X-RAY PHOTOELECTRON SPECTROSCOPIC STUDIES OF CARBON FIBRE SURFACES

Thesis submitted to the University of Newcastle upon Tyne for the degree of Doctor of Philosophy

by

Carol Kozlowski, B.Sc.

August 1984

ABSTRACT

The type and extent of surface oxidation of carbon fibres has been determined after electrochemically treating fibres in a variety of electrolyte solutions. The chemical and physical characteristics of these fibres have been evaluated using XPS, SEM, FTIR and UV spectroscopy. The fibres were anodically treated, both in a laboratory and in a commercial type cell. Fibres that have undergone commercial treatment were then incorporated into epoxy composites, the ILSSs of which were then measured.

The extent of oxidation and type of surface functionality produced as a result of electrochemical treatment is shown to depend upon several factors, ie the nature of the electrolyte, the anodic potential, reaction time, the structure of the fibre surface, the pH of the electrolyte solution, and the electrolyte concentration.

Surface nitrogen functionality is not produced as a result of polarising the fibres in nitric acid. It is produced, however, with treatments in solutions containing ammonium ions. The amount of surface nitrogen depends upon the concentration of these ammonium ions in the solution.

In most cases, polarisations in salt solutions produce similar changes in the fibre surfaces as treatment in the acid alone. The presence of bicarbonate ions tend to inhibit fibre surface oxidation.

In acidic solutions the fibres are shown to be extensively oxidised. Although the functionality of the oxide layer produced is very similar (ie. consisting of keto- and carboxyl/ester groups) after all the acidic treatments studied, the surface topography of the oxide layer produced is very different. In all cases this oxide layer is loosely bound to the bulk fibre.

In general, as reaction time increases, oxidation of the fibre surfaces also increases. Surface oxidation also increases with potential. However at high potentials (~3V) and long reaction times (>15mins) the detected functionality of type II fibres decreases. This is thought to be due to the formation of gaseous products such as carbon dioxide.

The reactivity of type I and type II fibre is shown to be different. The amount of carboxyl/ester functionality produced is far greater for type II fibres. It is concluded that carboxyl functionality is produced at the edge sites and keto-type functionality on the basal planes.

The amount of oxidation decreases as the pH increases. In alkaline solutions carboxyl and alcohol groups are produced, (the former being in greater quantities). The physical mechanism of oxidation is also different. Instead of an overall oxide layer being produced (in acidic solutions), holes are produced in the fibre surfaces. These holes are thought to be areas of localised attack.

It is also shown, using a small pilot plant, that both galvanostatic and potentiostatic control of electrolysis are satisfactory in producing treated fibres, which when incorporated into resins form composites with a high ILSS. The ILSS of the composites produced are dependent neither upon the amount of surface oxygen present nor upon the number of carboxyl groups present.

CONTENTS

CHAPTER 1

INTRODUCTION

Composite materials consisting of epoxy resins reinforced with carbon fibres are of great importance to the aerospace industry for structural applications. They have a considerably higher specific stiffness and strength compared to common engineering metals and glass fibre composites. The properties of fibre/resin composites are governed not only by the individual properties of fibre and resin, but also by the nature of the interface between these two components. When these composites were first developed some of the mechanical properties were disappointing. This was due to weak fibre/resin bonding which led to poor interlaminar shear strength (ILSS). Surface treatments of the fibres, usually oxidative in nature, have been found to greatly improve the ILSS (1).

The physical and chemical changes incurred during treatment have been studied by many workers in order to explain the observed improvements in ILSS (eg. 2,3,4,5). Many of these studies have been concerned with surface characterisation of the fibre using a variety of techniques including titration (6), microscopy (7), and spectroscopy (8). However, the reasons why these treatments are successful are still not known.

The effects of surface treatment can be as follows:-

(a) The surface topography may be altered by the

removal of carbon atoms in the form of gaseous and/or water soluble products during the oxidation process. This roughening of the surface will increase the area to which the resin can adhere and may lead to greater fibre-resin bonding.

(b) The chemical nature of the surface may alter. Several different functional groups are thought to be present on the fibre surface eg. alcohols, quinones, and carboxyl types (see Fig.1.1). One or more of these surface groups may react chemically with the resin or its curing agents and so increase fibre/resin bonding.

The relative importance of surface topography and surface functionality in composite properties is difficult to assess. This is because in most cases an increase in surface functionality is accompanied by a change in surface topography.

In this work, both the chemical and physical nature of the fibre surfaces before and after electrochemical oxidation in a variety of electrolytes are examined and the ILSSs of the corresponding composites measured. Electrochemical oxidation of the fibres is easily reproducible and the degree of surface oxidation can be readily controlled. This treatment can be carried out in the laboratory and easily adapted to work on a commercial scale to allow enough fibre to be treated and incorporated into composites, the mechanical properties of which can be tested.

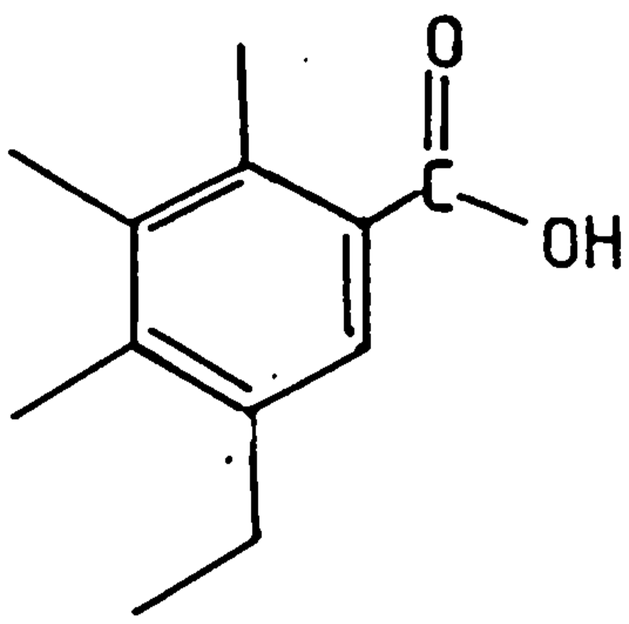

Carboxyl

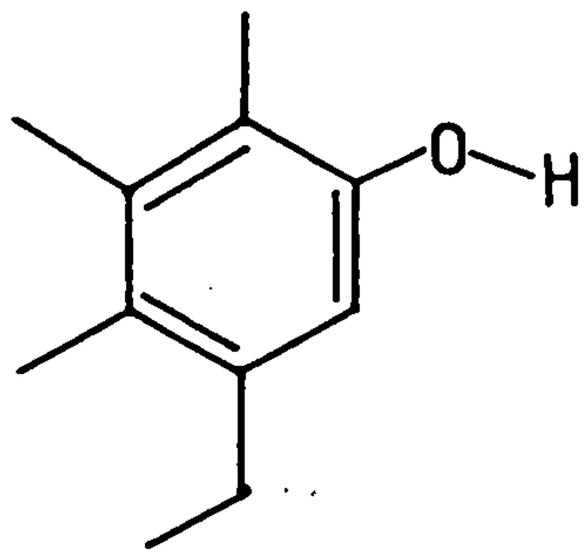

Phenolic Hydroxyl

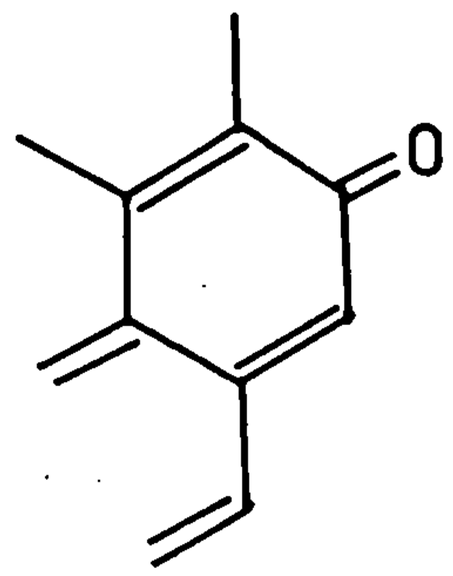

Quinone-type Carbonyl

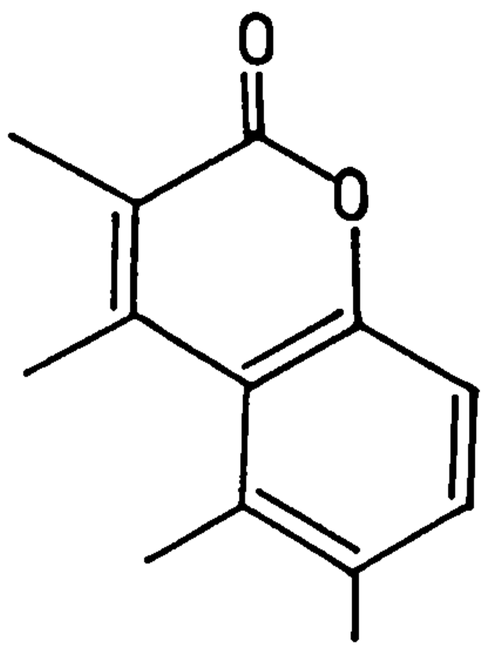

Normal Lactone

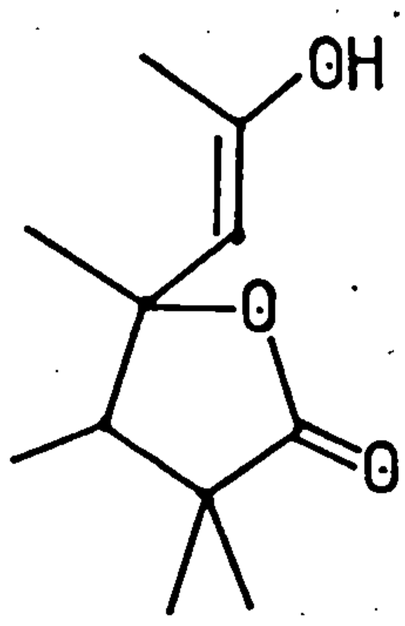

Fluorescene type Lactone

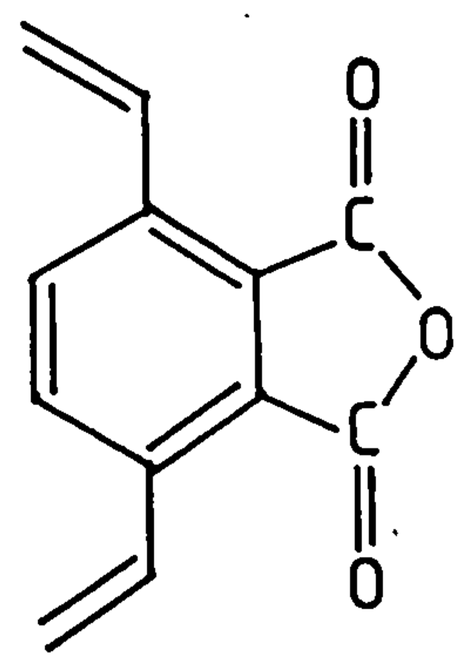

Carboxylic Acid Anhydride

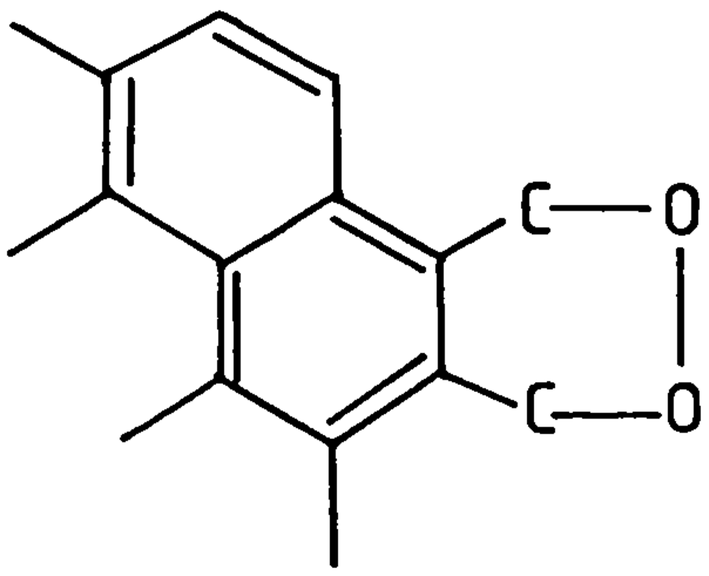

Cyclic Peroxide

Fig.1.1 Possible Functional Groups on Carbon Surfaces

The nature of electrochemical processes that occur on carbon electrodes depend upon:-

(a) the electrolysis conditions,

(b) the pH of the electrolyte solution,

(c) the concentration of the electrolyte,

(d) the specific nature of the electrolyte, and

(e) the nature of the carbon surface.

The aim of this work is to investigate all these factors and their effect on the type and the amount of surface functionality that is produced. The fibres have been treated in the laboratory and in a commercial-type pilot plant. The fibres anodically oxidized on a small scale, in the laboratory, are excessively over-treated compared to those used in commercial production. The reason for this is to produce the largest possible chemical modification of their surfaces. These large changes in surface functionality can be more easily detected than the smaller changes produced by commercial treatments. This aids the characterisation of commercial fibre surfaces treated under similar conditions. The changes in surface topography caused by different treatments are also studied.

Chemical characterisation of the fibres is carried out using X-ray photoelectron spectroscopy (XPS). Additional confirmation of results is obtained using Fourier transform infra-red spectroscopy (FTIR) and ultra-violet spectroscopy. The surface topography is examined using scanning electron microscopy (SEM).

A further aim is to observe and explain the effect of these chemical and physical changes on the shear properties of the

composites produced from fibres pretreated in a pilot plant.

It is hoped that the present work will lead to a better understanding of the changes induced on the fibre surface by electrochemical treatment, and to a greater insight into fibre-resin bonding.

CHAPTER 2

THE STRUCTURES AND SURFACE CHARACTERISTICS OF CARBON FIBRES AND OTHER CARBON MATERIALS

2.1 Introduction

To gain a better understanding of the effect of electrochemical treatment on the fibre surface, it is necessary to define the structure and the existing chemical nature of the fibre itself. The structure and properties of other types of carbon provide a good background for such an investigation. Many different types of surface treatments have been used and their effects on the fibres and resulting composites examined by a number of research groups. The types of surface treatment chosen for laboratory investigation by many workers are thought to resemble those used commercially (commercial treatments are mostly confidential), and are designed to produce detectable changes in the fibre surface. All commercial pretreatments are designed to produce the most desirable properties in the resulting composites. A short review of the changes induced by various pretreatments on fibre surfaces and composite properties is given below.

2.2 History

One of the first applications of carbonised materials was made, c1880, by Thomas Edison, who used carbonised cotton fibres as filaments for his incandescent lamp. These carbon filaments were later superceded by the more durable tungsten filaments.

In 1951, it was discovered that the strength of graphite increased by a factor of two from room temperature to 2500^{o}C and the Youngs modulus of elasticity by forty percent (9). This meant that graphite could be used for structural purposes at much higher temperatures than was possible with other materials. In the same year, Rosalind Franklin (10) showed that there was a pronounced increase in the basal plane alignment on heating a thin plate of anthracite; cut parallel to the bedding plane. These results were remarkably similar to those obtained when polyacrylonitrile (PAN) fibres were heated.

By the early 1960s there was a real need for a fibre with a high specific modulus and strength for reinforcing plastics. Bacon(11,12,13) had produced graphite whiskers with a tensile strength of 20 GPa and a Youngs modulus of 700 GPa. Asbestos fibres also proved very strong but were too short. Carbonised rayon fibres had a very low tensile strength and a lower Youngs modulus than graphite whiskers. This left the field open for a polycrystalline carbon fibre, with the necessary basal plane orientation parallel to the fibre axis, to be produced.

On heating PAN fibres to 200^{o}C, it was observed by L.N.Philips that a change in colour from white to black occured. These heated fibres were remarkably fireproof: when put into a flame they glowed red hot (14). This heating produced a ladder polymer and carbon fibres with the preferred orientation. PAN also gave a good carbon yield on heating.

In the period 1960-1965, Bacon (11), Shindo (15,16) and Watt

(17) separately showed that very high strength carbon filaments could be obtained by subjecting precursor fibres to a continuous tensile stress during high temperature treatments.

Carbon fibres are now produced from various precursor polymers, eg. PAN, cellulose and pitch. A typical process involves the following steps (1):-

1. Preoxidation at low temperatures (200-300°C).
2. Carbonization in an inert atmosphere at 1000°C.
3. Graphitization at 2500-3000°C.

There are three types of fibres produced from PAN. Each has undergone a different graphitization temperature: type I (high modulus) at 2800 °C, type II (high strength) at 1600°C, and type III (high strain) at 1100°C. These fibres have different mechanical properties and also show significant differences in structure and adhesion behaviour (18).

2.3 The Structure of Carbons

There are three allotropes of carbon; diamond, α-graphite and β-graphite. The structures are given in Fig.2.1.

2.3.1 Diamond

Diamond has a giant covalent lattice with extremely strong bonding throughout the crystal and is one of the hardest substances known. It has a highly symmetrical structure so that a large number of crystal faces may be formed and it is therefore an attractive gemstone. In the absence of impurities there is a large energy band gap of 6eV between the filled electron band and

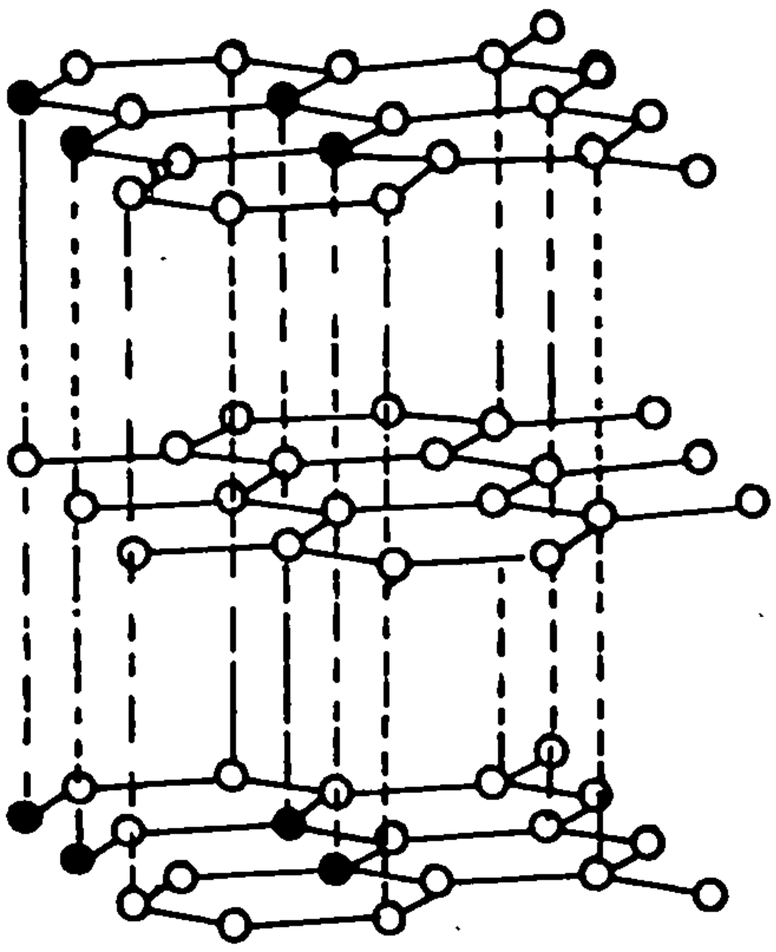

Structure of ∝-graphite

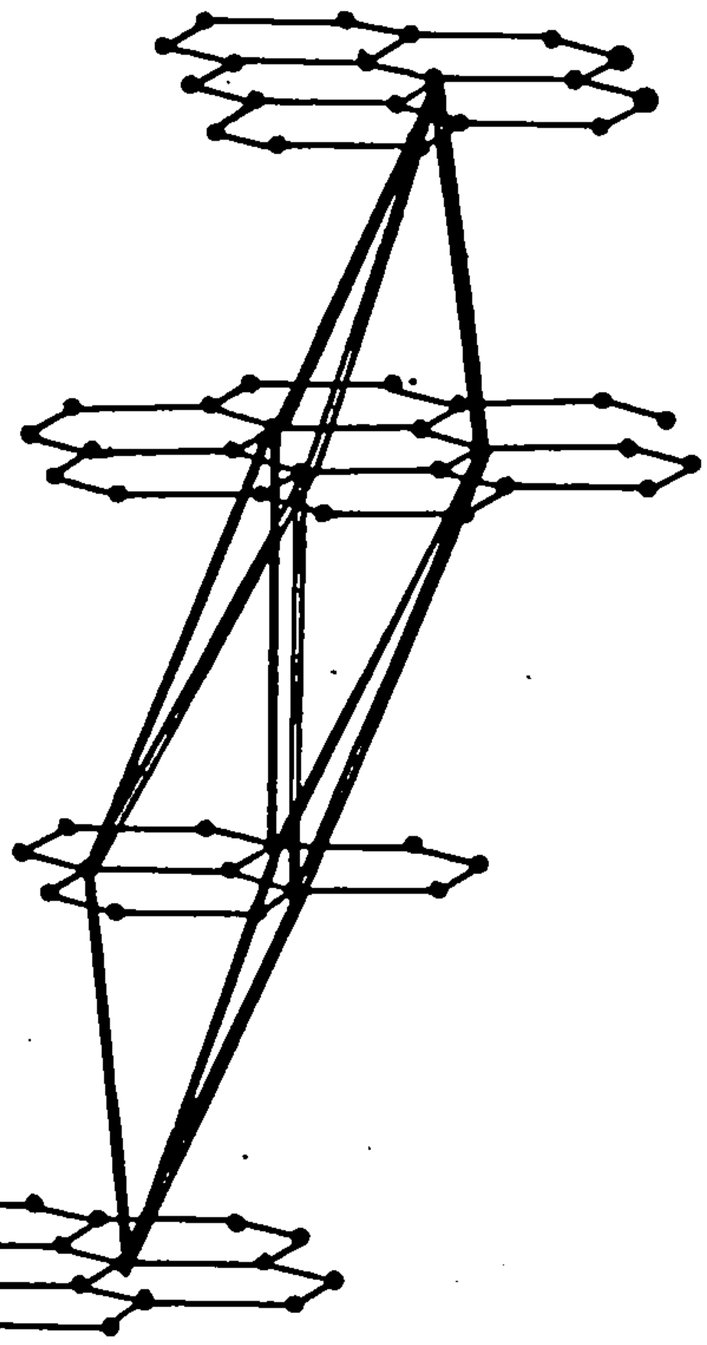

The lattice structure of rhombohedral β-graphite

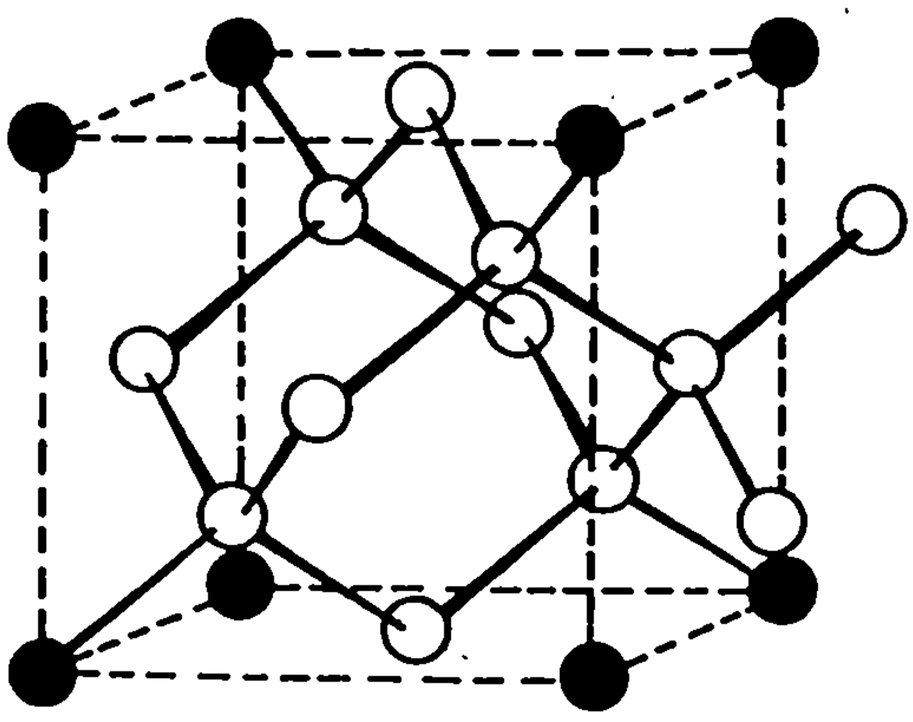

● marks the corners of the unit cell.

Structure of diamond.

Fig.2.1 Allotropes of Carbon

the next vacant band, so that it is colourless and does not conduct electricity.

2.3.2 α-graphite

Within each plane, each carbon atom is bonded to three other carbon atoms. The non-bonded p atomic orbitals overlap to give a completely delocalised system of molecular orbitals, thus allowing the transport of electrons throughout the crystal. Graphite is therefore a good conductor. The planes are held together by weak van der Waal forces. The interplanar distance is 0.33539nm, although this is slightly greater in incompletely crystalline carbons (19). The planes are so arranged that the carbon atoms of alternate layers are vertically above each other.

2.3.3 β-graphite

In β-graphite the planes are staggered such that the carbon atoms of every third layer are vertically above each other. This form is rare. It can be artificially produced by mechanical treatment, such as grinding of the α-form.

2.3.4 Pyrolytic Graphite

Pyrolytic graphite is produced by the deposition of carbon from the vapour phase onto the surface of a substrate. The result is a polycrystalline form of carbon, which is characterised by a high degree of orientation in the plane parallel to the surface of deposition.

2.3.5 Carbon Blacks

A number of models have been proposed for the structure of carbon blacks (20-24). Most of these models are over-simplified. The latest and most detailed is shown in Fig.2.2.

2.3.6 Carbon Whiskers

These were first produced by Bacon in 1960 (11). They are a form of highly purified artificial graphite in scroll-like formations continuous along a whisker length. They are extremely strong and are used as a strengthening filler for plastics and other matrix materials.

2.3.7 Carbon Fibres

On the basis of X-ray diffraction information, two basic models have been proposed for carbon fibre structure, one by Ruland (25,26), the other by Johnson and Tyson (27). The X-rays penetrate the whole fibre and thus the information obtained is representative of the bulk of the fibre. This technique leads to information about the degree of graphitization, and crystallite size and orientation. According to Ruland (25,26), all high modulus fibres consist of long thin fibrils and closed voids orientated in the direction of the fibre axis. There is also a lack of three dimensional order and the fibrils are stacked in a turbostratic manner (see Fig.2.3a). The model proposed by Johnson and Tyson (27) comprises of an array of crystallites of carbon stacked in columnar arrangements which may be slightly

Fig.2.2 Carbon Black

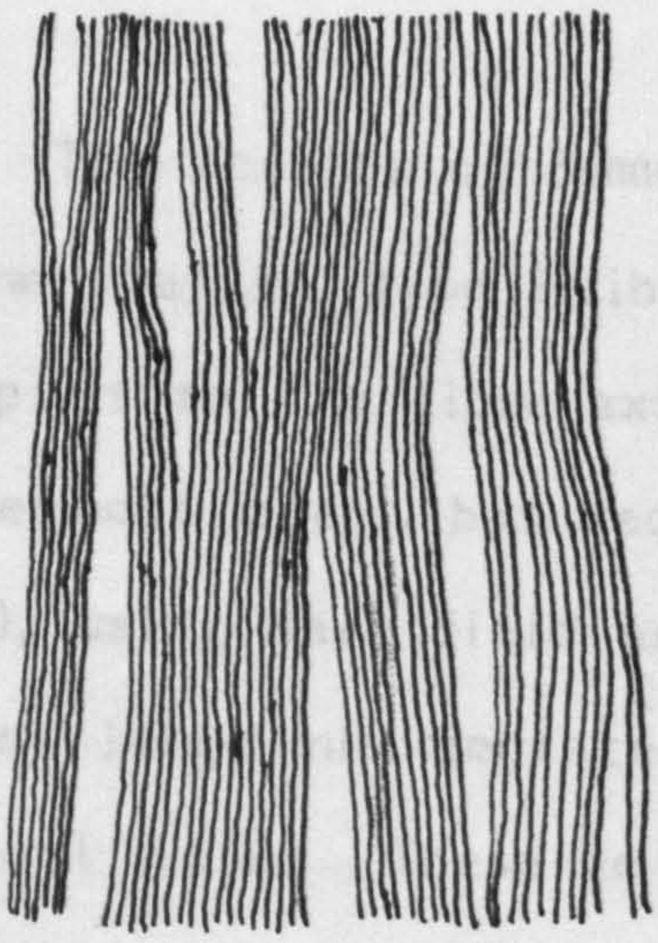

Fig.2.3a Ruland Model

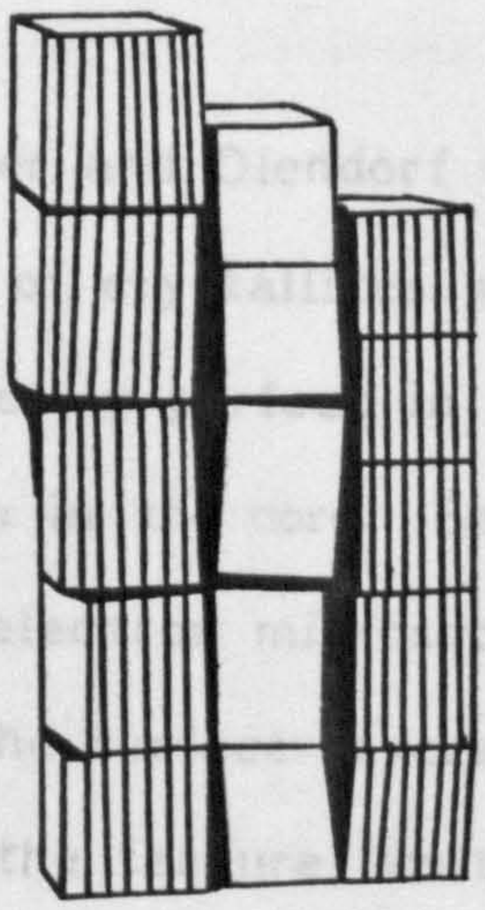

Fig.2.3b Johnson and Tyson Model

separated from each other. This slightly defective stacking, ie.tilting and/or rotating relative to one another, can cause voids. Low angle scattering measurements revealed the voids as having a mean width of 10Å (see Fig.2.3b).

Johnson and Watt (17), using X-ray and electron diffraction information, reported that high strength PAN carbon fibres consist of crystallites held together by a secondary carbon phase. The fibrils or crystallites themselves are composed of graphitic plates which can lie in random directions except for the a-axis which lies less than 10° from the fibril axis in the case of high modulus fibres. The fibrils can be regarded as polycrystalline with an average thickness varying between 250 and 1000 Å. Fibres prepared from PAN have a circular cross section and very smooth surfaces. These workers also reported that type I fibres were more graphitic in nature than type II.

The results of Bennet (28), and Butler and Diendorf (29) show that for type I fibres the alignment of crystallites with respect to the fibre axis appears to be nearly perfect in the outermost layers, but becomes more random in the core. Bennet (28), using dark field and lattice fringe electron microscopy, found large misorientated crystallites in the surface layers of type I fibres. These he considered to be the feature limiting their intrinsic strength. However, unlike other workers, he found no evidence of discrete fibrils. The strength of all fibres could be increased by small flaws and impurities. Moreton (29) stated that the strength of the fibres was a direct consequence of the external and internal cleanliness of the initial PAN fibres.

The ESR (electron spin resonance) results obtained by Robson et al (30) confirm those reported using X-ray diffraction techniques, in that the graphite crystallites have their basal planes parallel to the fibre axis. Raman studies show that type I fibres are more graphitic in nature than type II (31). The d spacings of graphite crystals in type I fibres are 3.39Å (32) compared to 3.35Å in natural graphite.

2.4 Surface Functional Groups on Carbons

All carbon surfaces, except the basal plane of highly orientated graphite, will contain a number of different functional groups. The nature of these functional groups is of fundamental importance to the understanding of most electrochemical processes occuring at carbon or graphite electrodes. The surface functionality of carbon surfaces has been reviewed by Donnet (33,34), Boehm (35), Rivin (36), Puri (37) and Deviney (38).

Most work has been carried out on amorphous carbons (such as carbon black) and activated carbons because of their large surfaces areas. These carbons consist mainly of graphite-layers of limited size, stacked parallel to each other without further order. The more random the order of these graphitic planes, the more susceptible the carbon is to oxidation and the adsorption of gases. In addition to the edges of layers, the basal planes also possess defects, eg. dislocations and discontinuities. Such sites are highly active. Physisorbed oxygen is present on all carbons at temperatures greater than -40^{o}C (39,40,41). This

physisorbed oxygen cannot easily be removed.

Two types of 'oxide' are present on carbons depending upon their pretreatment; acidic and basic oxides (43).

2.4.1 Acidic 'oxides'

Acidic surface oxides result from the treatment of carbon with oxygen at temperatures near the ignition point and are also formed upon reaction with oxidizing solutions at room temperatures. Surfaces of carbon rich in these oxides are hydrophilic. These oxide groups must include some strongly hydrophilic components such as carboxyl or hydroxyl functionalities.

Carbons with the highest surface areas permit the best functional group identification of surface oxides. The most detailed work has been conducted on carbon blacks. Functional group derivatization has been the most extensively used method for identifying the surface groups. The derivatization of functional groups present on polymer surfaces are discussed in section 2.4.5.

Boehm (51) performed some differential acidimetric determinations of active carbons. These functional titrations indicated the presence of carboxyl, hydroxyl, lactone and carbonyl groups on their surfaces. The surface concentration of each group was determined in the following way:-

(1) The carboxyl groups were titrated with sodium

bicarbonate ($NaHCO_3$).

(2) sodium carbonate (Na_2CO_3), which also neutralizes the carboxyls, allows the lactone cycles to open and to titrate the -COOH groups so formed.

(3) Sodium hydroxide allows the determination of phenolic functions together with lactone and carboxyl groups;

(4) Sodium ethoxide neutralizes the carbonyl functions, which are probably of quinoid type. This reagent also neutralizes the three other acid functionalities.

Fig.2.4 shows the structures proposed by Boehm (51,52,53,54) and Garten (55).

The infra-red spectrum of carbon black (56) showed -OH, -COOH and C=O to be present. The concentration of carboxyl groups depends on the temperature of oxidation; when this temperature exceeds 900^{o}C carboxyl groups are not formed, which is to be expected since decarboxylation is complete above 900 ^{o}C.

2.4.2 Basic 'oxides'

Basic oxides are formed when a carbon surface, freed from all surface compounds by heating in a vacuum or inert atmosphere, comes into contact with oxygen after having been cooled to a low temperature (43). Much less is known about the structure of these oxides. They absorb acids only in the presence of oxygen. A part of the acid absorbed in this way may be desorbed by certain solvents, such as toluene.

Garten and Weiss (55,57) proposed a chromene-type structure for the basic oxides (see Fig.2.5).

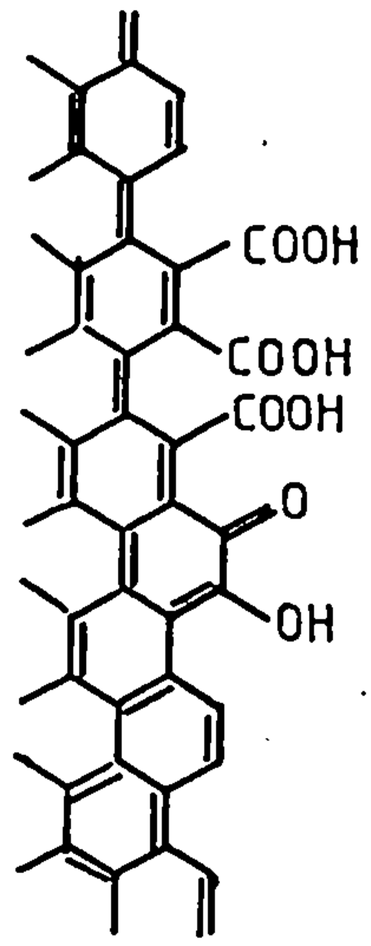

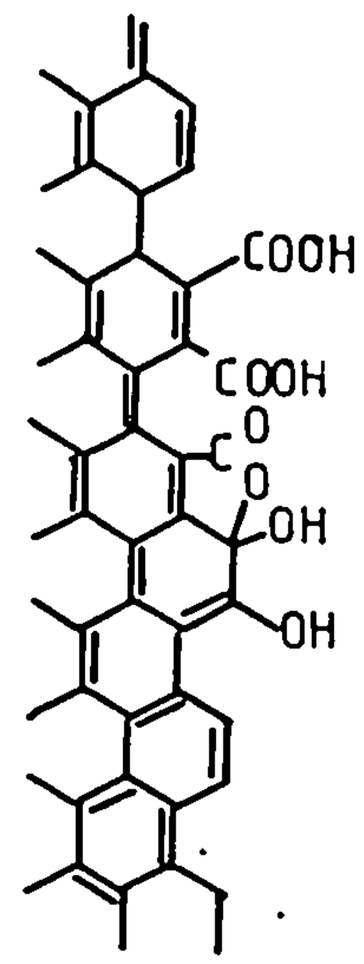

Fig.2.4 Surface Oxides of Carbons

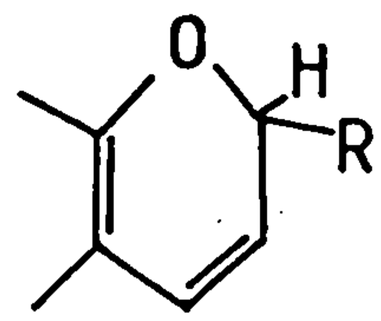

or

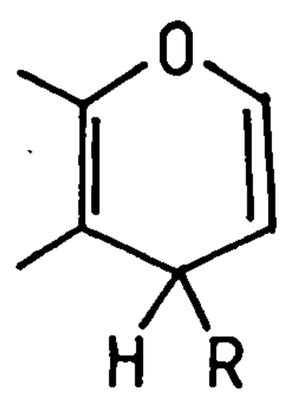

Fig.2.5 Chromene Structure

Donnet (56) suggests that the unexplained oxygen could be engaged in the basic groups capable of being formed between the basal planes of the graphitic layers.

2.4.3 Graphite

The rate of fixation of oxygen to a carbon surface decreases considerably when the degree of graphitization of the carbon increases (58). Hennig, using monocrystals of graphite, found the area of the graphitic layer may be multiplied by six without increasing the amount of oxygen fixed to the surface, providing the number of border atoms remains constant.

2.4.4 XPS of Organic and Polymer Systems

The most comprehensive study of these systems has been carried out by Clark and his co-workers (59-65), although other workers have examined smaller ranges of chemical compounds. The appendix contains a range of C1s and O1s binding energies and chemical shifts for a variety of compounds and polymers.

2.4.4.1 C1s Binding Energies

Clark (65) summarised the C1s chemical shifts by stating that each C-O bond present induces a 1.5eV chemical shift on the C1s signal. Fig.2.6 gives the approximate range of binding energies for several functional groups.

The chemical shifts for C/N functionalities are markedly

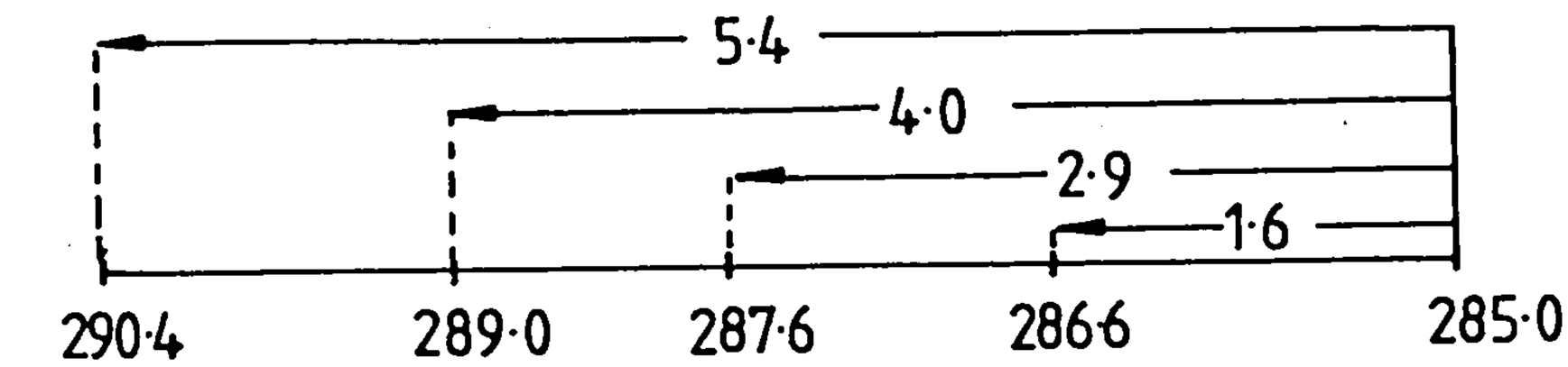

Fig.2.6 Carbon 1s- Shifts

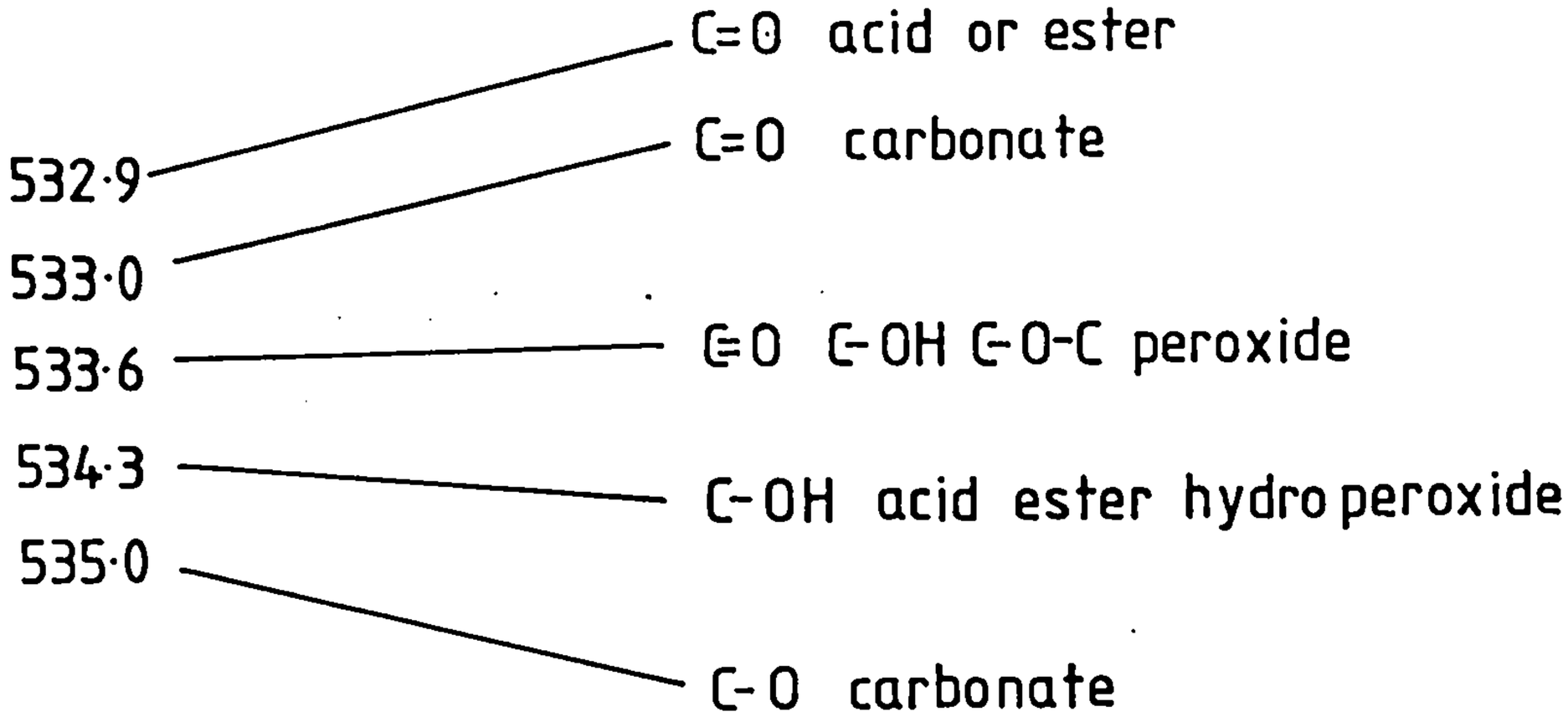

Fig.2.7 Oxygen 1s Shifts

dependent on the substituent. The chemical shifts for $-N(CH_3)_2$, $-NH_2$, -NCO, NO_2 and $-CONH_2$ are 0.2, 0.6, 1.8, 1.8 and 2.0eV. The C1s binding energy for amide groups is noticeably less than for carboxyl functionality.

2.4.4.2 O1s Binding Energies

The O1s signals for a variety of functional groups fall within a small range of binding energies ie. 532.8-535.0eV (Cf. C1s, 285.0eV). O1s binding energies are summarised in Fig.2.7 (64,65). The extremes in binding energies are seen in carboxyl and carbonate groups where the singly bound oxygen has the higher binding energy.

2.4.4.3 N1s Binding Energies

-CN, $-NH_2$,-OCONH- and $-CONH_2$ groups have N1s binding energies which fall within the range 399-401eV. Oxidized nitrogen functions have much higher binding energies eg.-ONO (408eV), -NO (407eV) and -ONO-(405eV).

2.4.5 Functional Group Labelling (derivatization)

For spectra with many overlapping peaks, or for functionalities that give rise to signals of similar binding energies, organic labelling reactions have been used to detect the presence of these individual groups. These reactions label specific functionalities with a distinctive element such as fluorine or thallium. A list of derivatization reactions are given in Table 2.1. The properties of a good labelling reaction

TABLE 2.1

Derivatization Reactions

Functional group	Reagent	Product	Ref.
$-CH_2OH$	$(CF_3CO)_2O$	$-CH_2OCOCF_3$	44
$-CH_2OH$	$Ti(acac)_2OPr^i_2$	$-CH_2OTi(acac)OPr^i$	45
$>C=\overset{|}{C}-OH$	$ClCH_2COCl$	$C=\overset{|}{C}-OCOCH_2Cl$	45
$>C=O$	$C_6H_5NH-NH_2$	$>C=N-NHC_6H_5$	44,46
$-COOH$	$BaCl_2$	$(-COO^-)_2Ba^{2+}$	47,48
$-COOH$	$TlOC_2H_5$	COO^-Tl^+	49
$-NH_2$	C_6F_5CHO	$-N=CHC_6F_5$	44

are:

(a) the reaction is specific to one functional group,

(b) the element introduced onto the surface has a large photoelectric cross section, producing high intensity photoelectron signals.

The main problem with using these derivatization reactions on polymers such as carbon fibres is that it cannot be assumed that surface functional groups react in the same way as normal organic compounds. The reactivity of a specific functional group may be affected by neighbouring functionalities. Steric hinderances will also influence reactivity. If the polymer has a roughened surface, unreacted chemicals may get trapped in surface pores, giving misleading results. Nevertheless, organo derivatization has been proved useful on polymers such as polythene (50).

2.5 Surface Treatments

Successful reinforcement of composites is only achieved by obtaining sufficient stress transfer between fibre and matrix. Such stress transfer can be realised by mechanical action, physical adhesion and chemical bonding. Composites made from untreated fibres and epoxy resins have poor mechanical properties (eg. ILSS and impact strength), particularly when the fibres have a high modulus (these also exhibit the highest degree of crystalline perfection). Surface treatments, mainly oxidative in nature, are known to greatly improve the ILSS and hence lead to improved fibre resin bonding. The types of surface treatment are as follows (1):-

(a) Wet Methods eg. the immersion of fibres in oxidizing agents such as nitric acid and potassium permanganate. This also includes electrochemical oxidation.

(b) Dry Methods, eg oxidation by air, oxygen or ozone.

(c) Coatings, eg. polymer grafting.

Electrochemical fibre treatments appear to be the most widely used in industry. Processes using various electrolytes have been developed and patented (66,67,68). Fig.2.8 shows an electrochemical cell suggested by Paul (69) for the treatment of fibres on an industrial scale.

2.6 The Effect of Wet Treatments on Fibre Surfaces.

There are two main types of wet treatment that can be used to treat the fibre (a) the use of strong oxidizing agents such as nitric acid, and (b) electrochemical oxidation in aqueous solution.

2.6.1 Nitric Acid Treatment.

Nitric acid oxidation of Thornel 25 fibres was found to increase the specific area and the concentration of carboxylic groups on the fibre surface (70). Carbon fibres are not homogeneous in their response to this chemical attack and a skin-like layer separates from the bulk of the fibre (71,72). This increase in surface oxygen concentration was also noted by Brewis (2). The oxygen 1s spectrum of treated fibres showed the presence of at least two different oxygen species (B.E.s, 531.7eV

and 533.4eV). The carbon 1s spectra of these fibres exhibited a shoulder to higher binding energy of the main peak (chemical shift 1.5eV) and a smaller peak 4eV from this main signal.

Goan (73) and Fitzer (18) found that type I and type II fibres varied in their susceptibility to chemical attack. On boiling in concentrated nitric acid (60-70% by weight), a 4% weight loss occured after 3 hours (unaffected by further treatment) with type I fibres, with no observable changes in surface topography (magnification x5000). Type II fibres underwent a 50% weight loss after 72 hours and several significant differences in surface topography were observed after treatment. The fibres were pitted throughout the fibre shell. The diameter of the fibres was reduced from 8 to 5.5 and the microscopic roughness (striations) was removed. The concentration of oxide groups produced on type I fibres was one order of magnitude less than for type II fibres (18) and the formation of these acid groups on type II fibres occurs rapidly (up to one hour) whereas type I fibres react much more slowly. The surface areas of both types of fibre initially increased upon oxidation, this increase being very small for type I fibres. After long oxidations the surface area of type II fibres decreased, indicating that the outer shell of the fibre had been completely oxidised to CO_2 and the fibre had become smooth.

These results for type I fibres were also found by Rand et al.(100), who found that electron microscopy revealed no marked differences in the fibres before and after treatment with fuming nitric acid. There was some evidence for conical pitting. The mean diameter of the fibres remained unchanged.

Other oxidizing agents have also been used such as Hummers reagent (74), chromic acid (75), and sodium hypochlorite (76).

2.6.2 The Electrochemical Oxidation of Graphite and Carbon Fibres.

Electrochemical oxidation is the most widely used industrial method of treating carbon fibres (66,67,68). The changes induced by such treatments will be governed by the structural and chemical nature of the fibre itself. Since the structure of carbon fibres, particularly type I fibres, is closely related to graphite, an outline of the electrochemical behaviour of graphite is given below to help explain some of the main features observed on carbon fibres in this work.

2.6.2.1 Graphite.

Electrochemical reactions may occur (77):-

(a) at edge atoms (at plane boundaries or defects);

(b) at exterior intraplanar atoms, and

(c) by intrusion between the planes.

The edge atoms of the carbon planes in graphite would be most reactive because the residual valence bonds lead to reactions that occur preferentially in the direction perpendicular to the graphitic planes. Edge attack is heaviest on less orientated graphite, whereas attack by intraplanar intrusion is more pronounced with highly orientated graphite electrodes, provided that some edge planes are exposed to the electrolyte. Intraplanar intrusion of ions into the lattice occurs with many

electrolytes, especially with nitric and sulphuric acids and their salts. Marsh et al.(78) found that pyrolytic graphite, unlike natural single crystal graphite, showed only a general overall eroding of the surface.

Bardina and Krishtalik (79) studied the oxidation of non porous pyrolytic graphite in phosphate solutions below the oxygen potential. A linear relationship between current and potential was obtained from 0.5-1.2V. An increase in pH from 1 to 9 had practically no effect on this curve. They suggested that the curve corresponded to the oxygen reaction and assumed that oxygen was given up from the graphite surface in the form of carbon dioxide.

Binder et al (80) studied the anodic oxidation of several types of carbon, including graphite, in acid and alkaline electrolytes. They concluded that 80% of the charge was used to oxidise the carbon electrode to CO_2 and 20% for the formation of oxygen containing compounds. The formation of the oxide layer preceeded the evolution of carbon dioxide. Redey and Lohonyai (81), using spectroscopic graphite, reported the formation of two types of oxidation, one occuring at 0.4V and the other at 0.9V.

Usually, polarisation in acid solutions above the oxygen potential results in the formation of carbon dioxide, and swelling of the electrode occurs, causing it to exfoliate. Strong anodic treatment in acid electrolytes leads to the formation of graphitic oxide (82).

In strong alkaline solutions, it has been suggested that an

equilibrium occurs on the electrode of the type (83):

$$OH^- = OH + e^- \qquad 2.1$$

Oxygen discharged from water molecules is exceedingly reactive, whereas oxygen from hydroxyl ions is much less so (77) The great difference in oxygen activities in acid and alkaline solutions suggests that the first step in the oxidation process from water molecules is:

$$C_{(s)} + H_2O \longrightarrow C(O)_{ads} + 2H^+ \; 2e^- \qquad 2.2$$

The corresponding step for the discharge of hydroxyl ions is

$$C_{(s)} + OH^- \longrightarrow C(OH)_{ads} + e^- \qquad 2.3$$

When oxygen is discharged from a water molecule, carbon dioxide can be formed by the following reactions

$$2\,C(O)_{ads} \longrightarrow CO_2 + C \qquad 2.4$$

$$C(O)_{ads} + OH^- \longrightarrow CO_2 + H^+ + 2e^- \qquad 2.5$$

$$C(O)_{ads} + H_2O \longrightarrow CO_2 + 2H^+ \; 2e^- \qquad 2.6$$

These reactions will involve C-C bond breakage. According to Kokhanov(84,86) the evolution of oxygen can occur with or without the participation of a surface graphite compound. He proposes a scheme for the evolution of oxygen, the overall equation with contributions from several reactions can be written as follows:-

$$4OH^- \rightarrow O_2 + 2H_2O + 4e^- \qquad 2.7$$

Bulygin (85) found that high chemical losses occurred in acidic solutions, which were independent of the specific

character of the anion. These were attributed to the oxygen discharged in these solutions being more active than that discharged in alkaline solutions. Oxidation in acidic solutions leads to the formation of pyromellitic acid and intermediate surface oxides, processes which evidently have lower activation energies than for the formation of the final product, carbon dioxide.

2.6.2.2 Carbon Fibres

Anodic oxidation in aqueous sulphuric acid has been carried out by several workers. Weinberg and Reddy (6) suggested that working potential has little or no effect on the surface oxide products, which were determined by titration with base after the fibres had been electrolysed. Proctor and Sherwood (87), polarising the fibres in two different electrolytic solutions (sulphuric acid and ammonium bicarbonate), found using XPS, that the total oxide concentration increases with fibre potential. The relative proportion of different surface groups varies with potential, C=O being dominant at low potentials and C-O at higher potentials. The relative amount of acid groups remained fairly constant at every potential. These effects were more pronounced using sulphuric acid as the electrolyte. Nitrogen groups were present on polarising fibres in ammonium bicarbonate solution and their surface concentration increases with an increase in potential.

Shindo (88) anodically oxidised Besfight type I and type II in aqueous solutions of sodium hydroxide and sulphuric acid using a batch continuous process. In aqueous sodium hydroxide, there

was no difference in tensile strength or weight loss at anodic potentials 1.0, 1.5, 2.0V, but there was a significant weight loss for fibres treated in sulphuric acid. He also found that the amount of decomposition products was greater for type II than type I fibres. This has also been observed for treatments in nitric acid. HM fibres treated in acidic solution exhibited a more rapid decrease in tensile strength than those treated in alkaline solution.

The tensile strength of type I fibres, treated in sulphuric acid, drops considerably only if potentials higher than 2.1V are used for treatment times of ten minutes (3). Fitzer distinguished between non-corrosive and corrosive treatments. The evolution of aqueous bi-products, CO and CO_2 , was caused by corrosive fibre damage. He concluded that anodic potentials lower than 2V must be applied to avoid large amounts of fibre damage. Washing removed all surface contaminants.

Most of the studies of the effect of surface treatments on carbon fibres have involved the use of wet chemical techniques. As this work mainly uses XPS as a tool for identifying surface functionality, a brief review of the work involving this technique in the study of carbon fibre surfaces is given here.

2.7 XPS of Carbon Fibres

The earliest X-ray photoelectron studies of carbon fibres were carried out by Barber et al.(89) in 1970. They found that there was a large increase in oxygen bound to the surface after oxidation, and at least two types of oxygen were present on all

oxidised fibres. The carbon 1s profile resembled that of graphite. Fibres baked in nitrogen at 1300K contained two types of nitrogen. In later studies, using graphite, he presented evidence for the presence of two types of oxygen on basal surfaces (90).

Donnet (74) has carried out a detailed examination of type I and type II fibres using anodic oxidation treatments in acid and alkaline solutions. There were two distinct features in the carbon 1s spectrum of fibres anodised in nitric acid; a main peak at 284eV and a chemically shifted component 3.7eV from the main signal (shown in Fig 2.9a). He attributed this chemically shifted species to C=O functionality. The carbon 1s spectrum of type I fibres treated in Hummers reagent possessed a chemically shifted species 2.1eV from the main peak (Fig 2.9b), this he assigned to C-OH groups. The chemical shift of cyclohexanol is 1.9eV. This type of structure seems unlikely to be produced on carbon fibres. The usual chemical shift induced by alcohol groups are in the range 1.6-1.7eV (see Fig.2.6).

In 1979, Brewis et al (2) used XPS to determine the degree and nature of oxidation of carbon fibres before and after various pretreatments. His results are shown in Fig.2.10. The spectrum of untreated fibres possesses a tailing towards higher binding energy (and also a small peak at 7eV, although they make no mention of it). A shoulder is present to higher binding energy of the carbon 1s primary peak for treated fibres and a peak is also present at 4eV from the main peak. The oxidation level increased fourfold on oxidation with at least two oxygen species being present. They concluded that alcohol and carboxyl type

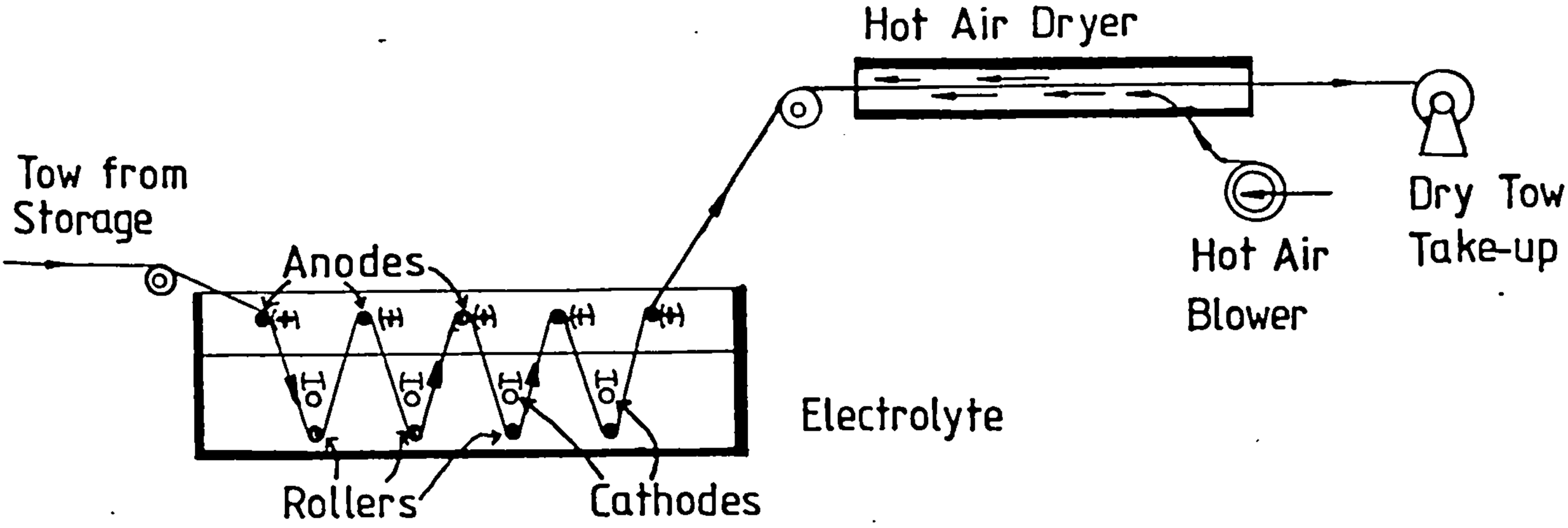

Fig.2.8 Paul's Electrochemical Cell and Industrial Plant

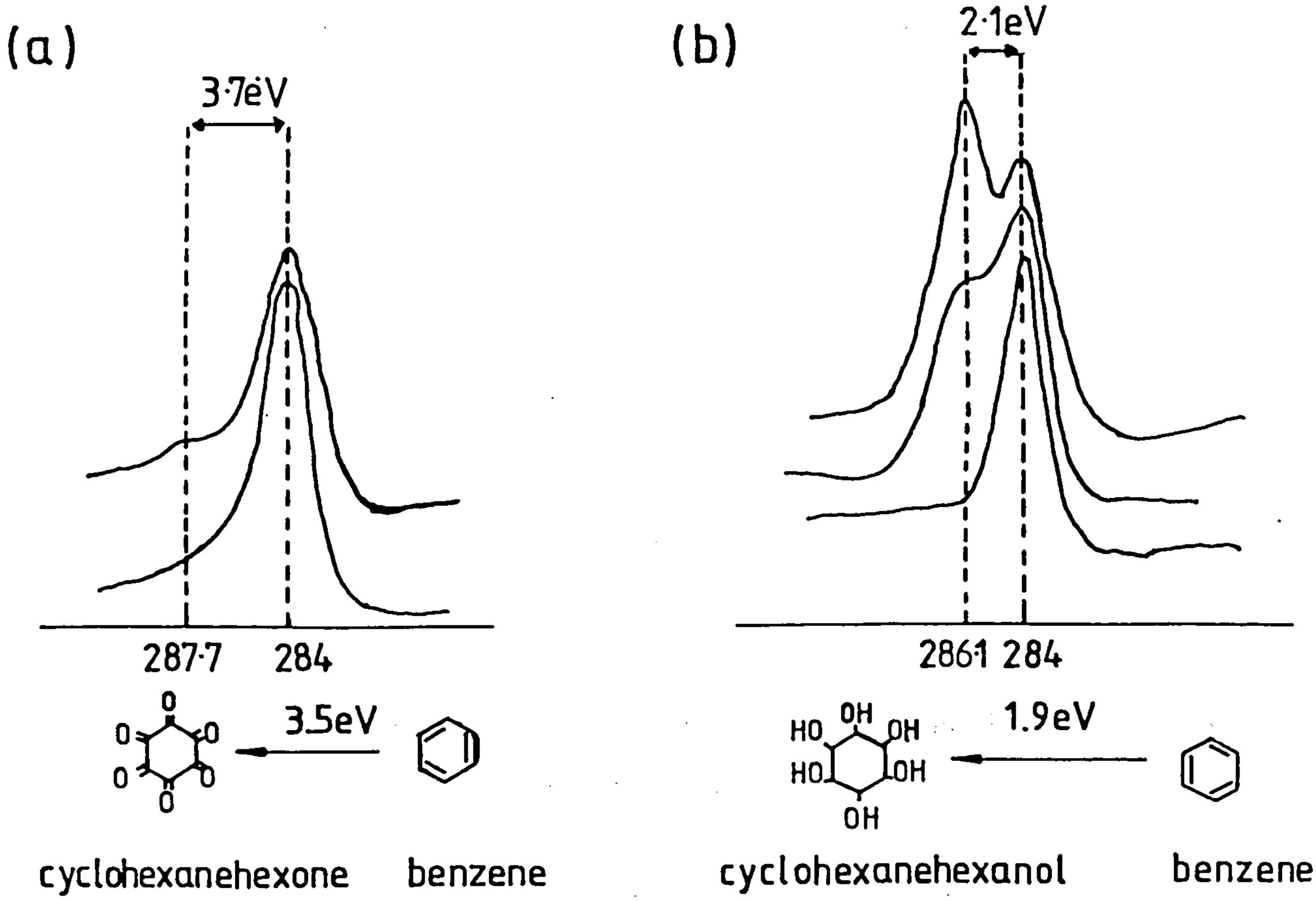

Fig.2.9 The C 1s Spectra of Fibres Treated in (a) Nitric Acid and (b) Hummers Reagent

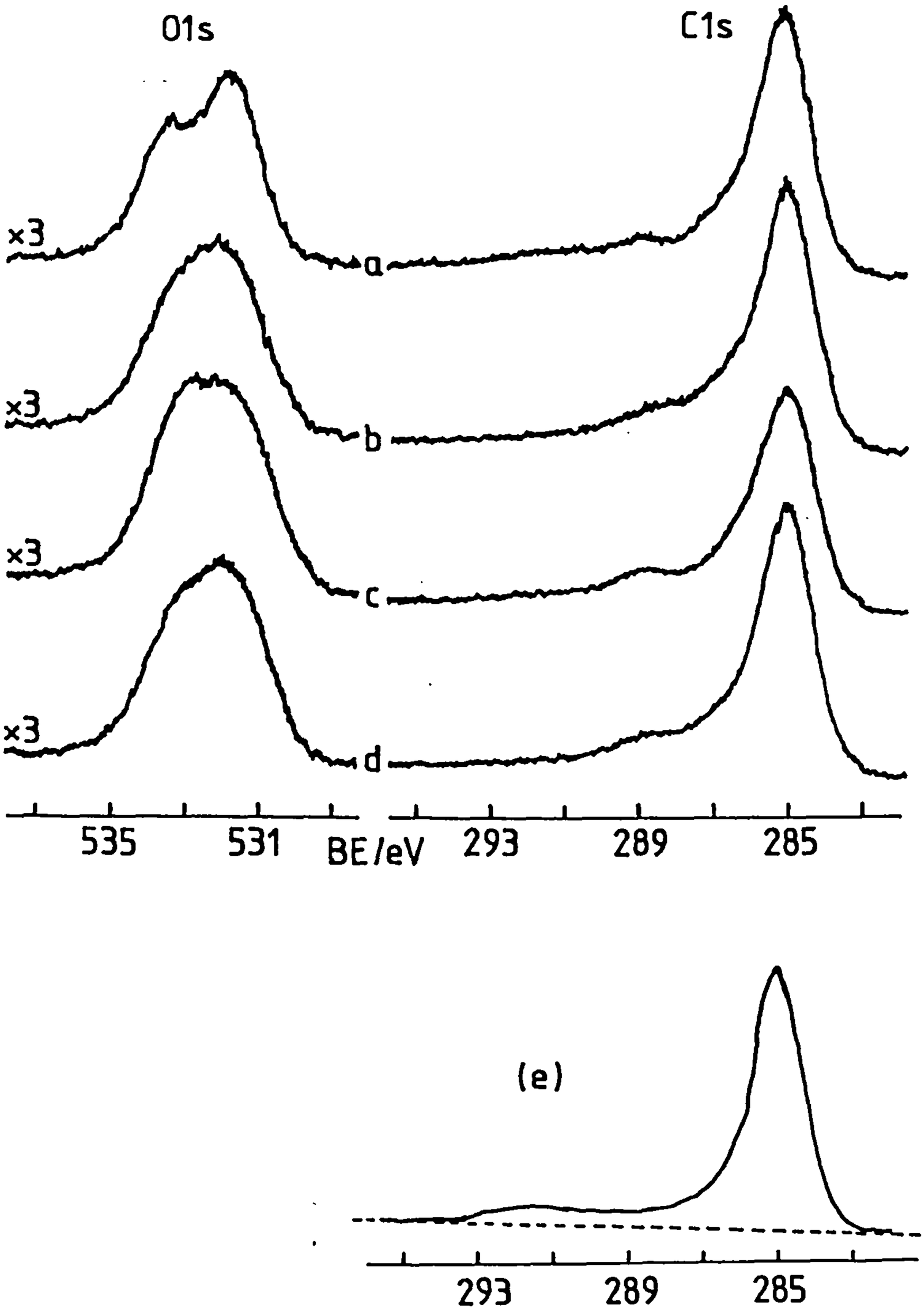

Fig.2.10 Effect of Oxidation on Carbon Fibre Surfaces (after Brewis et al) treated in

(a) Air
(b) Chromic Acid
(c) Nitric Acid
(d) Sodium Hypochlorite

and

(e) Untreated

groups were present on the fibre surface. They further stated that good adhesion can only be achieved if the fibres have a 4% O:C ratio, further oxidation resulting in only a moderate increase in adhesion.

Thomas et al.(91) found no significant differences in chemical environments of the elements on various fibres. The carbon 1s spectrum of type II fibres (treated) consisted of two chemically shifted species at 1.25eV (-C-O-) and 2.5eV (C=O) from the main signal. The former shift seems very small for alcohol groups. Nitrogen 1s- binding energies were said to correspond to N-O type linkages, although no binding energies were published.

Drzal (7) also found an increase in oxygen and nitrogen concentration from untreated to treated type III fibres. He suggested that the source of nitrogen could be from nitric acid treatments. Sodium contamination was also present. Nitrogen 1s binding energies of 400eV corresponding to C≡N and C-NH_2 linkages were also detected. These results are very simlilar to those found by Gynn et al (92). Heating to 300^{o} C reduces the surface oxygen concentration. Type I fibres gave different results to those obtained for type III fibres. The photoelectron peak width (FWHM) in the C1s spectrum is less for type I fibres than for type III; this being due to the greater degree of truly orientated crystallites. There was a definite relationship between the polar component of surface free energy and the amount of surface oxygen (measured by XPS).

Ishitani (93) found chemical shifts of 1.5eV, 2.5eV and 4eV in carbon 1s spectra of oxidised fibres and in a later

publication he claimed to have these results with the use of a digital difference technique (94). Proctor et al (95) used a different digital difference technique with which they were able to obtain detailed information about the very small changes in carbon 1s spectra of commercially treated fibres. Sherwood in a review of data analysis techniques has given a full explaination of this technique (140). Fourier transform infra red spectra of these fibres showed the presence of COOH group (although the noise level was very high).

Most commercial treatments only slightly oxidize carbon fibres to obtain a good ILSS in the corresponding composite whilst not damaging the fibre itself. This slight oxidation produces only very small changes in the carbon 1s spectrum of the treated fibres. Sensitive data collection techniques are needed to observe these subtle changes. In 1982-3 Proctor and Sherwood (95,87,96) showed how these changes could be investigated by using several data analysis techniques to obtain detailed information from digital carbon 1s spectra. These included non-linear background subtraction (97), smoothing (98) and curve fitting (99). They examined industrially treated samples from Courtaulds (96) and found that as the percentage treatment increased, there was an overall increase in the amount of C-O and C-N surface functionality. The oxygen 1s spectra of commercially treated fibres showed no difference in the relative proportion of oxygen species with the increase in commercial treatment. On heating the fibre (95) the effect of surface treatment was reversed, the carbon 1s spectra resembling those of untreated fibres.

2.8 The Effect of Surface Treatments on Carbon Fibre/Resin Composites.

It is known that surface treatments improve fibre resin bonding but the mechanism by which the adhesion takes place is not yet fully understood. There appear to be three major mechanisms contributing to the strength of the fibre resin bond (100):-

(a) The absorption (either physical or chemical) of the resin molecules onto surface complexes; usually acidic complexes have been considered to be of most importance (1).

(b) Physical adsorption onto the basal surfaces.

(c) A mechanical 'keying' effect when the resin penetrates pits and channels on the roughened surface brought about by oxidation.

In most cases an increase in the surface functionality is accompanied by an increase in surface area, and so the relative importance of these two factors is difficult to assess. Herrick (70), in 1968, reported that the treatment of Thornel 25 fibres in nitric acid increases their surface area and also the number of surface oxygen complexes. Similar results have been reported by Donnet (101), Fitzer (3) and Rand (100). The interlaminar shear strength of composites made from these treated fibres also increased. Some fibres, after nitric acid treatment, were heated in hydrogen to reduce the surface oxygen complexes. The ILSS of the corresponding composites decreased significantly suggesting that surface functionality was of most importance in enhancing

fibre resin bonding. Scola and Brooks (102), on the other hand, found no decrease in the ILSS for composites produced from treated Hitco HMG50 fibres that had been heated in hydrogen prior to incorporation into the composite.

It has been found by many workers (eg. 71,95) that heating the fibres removes acidic surface oxidation almost completely. The treatment of AG carbon fibres in Hummers reagent (71) produces a graphitic oxide type layer. This lamellar graphitic oxide can be destroyed by heating. The formation of this lamellar coat greatly improves the ILSS of composites, but the ILSS of composites made from treated fibres which had been heated decreased to a similar value to that of the untreated the fibre/resin composites. For AC fibres, heating did not produce such a marked effect. Although heating caused a substantial decrease in ILSS, the original value for the untreated fibre/resin composites could not be obtained.

Fitzer (3) has carried out a systematic study of the effect of fibre surface treatment using nitric acid on the shear strength of composites. He used titration methods to determine the surface oxide concentration, and blocking reagents such as diazomethane. Over-oxidation of the fibres was found to strongly influence composite fracture behaviour and so only short oxidation times were used. Over-oxidation of the fibres causes a brittle fracture in the short beam test and therefore is not an adequate indication of ILSS. An optimum level of surface oxidation was found for type II fibres to produce maximum ILSS.

Fig 2.11a shows the effect of using blocking agents on carbon fibres prior to their incorporation into the resin. These reagents are said to react with carboxylic and alcohol functionalities as shown in Fig 2.11b. Fitzer concluded that the amount of fibre-resin bonding is solely dependent upon the amount of acidic surface functionality.

Surprisingly, he found type I and type II fibres gave the same ILSS for their composites but type I had a surface oxide concentration one order of magnitude less than type II fibres. This indicates that other bonding mechanisms are involved as well, or instead of, the one suggested above.

Brewis (2), using a variety of pretreatments, found that at best only a moderate increase in ILSS was achieved. The largest increase in ILSS (35%) was observed for chromic acid treatment. He suggested that optimum adhesion occurs when the O:C ratio (measured by XPS) was 4%.

Thomas et al (91), using XPS, found a relationship between the amount of surface oxygen and ILSS. A similar relationship was also found for surface nitrogen concentration.

Brelant (104) has a completely different view on the subject. He suggests that the ILSS of fibrous composites is a function of resin strength and the size and distribution of voids at the fibre/resin interface. The limiting strength is said to be the stress required to propagate cracks through the voids along the fibre-matrix boundary. The increase in shear strength noted in the experiments carried out by Fitzer (3), for short the

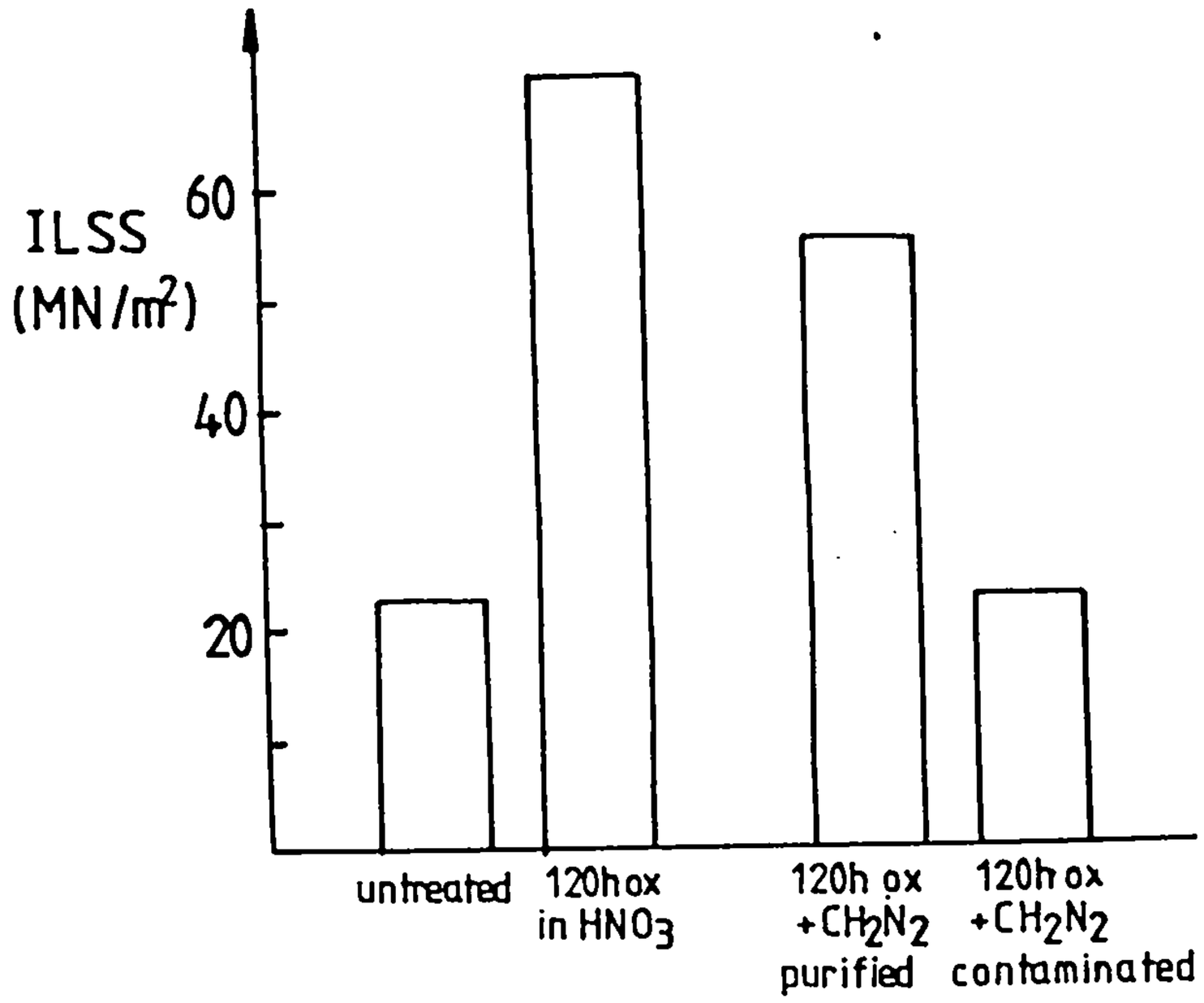

Fig. 2.11a Effects of Blocking Agents on ILSS

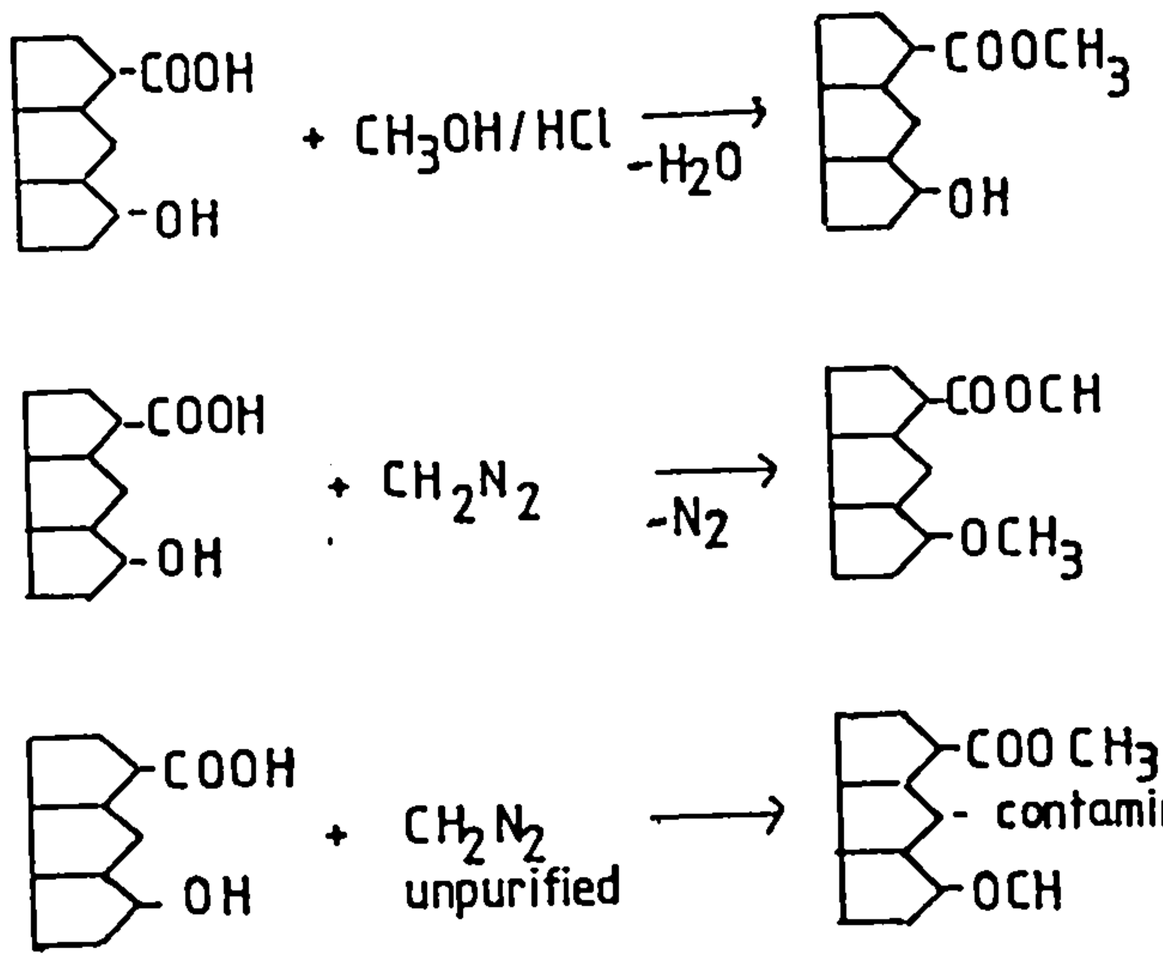

Fig. 2.11b Reactions of Blocking Agents

treatment times he proposed, could be attributed to the removal of contaminants or the reduction of protruberances which facilitate void formation. He suggests that fibre/resin bonding is primarily physical in nature.

The electrodeposition of polymers and co-polymers onto fibre surfaces has been found to increase the ILSS of composites (103). Significant improvements were found for a three copolymer system containing maleic anhydride (149). This functionality has a high affinity for bonding to epoxy resins and there is some indication that interlaminar shear strength may be related to the maleic anhydride level in the deposited polymer.

2.9 Summary.

Much research has been directed towards the nature of fibre resin interaction. The analysis of fibre surfaces by wet chemical techniques can lead to conflicting results. More recently, XPS has been used to examine fibre surfaces because it is essentially a non-destructive technique, and from chemical shift values new information about surface functionality has been obtained. Most XPS studies, unfortunately, have not fully exploited the uses of detailed analyses of spectra in order to obtain the maximum information about the sample surface.

There is still much debate concerning the nature of fibre/resin bonding as to whether it involves physical or chemical interactions, or both.

CHAPTER 3

X-RAY PHOTOELECTRON SPECTROSCOPY

3.1 Introduction

XPS experiments are based upon the properties of photoelectrons emitted from a sample on irradiation with X-rays. Most of these experiments have involved the precise measurement of the kinetic energy of these emitted electrons. The kinetic energy (KE) of an emitted electron is characteristic of both the electron energy level from which it originated and the energy of the incident radiation. Photoelectrons can be emitted from valence (those which take part in chemical bonding) and core energy levels (those which are generally not involved in chemical bonding). The photoelectrons emitted from core levels have kinetic energies which are characteristic of the atoms from which they originated. However, small changes in the detected binding energies (chemical shifts) do occur, and these changes depend on the chemical environment of these atoms. The analysis of chemical shift data provides valuable information concerning the chemical characteristics of the sample under investigation.

The majority of this work focusses on the chemical characterisation of fibre surfaces using XPS. This chapter explains the basic principles of the technique and outlines the information that can be obtained from detailed spectral analysis, especially with reference to carbon polymers.

3.2 The Photoelectric Effect

In 1887, Hertz (105) observed that if a spark gap was illuminated with ultraviolet light it could discharge more readily. Lenard, in 1899, built an apparatus for measuring the velocity of the electrons ejected from a metal sample when the sample was exposed to ultraviolet light. This phenomenon was explained by Einstein (106) in 1905, using quantum theory from which he derived the relationship

$$K.E.(\text{ejected electrons}) = h\nu - B.E. \qquad 3.1$$

where $h\nu$ is the energy of the incident radiation.

B.E. is the binding energy of the electron, ie. the energy of the electronic energy level from which the electron was ejected.

K.E. is the kinetic energy of the electron.

The ejection of electrons from a sample on its exposure to electromagnetic radiation is known as the photoelectric effect. Between 1913 and the 1930's, Robinson and Rawlinson tried to develop the idea of XPS, however, the poor resolution of electron spectrometers at the time prevented the extraction of most of the information contained in photoelectron spectra.

It was not until the late 1950s and early 1960s that experiments using high resolution electron spectrometers made it possible to obtain detailed information about the energy

distribution of electrons in the molecules of solids and gases (107,108). In 1964 Seigbahn (109,110) and his co-workers established a correlation between chemical oxidation state and electron binding energy shifts. Both soft X-ray photoelectron spectroscopy (XPS) and ultraviolet photoelectron spectroscopy are extensively used for the examination of solids, liquids (111,112) and gases (113,114). UPS only allows access to the valence electrons (those which take part in chemical bonding), whereas XPS is used for both valence and core electron energy levels. This work uses XPS as a tool for examining solid surfaces.

3.3 Photon Absorption

There are several different processes which can occur when a sample atom, A, is irradiated with X-rays of energy hν. These processes are shown in Fig.3.1. The emission of a photoelectron leaves behind a singly charged atom A. This excited, positively charged atom emits an X-ray of lower energy than the incident radiation hν, or ejects an Auger electron (115,116). Fig.3.2 shows the relative probabilities of X-ray emission and Auger electron emission in the decay of K(1s) holes in the lighter elements. From this graph, it can be seen that for lighter atoms Auger electron emission predominates. Normally, both Auger electron emission and X-ray fluorescence are very rapid processes and the core hole states are very short lived.

The energies of Auger electrons are solely dependent on the energy levels in the sample and not on the energy of the incident radiation. So, in order to distinguish between a photoelectron signal and an Auger electron signal, the energy of the radiation

source must be altered. This will result in a change in the kinetic energy of the photoelectron signal but not in that of the Auger electron.

3.4 The Photoelectron Spectrum

As stated previously, XPS essentially entails the irradiation of a sample by X-rays of energy hν. This results in the ejection of photoelectrons for which the kinetic energy can be measured. The number of electrons is plotted against their kinetic energy. This plot is known as the photoelectron spectrum. The main features of an X-ray photoelectron spectrum are signals due to core electrons and valence electrons. Other signals that may be present include Auger electron signals and signals due to satellites.

3.5 Binding Energy

X-rays incident on a sample give rise to photoelectron emission according to the basic equation as shown above (Eqn.3.1). This equation does not take into account the energy needed for an electron to escape from the surface of a material, ie. the work function of the sample. The work function of the sample is a combination of two effects; the surface dipole and the average internal electrostatic potential, the latter being a property of the bulk sample. Experimentally it is impossible to distinguish between the two. In the space between the source and the entrance slit to the spectrometer, there exists a small electric field, because grounding the source and the spectrometer material means that their Fermi levels are the same. This gives

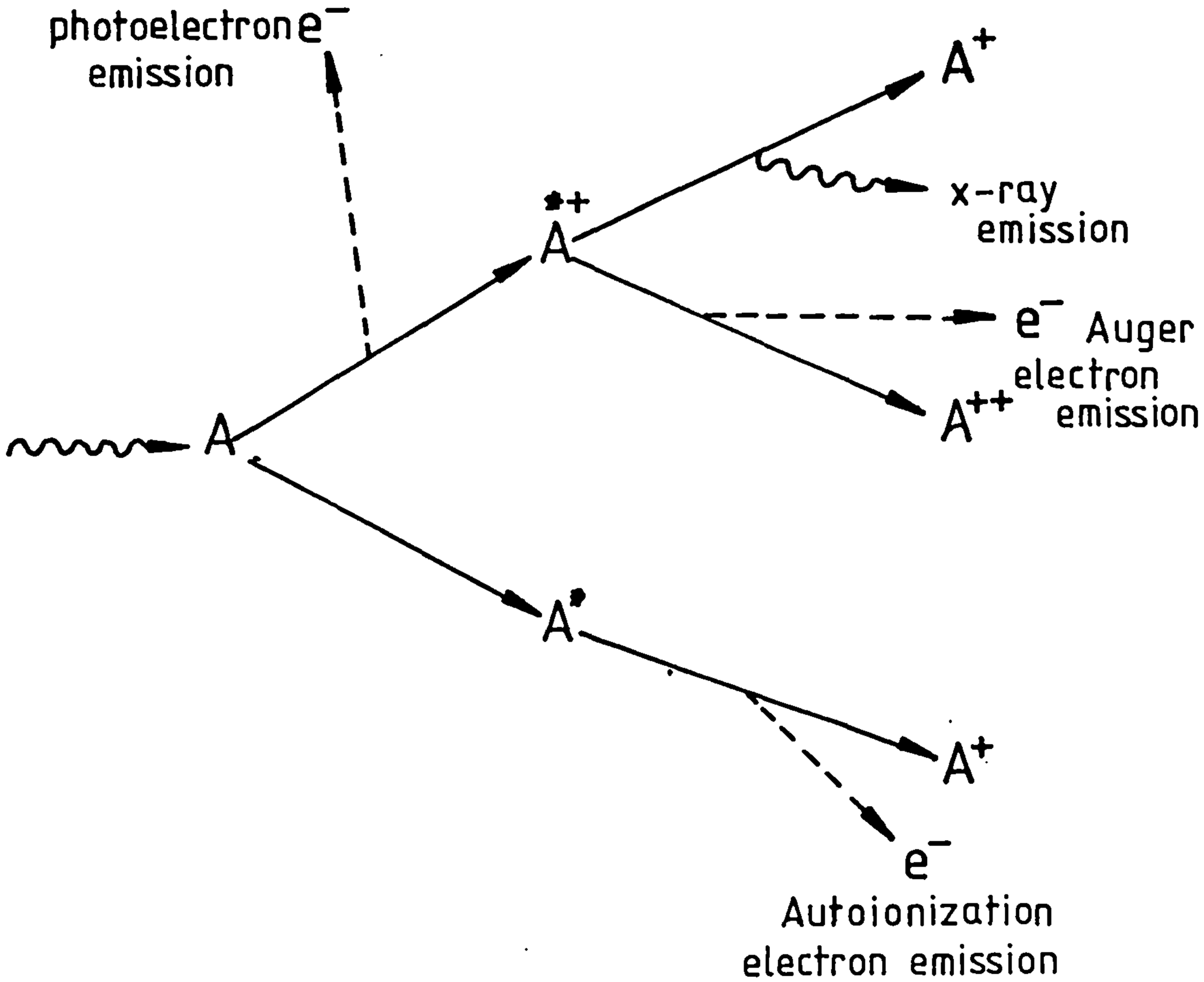

A - sample atom

A^* - excited sample atom

A^+ - a singly ionized sample atom

A^{++} - a doubly ionized sample atom

FIG. 3.1 Processes that can occur when a sample atom is irradiated with X-rays.

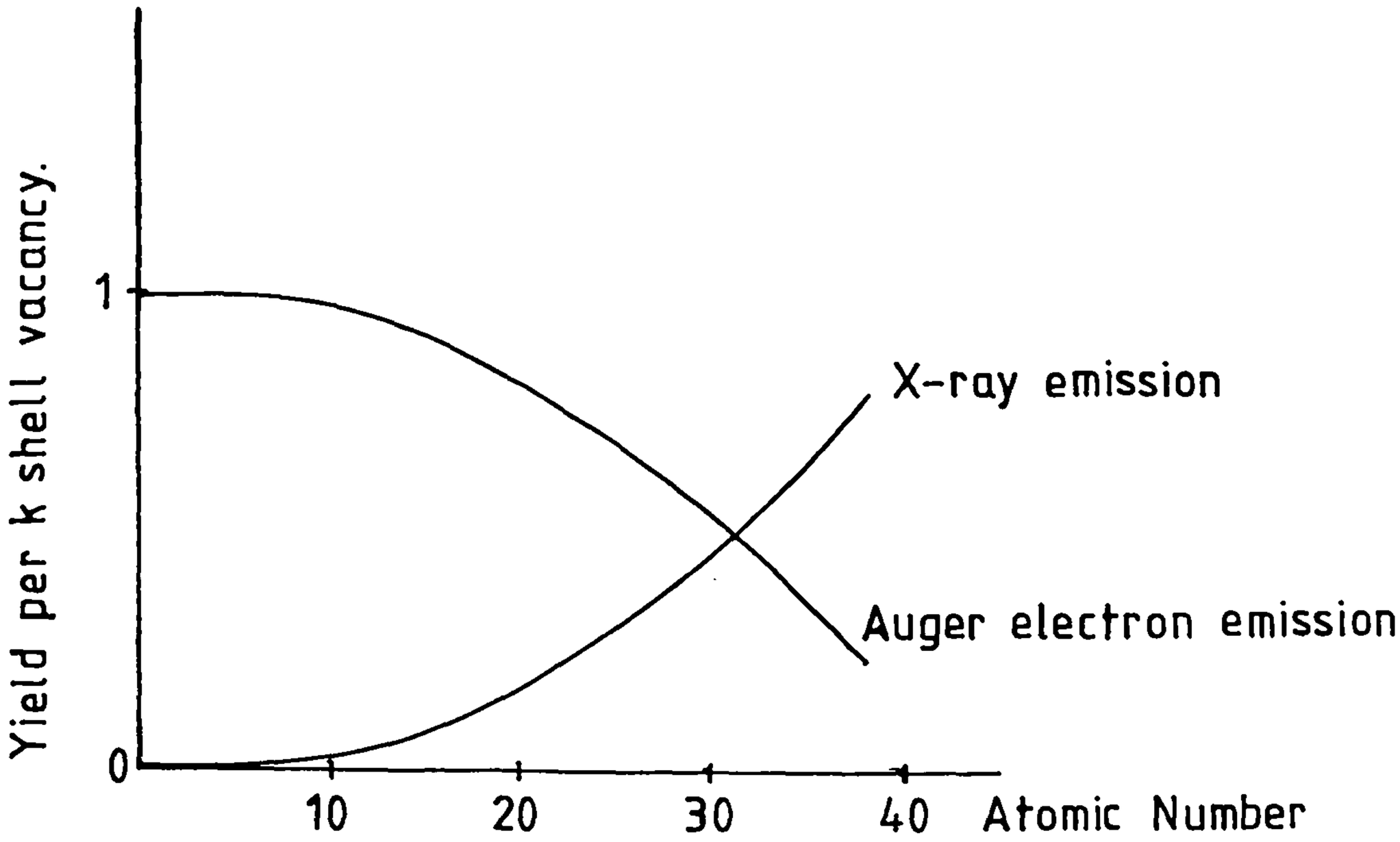

FIG.3.2 Relative probabilities for the emission of an Auger electron and an X-ray photon.

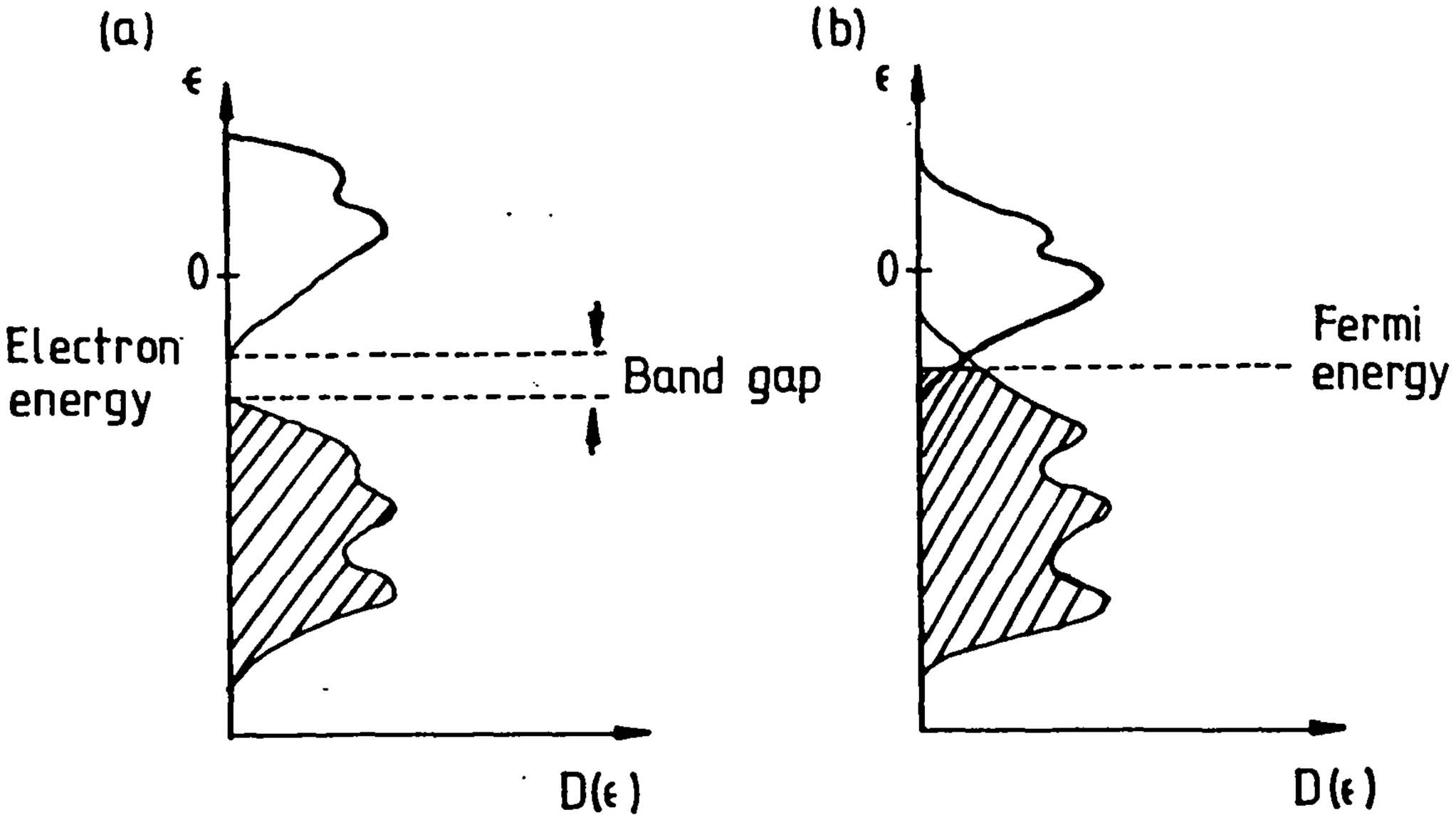

Fig.3.4. Density of states for (a) an insulator and (b) a metal.

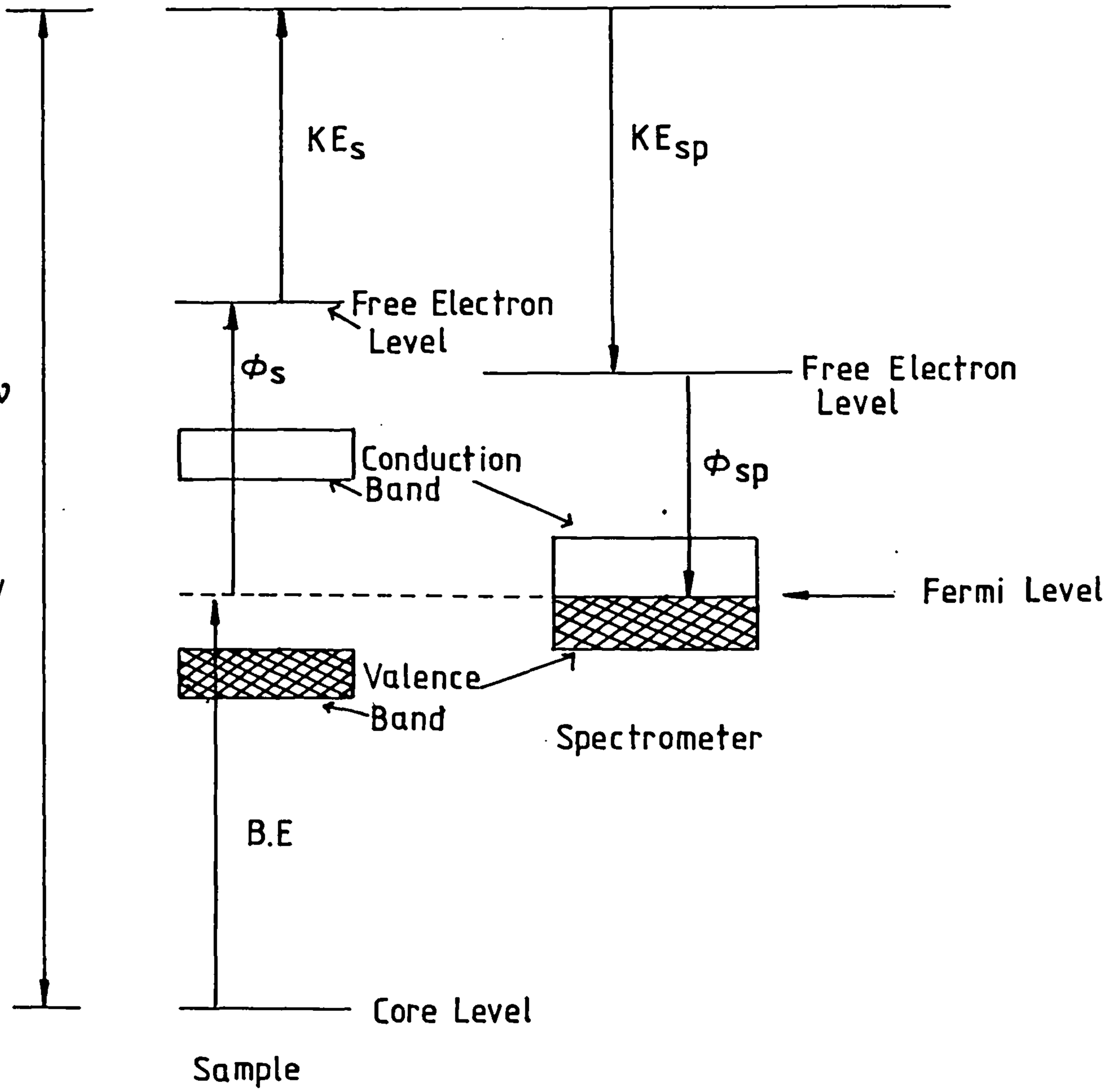

FIG.3.3 Energy Level Diagram for an Electrically Conducting Sample in Contact with the Spectrometer

rise to a contact potential if there is a difference in the work function of the source material and the spectrometer material. The above equation has to be modified to account for these two effects.

$$K.E. = h\nu - B.E. - (\Phi_{sp} - \Phi_{cpd}) \qquad 3.2$$

where Φ_{sp} is the work function of the sample,

Φ_{cpd} is the work function of the spectrometer,

B.E. is the binding energy with respect to the vacuum level.

If the binding energy is referenced to the Fermi level rather than the vacuum level, the above equation becomes

$$K.E. = h\nu - B.E._F - \Phi_{sp} \qquad 3.3$$

because

$$B.E._F = B.E._v + \Phi_{cpd} \qquad 3.4$$

This eliminates the need to experimentally determine the work function of the sample, which in practice is a very difficult task. The above equation applies to metals and other conductors. Fig.3.3 shows an energy level diagram for an electrically conducting sample in contact with the spectrometer.

For insulators, eg. powders and some polymers, where the electron transport through the sample is limited, the continuous loss of electrons causes a build up of positive charge, and the photoelectron signals tend towards lower kinetic energy. In calculating the binding energy for a particular photoelectron,

this charging has to be taken into account as follows

$$K.E = h\nu - B.E._F - \Phi_{sp} - S \qquad 3.5$$

where S is the sample charge.
Charging with particular reference to the KRATOS (AEI) ES 100, 200A and 200B spectrometers has been discussed by Povey et. al.(118).

Shifts due to charging are only a few eV, which is lower than expected, being countered somewhat by stray electrons in the sample chamber. Fig.3.4 shows the density of states for (a) an insulator and (b) a metal or conductor (117). In the case of an insulator, the conduction band and the fully occupied valence band are separated by a band gap, whereas in metals these bands overlap. The position of the Fermi level in metals is well defined as the uppermost occupied state, but for insulators this position is generally not known and the use of the Fermi level is somewhat arbitrary.

X-radiation (eg. MgKα X-rays) gives a photoelectron spectrum as a series of peaks which reflect the discrete binding energies of the electrons present in the solid. Discrete peaks occur at energies given by the above equations, which apply to photoemission processes that are elastic. (Inelastic processes will be discussed later in this chapter.)

3.6 Binding Energy Calibration

When a sample is introduced into the spectrometer, contamination can occur by the adsorption of residual gases,

especially if the instrument uses oil diffusion pumps. This contamination is in the form of saturated hydrocarbons, adsorbed water and gases, and the hydrocarbons can be used as a reference for the sample. The binding energy for the carbon 1s photoelectron for hydrocarbon is 284.6eV. It is assumed that the hydrocarbon will be subjected to the same static charge exhibited by the sample (which, of course, will be the same). Therefore calculation of the binding energy of the unknown photoelectron peak can be carried out as follows:-

$$B.E.(sample) = B.E.(ref.) + K.E.(ref) - K.E.(sample) \quad 3.6$$

Another calibrant which is commonly used is gold. This may be used in two different ways: the sample can be mounted in electrical contact with a gold plate, or a thin film of gold can be vaporised onto the sample surface. The Fermi level of the conducting sample and the gold will equilibrate. If the sample is non-conducting differential charging may result. This was not used for this work because the carbon contamination of the gold would greatly affect the carbon fibre carbon 1s spectrum and it would be extremely difficult to obtain any meaningful results.

3.7 The Interpretation of Photoelectron Spectra

The binding energy calculated from the photoelectron spectrum, using equation 3.5, is sometimes taken as the orbital energy from which the photoelectron originated. This assumes that when a core electron is emitted, the energies of all the other electrons in the atom remain constant during the ionization process. This is known as Koopman's Theorem (119) and can be

written as:-

$$E = -B.E \qquad 3.7$$

where E = orbital energy level, and

B.E.= binding energy of the photoelectron.

If Koopman's Theorem holds, the binding energy of an electron is the difference in energy between the vacuum level and the electron orbital energy. This is not the case.

When a photoelectron is ejected from a core level, the other electrons experience a greater effective nuclear charge and are drawn closer to the nucleus. This, in turn, gives greater shielding of the nuclear charge towards the photoelectron and results in a gain in kinetic energy (which equals the loss of potential energy of the remaining electrons). This is known as the relaxation energy.

Electron correlation energy is dependent on the number of electron pairs in the atom or ion. The ion produced after photoelectron emission has a smaller number of electron pairs and hence a smaller correlation energy. Relativistic effects may also be taken into account, especially for heavier atoms. Both correlation and relativistic contributions are usually very small.

3.8 Core Electron Signals

Core electrons do not play a major role in chemical bonding and their binding energies are specific to the particular atom

from which they originate. There are, nonetheless, small but measurable changes in their binding energies depending on the total chemical enviroment of the atom. These are due to a change in the electronic charge distribution in the valence shell which occurs when an atom changes its chemical environment from compound to compound. This affects all the core electrons and is revealed in the photoelectron spectrum. A small change in the binding energy is known as a chemical shift. These chemical shifts provide useful information about the surface functionality of a sample and are of particular interest to chemists.

The carbon 1s spectrum of benzadicarboxylic acid (see Fig.3.5) consists of two signals; one being due to the carbon atoms in the benzene ring, the other to the carbon atoms in the carboxyl group. Oxygen has an electronegativity considerably higher than the electronegativities of carbon and hydrogen so that there will be less negative charge within a certain atomic distance around the nucleus for a carboxylic group than for a carbon atom in a benzene ring. The electrons associated with carbon in the carboxyl group will experience a greater effective nuclear charge and therefore have a higher binding energy than those in the benzene ring. The chemical shift in this case is 4.0V.

Fig.3.6 shows the sulphur 2p spectra of sodium thiosulphate and sodium sulphate. There are two signals for $S_2O_3^{2-}$ ie. sulphur is present in two different chemical environments. The central atom has less valence electron density associated with it than the other sulphur atom, so any core electron would experience a greater effective nuclear charge. The binding

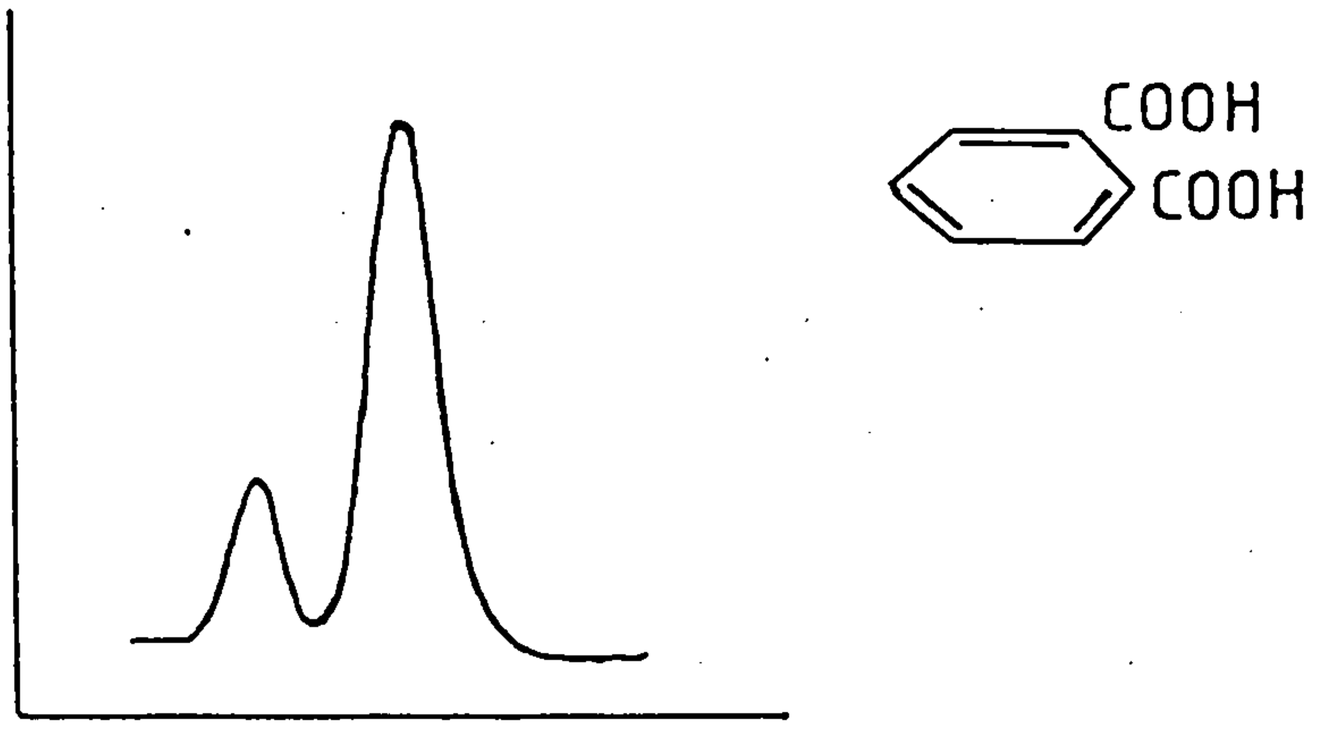

Fig.3.5 The C1s Spectrum of Benzadicarboxylic Acid

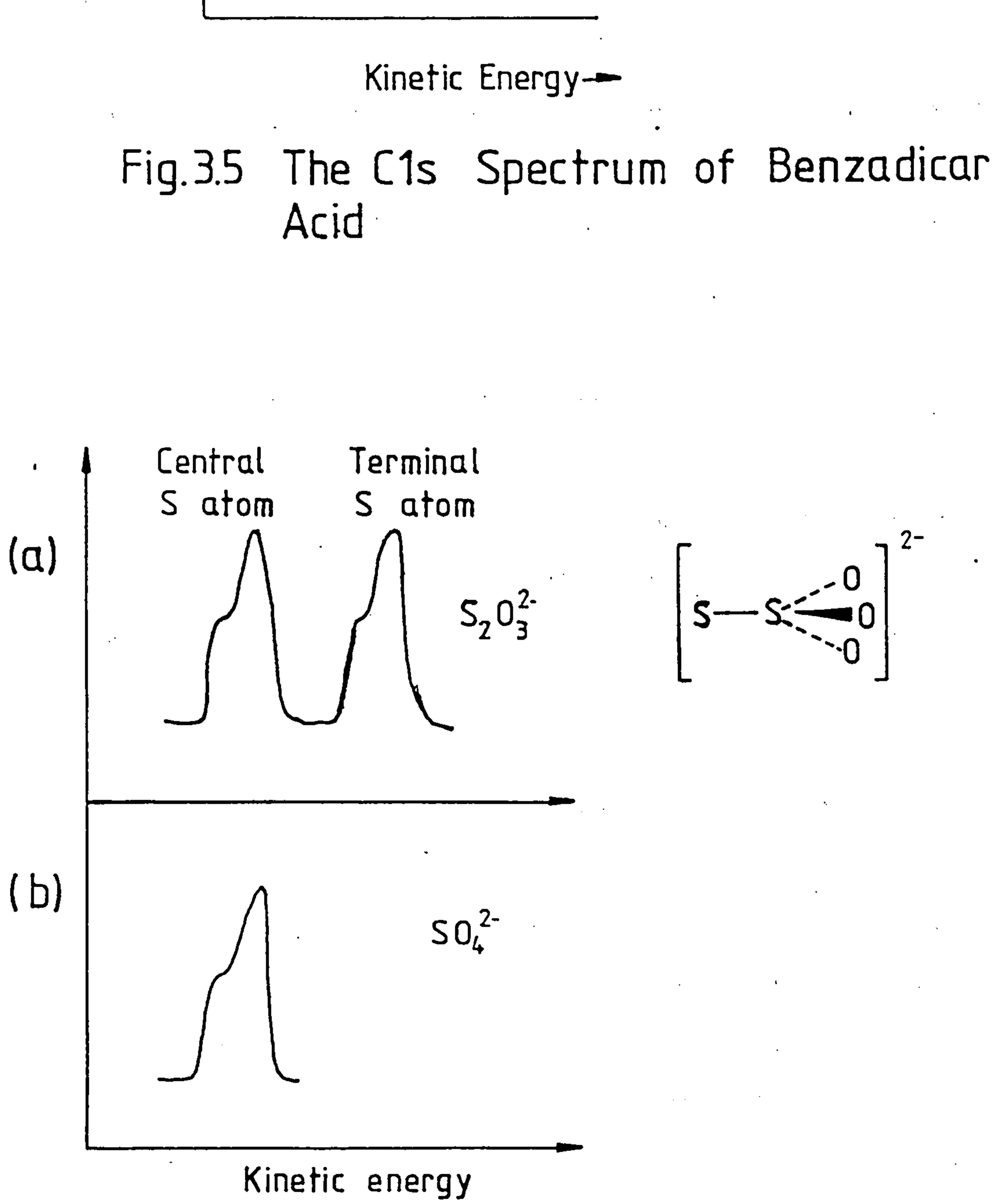

FIG.3.6 The S2p- spectra of sodium thiosulphate and sodium sulphate.

energy of this electron would be slightly greater, and hence the kinetic energy would be slightly less.

These simple explanations do not take into account effects due to the photoelectron emission process itself eg. relaxation effects. When a core electron is removed, the valence electrons will experience a greater effective nuclear charge and will be drawn towards the nucleus. This acts to shield the photoelectron from the nucleus and leads to the photoelectron gaining kinetic energy. Relaxation does depend upon chemical environment, having significantly different values for different compounds. In some cases this effect may be of a similar magnitude to the chemical shift.

3.8.1 Theoretical Calculations of Binding Energies

The binding energy of a photoelectron is the difference in energy of an atom before and after photoionization. It is therefore the difference between the initial(A) and the final(A^{+*}) states.

$$B.E. = E(final) - E(initial) \qquad 3.8$$

The most accurate method of determining this binding energy is provided by ab initio calculations of the total energies of the inital and final states. These types of calculations are ideal for atomic gases and other small systems (120,121,122), but for large molecules they entail unacceptable use of computer time.

There have also been many calculations solely involving the neutral atom, assuming Koopman's Theorem. The two most common methods are the Xα (and related methods) and CNDO (complete neglect of differential overlap) calculations. Both are carried out using computer programs which involve adjustable parameters that are determined by minimizing the total energy. Both these methods have been adapted to take into account relaxation energy. The merits of various calculations have been reviewed by Shirley (123). The model involving CNDO calculations works well for the core region (124) and will be described below.

3.8.1.1 The Ground State Potential Model (GPM)

This electrostatic model was developed by Siegbahn and his co-workers (125).

Consider the atom, from the core electron is ejected, as a hollow sphere with charge q_i which is equal to the charge on the nucleus (the number of protons) less the charge from the electrons. When an atom is on its own this charge will be zero, but any neighbouring atoms will affect the valence electrons of this atom. This gives rise to a slightly positive or negative charge on the atom itself. The potential energy inside this hollow sphere of radius r_i can be written as

$$\text{Potential energy} = q_i / r_i \qquad 3.9$$

Consider a surrounding atom as a point charge q_j a distance r_j from the sphere. The potential energy induced at the original atom will be

$$\text{Potential energy} = q_j / r_{ij} \qquad 3.10$$

The overall effect will be the sum of these terms. The potential effect of all other atoms has to be taken into account.

$$\text{Potential energy} = q_i / r_i + \sum_{i \neq j} (q_j / r_{ij}) \qquad 3.11$$

This equation will represent the difference in binding energy between an atom of charge zero and an atom of charge q_i in some chemical enviroment containing other atoms of charge q_j . For most purposes, this has to be referenced to a calibrant atom and the full equation is written as

$$E_a = k_a q_i + \sum_{i \neq j} (q_j / r_{ij}) + K \qquad 3.12$$

K is a constant which depends upon the reference level chosen, and k_a is a constant for the particular core level chosen.

The difference in electronic potential, V, between an atom of zero charge A and an atom in a particular chemical state A' has the same value as the difference in binding energy ie. chemical shift E .

$$E = BE(A) - BE(A') = V(A) - V(A') = -V \qquad 3.13$$

The electronic potential can be determined using CNDO calculations. The electron potential, V can be defined as

$$V = \text{Electronic charge} / r \qquad 3.14$$

3.8.1.2 Relaxation Potential Model

The inclusion of relaxation effects is carried out using the equivalent cores approximation. First the electronic potential for an appropriate cluster (which represents the atom and its surrounding neighbours, normally the next nearest neighbours) is calculated (giving V). Then the calculation is repeated replacing the atom concerned with an atom whose nuclear charge is increased by one and repeating the CNDO calculation to obtain V'. The relaxation energy is half the difference between V' and V (126) .

$$\text{Relaxation energy} = 0.5 (V' - V) \qquad 3.15$$

This leads to

$$V(\text{RPM}) = V (\text{GPM}) - \text{Relaxation Energy.} \qquad 3.16$$

The situation is far more complex for metals (127,128).

3.9 Spin Orbit Splitting

In Fig.3.6a the peaks corresponding to the three sulphur 2p signals exhibit shoulders on the higher binding energy side. This is due to spin orbit coupling. The total angular momentum of a single isolated electron is obtained by the vector summation of the indiviual electron spin, (s), and the angular momentum,

(l),

$$j = l + s \qquad 3.17$$

where l = 0,1,2,3 for s,p,d,f respectively

$$s = \pm 1/2$$

In the case of the sulphur 2p orbital j=1/2 and 3/2, and both signals are seen in the photoelectron spectrum. Their relative intensities are given by the ratio of their respective degeneracies, (2j+1). In this case it is 1:2. Table 3.1 shows the j values and their respective area ratios for different types of orbitals. The theory of spin orbit splitting has been discussed in detail, using a combination of wave mechanics and the theory of relativity, by Dirac (133).

3.10 Peak Shape

The peak shape for a photoelectron signal has a mixture of Gaussian and Lorentzian character. The Lorentzian character is imparted by the electron emission process, and the Gaussian character by the kinetic energy measurement process in the spectrometer. Solid samples will always produce inelastically scattered electrons which show up on the low-energy side of a photoelectron peak. Energy losses are usually spread over a very large range, resulting in an overall background in the photoelectron spectrum.

The signals from conductors, usually metals, exhibit a tailing towards higher binding energy. The reason for this has been explained by Mahan (129) and by Nozieres and de Dominics

TABLE 3.1 Spin orbit splitting parameters.

Orbital	j values	Area ratio
s	$\frac{1}{2}$	-
p	$\frac{1}{2}, \frac{3}{2}$	1:2
d	$\frac{3}{2}, \frac{5}{2}$	2:3
f	$\frac{5}{2}, \frac{7}{2}$	3:4

(130). Essentially, this tailing is caused by the interaction of the positive core hole formed as a result of the primary photoemission process with the conduction band electrons, and is known as conduction band interaction (CBI). The CBI is intrinsic to the photoelectron process and is not caused by extrinsic processes involving energy loss upon transport through the material. Doniach and Sunjic (131) calculated a line shape with a tailing towards higher binding energy, but to apply this to a carbon 1s spectrum of carbon fibres all the instrumental factors would have to be removed. Instead, Proctor and Sherwood (95) found a much simpler lineshape to account for both instrumental and conduction band effects. An exponential tail was found to be suitable for describing this asymmetric tail and will be used in this work.

3.11 Peak Width

The peak width is normally defined as the full width at half maximum (FWHM) in electron volts. This is dependent upon three factors:-

(a) the intrinsic width, determined by the uncertainty principle from the life time of the ion remaining after photoemission (Ag3d $t=10^{-14}$ s). The transition between the initial state and the final state may also contribute to this since it will involve the relaxation of the valence electrons. It can therefore be assumed that the intrinsic line width is dependent upon chemical environment.

(b) the width of the X-ray radiation. Mg Kα X-radiation has

a line width of 0.7-0.85eV. This can be greatly improved by using a monochromator on the incident radiation, although this greatly reduces the photoelectron intensity.

(c) the analyser resolution.

$$R = E / FWHM \qquad 3.18$$

where R= resolving power of the analyser.

E= energy of the photoelectrons.

The above equation implies that, if R is constant, the FWHM will increase with increasing photoelectron energy. Retardation of these electrons can increase the resolution.

3.12 Peak Intensity

The area under a particular photoelectron peak is proportional to the number of atoms of a given type present on the sample surface. Its intensity (I) is governed by many factors and is given by the following equation

$$I = I_o \alpha C K x \qquad 3.19$$

where I_o = the intensity of the incident radiation,

α= photoelectric cross section,

K = instrument factor (dependent upon instrument design),

x = thickness of the sample,

C = concentration of molecules.

The photoelectric cross section is defined as the transition probability per unit time for exciting a photoelectron from a subshell with a photon flux of given energy. k is dependent on

instrument design and if the electrons are retarded, it is also slightly dependent on their kinetic energy. It may be considered constant for electrons emitted with comparable kinetic energy.

This equation assumes that no collisions occur before the electron enters the spectrometer. But, in reality, there are many atoms and molecules present in the sample and collisions must occur. Electrons which originate from a greater depth in the solid undergo an increasing number of collisions and some do not escape from the surface (see Fig.3.7). This loss of electrons is accounted for by an attenuation factor (σ). This loss depends upon the electron kinetic energy and the nature of the material. This is an exponential loss and is defined as $e^{-\sigma x}$, where x is the depth in the material from which the electron travels. The escape depth can be written as

$$\lambda = 1 / \sigma \qquad 3.20$$

Practically no electrons are seen from a depth greater than 3λ. The above equation must be modified to allow for collisions between photoelectrons and atoms. For a homogeneous solid with a mean escape depth,λ, of the photoelectrons (if elastic scattering is neglected) the intensity expression becomes:

$$I = I_o \alpha D k \lambda \ (1-e^{-x/\lambda}) \qquad 3.21$$

where D is the density of the atoms under investigation and

α is the total probability of ionizing a sample atom with a photon of given energy.

This leads to an expression for determining the thickness of very thin films on the sample surface

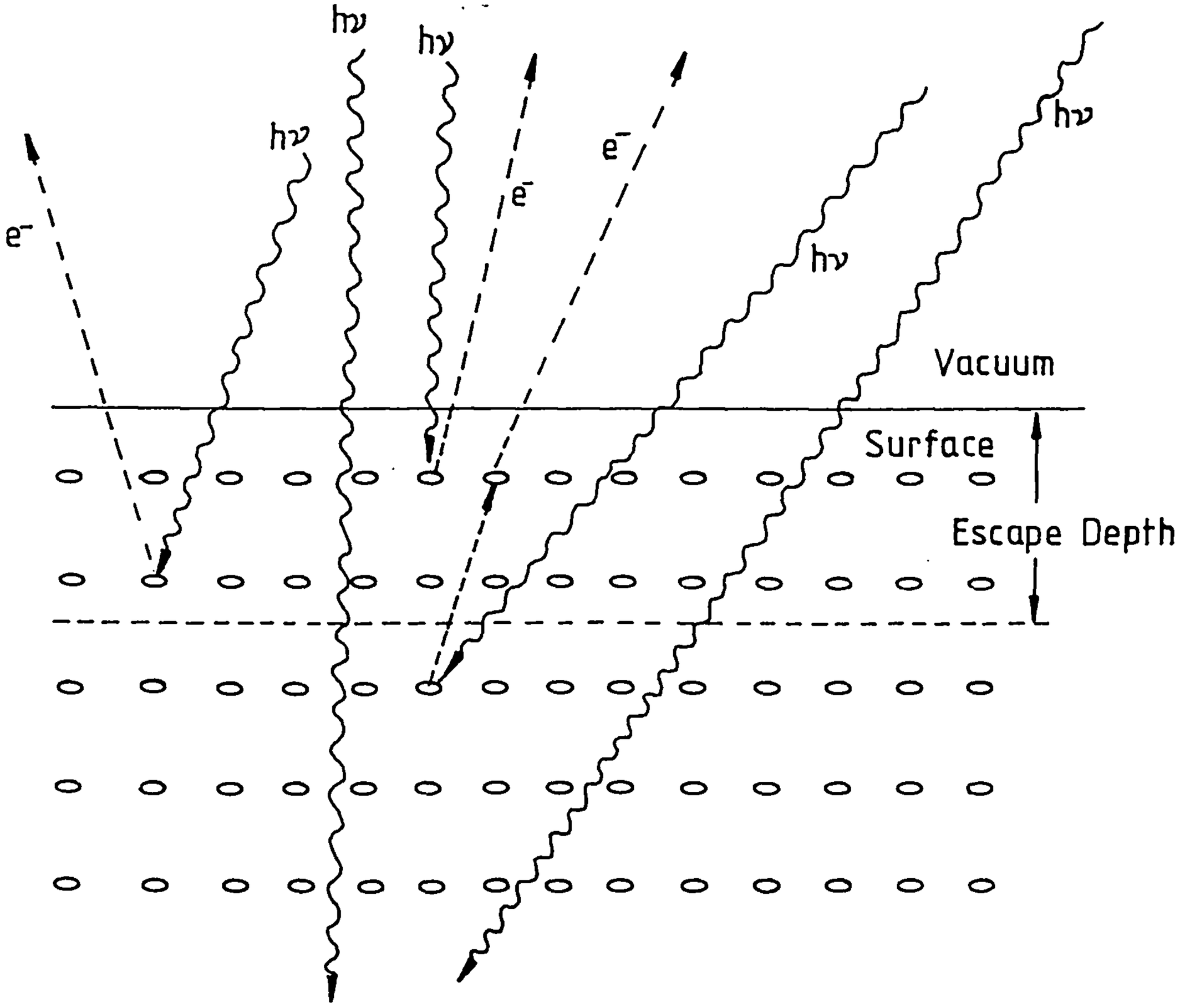

Fig.3.7 Escape Depth of Photoelectrons

$$K \frac{I_{ox}}{I_m} = x\sigma_{ox} \qquad 3.22$$

where K is the intensity of the two pure materials, and

x is the thickness of the oxide layer

This mean escape depth is markedly dependent upon the kinetic energy of the photoelectron.The photoelectron spectrum of a lower binding energy orbital will be more representative of layers deeper into the solid.

Full quantitative analysis of solid surfaces by means of XPS is difficult due to many factors, for example pitting caused by surface treatment greatly complicates accurate determination of surface concentration.

3.13 Valence Electron Levels

The photoelectrons from these valence levels have binding energies between 0 and 20eV. These valence electrons are involved in delocalised or bonding orbitals. A spectrum of this region consists of many overlapping peaks, which closely reflects the initial density of states.

3.14 Satellites

All other peaks present in a photoelectron spectrum are termed satellites. They arise for the reasons indicated below.

3.14.1 X-ray Satellites

Fig.3.8 shows the unmonochromatised X-radiation from a magnesium target. It shows that the most X-radiation is the K_α doublet. This arises from the electron transition 2p to 1s. Additional X-ray peaks, known as satellites, are associated with each of the main (eg.K_α) peaks. Table 3.2 (134) shows the observed line positions and intensities.

The continuous region gives rise to photoelectrons which contribute to the general background (known as Bremsstrahlug radiation). Problems can arise when interpreting core level spectra if a photoelectron peak excited by this radiation overlaps the photoelectron peak excited by the main (K_α) X-radiation. Such a peak is called an X-ray satellite.

Small signals can arise from secondary electrons hitting the aluminium window leading to the production of aluminium K_α X-radiation. These 'ghost' peaks are at 233.0eV to higher kinetic energy of those excited by Mg K_α. Old or damaged targets can give rise to Cu L_α radiation, these appear at 233.9eV to the lower kinetic energy of Mg K_α .

3.14.2 Multiplet Splitting

The ejection of a core electron from a paramagnetic species, ie. one with unpaired electrons in the valence band, produces a further unpaired electron. If the unpaired core electron spin is parallel to that of the unpaired valence electron, then exchange interaction can occur, resulting in a lower energy than for the

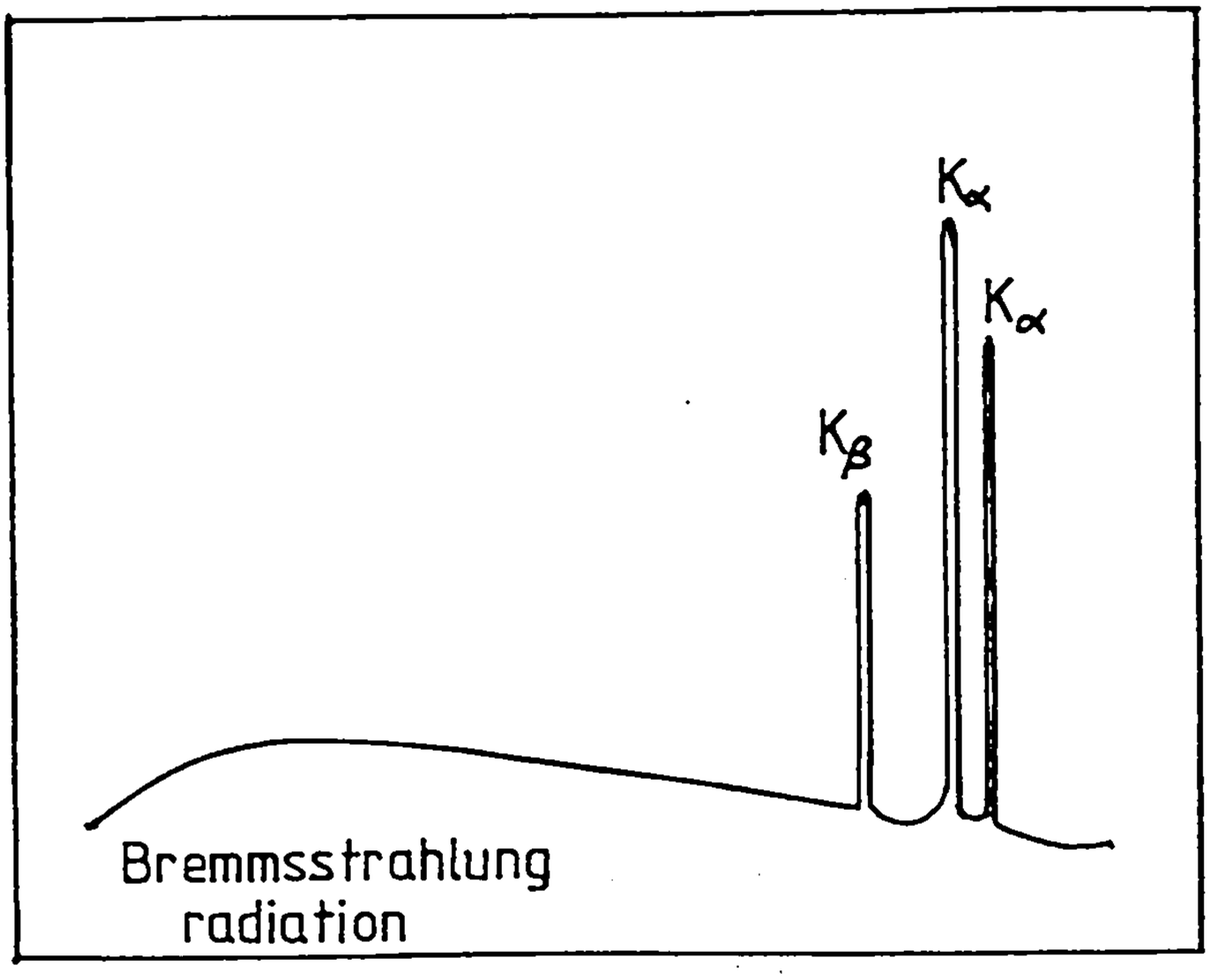

FIG. 3.8 Unchromatised X-radiation from a magnesium target.

TABLE 3.2 High energy satellite lines for Mg.

X-ray line	Separation from $K_{\alpha_1\alpha_2}$ (eV) and Relative intensity ($K_{\alpha_1\alpha_2}=100$)
K	4·5 (1·0)
K_{α_3}	8·4 (9·2)
K_{α_4}	10·0 (5·1)
K_{α_5}	17·3 (0·8)
K_{α_6}	20·0 (0·5)
K_β	48·0 (2·0)

case of an anti-parallel spin. The core level in the case of an s level will appear as a doublet corresponding to the two possible spin states for the unpaired core electron. Examples of multiplet splitting are the 4s levels of rare earths (unpaired 4f levels), spectra of organic radicals, and the 1s level of molecular oxygen.

3.14.3 Shake-up and Shake-off Satellites

Core electrons almost completely screen the valence electrons from the nucleus. Core electron removal is accompanied by reorganisation of the valence electrons in response to an increase in the effective nuclear charge. This reorganisation can give rise to the excitation of a valence electron. This electron can either be completely ejected from the atom (shake-off), or moved to an unoccupied level (shake-up). These processes give rise to signals to the low kinetic energy side of the main photoelectron peak and are sometimes called configuration interaction satellites. The processes are outlined in Fig.3.9.

3.14.4 Plasmon Loss Features

An electron is said to have suffered a plasmon loss when it has given up energy equal to the characteristic energies for an oscillation of the conduction band. These oscillations have frequencies characteristic of the solid material ω. There are two types of processes by which oscillations can occur (134,135):

(a) an intrinsic process resulting from the coupling of the

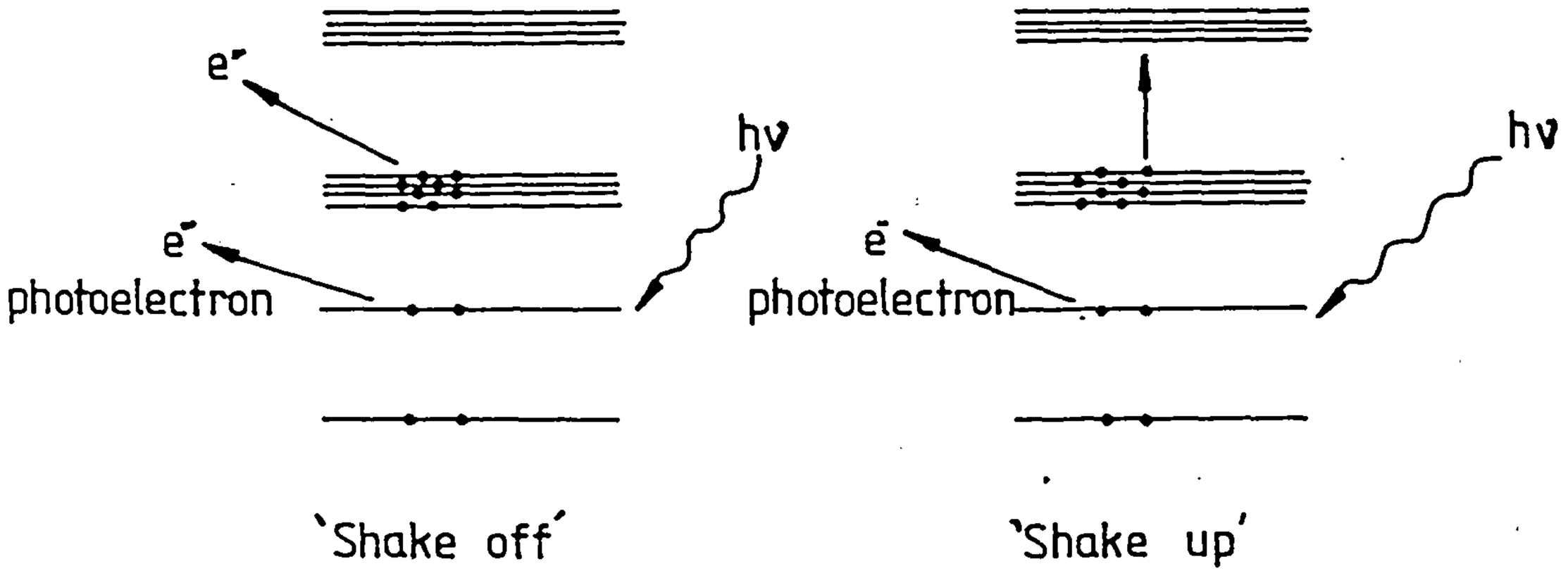

Fig.3.9 Shake off and shake up satellites.

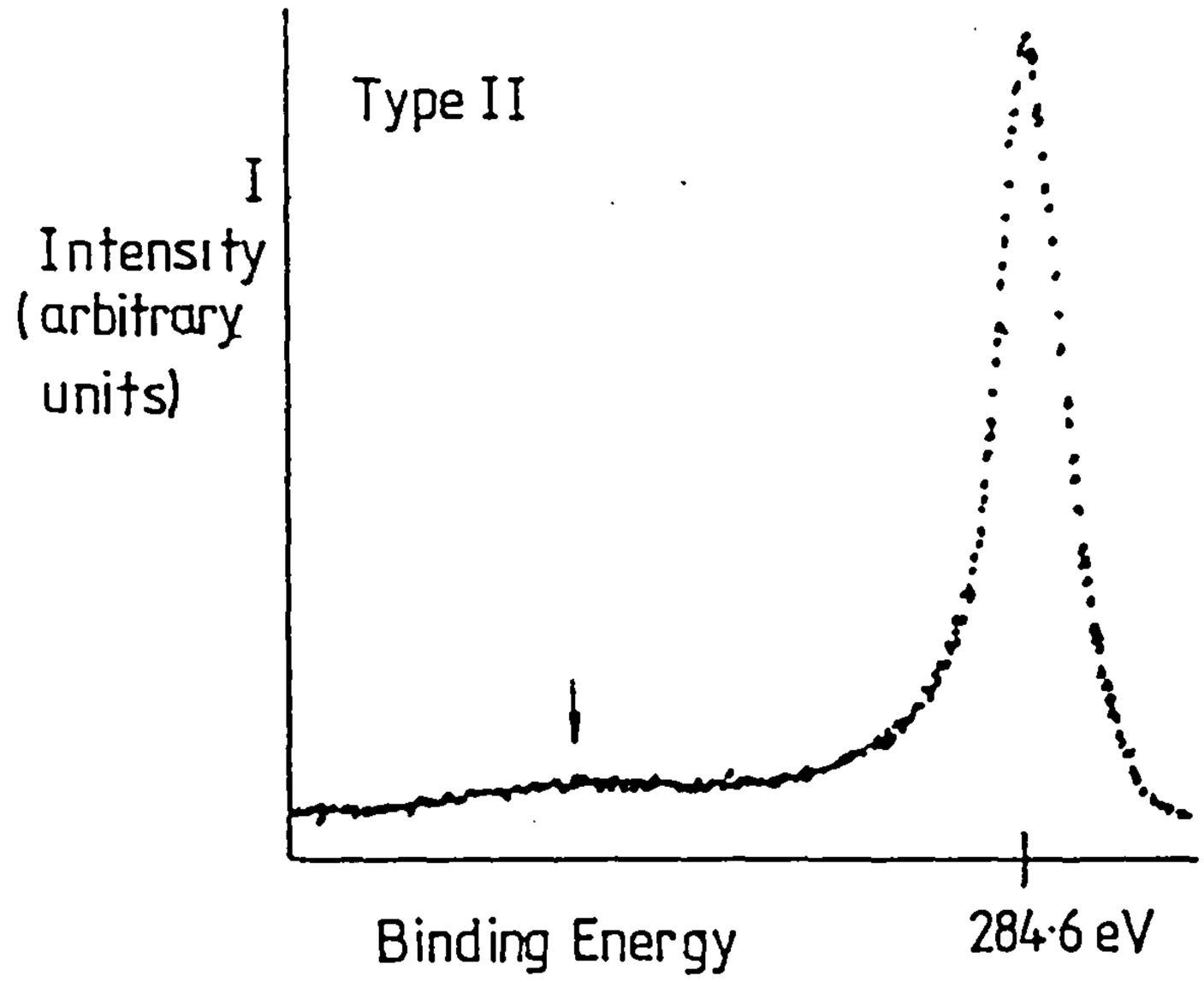

Fig.3.10 C 1s Spectrum of Untreated Fibres.

core hole to collective oscillations of the valence electrons, or

(b) an extrinsic process, where an electron passing through a solid can couple with electron density fluctuations.

The extrinsic processes can be further classified as being representative of either the surface or the bulk of the solid. Within the solid, the loss is said to be a 'bulk' plasmon and have an energy $h\nu$. Electrons that have suffered a plasmon loss can undergo several further plasmon losses. This results in a series of signals with the same separation ,$h\nu$, but with decreasing intensity (136,137). At the surface of a solid a localised oscillation can occur with a different frequency to that of the bulk conduction band. This gives rise to surface plasmons.

It very much depends upon the nature of the conductor and the cleanliness of the sample surface whether or not plasmon loss features are discernable. Although there is some direct evidence for the existence of intrinsic plasmons for sodium (138), it is widely held that extrinsic plasmon loss is the main contribution to the overall observed energy loss features in the XPS of simple metals (139).

3.15 The Main Features of the Carbon 1s Spectrum of Carbon Fibres.

Fig.3.10 shows the carbon 1s spectrum of untreated type II fibres. The main peak exhibits an asymmetric tailing towards higher binding energy similar to that observed for graphite (139)

and metals. This is due to conduction band interaction (see section 3.10).

The arrow indicates a plasmon feature at 7eV from the main peak (87,95,96). This is similar to that observed on graphite (141,142,143,144). Bradshaw (142), on the basis of results obtained from graphite using soft x-ray potential spectroscopy, photon induced Auger and XPS, suggests that this is an intrinsic plasmon. His results are confirmed by Brenig et al (143). Houston (145), using soft xray appearance potential (SXAPS), commented that Bradshaws results are a result of band structure variations and showed negligible plasmon effects. Proctor and Sherwood (87) suggest that the plasmon is a result of an extrinsic process because upon heating the fibres to 1400^{o}C its intensity increases, while the surface oxygen concentration decreases and so the plasmon intensity is dependent upon the nature of the surface itself.

3.16 Conclusions

The most valuable information that can be obtained from XPS is that of chemical shifts. This allows the chemical characterisation of carbon fibre surfaces. Although full quantitative analysis cannot be achieved, valuable information can be obtained from relative intensity ratios of chemically shifted species. This technique is one of the most useful methods for examining surfaces, but complimentary information from other techniques is always desirable.

CHAPTER 4

EXPERIMENTATION

4.1 Introduction

The aim of this work is to characterise the physical and chemical nature of the carbon fibre surface before and after surface treatment. It was essential to use several different techniques to obtain complimentary and reliable results.

Surface treatment was carried out electrochemically. Electrochemical oxidation provides easily controllable and readily reproducible conditions, and allows many parameters to be kept constant throughout a series of experiments. Treatments can be carried out on a small (in the laboratory) or large scale (in industry). Two types of cell were used. One was a standard three electrode glass cell; the other, a pilot-plant cell for use with a continuous tow of fibres. The fibres treated in the pilot plant were collected and incorporated into resin composites.

The chemical nature of the surface was examined by X-ray photoelectron spectroscopy and in some cases Fourier transform infra-red spectroscopy. The physical nature of the surface was studied by electron microscopy.

4.2 Electrochemistry

4.2.1 Laboratory Equipment and Procedure

The electrochemistry was carried out using a standard three electrode glass cell (Fig.4.1). A bundle of carbon fibres (ca.3000 filaments) acted as a working electrode and a piece of platinum foil as the counter electrode. A reference electrode was placed as close as possible to the working electrode by means of a Luggin capillary. A saturated calomel electrode was used for acid and salt electrolytes, whereas a mercury/mercury oxide electrode was used for basic electrolytes.

All solutions used triply distilled water and AristaR chemicals (or AnalaR if the AristaR grade was not available). These solutions were thoroughly de-aerated prior to use. The fibres were immersed and removed from solution whilst still in circuit. They were then washed thoroughly in triply distilled water and dried in an oven at 100^{o}C for 30 minutes. All sample transfers were made in air.

The samples for XPS analysis were prepared by polarising the fibres to various potentials for a fixed time. The polarisation was carried out using either a precision MINISTAT potentiostat, or a Chemical Electronics Type 2B potentiostat. The former was connected to a PRECISION 16BIT ramp generator for cyclic voltammetery studies; the latter to a custom built function generator.

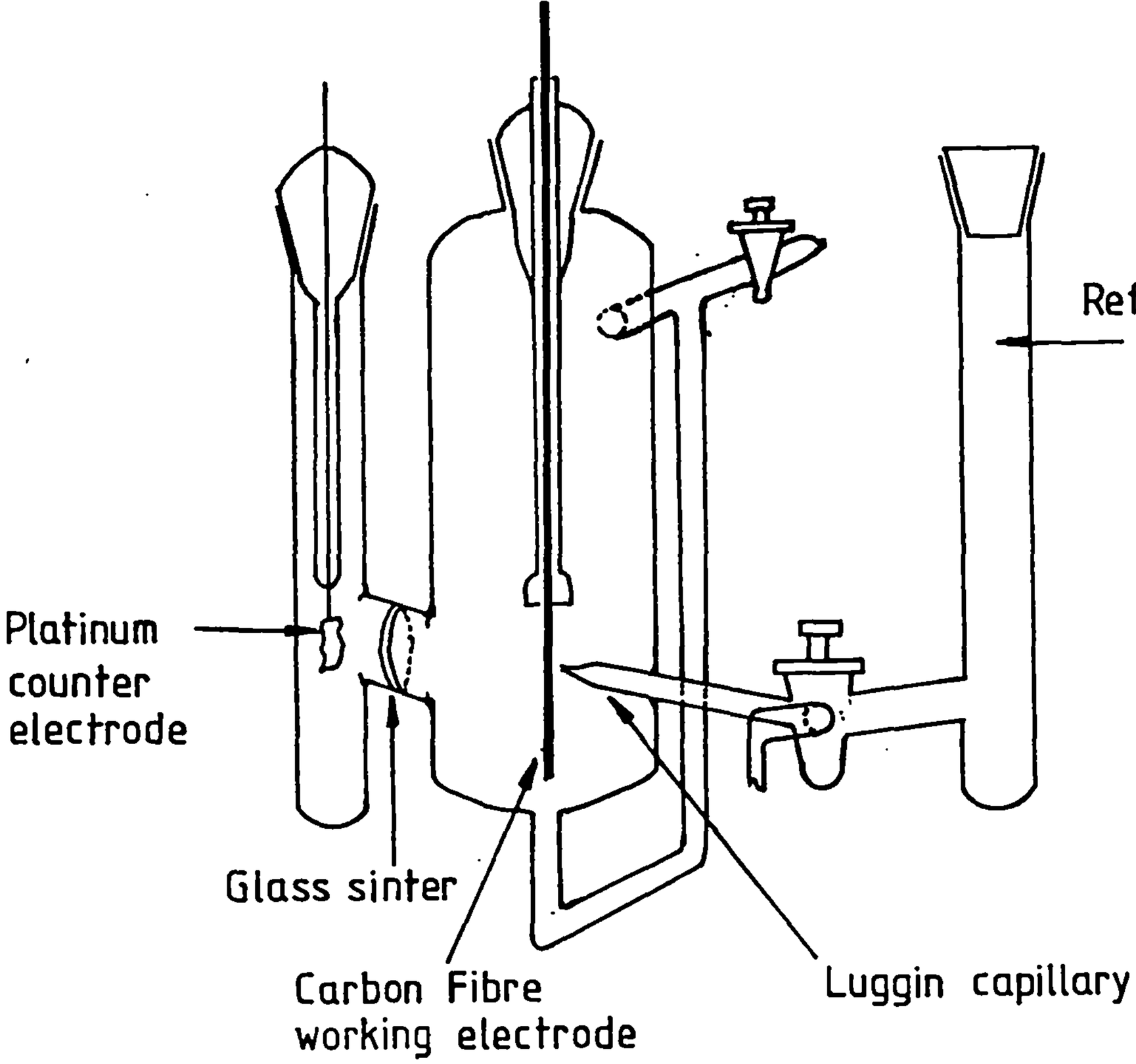

Fig.4.1 Standard 3-Electrode Glass Cell

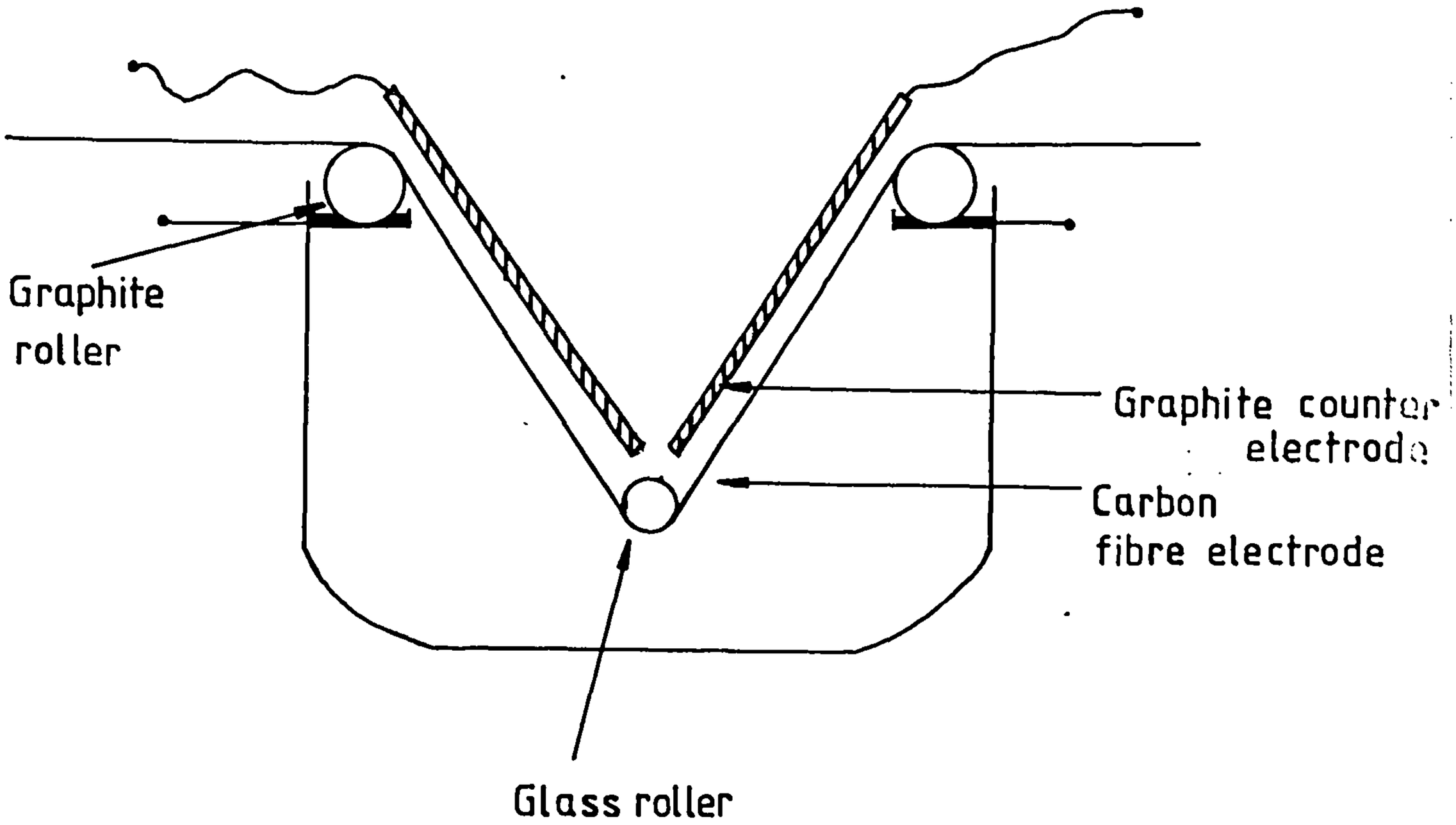

Fig.4.3 'Industrial'-type Cell

4.2.2 Semi-Industrial Procedure

For composites to be made it was necessary to treat large amounts of carbon fibres, ~7grams, to make a 1 by 0.2 by 8cm composite bar. A pilot plant was built and is shown in Fig.4.2. The cell (Fig.4.3) consisted of a tow of fibres acting as the working electrode and two graphite plates as the counter electrode. For some treatments the cell current was kept constant by means of a power supply (galvanostat). For constant potential treatments, a reference electrode was placed as close as possible by means of a Luggin capillary. The potential was controlled using a potentiostat.

All solutions were made with distilled water and AnalaR grade chemicals.

4.3 Composite Production

Fibre/resin composites were made in the following way:

A mould (Fig.4.4) was treated with ROCOL(PTFE) release agent and preheated to 60°C. A resin mixture was prepared, consisting of Shell Epikote 828(2,2-diphenyl propane-p, p'diglycidine ether), 100 parts by weight; methyl nadic anhydride, 90 parts by weight; and Shell Epikure K618, 4 parts by weight, and warmed to 60°C. Thirty lengths of treated carbon fibre was impregnated by placing in the resin mix for 5 minutes at 60°C. The bundle of tows were then removed; the excess resin drained off and the bundle of tows placed in the mould which was clamped in position with 2mm spacers . The bar

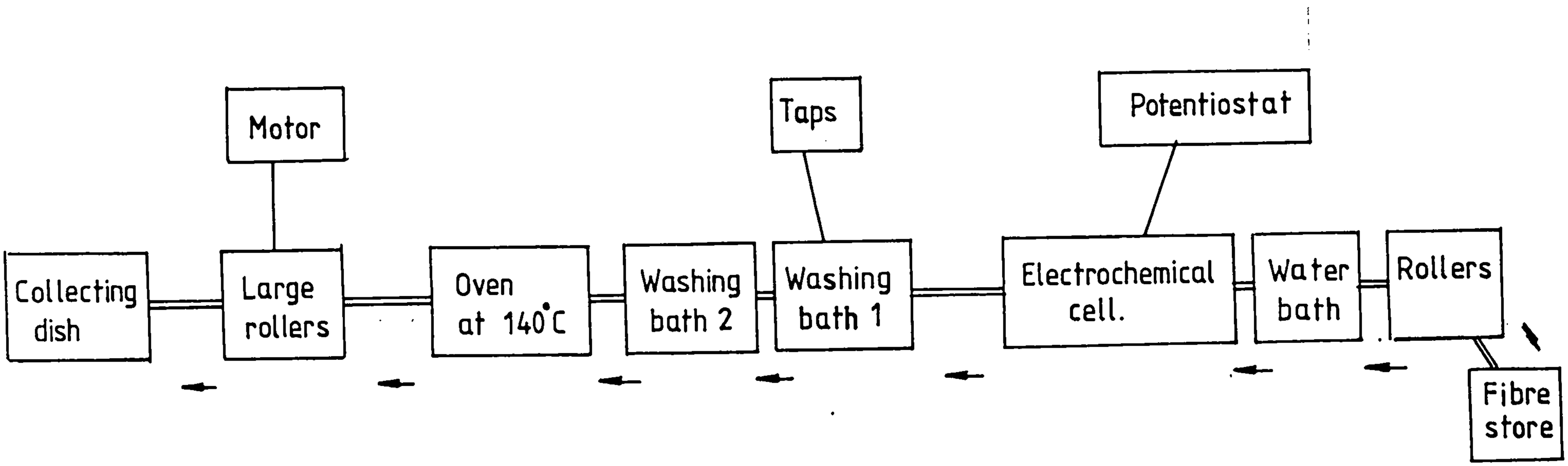

FIG.4.2 PILOT PLANT

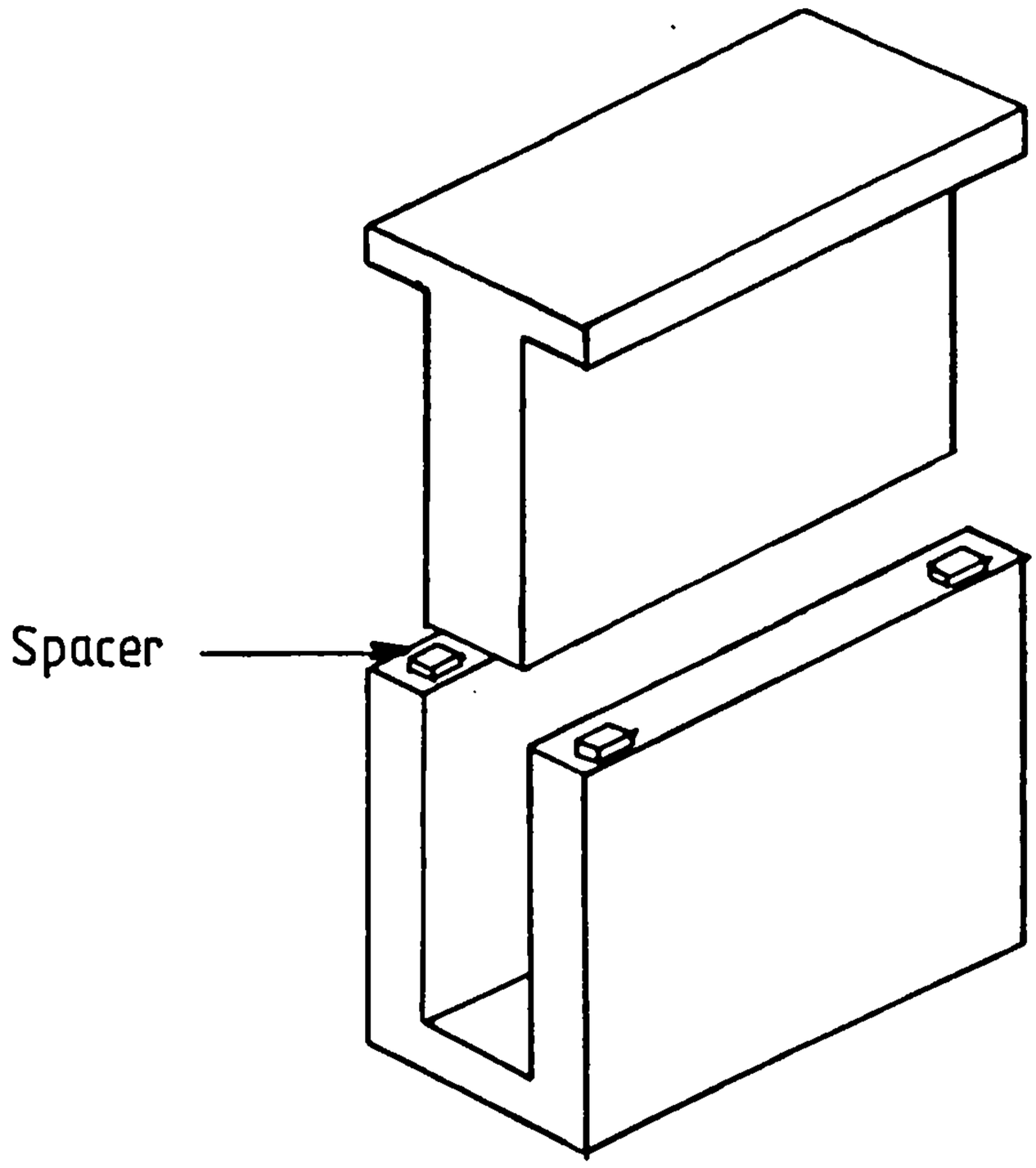

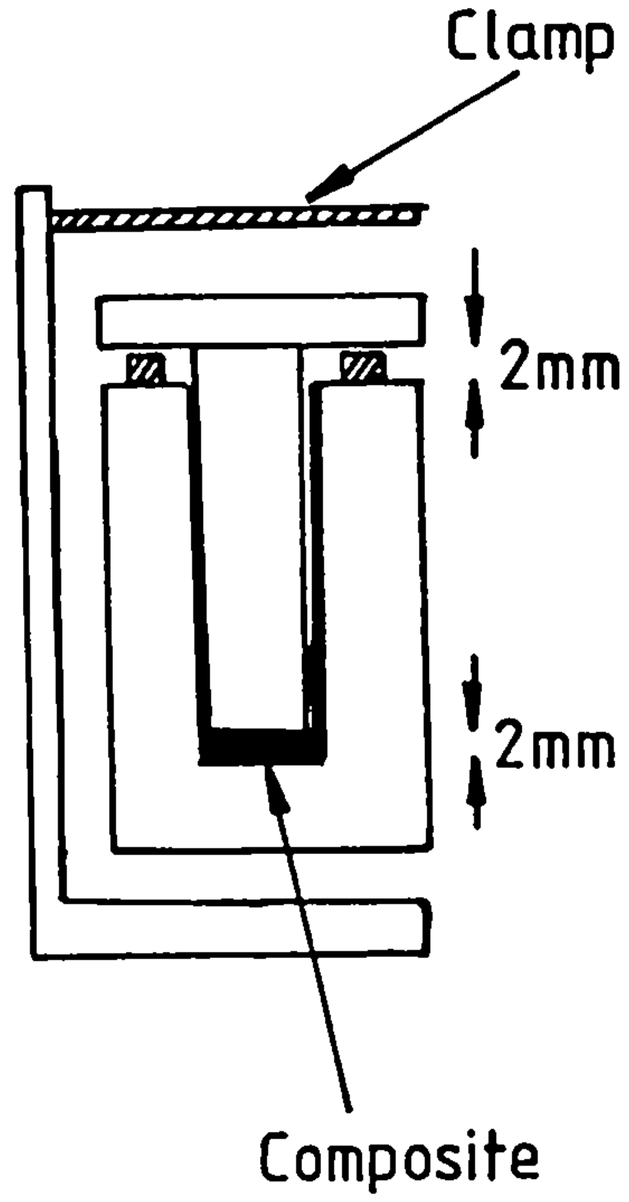

FIG.4.4 Mould used for composite production.

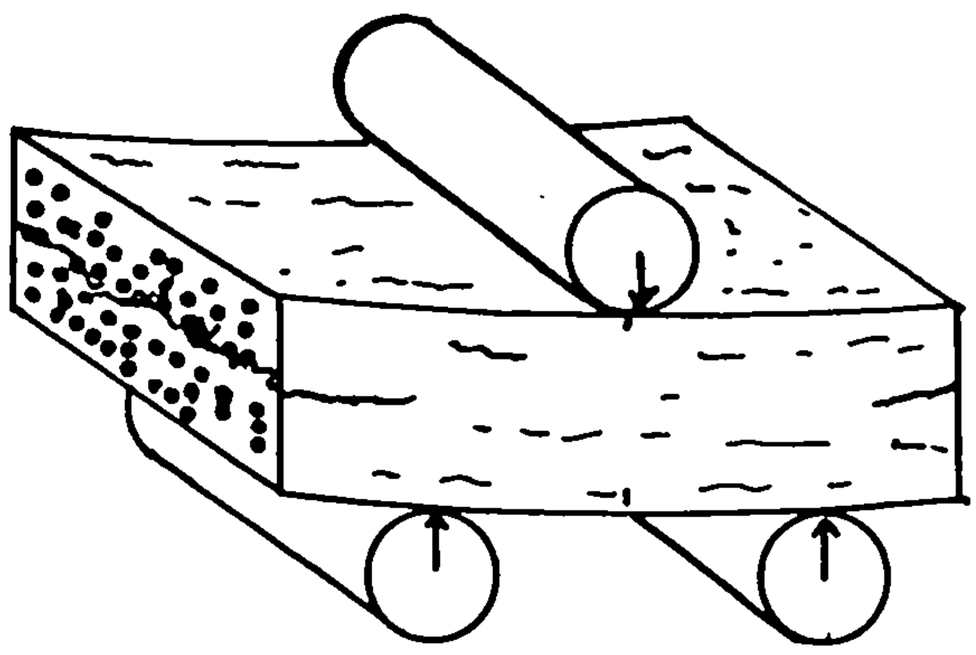

FIG.4.5 Short beam shear test configuration.

was then cured at 120°C for 2 hours and post cured at 180° C for 16 hours. The mould was allowed to cool; the bar removed, and the edges and ends trimmed. The bar was weighed and its dimensions measured. It was then cut into eight specimens (1cm in length) for interlaminar shear testing.

4.4 Interlaminar Shear Strength Test

The ILSS was measured by using a short beam shear test. The configuration is shown in Fig.4.5. Only unilaminates can be used for this test. The load was applied and measured with an Instron testing machine.

4.5 The Spectrometer and Spectral Collection

The spectrometer used was an AEI(KRATOS) ES200B. The main features of an X-ray photoelectron spectrometer are shown in Fig.4.6. X-rays are produced by the bombardment of electrons on to a magnesium target from a tungsten filament. The filament current used was 20mA with a high voltage of 12kV. The X-rays pass through a thin aluminium window into the sample chamber to filter out any stray electrons present in the gun chamber before sample irradiation takes place. The pressure inside the sample chamber was 10^{-8} to 10^{-9} Torr. The sample was introduced into the spectrometer via an insertion lock.

In order to determine the kinetic energy of the photoelectrons they are directed through an electrostatic analyser. This type of analyser uses an electrostatic field between two concentric spherical domes. The photoelectrons are

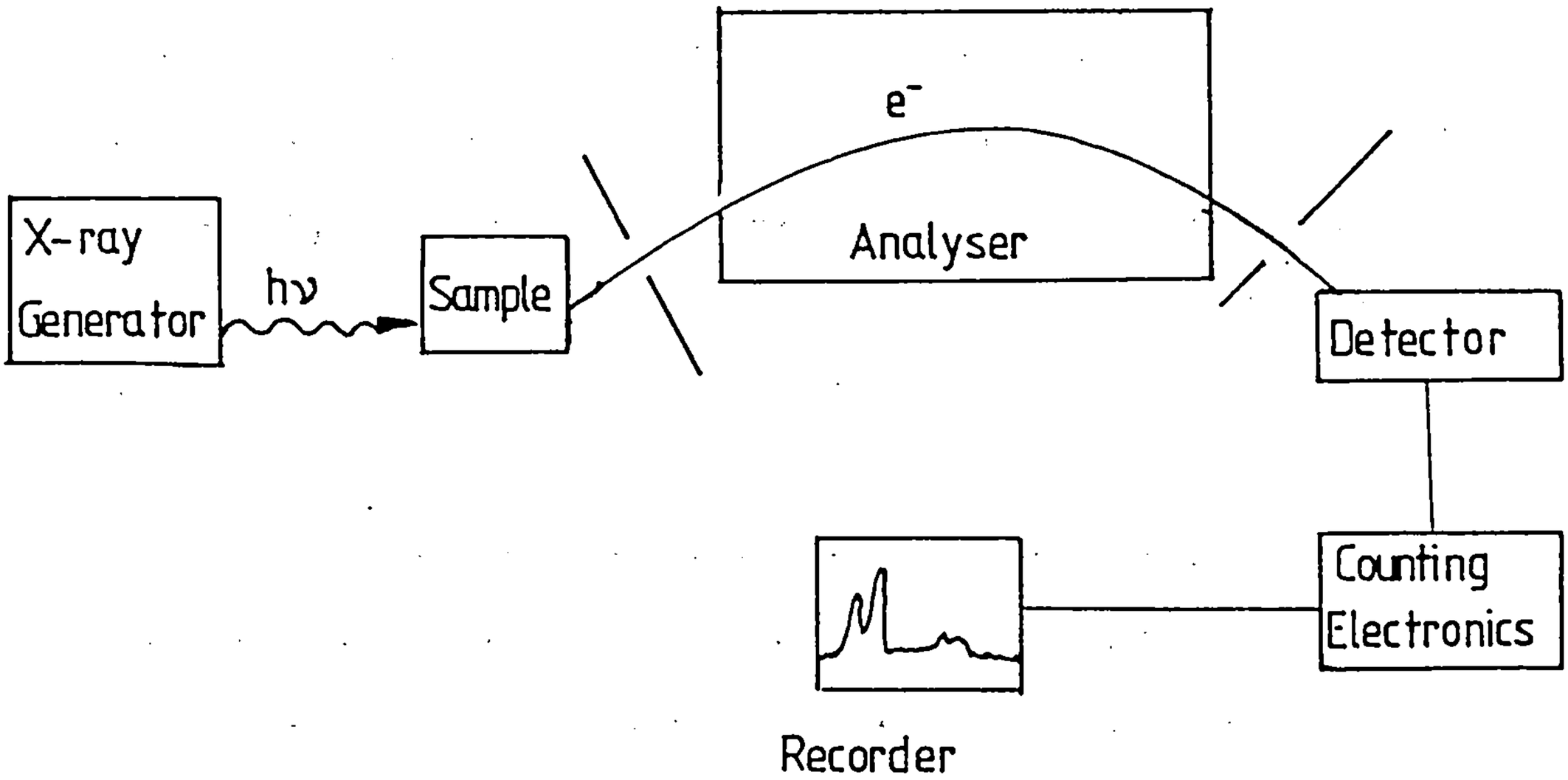

Fig. 4.6 Basic Features of X-ray Photoelectron Spectrometer

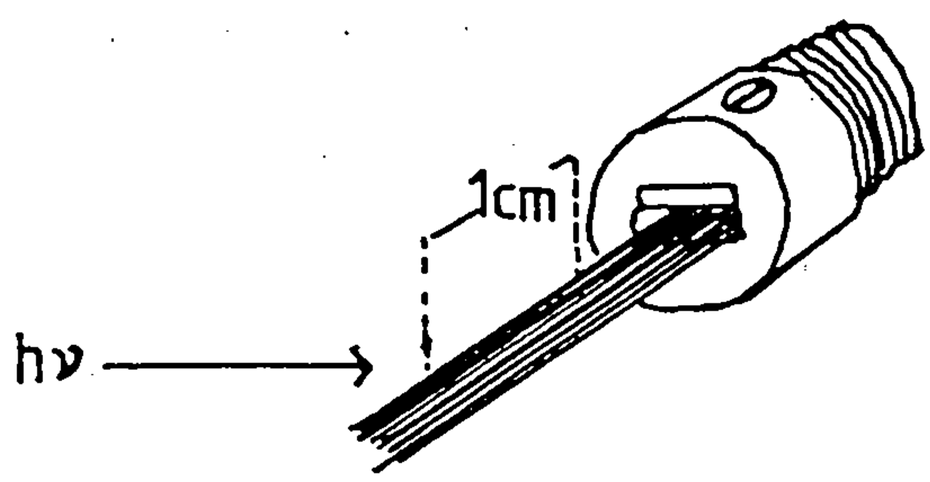

Fig. 47 Sample Holder

deflected in roughly circular orbits. It was operated in the fixed retardation mode (FRR) for most spectral collection. In FRR mode, all electrons are retarded down to 1/23rd of their original energy. This increases the sensitivity and also decreases the width (PWHM) of the photoelectron peak. This retardation is carried out in the lens system and a spectrum is obtained by scanning the voltages applied to the analyser. For constant resolving power, peak widths will vary with kinetic energy.

If the photoelectrons have low kinetic energy, there is a greater probability of them being scattered by residual gas molecules because of the time spent in the analyser. So, the intensity for low kinetic energy photoelectrons is poor. The alternative mode is the Fixed Analyser Transmission (FAT) mode. In this mode, the analyser voltages are kept constant whilst the lens potentials are scanned.

The photoelectrons are detected by an electron multiplier and a plot of electric current incident on the detector against kinetic energy is recorded in analogue form on an x-y plotter. This information can also be collected in digital form using an Apple II microcomputer.

4.6 Sample Handling

The carbon fibre samples, examined by XPS, consisted of a bundle (ca 3000 filaments) bound together by a small piece of aluminium foil. This was placed into a specially designed sample holder (Fig.4.7) made from deoxygenated copper. This design

ensured that only the carbon fibres themselves were exposed to the X-rays.

Powdered samples (model compounds) were mounted on a copper block using double sided adhesive tape. The use of adhesive tape does introduce slight sample charging. Most of these compounds are volatile so they were cooled to liquid nitrogen temperatures. This was done by passing liquid nitrogen through the inside of the sample probe. The cooling commenced when the sample was placed in the insertion lock.

4.7 Argon Ion Etching

The fibres could be bombarded with argon ions from an Ion Tech B22 etcher. The ion beam can be mechanically scanned and fro to provide uniform ion bombardment. The current used is usually 2mA with a voltage of 5KV. This technique was not used to clean the surface of the fibres prior to electrochemical treatment because severe damage to the fibre would ensue (see section 5.2). It was only used for specific experiments concerned with disrupting the outer fibre layers.

4.8 Data Collection

Data were collected using an AppleII microcomputer linked to an IBM 370/168 mainframe computer. The advantage of collecting digital data is the ability to collect multiple scans which greatly improves the statistical validity of any small feature appearing in the spectrum. In digital form, spectral information can be stored and analysed using computer facilities. This

increases the amount of information that can be extracted from a spectrum.

The spectrometer was set up to collect the number of photoelectrons ejected in a pre-set time period over a small energy range. This energy range was usually 1/30eV. The spectra obtained consisted of 357 points in a 12.5eV scan.

4.9 Data Analysis

The full system at Newcastle is shown in Fig.4.8. The spectra are recorded on floppy disc, and the data is stored on magnetic tape on the main frame. The data can therefore be analysed using both micro and main frame facilities.

4.9.1 Data Operations

The data operations carried out are listed below.

Microcomputer

1. Spectral display.
2. Integration and area measurements.
3. Spike removal.
4. Binding energy estimation.

Main Frame

1. Spectral smoothing.
2. Derivative spectra.
3. Non-linear least squares curve fitting.

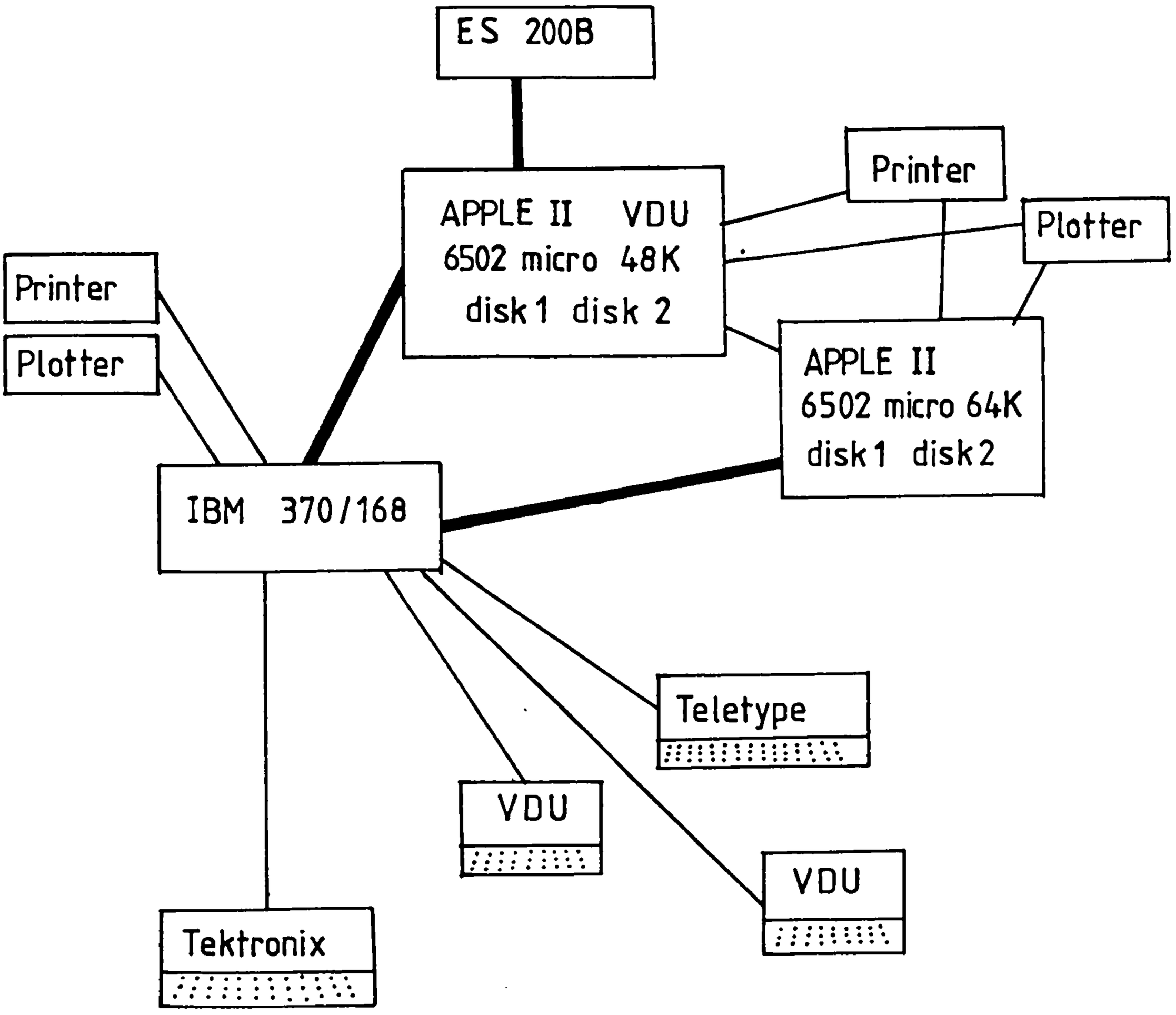

FIG.4.8 Digital Data Collection and Handling Arrangement.

4.9.1.1 Microcomputer Analysis

Most of the above operations are self explanatory (a fuller explanation is given by Sherwood(140)). The area measurements enable O1s:C1s area ratios to be calculated very quickly. The binding energy estimation provides good initial guesses for the non-linear least squares curve fitting program (explained below).

4.9.1.2 Main Frame Analysis

In many cases, a photoelectron spectrum consists of many overlapping peaks, often of different shapes and intensities. There are two main methods of trying to resolve spectra into their component signals, namely deconvolution and curve fitting. The method used in this case was curve fitting. This relies upon a series of initial guesses for the parameters of each component peak eg. peak width and shape. The number of component peaks has also to be guessed. These parameters are then fed into a computer program to obtain a good theoretical fit to the experimental data. These initial guesses have to be reasonably accurate in order for the program to converge. To help arrive at suitable initial guesses, derivative and smoothing techniques are used. These are explained below.

4.9.1.2.1 Spectral Smoothing

In general, it is always better to analyse unsmoothed data, but when it becomes impossible to collect good statistical data, smoothing results in a much improved signal to noise ratio. This enables the important features of the spectrum to be obtained.

There are two different types of smoothing processes that could be employed, namely the least squares central smoothing technique and related methods, and the fourier transform approach. The first method (98) is the most common and is the one used in this work.

4.9.1.2.2 Derivative Spectra

Derivative spectra (97) cannot give accurate peak positions because, if there is more than one peak present in the spectrum, the observed minima will always be shifted slightly. Nevertheless, it can be useful to give rough estimates of peak positions. Fig.4.9 shows a C1s spectrum and its derivative. The ratio Q (A/B) gives some indication of the peak asymmetry in the same way as the peak width could indicate peak asymmetry, but Q is more easily obtained. (The data has to be smoothed slightly before the second derivative is calculated.)

4.9.1.2.3 Non-linear Least Squares Curve Fitting

The aim of non-linear least squares curve fitting is to resolve a spectrum into a number of component peaks whose algebraic sum superimposes the experimental data collected. The curve fitting program, GAMET, requires a series of initial guesses to describe the individual peaks, eg their positions, intensities, and widths (99).

The functions most commonly used for peak shape are Gaussian and Lorentzian. This study uses a mixed Gaussian-Lorentzian function (the reason for this is explained in section 3.10)

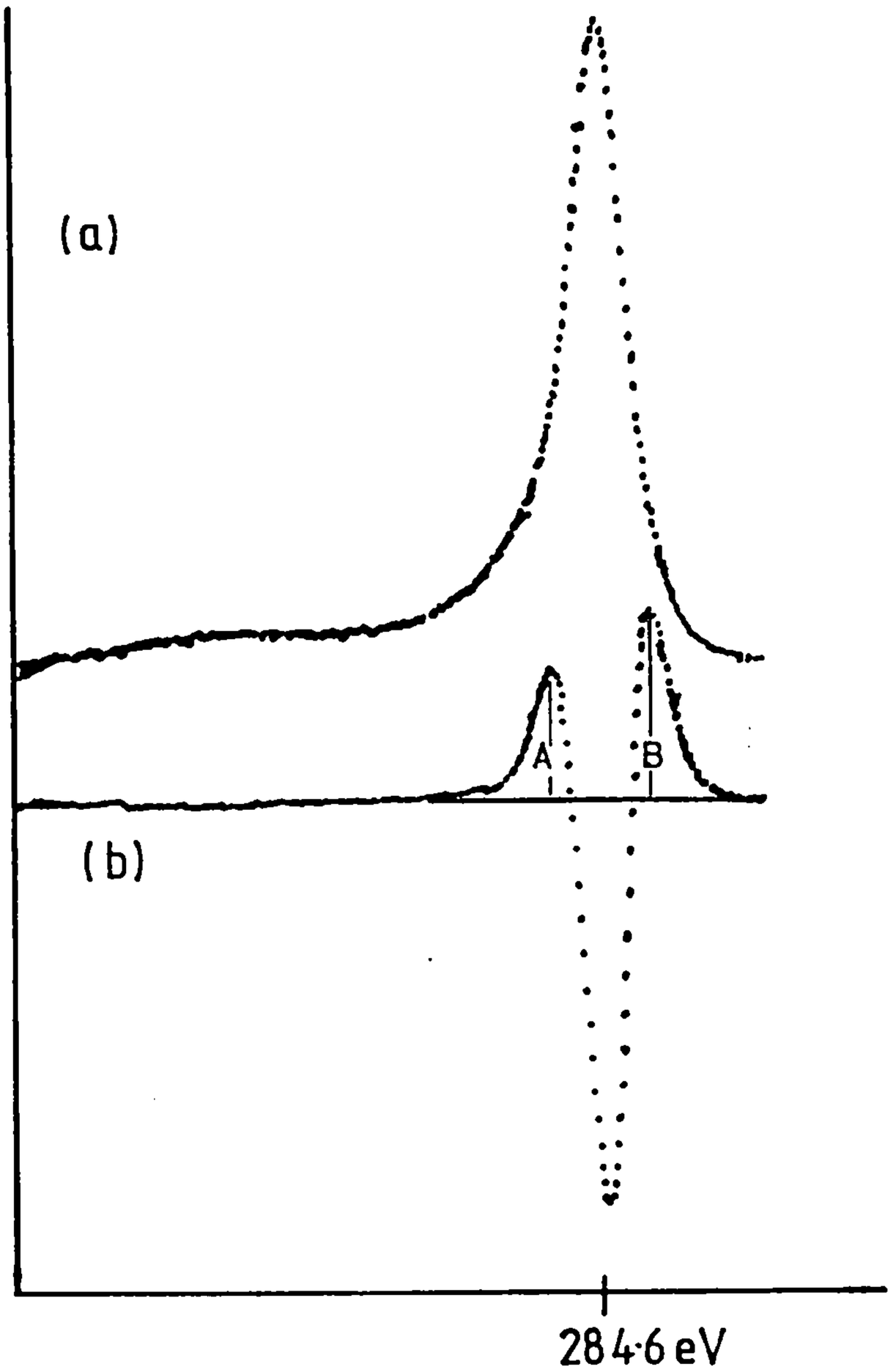

Q = A / B

(in this case Q=0·67)

Fig.4.9 (a) C1s of Untreated Fibres
(b) Second Derivative

$$f(x) = \frac{\text{Peak Height}}{(1+M(x-x_o)^2/\beta^2)\exp\{(1-M)[\ln 2(x-x_o)^2]/\beta^2\}}$$

where x_o is the peak centre and β is a parameter that is nearly 0.5(FWHM). The actual FWHM is calculated from β using an iterative method. M is the mixing ratio and takes the value 1 for a pure Lorentzian peak and the value 0 for a pure Gaussian peak.

The program involves the minimisation of chi square with respect to the free parameters. The weighted chi square, χ^2,which is defined as:

$$\chi^2 = \sum_{r=1}^{n} w_r[y_r - f(x_r/q)]^2$$

where y_r is the observed count at $x=x_r$, $f(x/q)$ is the fitted peak envelope, k is the total number of points in the spectrum,and w_r is a weighting function which in this case is chosen as y^{-1}_r, thus making χ^2 equal to the χ^2 statistic.

The chi square of different spectra should not be compared unless the number of degrees of freedom and the intensity of the peak are the same. This rarely occurs. The comparison of chi square is valuable in comparing different curve fits to the same spectrum to determine the best fit.

Each individual peak can be defined by the following parameters:-

1. peak position
2. peak intensity
3. peak width
4. Gaussian-Lorentzian peak shape mixing ratio
5. constant tail height
6. exponential tail
7. constant/exponential tail mixing ratio

These parameters may be fixed or allowed to float. The program uses an iterative method to find the best values for the floated parameters for the minimum chi square. No unique solution can be obtained, but the overall best fit is selected on the basis of a good statistical fit consistent with chemical and spectroscopic knowledge.

This data analysis technique is preferable to analogue curve synthesis techniques because it provides peak parameters which are reproducible, and also guages the quality of the fit.

The carbon 1s spectrum, as already explained, consists of a main graphitic peak and a number of chemically shifted peaks. The exponential tail found most suitable for the graphitic signal was 0.0275, its Gaussian-Lorentzian mixing ratio was given a value 0.84. All the chemically shifted signals were given a G-L mixing ratio of 0.5 with no exponential tail. The widths of these chemically shifted peaks were the same for a particular spectrum although the actual value was allowed to vary.

4.10 Scanning Electron Microscopy

SEM analysis was performed using a Joel JSM T20 microscope. The vacuum inside the sample chamber was 10^{-6} Torr, with a beam current of 10 μAmp. The resolution of this electron microscope was approximately 150 Å.

4.10.1 Sample Preparation

Small samples of fibres were embedded into a resin block with the ends of the fibres protruding. The length of the fibres protruding out from the block was as short as possible. This was to prevent the fibres from moving in the electron beam (due to charging). In this arrangement it was possible to see the ends and the sides of the fibres. The samples were then coated with a thin layer of gold to aid definition in the SEM photographs produced.

4.11 Fourier Transform Infra-red

FTIR spectra were collected using a Digil lab STS-10m spectrometer. Transmission spectra were recorded. (No signals could be detected using reflectance infra-red.) A small mesh of fibres was clamped into a sample holder and placed in the beam.

4.12 Ultra-violet Spectroscopy

The ultra-violet spectra were collected using a

Perkin-Elmer Lambda 5 UV/VIS spectrometer. Sample solutions were diluted to approximately 1/1000th of the original concentration to obtain a suitable spectrum.

CHAPTER 5

THE EFFECT OF ELECTROCHEMICAL OXIDATION ON CARBON FIBRE SURFACES USING ACIDIC ELECTROLYTE SOLUTIONS

5.1 Introduction

The aim of this chapter is to explain the surface changes induced on carbon fibres as a result of electrochemical oxidation in acidic electrolyte solutions. The results obtained from the variation in potential, concentration and reaction times are discussed. Comparisons between the use of different acids are made, and the differences in the behaviour of type I and type II fibres are also shown.

Some preliminary work was also carried out to find the chemical shifts of carbon 1s photoelectrons from a number of functional groups attached to aromatic rings. CNDO calculations were performed on a series of aromatic molecules to determine the extent of relaxation within the fibre lattice and to aid the assignment of photoelectron signals to particular functional groups.

5.2 Preliminary Investigations

5.2.1 Argon Ion Etching

The carbon 1s spectra of untreated type I and type II fibres are shown in Fig.5.1. Upon etching, the main peak broadens significantly. Unfortunately, the pressure inside the sample

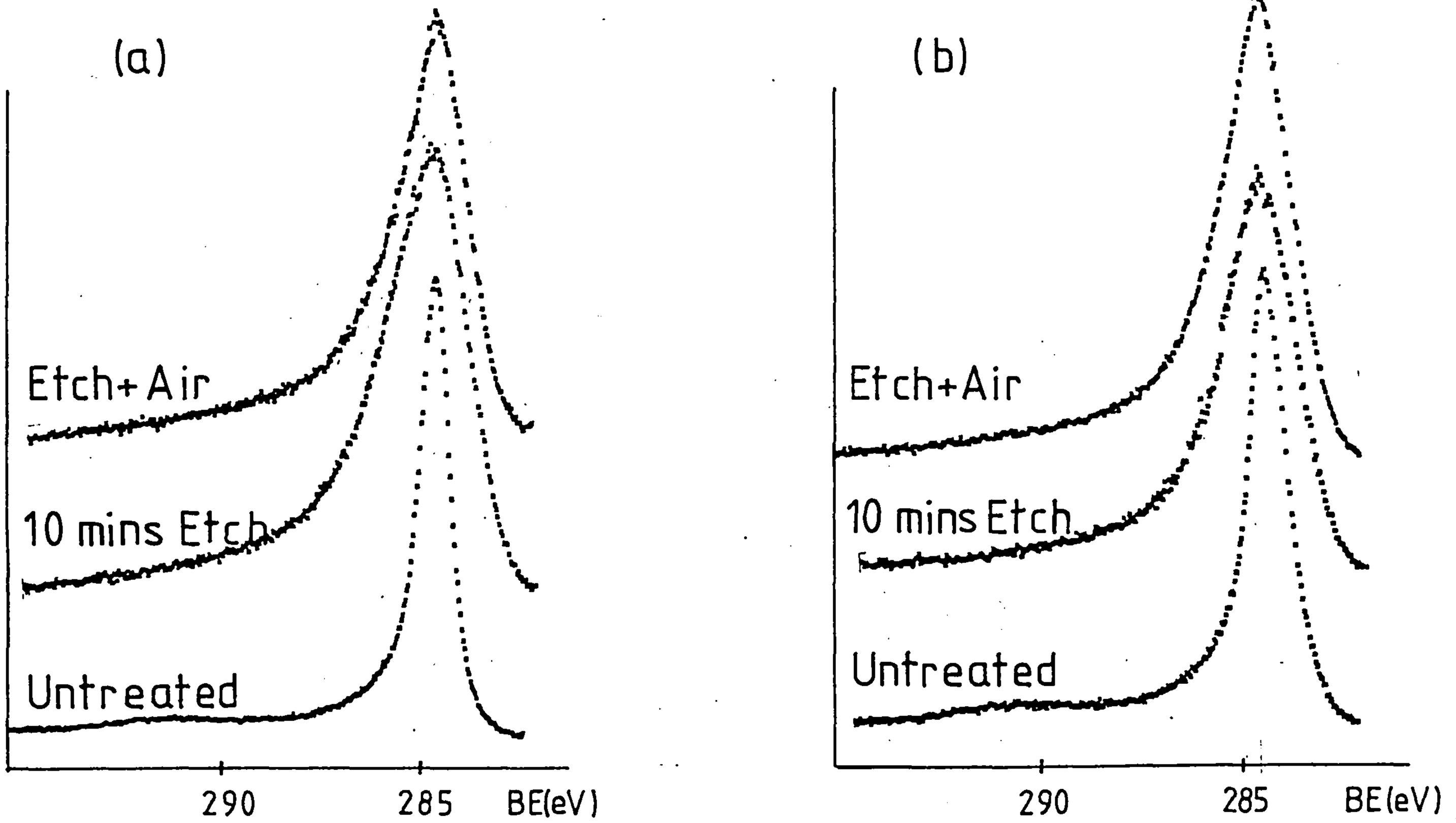

Fig.5.1 C1s Spectra of (a) Type I and (b) Type II Fibres

chamber during the etching process was quite high, 10^{-4}-10^{-5}Torr. Argon ion etching removes the outer layer of the surface. This will lead to the production of carbon atoms with unsatisfied valencies on the fibre surface. The surface carbon atoms will freely react with any oxygen present in the sample chamber and hence lead to an increase in surface oxygen concentration. There was also an increase in the amount of surface nitrogen. When the original PAN fibres are graphitised the outer layers of the fibres are fully converted into the carbon fibre lattice. This reaction however occurs to a slightly lesser extent for the more inner regions of the fibre. The middle of the fibre probably contains approx.5% of un graphitised ladder polymer. So, the increase in nitrogen detected after etching most probably arises from the larger concentrations of ladder polymer in the bulk fibre. The fibres, having been subjected to etching for 10 minutes, were then exposed to air for a further 10 minutes and earthed. The amount of surface oxygen increased slightly, but the nitrogen level remained constant.

For the case of metals, a standard sample preparation has been to etch the surface before electrochemical treatment to remove surface contaminants (eg.146). The above results show that etching carbon fibres results in a major breakdown of surface structure and if used as a standard sample preparation will lead to misleading electrochemical behaviour.

Unless the pressures inside the sample chamber during the etching process are very low, 10^{-9}Torr, it seems unlikely that depth profiling will lead to any conclusive results.

5.2.2 The Examination of Aromatic Compounds by XPS

A number of aromatic compounds were examined to find the range of chemical shifts induced by a particular functional group. All of these samples were cooled to liquid nitrogen temperature in order to prevent volatilisation of the compound in the ultra high vacuum of the sample chamber. The carbon 1s binding energies and chemical shifts calculated from curve fitting the carbon 1s spectra of a number of compounds are given in Table 5.1. (The spectra are shown in the Appendix.) The results are described below.

Phenol type groups induce chemical shifts in the range 1.35eV-2.18eV depending on the environment of the carbon atom in that functional group. Phenol itself gives rise to a chemically shifted signal at 1.6eV, which is the same as methanol and ethanol (see Appendix). The chemical shift decreases to 1.34eV and 1.49eV if another aromatic ring, or another phenol group, is present on an adjacent carbon atom. Carboxylic groups attached to carbons adjacent to that of the phenol group have the opposite effect. For ortho-hydroxy-benzoic acid (salicyclic acid), the chemical shift of the phenol carbon is 1.80eV. In the case of para-hydroxy-benzoic acid this shift is much greater, ie 2.18eV.

The carbon 1s spectrum of mellitic acid consists of two main chemically shifted signals at 1.44eV and 5.09eV from the hydrocarbon peak (BE=284.6eV). The carboxylic acid groups give rise to a chemical shift on the photoelectron signals from adjacent carbon atoms. These types of shifts have been described as β-shifts. Lindberg (147) listed a series of β-shifts and

TABLE 5.1

Carbon 1s Binding Energies of Chemically Shifted Species for a number of Aromatic Compounds (Cf. B.E. of C1s Hydrocarbon=284.6eV).

Compound	Molecular Structure	Functional Groups	Binding Energy (eV)	Chemical Shift (eV)
Benzoic Acid	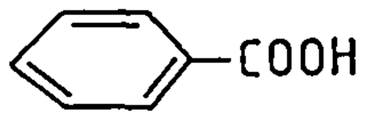	-COOH	288.95	4.35
Salicylic Acid	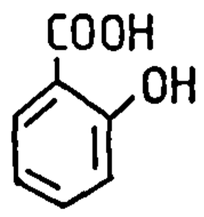	C-OH -COOH	286.4 289.2	1.80 4.68
Parahydroxy-benzoic Acid	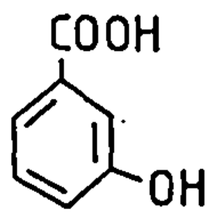	C-OH -COOH	286.78 288.90	2.19 4.30
Mellitic Acid	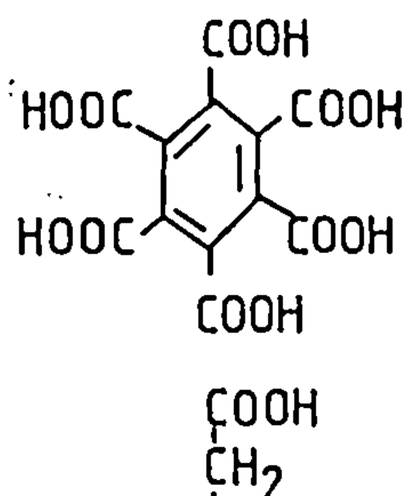	-COOH β-shift	289.69 286.04	5.09 1.44
Phenyl-acetic Acid	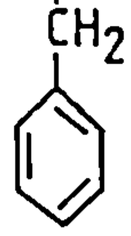	-COOH	289.3	4.70
Phenol		C-OH	286.22	1.62
Napthol	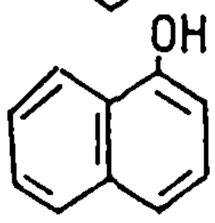	C-OH	285.94	1.34
Catechol	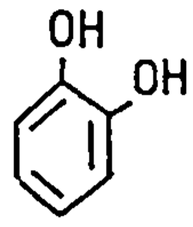	C-OH	286.09	1.49
Hydroquinone	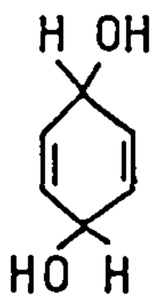	C-OH	286.30	1.70
Benzoquinone		>C=O	287.22	2.62
Graphitic Oxide	(See Appendix)		288.67 286.97	4.07 2.37

primary shifts for a number of methyl compounds. These are given in Table 5.2. The β-shift induced by carboxylic acid groups is reported as 0.7eV. In the case of mellitic acid, this β-shift is 1.44eV, which is roughly twice the value noted by Lindberg. This is to be expected since the adjacent carbon atoms themselves may also be affected by the other carboxylic groups in the molecule. β-shifts were not detected for compounds with only one carboxyl group attached to the ring. This may be due to relaxation effects lowering the magnitude of the shift which may not lead to resolvable signals.

Graphitic oxide was prepared according to Hummer's method (148). The compound produced was not yellow as obtained by Hummer, but grey/black due to the presence of unreacted graphite, as is the case when graphitic oxide is prepared electrochemically (82). The carbon 1s spectrum consists of two main chemically shifted species at 2.37eV and 4.07eV, as well as a main carbon signal. A structure of graphitic oxide has been proposed by Clauss and Boehm (159) and is shown in the Appendix.The chemical shift at 2.37eV is slightly higher than that detected by Evans (160).

For all the compounds, satellite features were detected between 5.9 and 8.0eV from the hydrocarbon peak. The satellite peaks have also been seen by Clark (63) for polyaromatic systems.

5.2.3 Theoretical Determination of Relaxation Effects

The experimental binding energies of a number of aromatic compounds have been reported above. These compounds have, at

TABLE 5.2

Chemical Shift Data for a Series of Methyl Compounds

Compound	C1s Shift (eV)	
CH_3-X	CH_3 (β)	X (primary)
$-CH_3OH$	0.1	1.5
$-CH_2OC_2H_5$	0.4	1.8
$-CH_2CO(OCH_3)$	0.6	2.1
$-CH(OH)CH_3$	-	1.4
-CHO	0.6	3.2
$-COCH_3$	0.6	3.1
-COOH	0.7	4.5
-COO-	0.6	4.4

most, two aromatic rings in their molecules. To apply these chemical shifts to spectra of carbon fibres, relaxation effects have to be taken into account. Relaxation effects are expected to be quite large due to the extended π system that exists throughout the lattice.

Shirley et al. (150) carried out a series of CNDO/2 calculations and applied a RPM to predict the relaxation energy of carbon atoms in a graphitic lattice. Their calculations involved the most central atoms of a series of aromatic molecules with an increasing number of aromatic rings. They plotted relaxation energy against $n_c^{-\frac{1}{2}}$ (where n_c is the number of carbon atoms) and extrapolated the graph to $n_c^{-\frac{1}{2}} = 0$. They concluded that the relaxation energy in graphite was that of benzene + 1.6(±0.2)eV.

For an approximation to the outer layer of carbon fibres, CNDO/2 calculations, using the RPM, were carried out on the outer atoms of a similar series of molecules. The atomic coordinates were taken from X-ray and neutron diffraction data in the literature. The calculated relaxation energies are given in Table 5.3. From these results, relaxation energy effects appear to be greater in linear aromatic molecules than in coronene type molecules. In both cases the relaxation energy increases with the number of aromatic rings in the molecule. It therefore can be assumed that relaxation effects play a major role in the detected chemical shift in spectra from carbon fibres.

TABLE 5.3

Relaxation Energies for a series of Compounds Calculated obtained from CNDO calculations and applying a RPM

Compound	Molecular Structure	Calculated Relaxation Energy (eV)
Benzene (151)	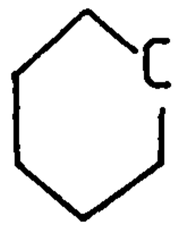	18.46
Napthalene (152)	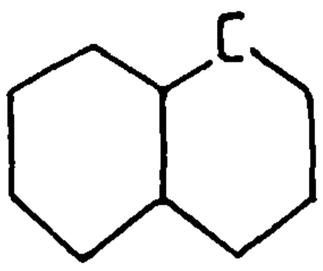	18.95
Anthracene (153)	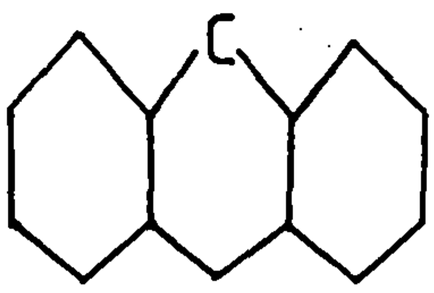	19.87
Tetracene (154)	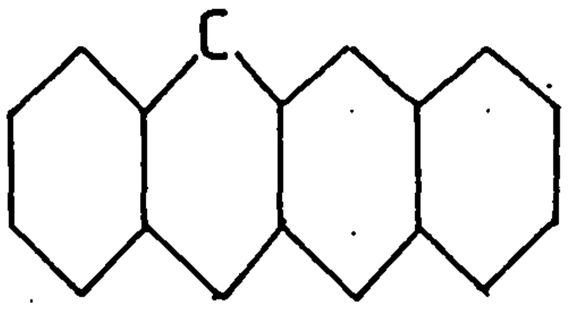	20.74
Pyrene (155)	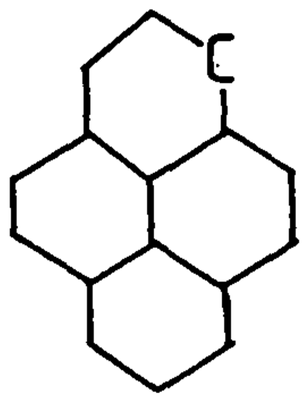	18.76
Perylene (156)	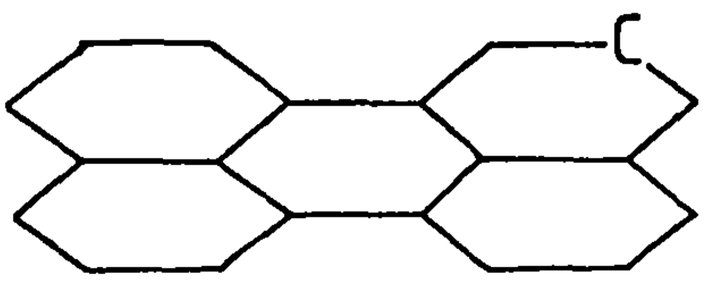	19.03
Coronene (157)	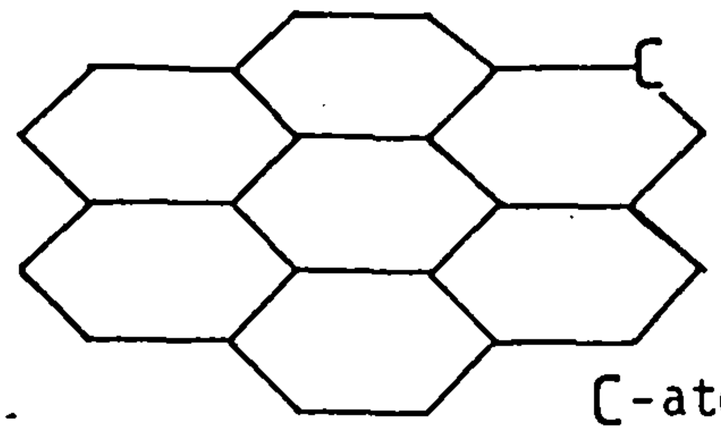	19.34

C-atom under consideration.

5.3 The Electrochemical Oxidation of Carbon fibres

5.3.1 Electrochemistry and Cyclic Voltammetry

No fine structure was observed in the cyclic voltammogram for nitric acid solution for a potential sweep using limits 0.0V to +1.2V(SCE). At +1.2V the increase in current was due to oxygen arriving at the electrode. This oxygen reacted with the surface of the carbon fibre causing the evolution of carbon dioxide. Similar results occured for a sweep from -1.0V to +2.0V(SCE).

The cylic voltammogram recorded for phosphoric acid is shown in Fig.5.2. There is an increase in the current at +0.4V. The process occuring at this potential appears to be reversible because of the negative current increase at +0.05V on the reverse potential sweep. This may correspond to the adsorption of phosphate ion onto the fibre surface, these phosphate ions being weakly bound to the fibre. As with the cyclic voltammogram obtained for nitric acid, there was a large increase in current at 1.1-1.2V(SCE). This again coincided with the evolution of gas.

Since no clear features appeared in the cyclic voltammogram in nitric acid, other than the oxygen potential at 1.2V, it was decided to polarise the fibres to a range of potentials, namely 0.5, 1.0, 1.5, 2.0, 2.5 and 3.0V(SCE) for a set time period (usually 20mins). The same set of potentials was chosen for phosphoric acid in order to make a good comparison between the two electrolytes.

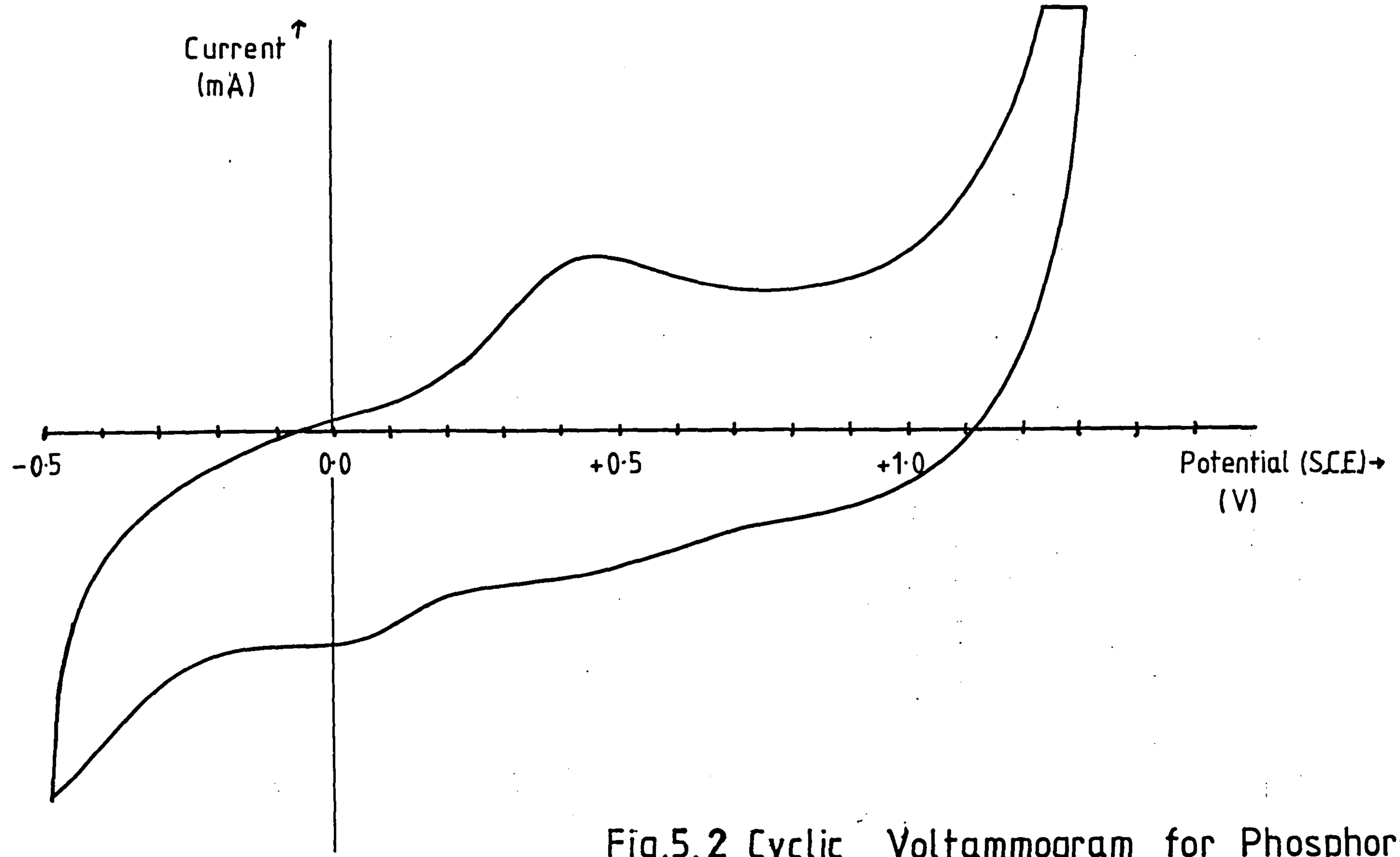

Fig.5.2 Cyclic Voltammogram for Phosphoric Acid Electrolyte

5.3.2 Fibre Surface Decomposition

The carbon 1s spectra recorded for samples polarised to potentials greater than 1.5V(SCE) were found to change with time.

The carbon 1s spectrum can be separated into 'graphitic' and 'oxide' parts, the latter being chemically shifted from the former by between 1 and 6eV. This latter region contains a number of signals due to carbon/oxygen complexes. The 'oxide' intensity decreased on exposure to X-rays (due to either the X-rays themselves or the heat from the X-ray gun). The samples did not decay when placed in the vacuum alone for the same length of time. Fig.5.3a shows a plot of the ratio of 'oxide' intensity (C_{ox}) and the 'graphitic' peak intensity (C_{graph}) against time. Figs.5.3b and c show the carbon 1s spectra after timed exposure to X-rays for fibres treated in nitric acid. Similar decomposition is observed for fibres treated in phosphoric acid. These spectra illustrate the general loss of 'oxide' and the change in the relative amounts of the oxygen species with time.

Having established that decomposition occurs on exposure to X-rays, it was necessary to take care with subsequent samples. Thus, spectra were recorded for the same fixed time, this time being as short as possible whilst still consistent with acceptable statistics.

(a)

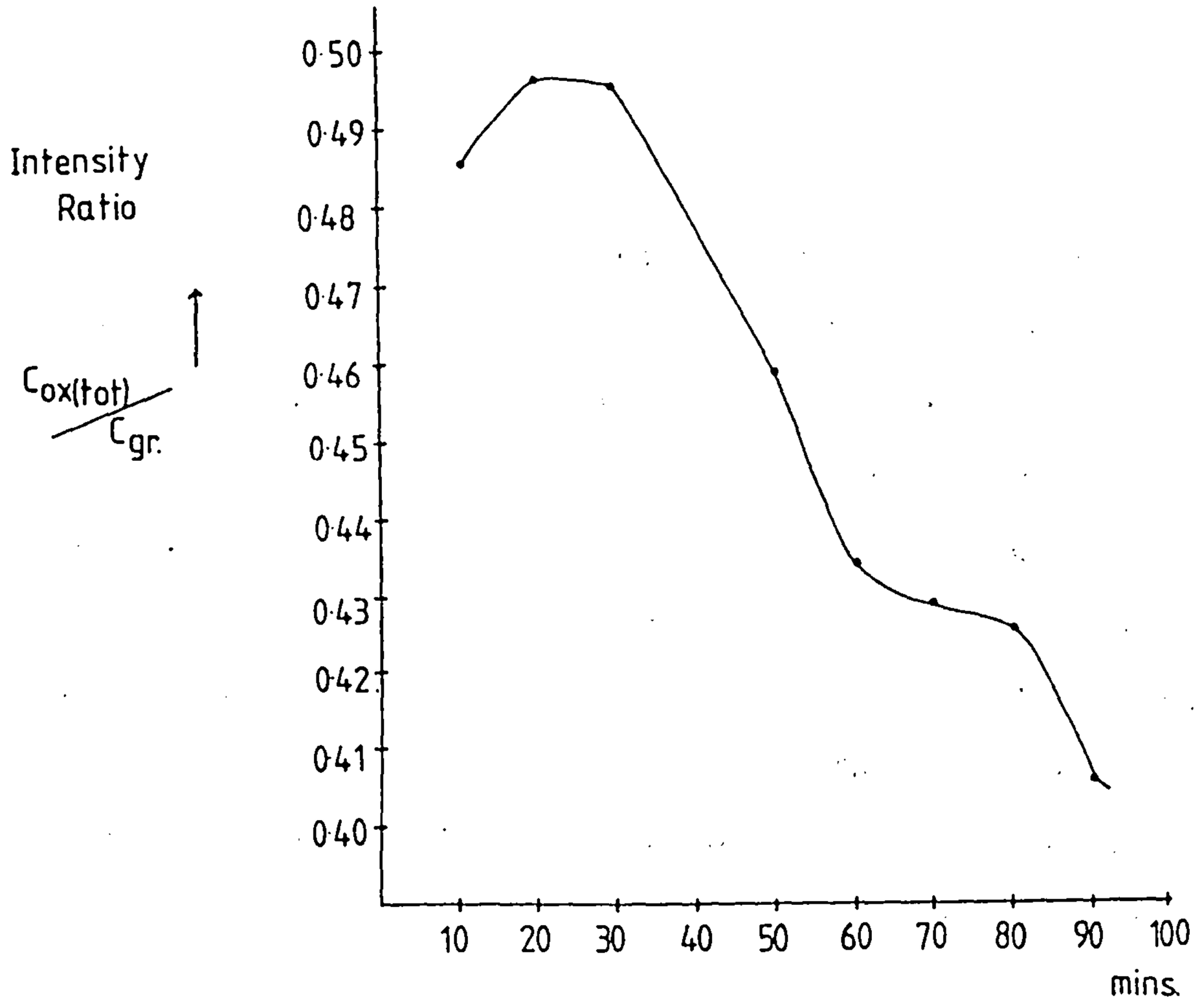

(b) C1s Spectrum after 10 mins

(c) C1s Spectrum after 90 mins

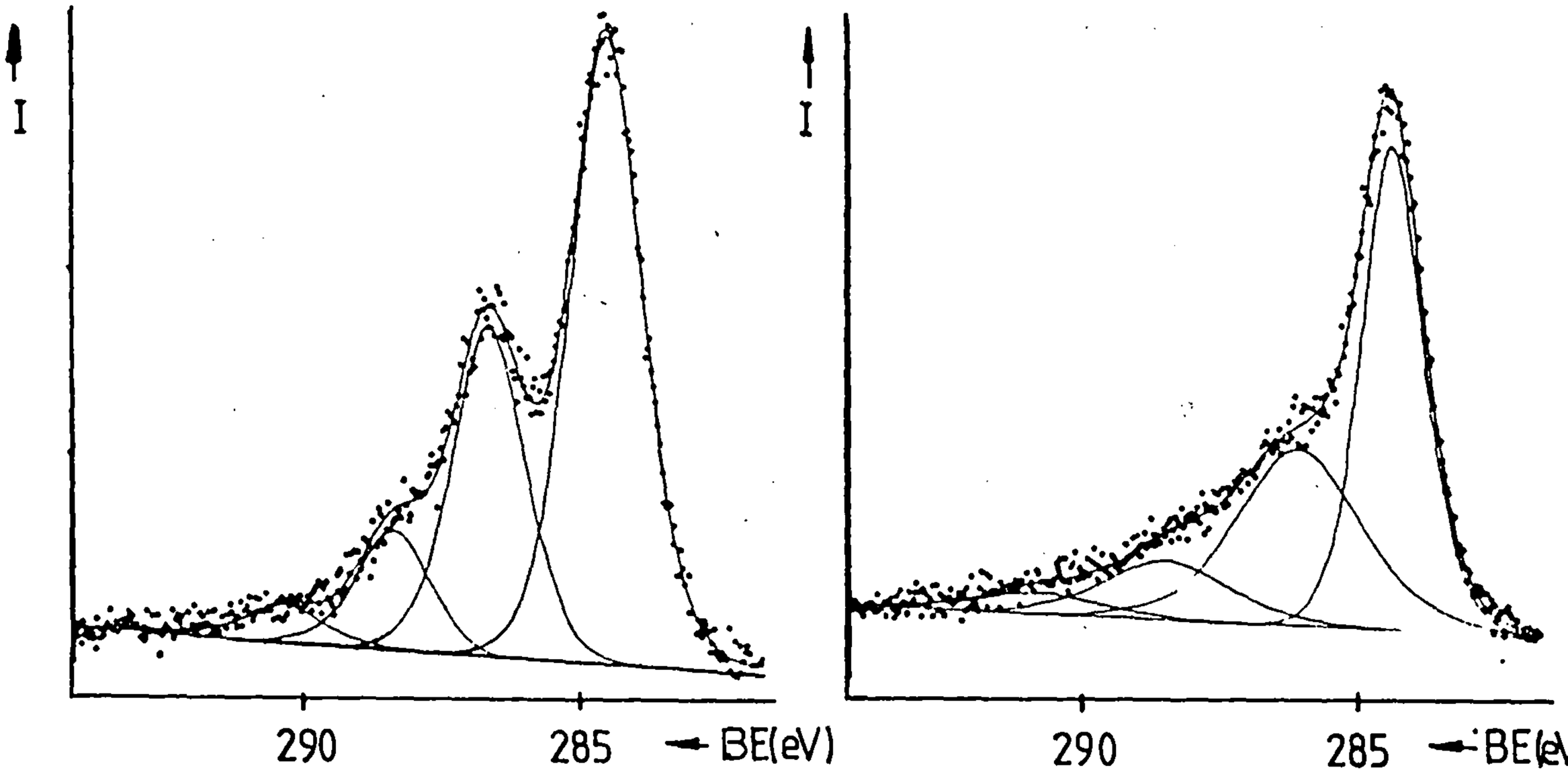

Fig.5.3 Decomposition of the Fibre Surface

5.3.3 Carbon 1s Spectra

5.3.3.1 Features of the 'Graphitic' Carbon 1s Spectrum

The carbon 1s spectrum of untreated type II fibres has been discussed previously (see section 3.15). In untreated fibres and in fibres with little surface functionality, the main graphitic carbon 1s signal exhibits an asymmetric tailing towards higher binding energy due to conduction band interaction. As the degree of surface functionality increases, this tailing is lost because of exfoliation of the fibre surface, which results in the loss of the surface conductive properties. The graphitic rings are altered by C/O groups, which can break up the extended π-electron system that is responsible for fibre conductivity.

The conducting nature of the lattice also gives rise to a plasmon loss feature (see section 3.14.4) some 6.9-7.0eV from the 'graphitic' peak. As might be expected, this feature is not present when there is any significant amount of surface functionality.

5.3.3.2 Features of the 'Oxide' Carbon 1s Spectrum and FTIR Data

All the FTIR spectra were carried out using fibres treated with nitric acid. The chemical shifts observed in the carbon 1s spectra for fibres treated with nitric and phosphoric acids are the same, and so it may be assumed that these chemically shifted signals may correspond to the same type of functionality.

In both cases (nitric and phosphoric acid treatments), the

carbon 1s spectrum consisted of a peak 2.1eV from the main peak. This corresponds to keto- type groups, and was confirmed by FTIR with absorbances at 1700-1690cm^{-1} and 1660cm^{-1} (oxide 1). The second chemically shifted species occurs at 4.0eV from the main peak. This was assigned to ester functionality, confirmed by FTIR with a stretching frequency 1730-1740cm^{-1} (oxide 2). In the spectra of fibres that have been extensively oxidised, a signal at 6.0eV is also present. The assignment of this peak is less certain. It is unlikely that it is caused by carbonate groups although carbonate functionality has been produced on graphite with potassium hydroxide (80). The other alternative is a shake-up satellite, this satellite being produced from transitions of electrons affecting the photoelectron (see section 3.14). This feature has been observed for all aromatic polymers. Its relative intensity, with respect to the 'graphitic' peak, remains constant within ±0.01.

No phenolic or alcohol type groups are present in the FTIR spectra and no appropriate peaks are seen in the carbon 1s spectrum. These alcohol groups would be expected to have a chemical shift of 1.6eV. The spectra are very similar to those produced by graphitic oxide (see Appendix).

In previous work carried out by Proctor and Sherwood (87,95,96), a β peak was included (see section 5.2.2). It is not included in this work because it is thought that there would be varying β contributions from carbons associated with several carbon/oxygen functionalities. It is noted that as functionality increases, the width (PWHM) of the main signal increases.

5.3.3.3 Studies in Nitric Acid

Figs.5.4 and 5.5 show the curve fitted spectra of fibres polarised to several potentials in 2.7 and 0.22 M nitric acid solutions respectively. There are two main 'oxide' signals, one due to 'graphitic' carbon and one to a plasmon or shake-up satellite. The binding energies of these 'oxides' vary slightly (±0.2eV) as potential varies. This is to be expected because of the large variation in local environment as the surface functionality increases.

Fig.5.6 shows the variation of the total 'oxide' intensity for the two different nitric acid concentrations. Clearly, there is a difference in the total amount of 'oxide' formed in the more dilute acid, but at 3.0V the situation is reversed, ie.'oxide' build up is greater in the stronger acid.

Figs.5.7 and 5.8 show how the individual 'oxide' intensities vary for each concentration.

5.3.3.3.1 2.7M Nitric Acid

Fig.5.7 shows that the relative area of 'oxide' 1 remains fairly constant until 2.5V(SCE) where there is a sharp increase in relative intensity, with respect to the main peak, from 0.089 to 0.836. 'Oxide' 2 (ester) shows a steady increase with potential from 0.06 to 0.28. The satellite/ plasmon intensity remains fairly constant at 0.04-0.05.

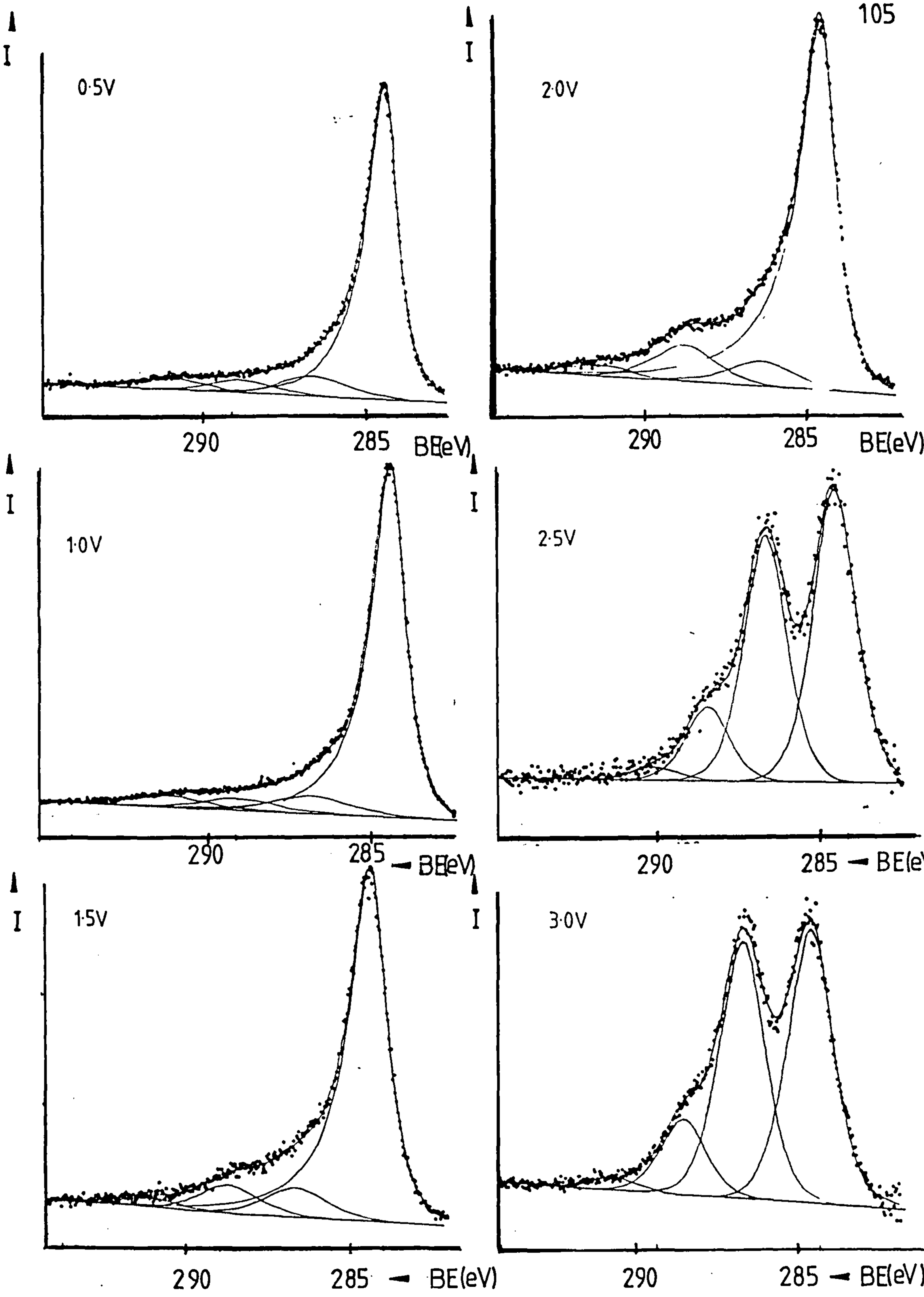

Fig.5.4 C1s Spectra of Fibres Polarised in 2·7M Nitric Acid

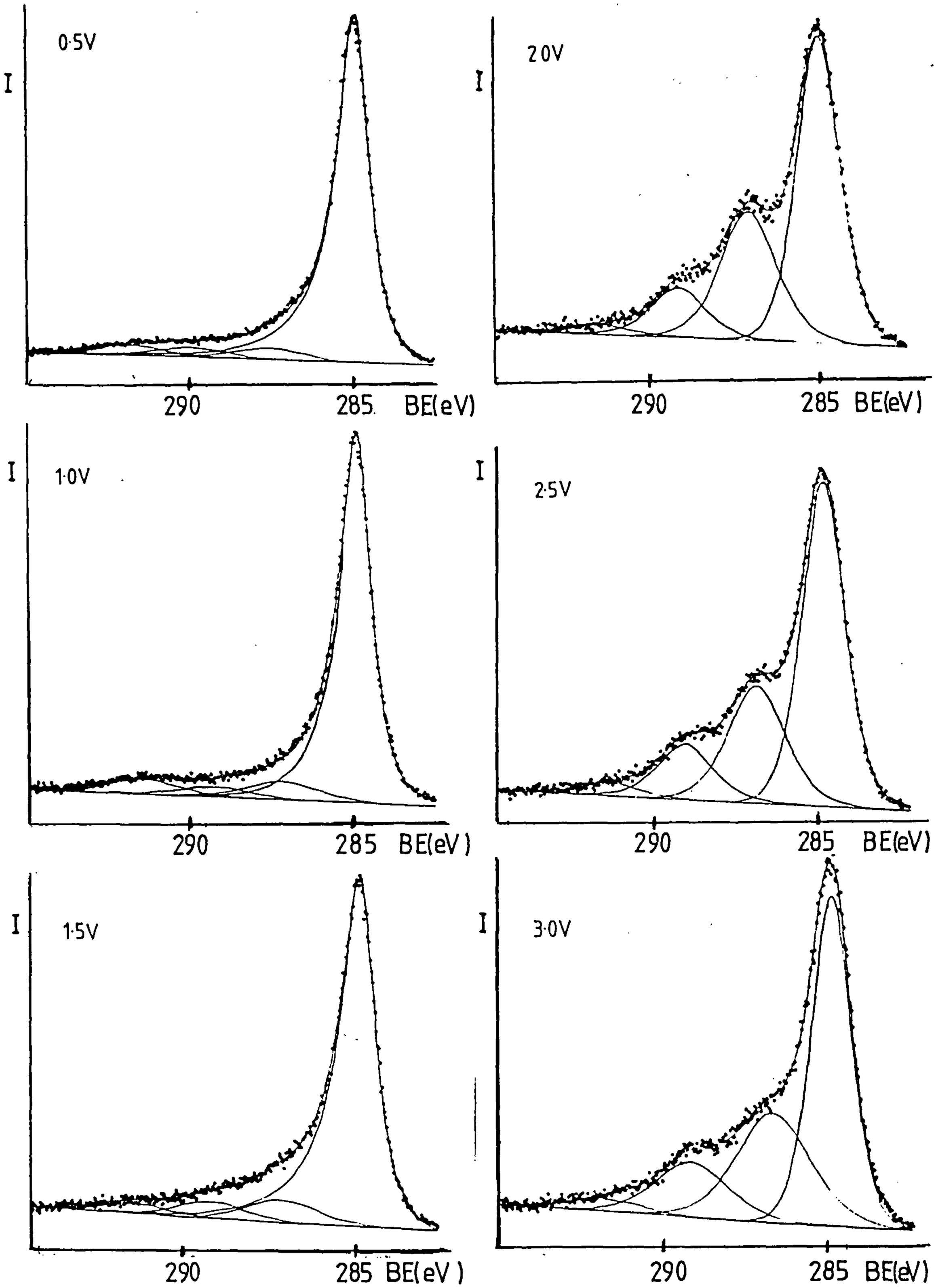

Fig.5.5 C1s Spectra of Carbon Fibres Polarised in 0·22M Nitric Acid

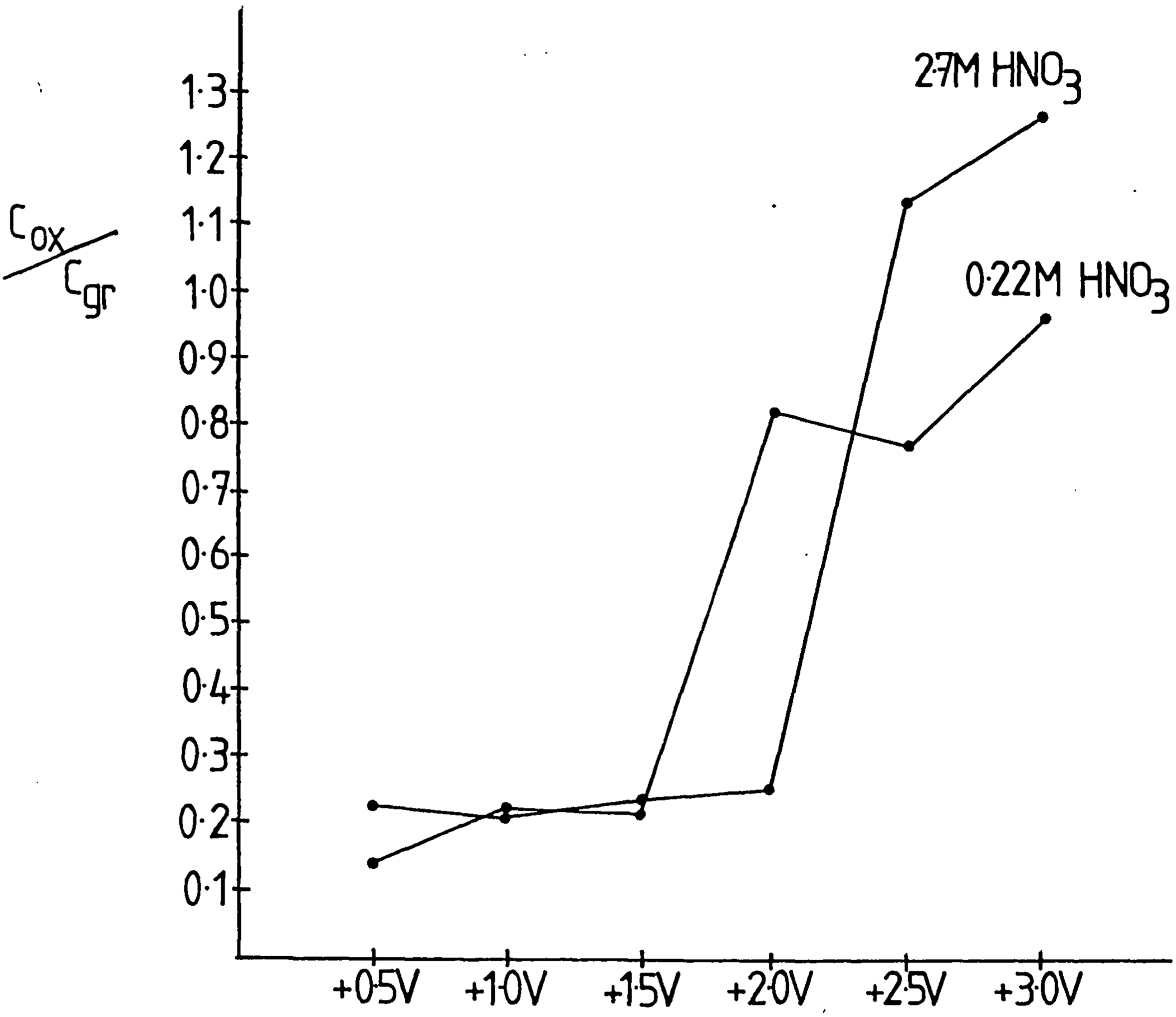

Fig.5.6 Variation of Total Oxide Intensity

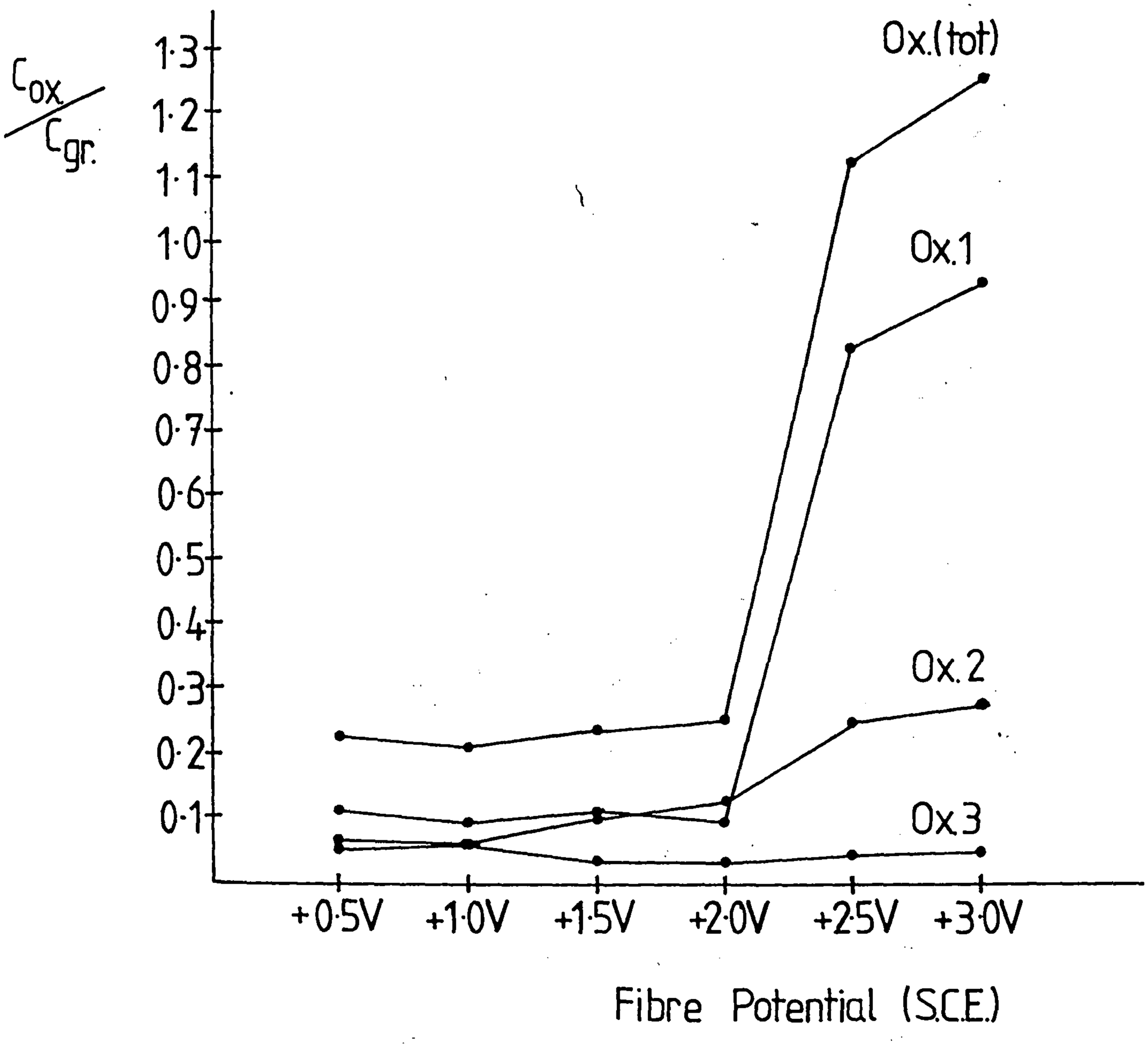

Fig. 5.7 Variation of Intensity of Shifted Carbon Species with Fibre Potential in 2·7M HNO_3

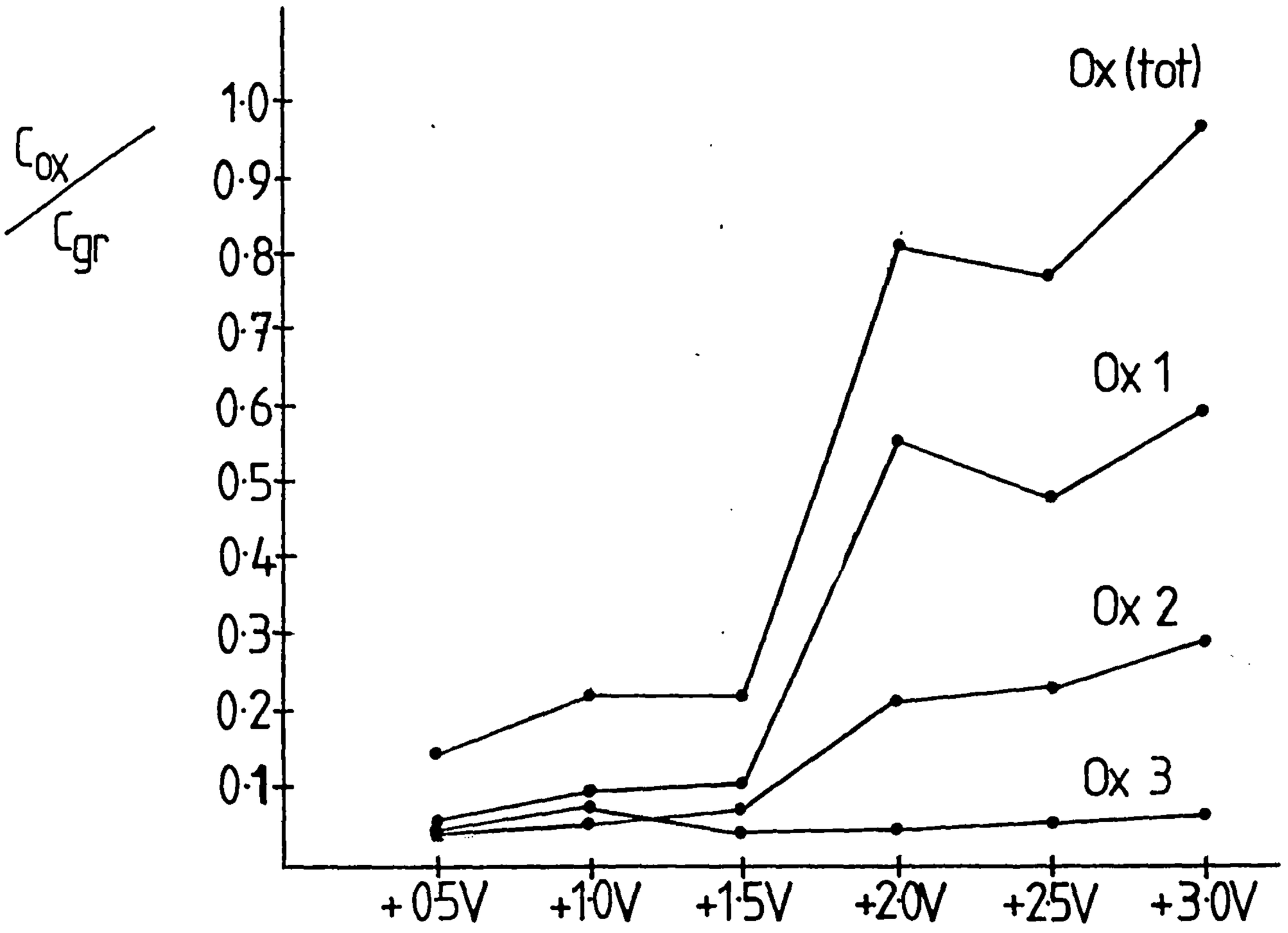

Fig.5.8 Variation of Intensity of Shifted Carbon Species with Fibre Potential for 0·22M HNO_3

5.3.3.3.2 0.22M Nitric Acid

Fig.5.8 shows that 'oxide'1 intensity increases with potential with a sharp rise between 1.5 and 2.0V(SCE), 'oxide'2 (ester) increases steadily from 0.04 to 0.278; plasmon/satellite intensity remains constant within ±0.01.

5.3.3.4 Studies in Phosphoric Acid(H_3PO_4)

Fig.5.9 shows the fitted spectra for fibres polarised to several potentials in phosphoric acid. These spectra are very similar to those obtained for nitric acid treatment. They consist of two main oxygen species with chemical shifts of 2.1eV (±0.2eV) and 4.0eV (±0.1eV), these most probably being due to carbonyl type and ester type groups respectively. Fig.5.10 shows how the C_{ox}/C_{graph} area ratio varies with potential. The total oxide generally increases with potential, with a sharp rise from 1.5V to 2.0V(SCE). There is a slight drop in intensity at 3.0V. 'Oxide' 1 and 'oxide' 2 behave in a similar manner but the maximum area ratio is much greater for 'oxide' 1 (0.84 compared to 0.30). The satellite/plasmon intensity remains constant.

5.3.4 Other Features

Nitrogen was not present in fibres treated in either acid. This is very surprising because nitric acid intercallates with graphite and these intercallation compounds are very difficult to remove by washing (1).

Phosphorus was present on fibres polarised to potentials

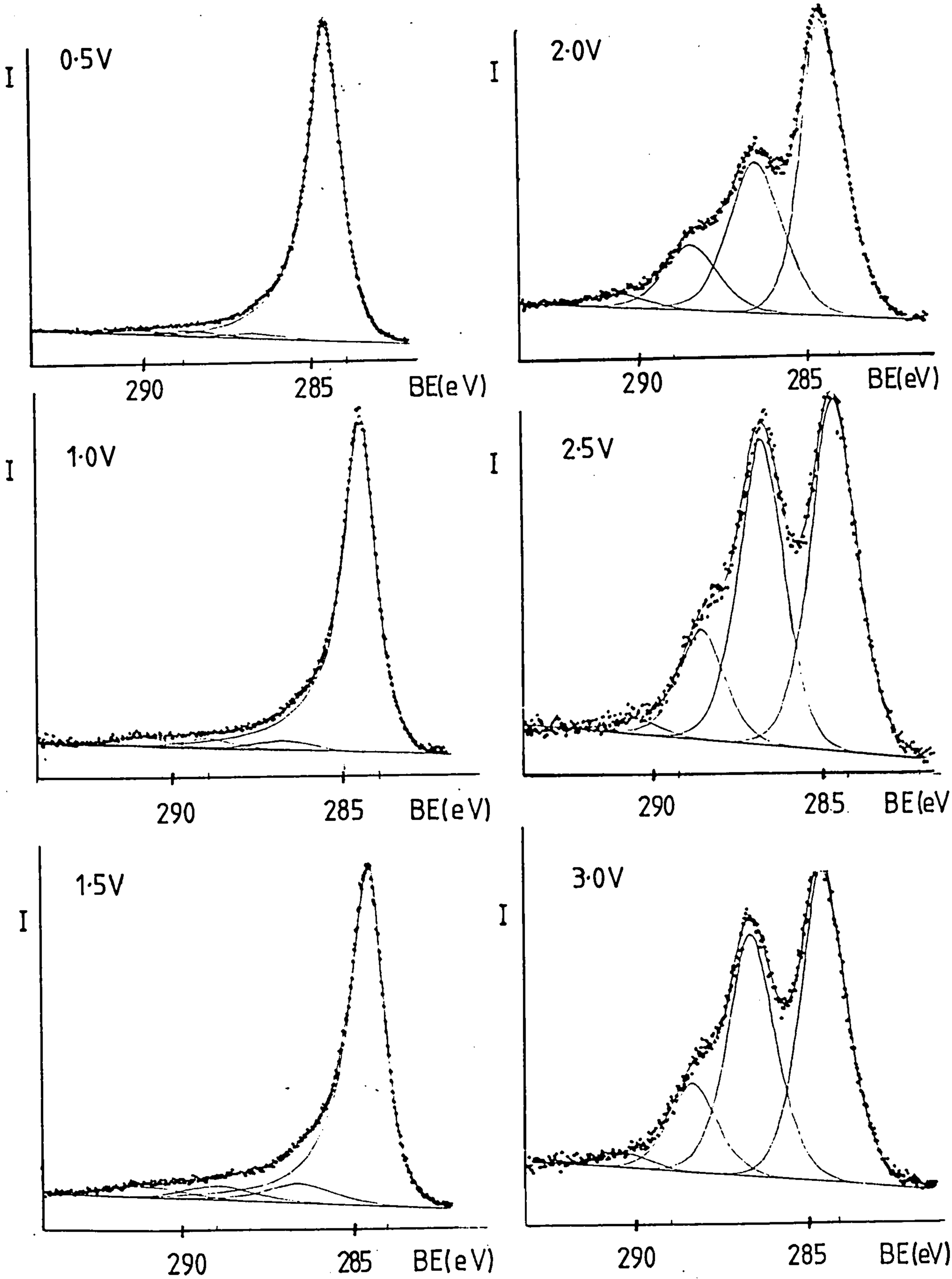

Fig.5.9 C1s Spectra of Fibres Polarised in Phosphoric Acid

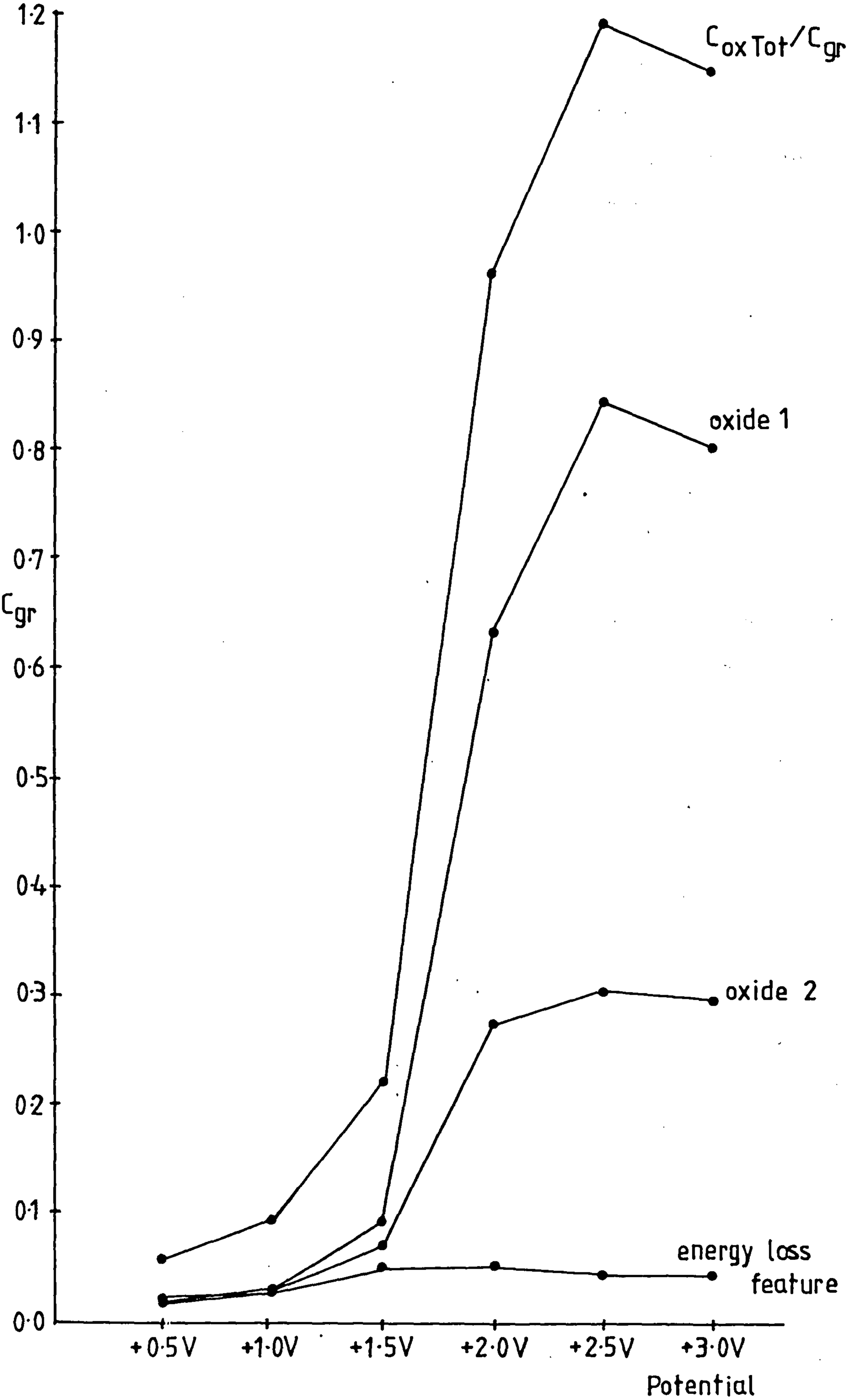

Fig.5.10 Variation of Chemically Shifted Species with Fibre Potential in H_3PO_4

above +1.0V in phosphoric acid, the binding energy of which corresponds to that of phosphorus in phosphate ions. This implies that phosphoric acid is trapped within the graphitic oxide type structure and is not removed by washing.

5.3.5 Oxygen 1s Spectra of The Fibre Samples

The oxygen 1s spectra of fibres treated in nitric acid consisted of one type of oxygen with binding energy 531.8eV. This lies between the binding energies for C=O and C-O type groups.

The oxygen 1s spectra of fibres treated with phosphoric acid consist of two main oxygen species with binding energies 531.3eV (±0.2eV) and 533.0eV (±0.5eV). The area ratio of the higher binding energy component to the lower binding energy component increases with increasing potential. At higher potentials, a third oxygen peak appears in the oxygen 1s spectra. This may arise from adsorbed water. The binding energy of this peak can vary depending upon how tightly the water is bound to the surface. This third peak may also arise from other hydroxy-type species, but the presence of physisorbed hydroxy species other than water seems unlikely. Table 5.4 gives the details of binding energies and area ratios obtained from curve fitting results.

5.3.6 Reaction-time Dependent Studies

Fibres were also polarised for different periods of time in the two acids.

Sample	Binding Energy/eV			Area Ratio		
	1	2	3	1	2	3
0·5V		533·5	532·3		0·318	0·682
1·0V		533·9	532·5		0·198	0·802
1·5V	535·6	533·0	531·3	0·016	0·490	0·494
2·0V	536·0	532·9	531·2	0·049	0·609	0·342
2·5V	535·9	532·6	531·2	0·036	0·691	0·273
3·0V	536·0	532·9	531·2	0·044	0·641	0·315
				(Peak area/total area)		

TABLE 5.4 Results of curve fits to O1s spectra of fibres treated in phosphoric acid

5.3.6.1 In 0.18M Nitric Acid at 2.0V

Fig.5.11 shows the variation of C_{ox}/C_{graph} with reaction time. Even after only ten seconds there was a significant amount of oxidation, since approximately one half of the total carbon 1s intensity was due to 'oxide'. The above ratio increases to a level of 0.98 after 12 minutes treatment. Further treatment leads to a slight decrease in this ratio. This suggests that the 'oxide' already produced reacts further to produce gaseous products (such as CO_2). The activation energy for the formation of carbon dioxide is probably smaller than for further oxidation of the bulk fibre.

5.3.6.2 In 4M Phosphoric Acid

Fig.5.12 show the fitted carbon 1s spectra for fibres polarised for sixty seconds and one hour. After only one minute of polarisation the fibres are extensively oxidised. These results are similar to those found with nitric acid.

The amount of phosphate present on the surface increases slightly with reaction time.

5.3.7 The Effects of Sulphuric Acid Treatment

The carbon 1s and oxygen 1s spectra of fibres polarised at 2.0V in 2M sulphuric acid for 20 minutes are shown in Fig.5.13, in which the binding energies and area ratios are also given. These results are very similar to those obtained for phosphoric

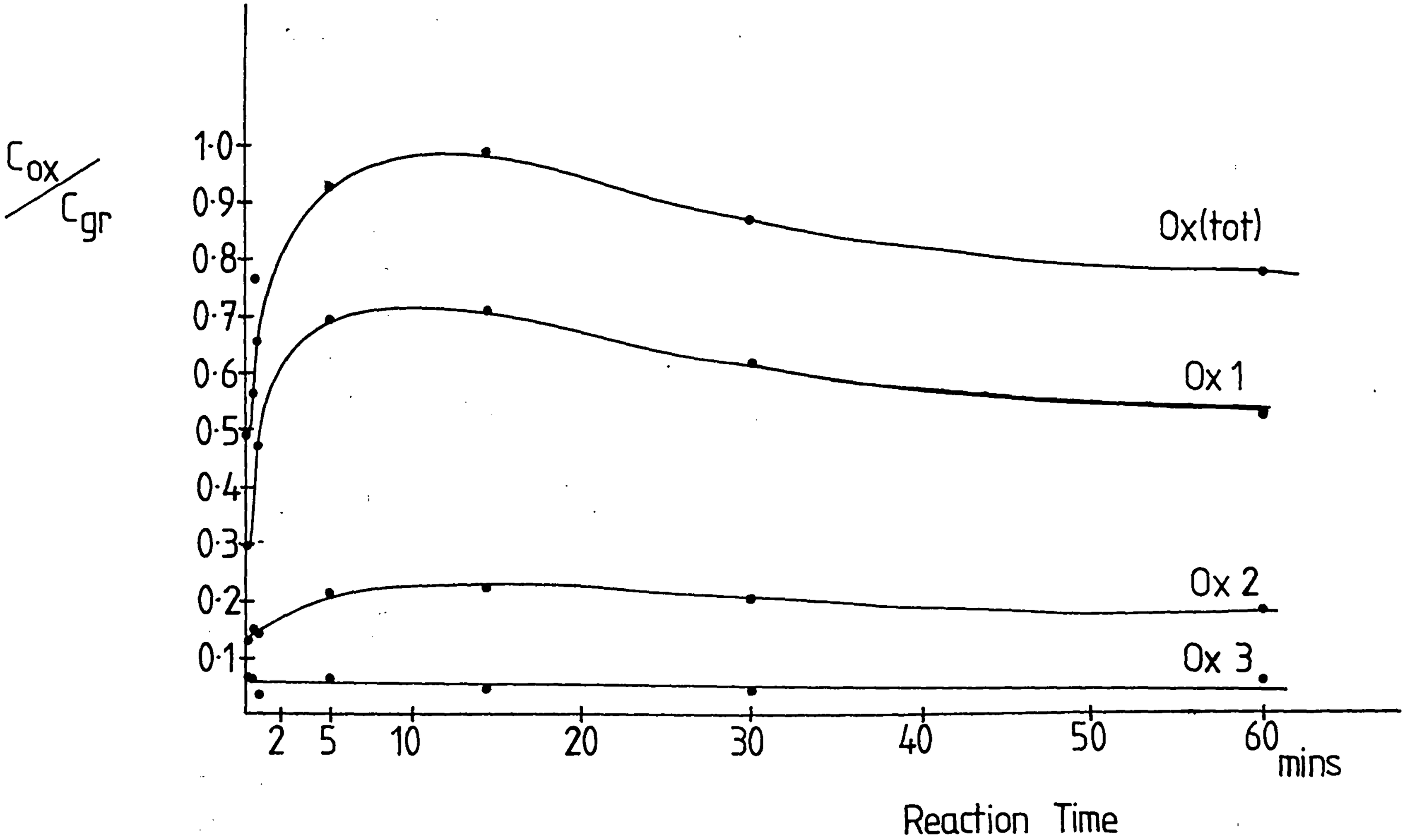

Fig.5.11 The Variation of the Intensities of Chemically Shifted Species with Reaction Time in HNO_3

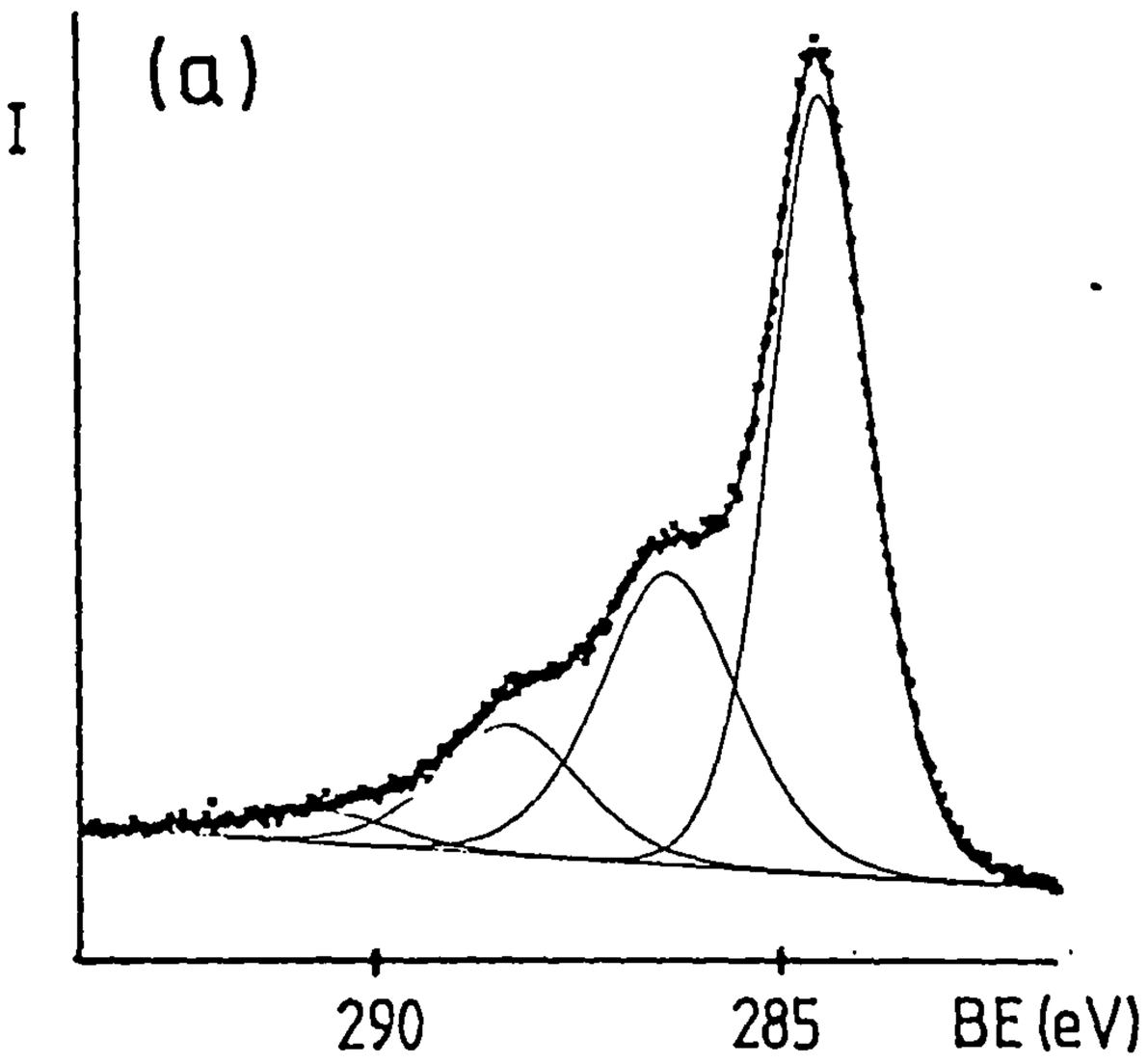

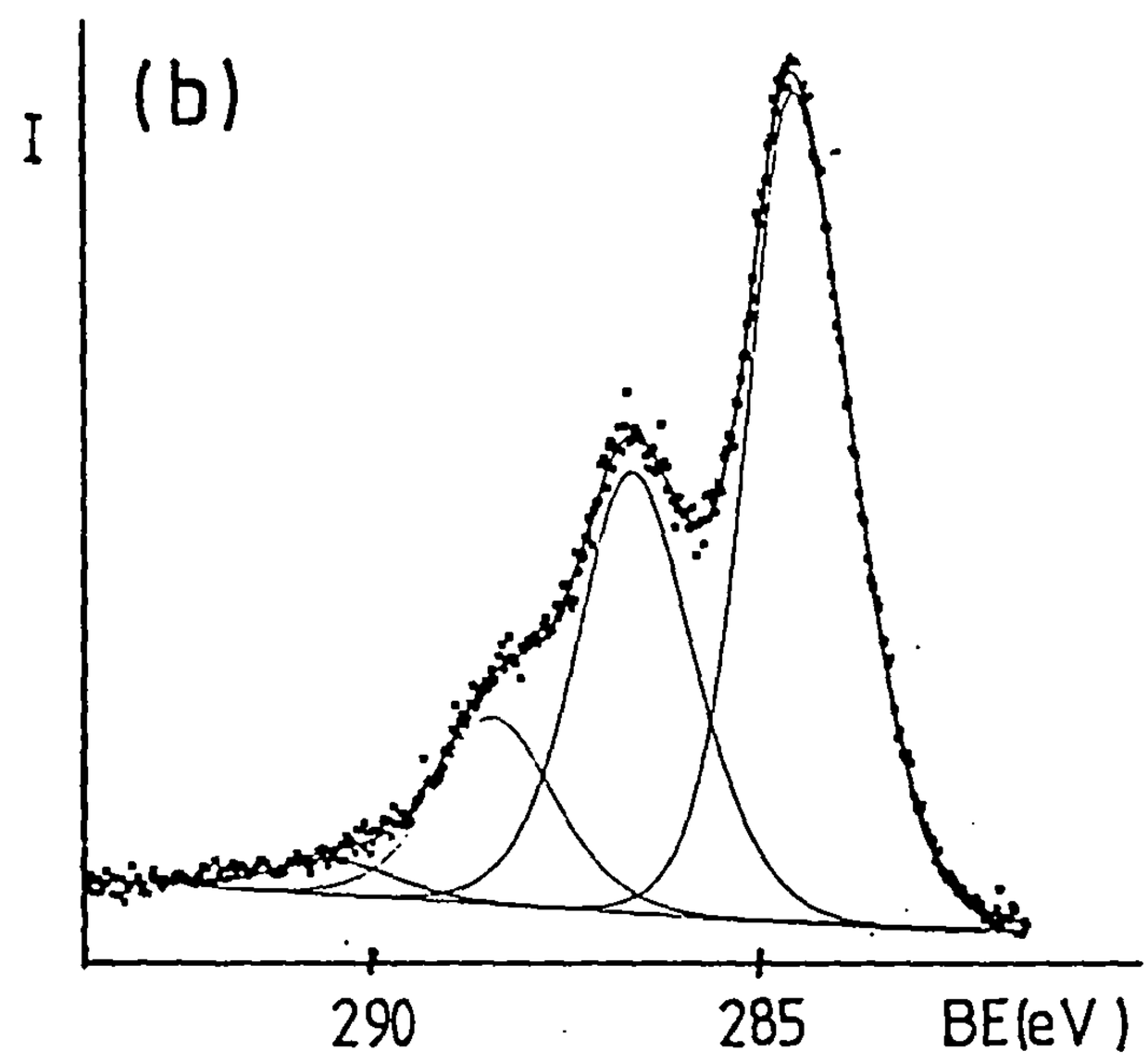

Fig.5.12 C1s Spectra of Fibres Polarised to 3V for (a) 60 secs and (b) 1 hour in H_3PO_4

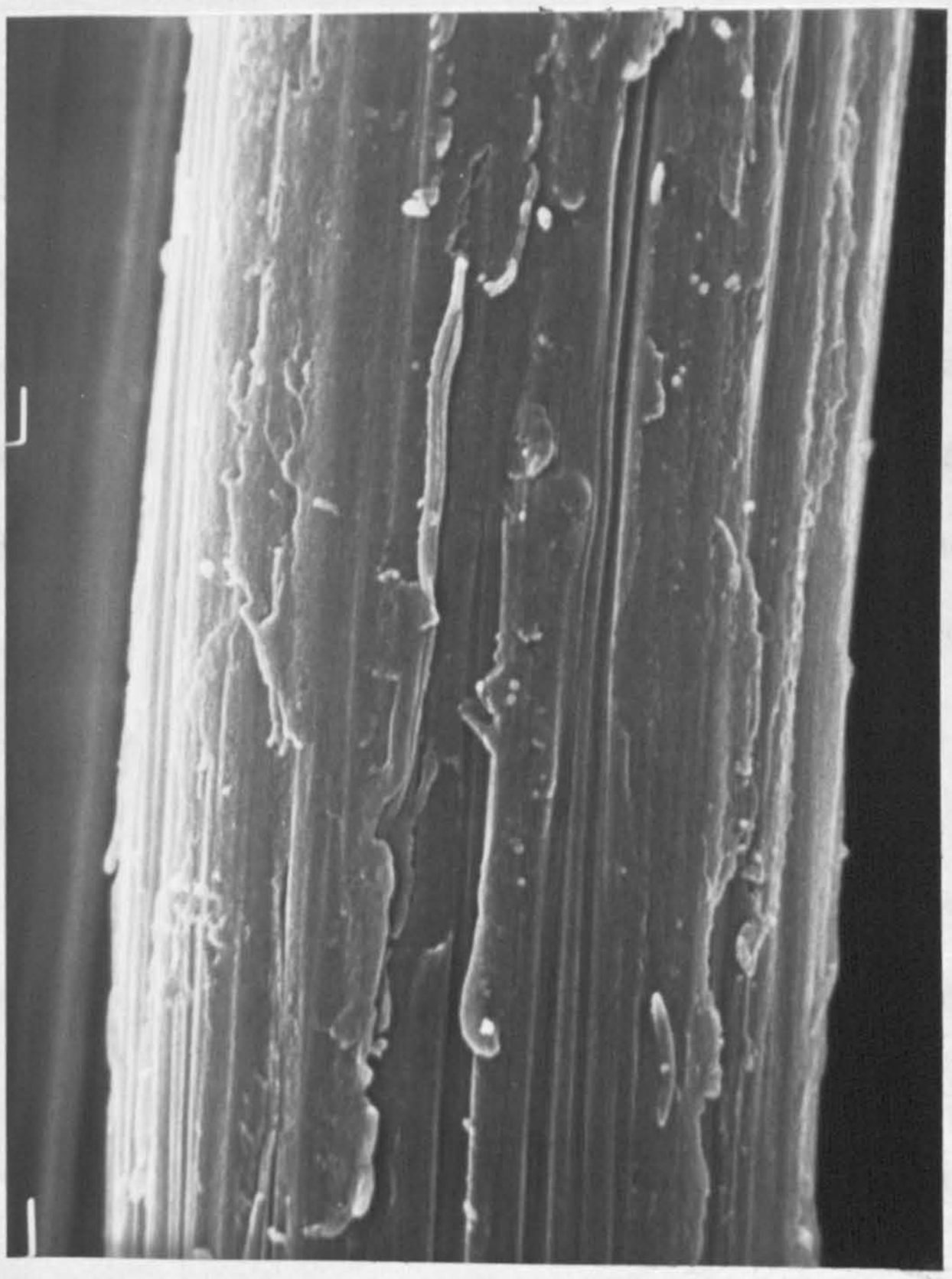

Plate 5.4 SEM Photograph of Carbon Fibres Polarised at 2·0V in Sulphuric Acid (2M)

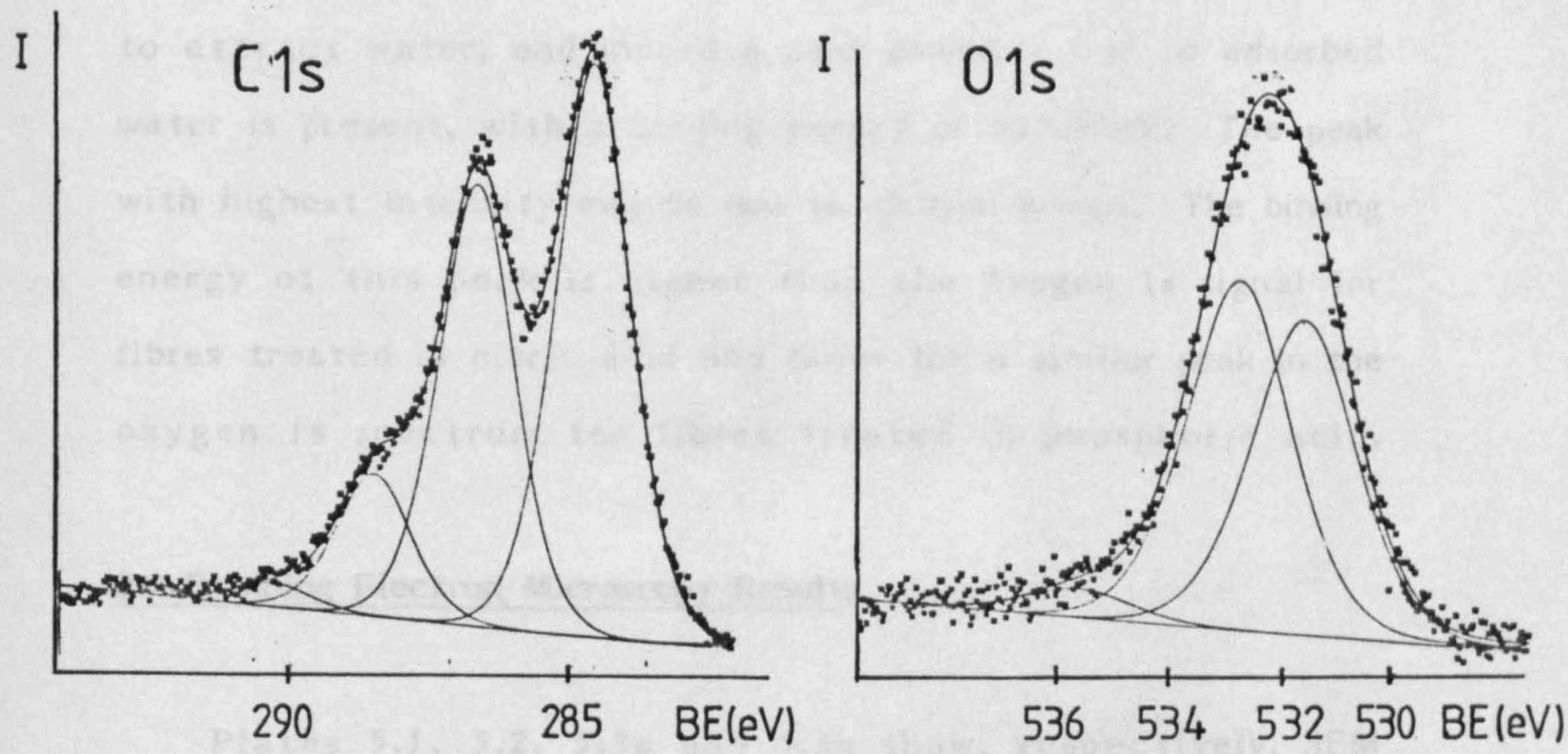

Fig.5.13 C1s and O1s Spectra of Fibres Polarised at 2·0V in Sulphuric Acid (2M)

acid. The carbon 1s main peak has lost its graphitic character due to exfoliation of the fibre surface. This can be inferred from the loss in exponential tail of this main peak. The 'oxide' region of the carbon 1s spectrum consists of three chemically shifted species with shifts of 2.15eV, 4.04eV and 5.89eV. Again, 'oxide' 1 has the greatest intensity and 'oxide' 2 only accounts for 23% of the total intensity of the chemically shifted species.

Sulphur is present in small amounts, the main sulphur 2p component having a binding energy of 168.3eV. This is in the region expected for sulphate ions (124). These sulphate ions would also be expected to give rise to an oxygen 1s signal with a binding energy of 531.6eV (±0.2eV). This is indeed the case.

The oxygen 1s spectrum consists of three resolvable peaks with binding energies 535.87, 532.86 and 531.60eV. The peak at 531.6eV corresponds to =O type groups and, as already stated, these arise from sulphate ions. These sulphate ions are likely to attract water, and indeed a peak probably due to adsorbed water is present, with a binding energy of 535.87eV. The peak with highest intensity may be due to -O type groups. The binding energy of this peak is higher than the oxygen 1s signal for fibres treated in nitric acid and lower for a similar peak in the oxygen 1s spectrum for fibres treated in phosphoric acid.

5.4 Scanning Electron Microscopy Results

Plates 5.1, 5.2, 5.3a and 5.3b show, respectively, SEM pictures of untreated fibres, fibres polarised to 3.0V for twenty minutes in nitric acid, and fibres polarised to 3.0V for

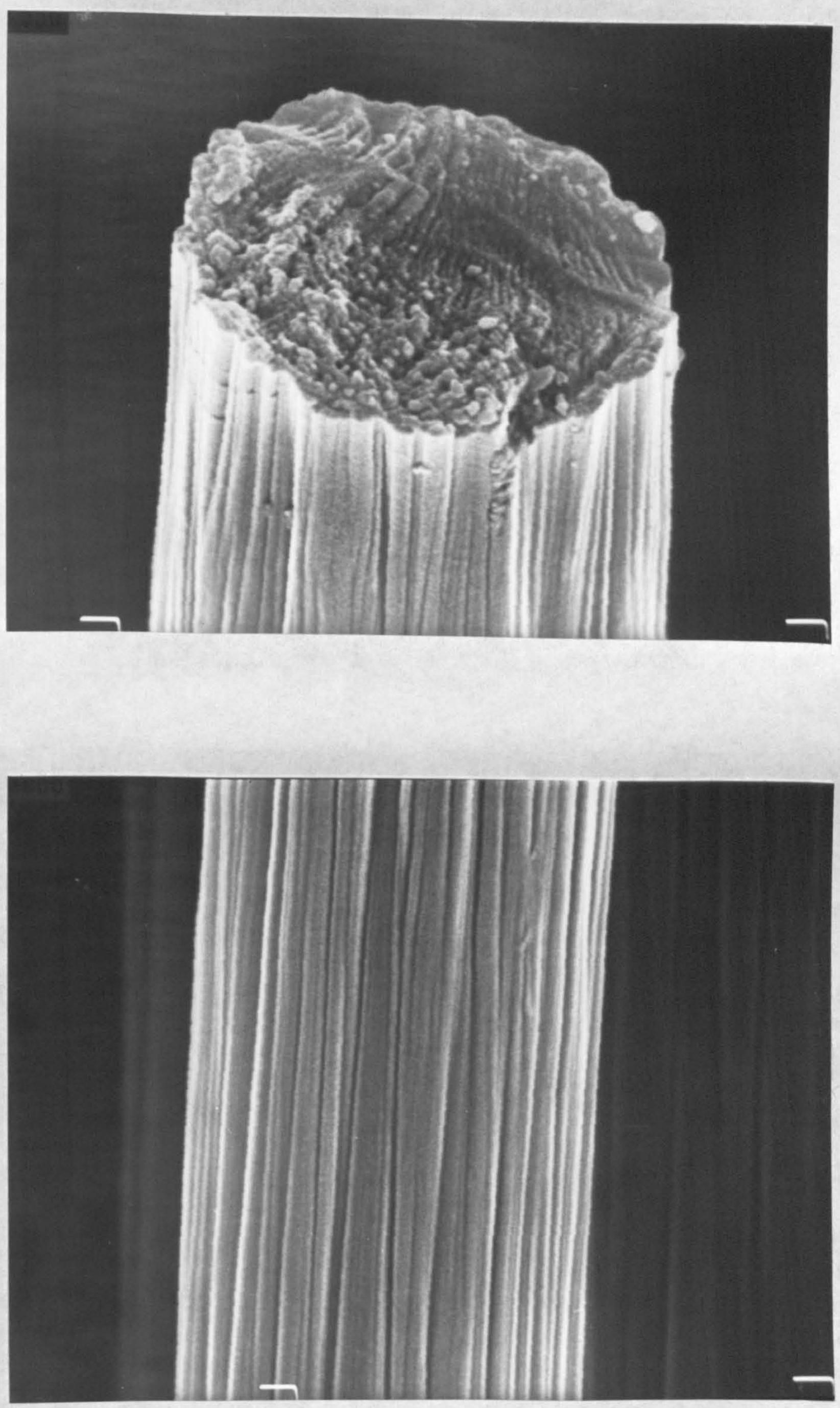

PLATE 5.1 SEM Photographs of an Untreated Carbon Fibre.

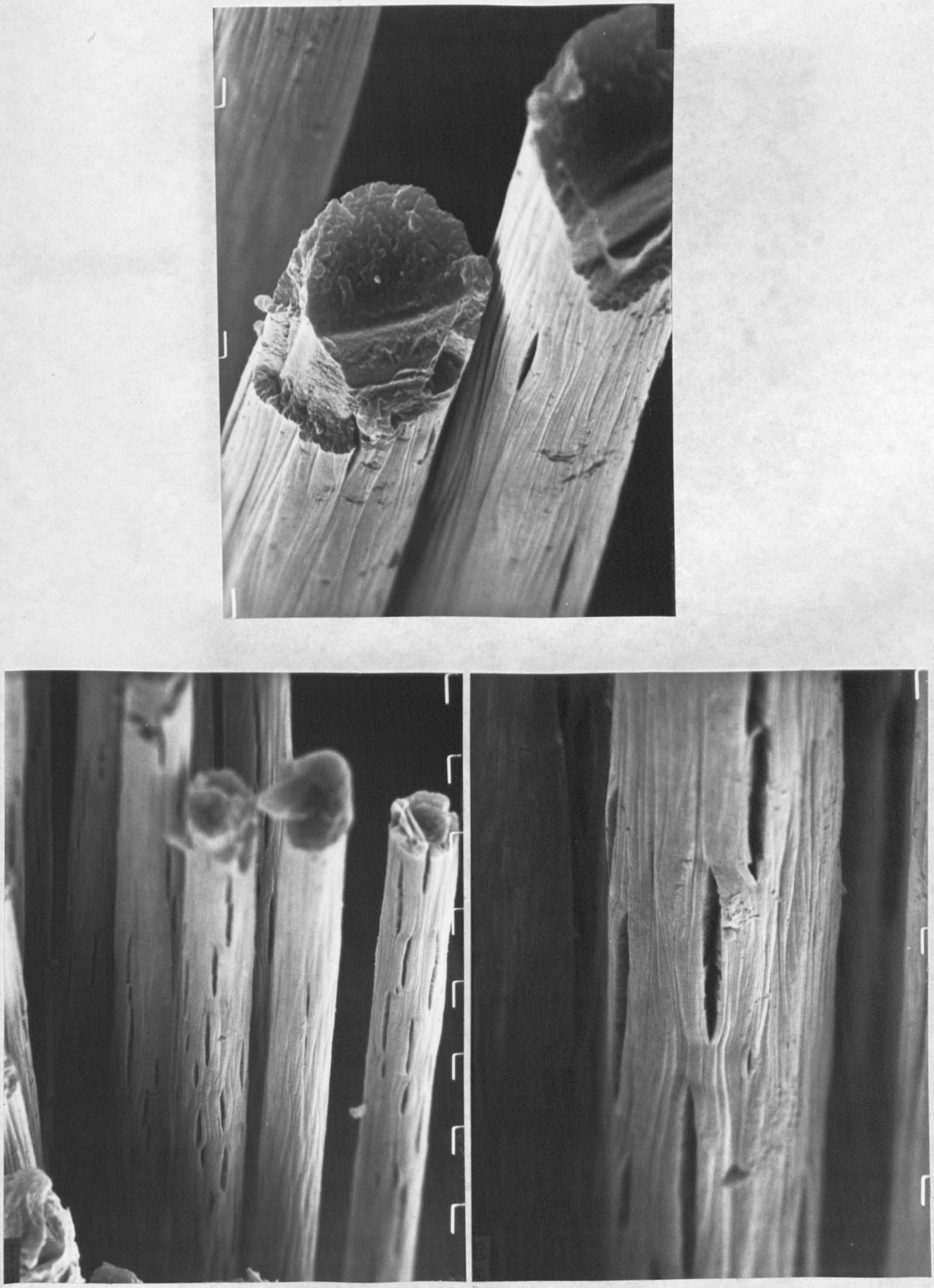

PLATE 5.2 SEM Photographs of Carbon Fibres Treated with Nitric Acid.

10 seconds

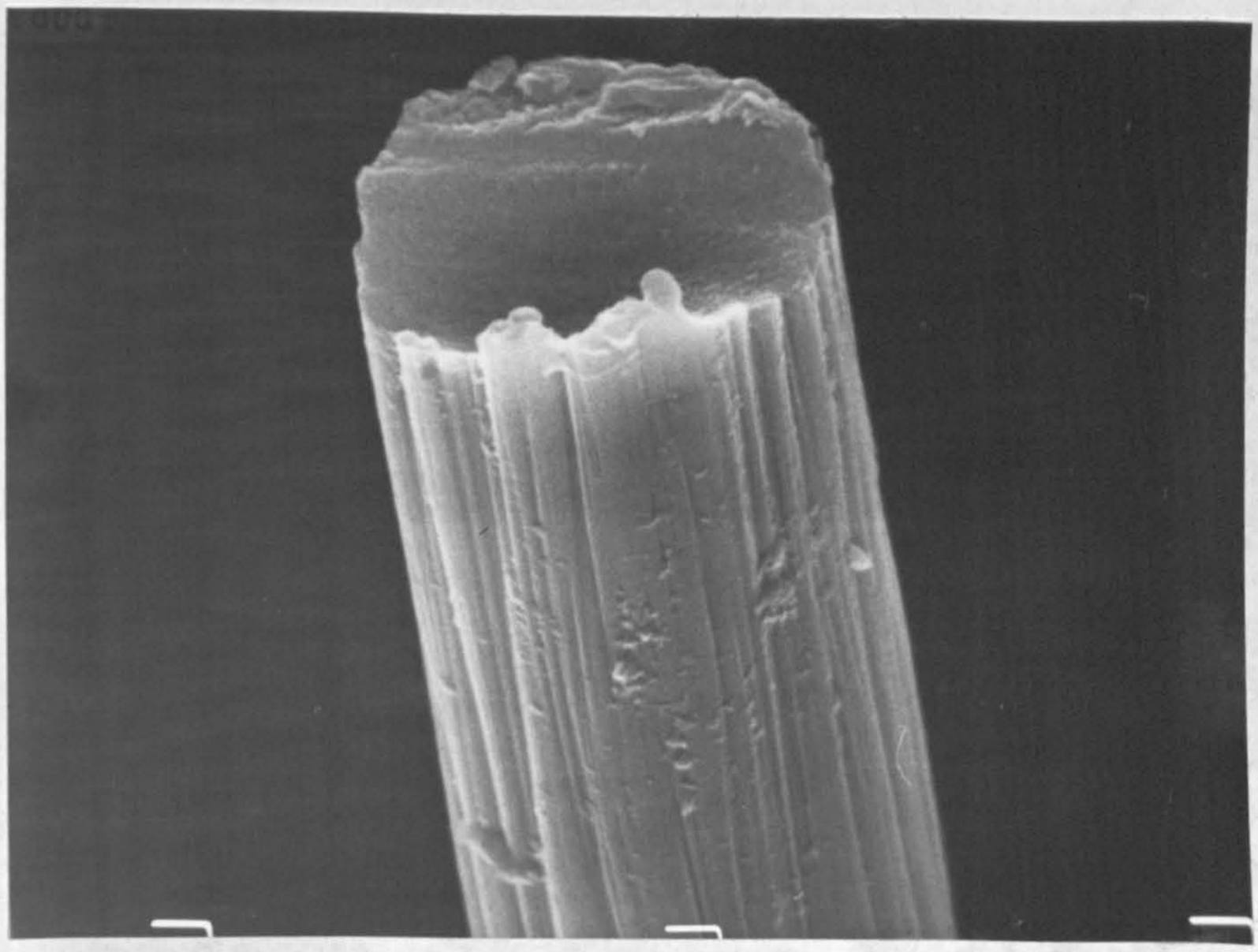

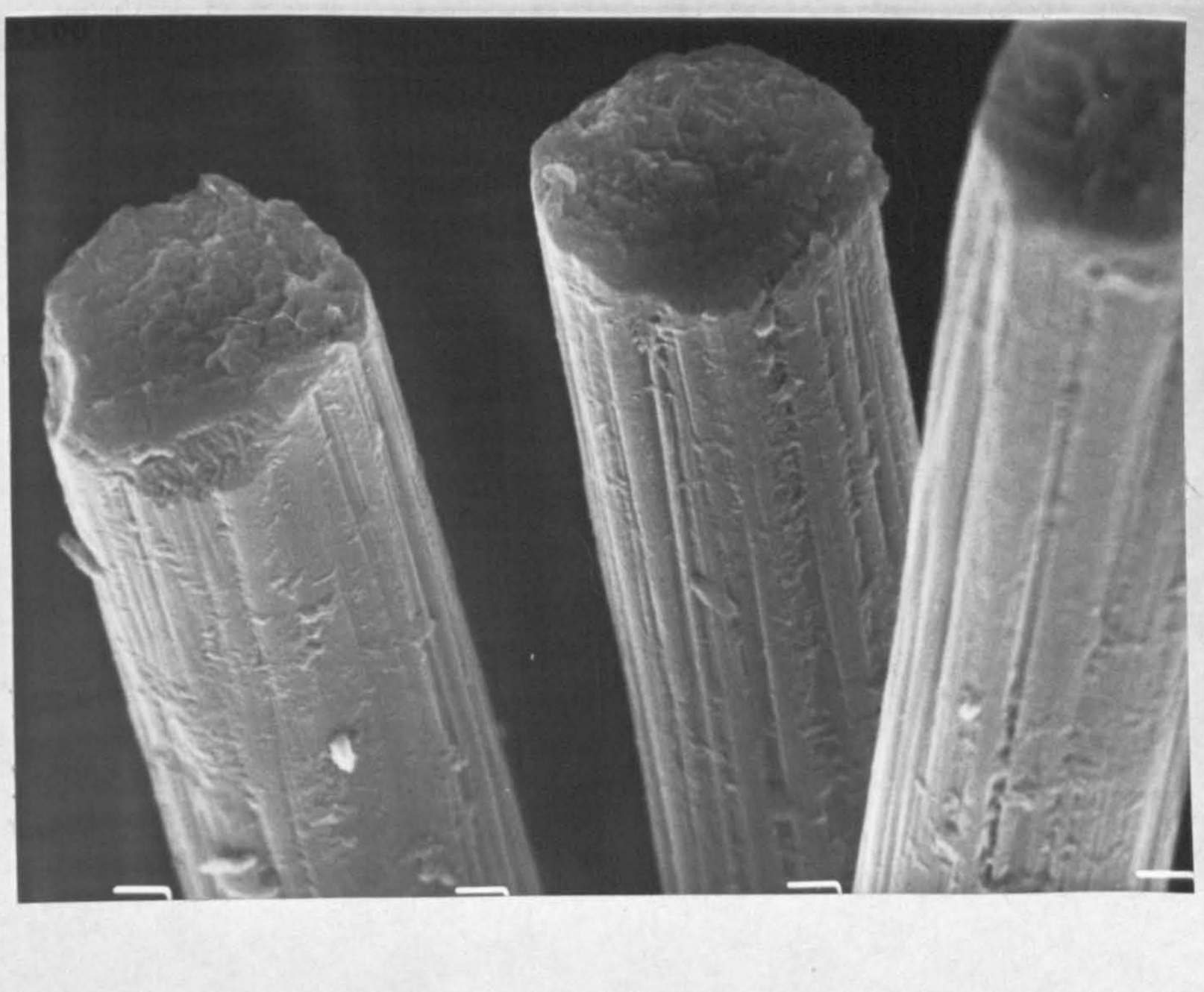

60 seconds

PLATE 5.3a SEM Photographs of Carbon Fibres Treated with Phosphoric Acid.

10 minutes

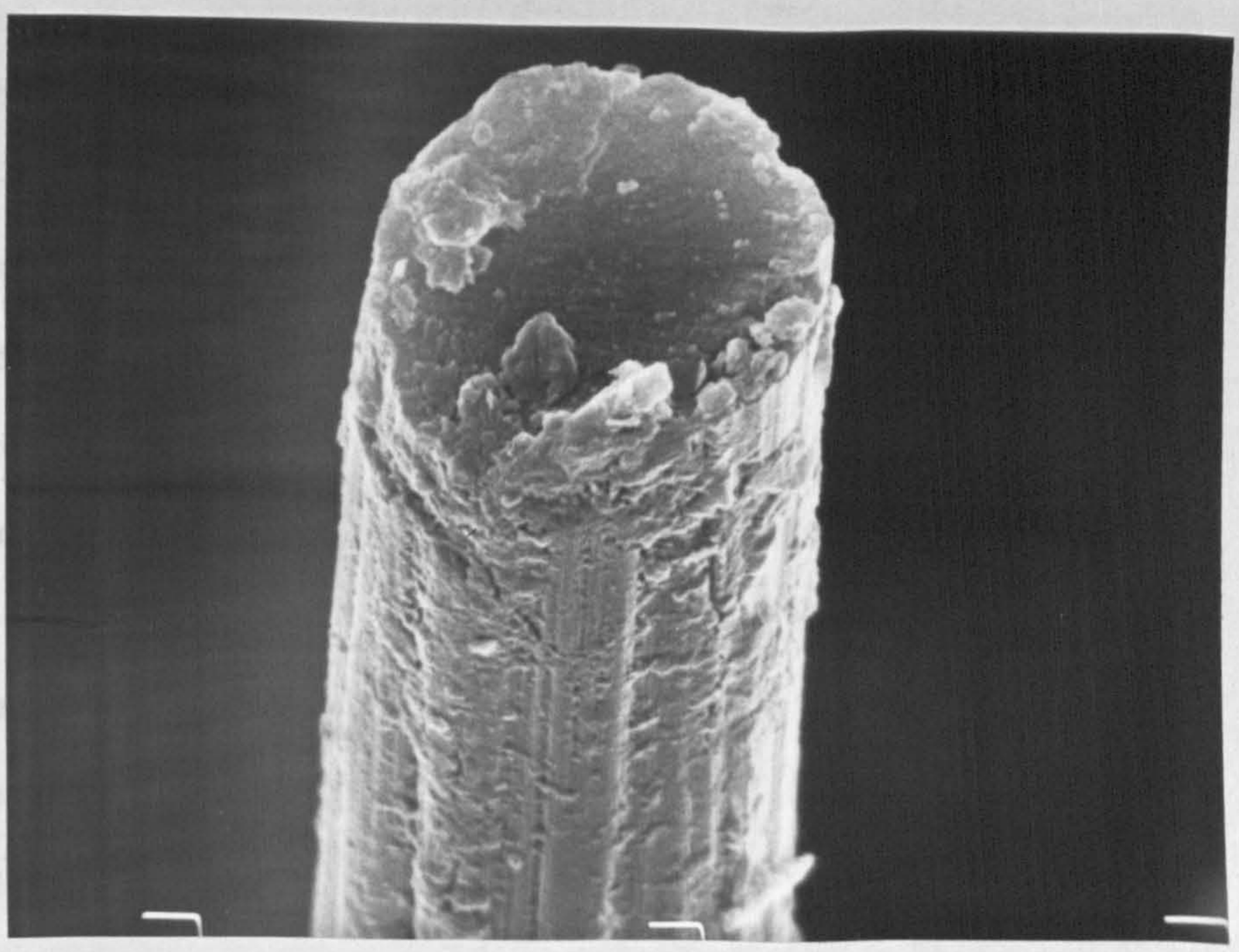

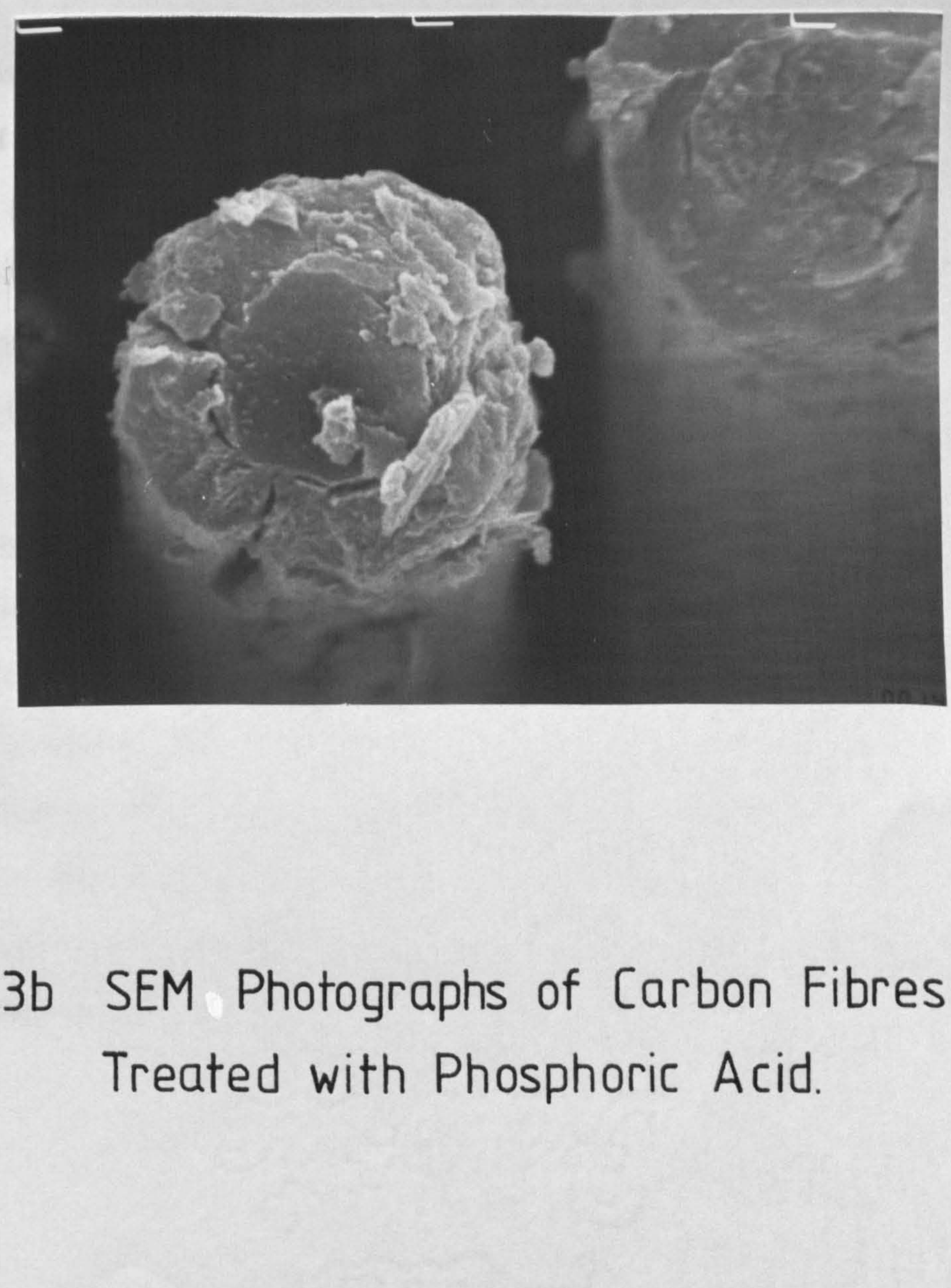

1 hour

PLATE 5.3b SEM Photographs of Carbon Fibres Treated with Phosphoric Acid.

different periods of time in phosphoric acid. There is a marked difference in surface topography between the treated and untreated fibres. The untreated fibres have long thin longitudinal grooves on the surface and appear smooth. The fibres treated in nitric acid are split parallel to the fibre axis. These splits are roughly the same length. These treated fibres have an apparently less dense outer layer compared to that of the bulk fibre. This decrease in density would cause considerable stress on the fibre surface and would give rise to the regular splitting observed on the surface. This 'less dense' outer layer is also present on fibres treated in phosphoric acid although no splitting was observed. The outer layer is slightly separated from the bulk of the fibre. Unlike fibres treated in nitric acid these fibres are blistered over their surfaces. The amount of blistering increases with treatment time. Clearly the oxidation process occurs by a different physical mechanism in the two acids. The blistering, produced even after a short treatment time, may provide a good physical key by which the resin may become attached.

Sulphuric acid causes extensive damage to the fibre surface. Flaking of surface layers occurs (see Plate 5.4). This will almost certainly lead to a weakening of the fibre/resin bond. Shindo(88) found that composites prepared from sulphuric acid treated fibres had a lower ILSS than those treated in sodium hydroxide. This 'oxide' layer does not appear to bond very well to the bulk fibre, and shear within this layer may cause the observed lowering of the ILSS .

5.5 A Comparison of the Behaviour of Type I (HM) and Type II (HT) fibres

Fig.5.14 shows the carbon 1s spectra of fibres (HM and HT) polarised at 2.0V for twenty mintutes in 2M nitric acid and 4M phosphoric acid. The amount of 'oxide' 1 produced is greater for type I fibres than for type II fibres. The opposite is the case for 'oxide' 2 where the larger amount is present on type II fibres. Both these features are seen for fibres treated in either acid. As already stated the 'oxide' 1 signal most probably arises from keto-type groups and 'oxide' 2 from carboxyl/ester type groups. The structures of type I and type II fibres differ in that there are more edge sites present in type II fibres. These edge sites are positions of unsatisfied valencies which become satisfied by the reaction of these outer atoms with other atoms such as oxygen. On electrochemical oxidation these edge site functionalities are further oxidised probably to acid type groups. If this is the case, then the larger the number of edge sites the greater will be the number of carboxyl-type functionalities produced on electrochemical oxidation. For type I fibres the carboxyl intensity ranges from 10-13% of the total intensity of the chemically shifted species. For type II, where the number of edge sites is larger than for type I fibres, the carboxyl intensity accounts for 21-29% of the total intensity of the chemically shifted species.

The oxidation of the ideal fibre surface would be one where there are no edge sites present, this will result in the formation of 'oxide' 1. This will be very similar to the oxidation of the basal plane of pyrolytic graphite, observed by

Type I

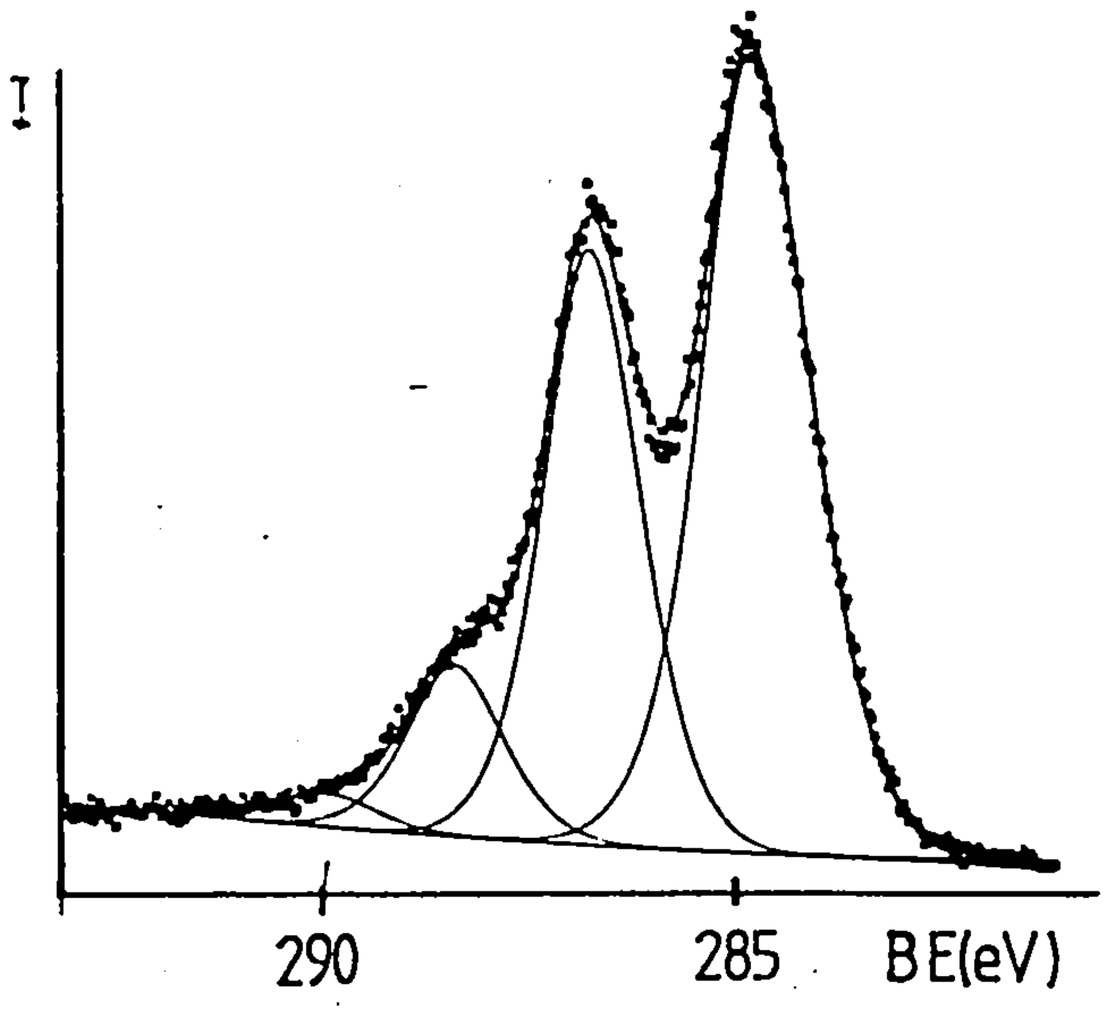

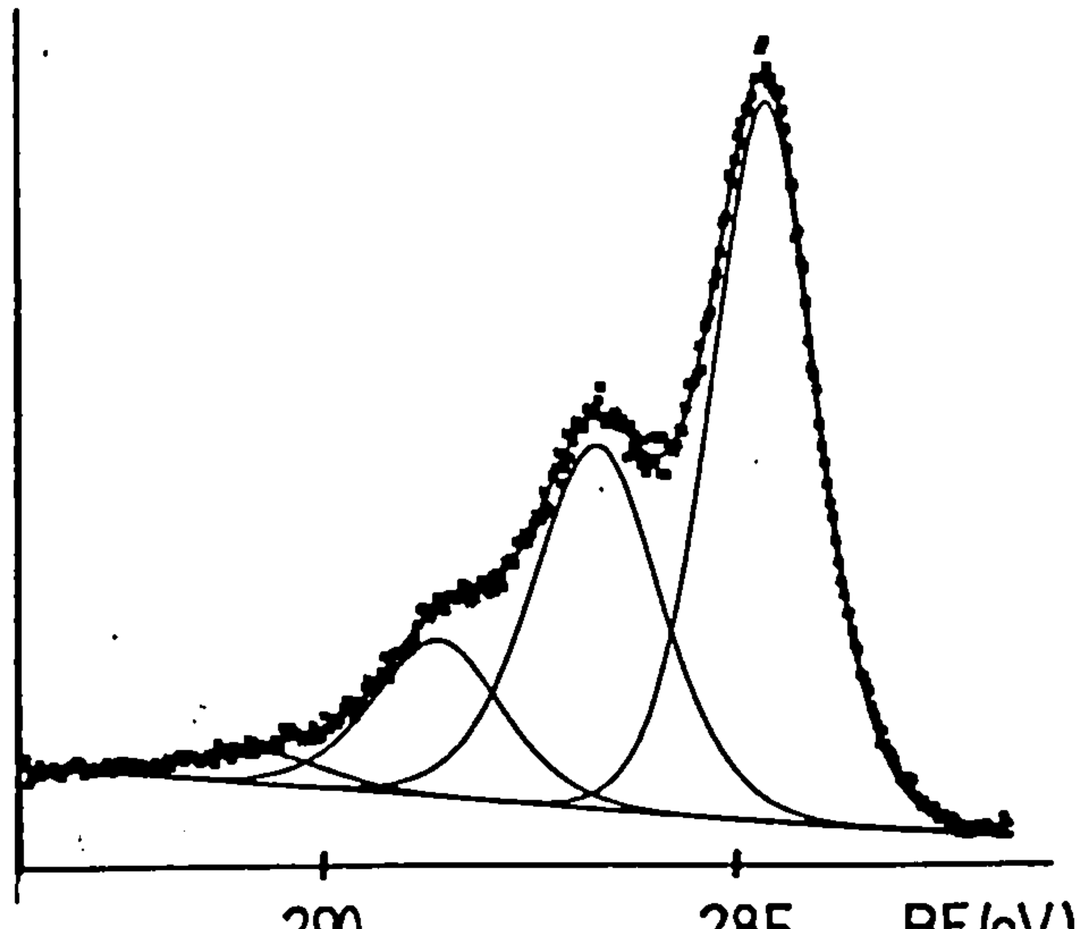

Type II

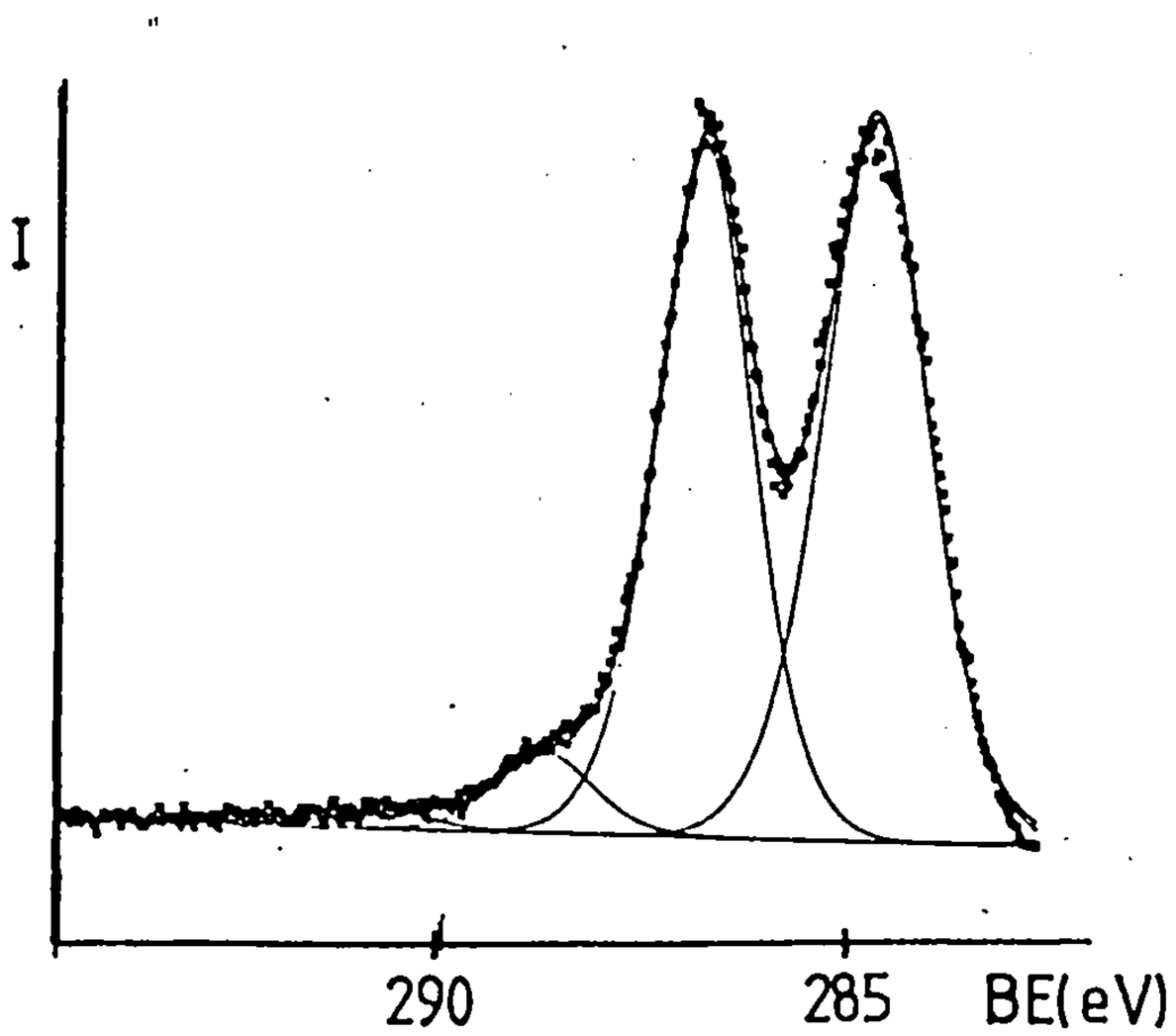

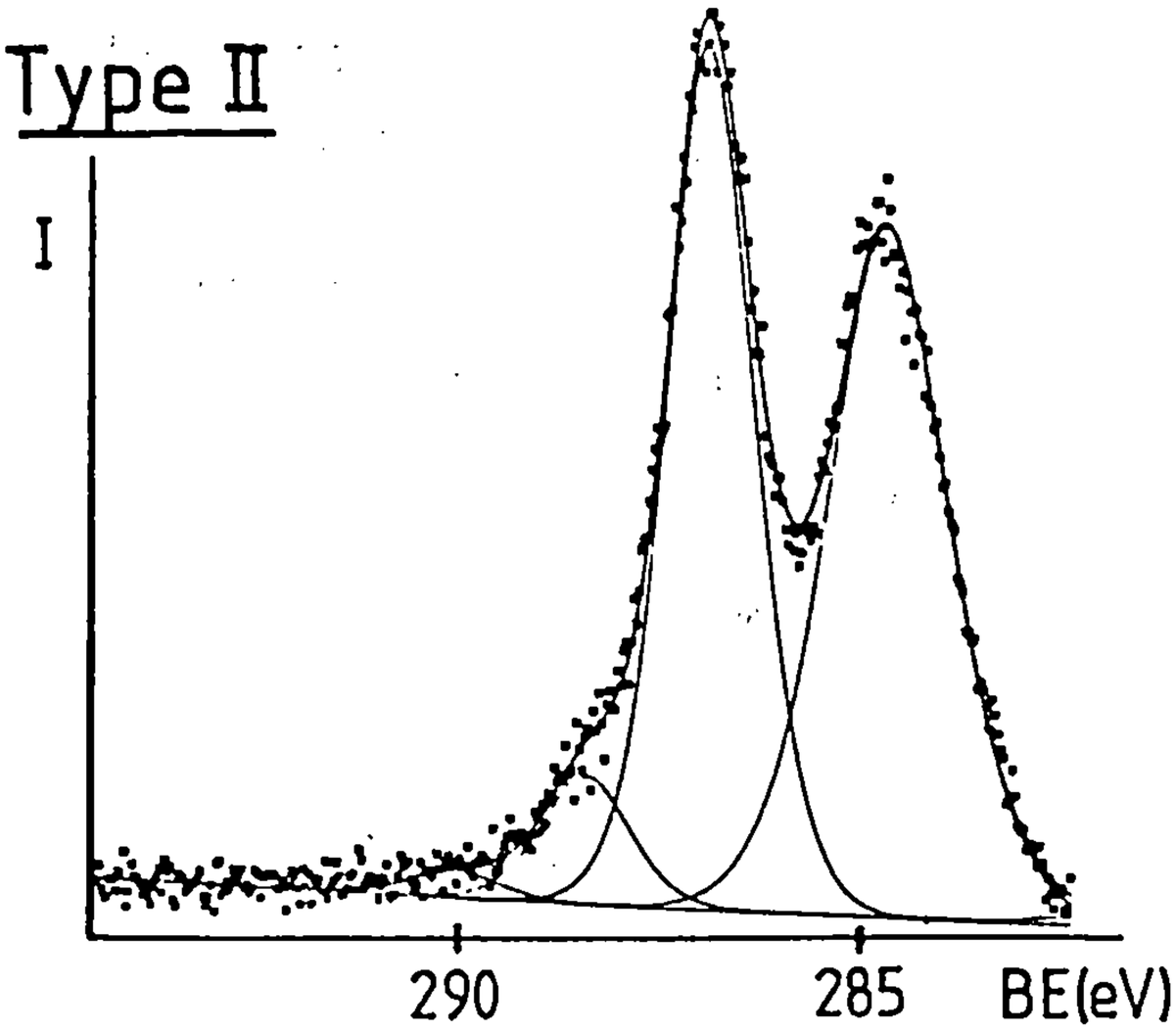

(a) Nitric Acid (2M) (b) Phosphoric Acid (4M)

Fig.5.14 C1s Spectra of Type I and Type II Fibres Polarised to 2·0V in Acid Electrolyte

Marsh et al.(78).

There is little difference between the same type of fibres treated in different acids, except that in the phosphoric acid case the anion (phosphate) is left in the oxide layer for both type I and type II fibres. Nitric acid treatment does not result in surface nitrogen functionality.

5.6 Conclusions

This chapter shows that XPS, FTIR spectroscopy, electrochemistry and SEM provide valuable and complimentary information about carbon fibre surfaces. It shows that high levels of surface treatment (ie. those producing a large amount of surface oxidation) are possible using acidic electrolyte solutions, and the 'oxide' formed is influenced by potential, reaction time and electrolyte concentration. The carbon 1s spectra collected for each acid treatment are very similar for a given potential. The major 'oxide' component arises from keto-type groups. Carboxyl/ester type groups are also produced and appear to be formed at edge sites on the fibre surface. After nitric acid treatments nitrogen was not produced on the surface, but in the case of sulphuric and phosphoric acids, sulphate and phosphate ions were detected in the oxide layer.

The considerable surface oxidation caused by electrochemical treatment clearly results in substantial topographical changes. The changes are different for treatments in different acids (see plates 5.1, 5.2, 5.3a, 5.3b and 5.4).

The properties of resulting composites must be influenced by the substantial changes in surface functionality and topography. It is most probable that the incorporation of acid anions into the surface oxide layer is undesirable because of their high polarity and their ability to attract water, as water denatures the resin.

CHAPTER 6

THE EFFECT OF pH ON SURFACE OXIDATION

6.1 Introduction

In this chapter the results of the anodic oxidation of type II fibres in sodium hydroxide and sodium nitrate are discussed. It has been found that graphite behaves differently in acidic and alkaline electrolytes. With the aid of the analysis of spectra recorded from fibres treated in solutions of different pH values, the different mechanisms of surface reactions are discussed.

An overall XPS spectrum for any of these fibres has not been shown, since they are all essentially similar showing only a carbon 1s peak and an oxygen 1s peak in the case of oxidised fibres (and in some cases sodium was present). No nitrogen 1s peak could be detected. Checks were made for any fibre surface decomposition , but no significant decomposition occurred during the collection time of the spectra reported here, except in the case of nitric acid (2M) as previously reported (see chapter 5).

6.2 Anodic Oxidation in Sodium Hydroxide Solution

The details of the spectra for fibres polarised in 0.5M sodium hydroxide are given below, though similar results were obtained at substantially greater concentrations.

6.2.1 Features of the Carbon 1s Spectra

Fig.6.1 shows the fitted carbon 1s spectra of fibres polarised to several potentials. Much less surface oxidation is seen than in previous studies in nitric acid. The 'graphitic' carbon 1s peak exhibits an asymmetric tail towards higher binding energy as seen in untreated fibres (87), but unlike the nitric case, it is retained even when the fibres are polarised to high anodic potentials. This suggests that the graphitic nature of the fibre surface remains largely intact even after vigorous electrochemical oxidation.

The XPS peak width, expressed as FWHM (full width at half maximum) of the 'graphitic' peak remains constant at 0.98eV (±0.01eV) after different electrochemical treatment, except for fibres treated at 2.5V, where the peak broadened to 1.04eV. The increased peak width at 2.5V most probably arises from unresolved β carbon peaks (147) that occur as a result of chemically shifted carbon atoms adjacent to the oxidised carbon atoms. The substantial rise in surface carboxylic/ester type groups at this potential would be expected to give a large (0.7eV) β shift (147).

The 'oxide' region of the carbon 1s spectrum consists of two main oxide components with chemical shifts of 1.6eV (±0.1eV) and 4.0eV (±.1eV) from the 'graphitic' peak. Two other components are observed with shift of 6.0eV and 6.9eV in all cases. The main components arise from alcohol (-OH) groups (1.6eV) and carboxylic acid/ester (-COOH) groups (4.0eV). This

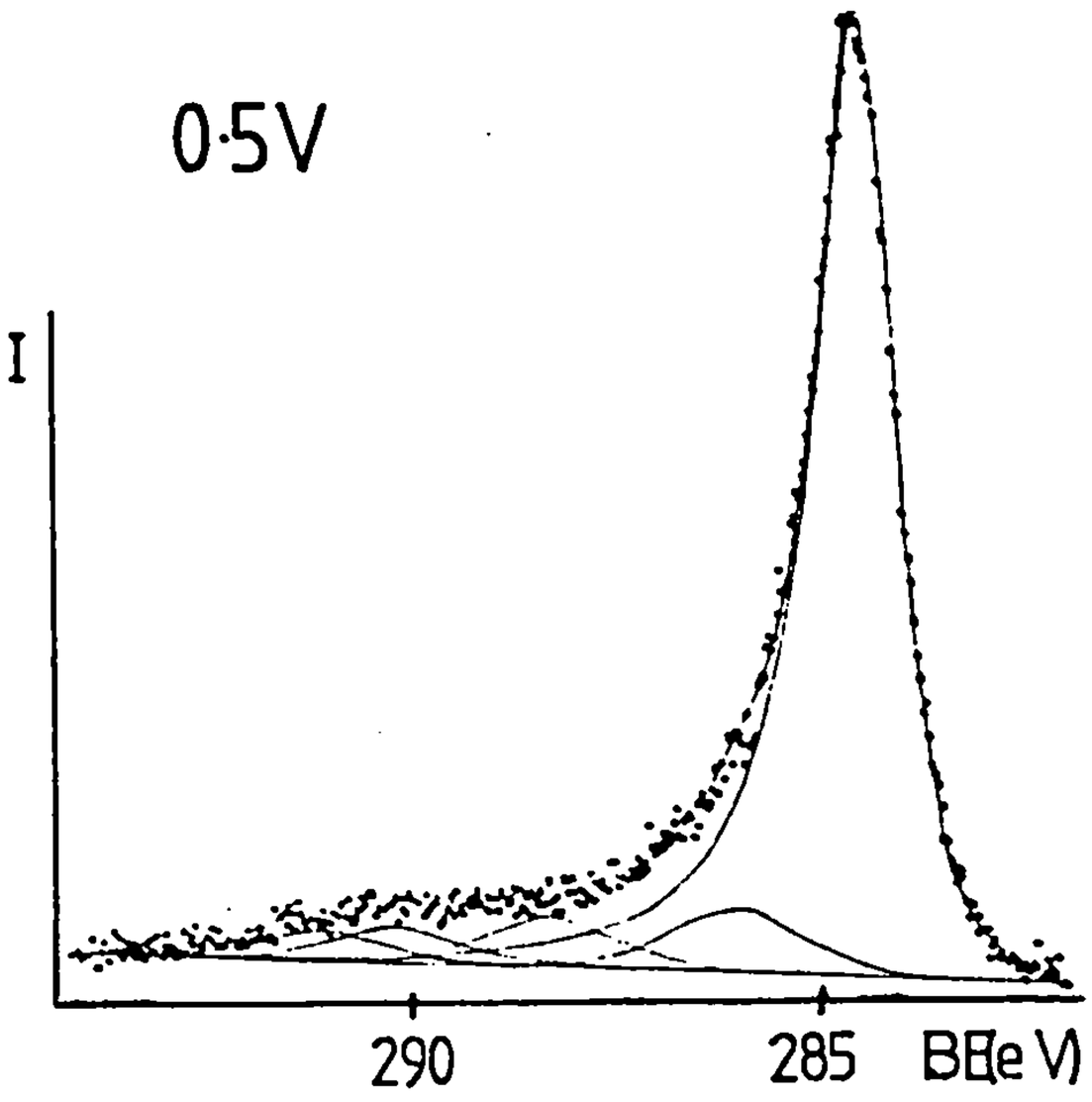

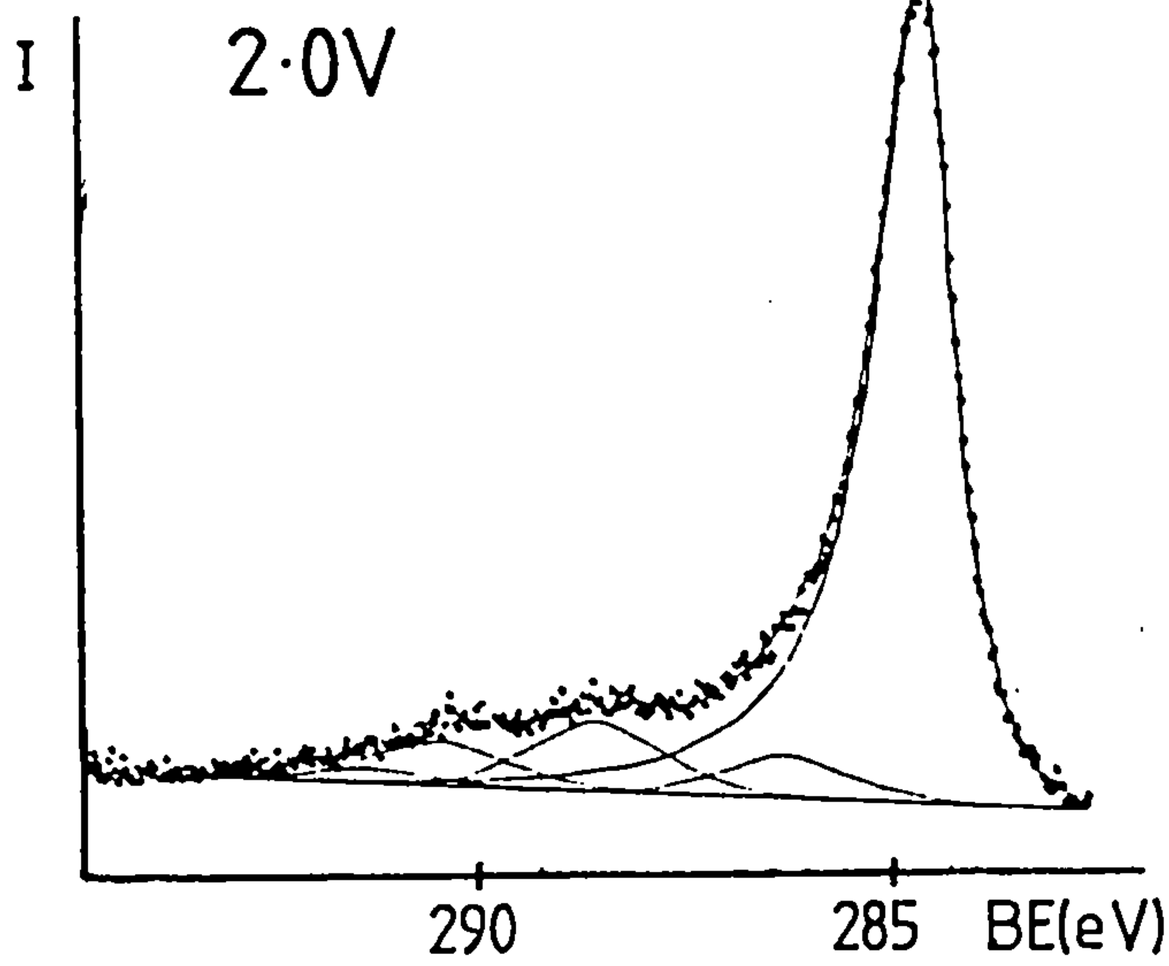

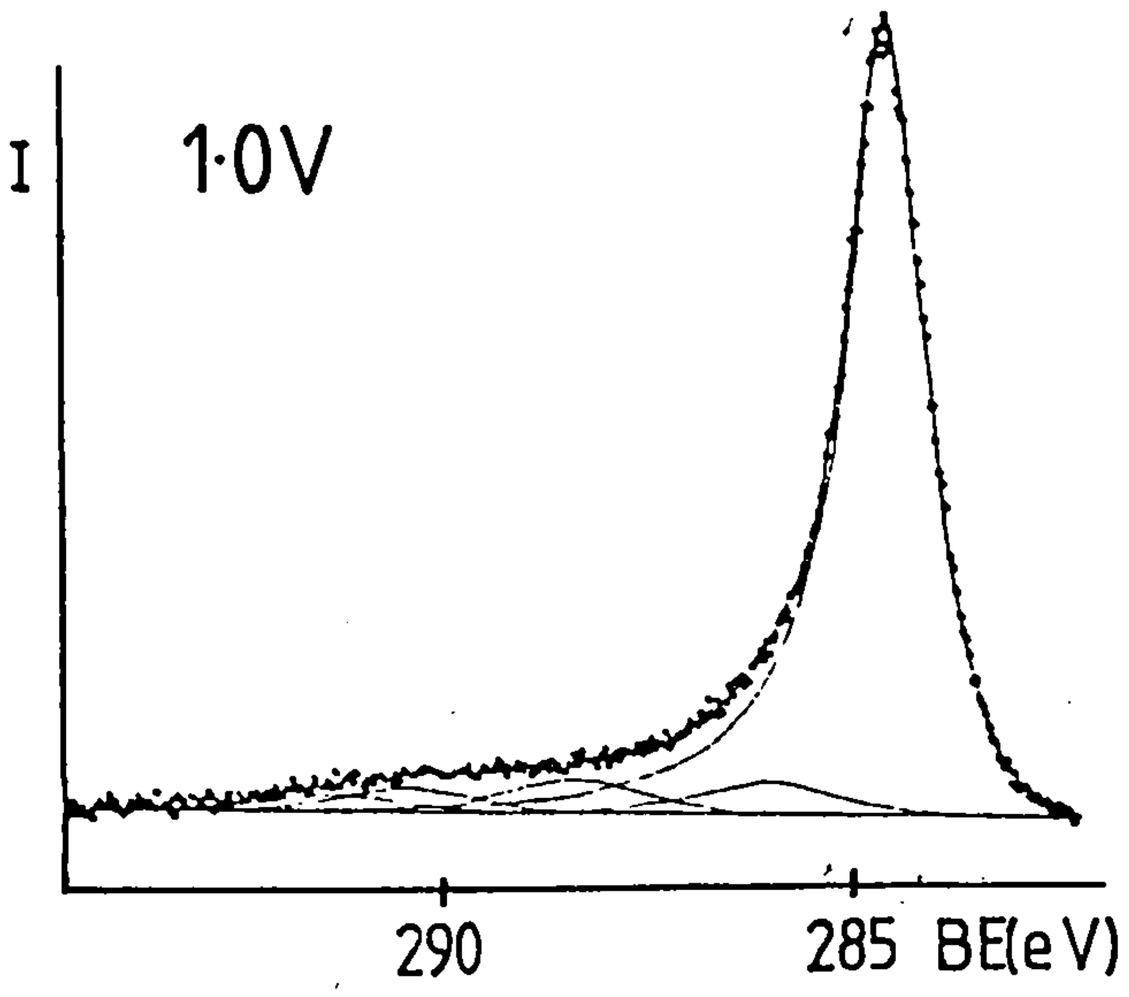

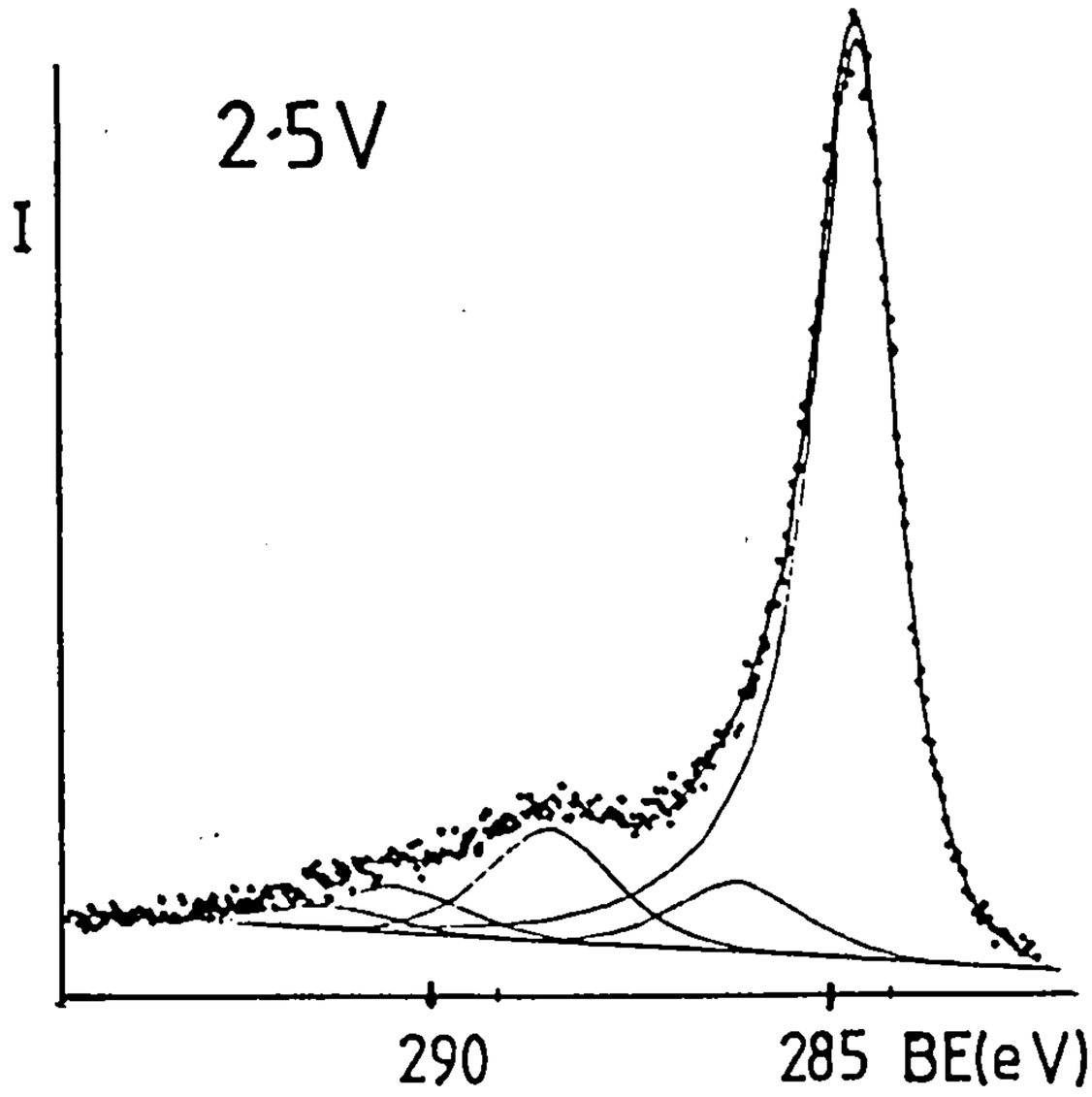

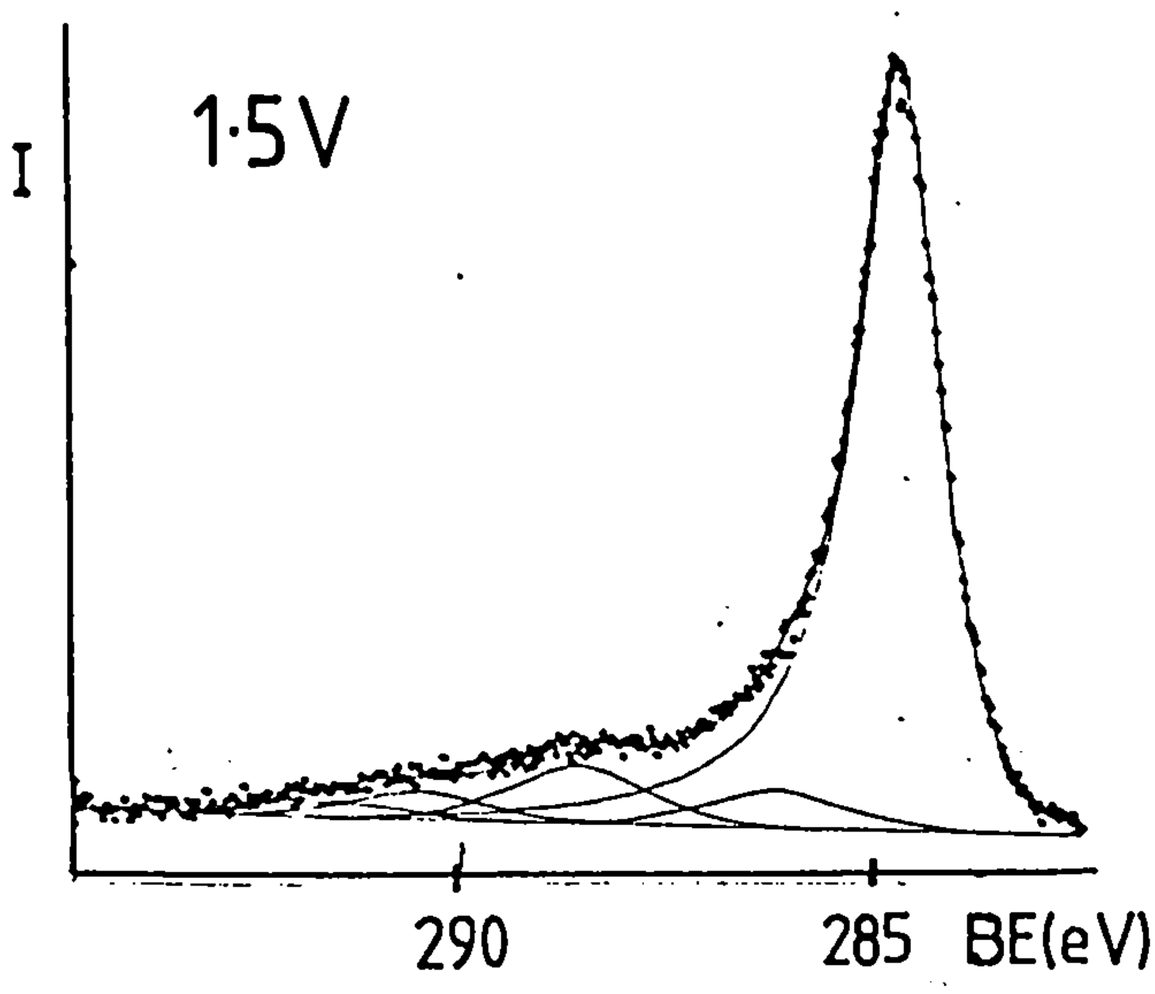

Fig.6.1 C1s Spectra of Fibres Polarised in 0·5M NaOH

alcohol functionality was not found in fibres treated in nitric acid and provides a useful clue to the surface oxidation mechanism. Table 6.1 shows how the relative peak areas with respect to the 'graphitic' peak vary with potential for each chemically shifted species. It can be seen that carboxyl type functionality predominates at the higher potentials, in contrast to the nitric acid results.

The plasmon loss feature at 6.9eV is present at each potential, although its intensity fluctuates slightly, suggesting that there may be some extrinsic character as suggested previously (section 5.2).

The assignment of the species at 6.0eV is less certain. It may arise from carbonate type groups, as carbonate is formed on graphite polarised in potassium hydroxide (80). However, it may also partly or wholely arise from π to π^* shake-up satellite contributions. Its intensity increases slightly with potential.

6.2.2 Features of the Oxygen 1s Spectra

Fig.6.2 shows the fitted oxygen 1s spectra of the fibre samples. At low potentials two oxygen species are present, but as the carboxyl functionality increases (as shown by the carbon 1s spectra) the fibres become increasingly polar leading to the physisorption of water, and so to a third peak (535.5eV) in the oxygen 1s spectrum. The two main components of the spectrum are due to >C=O (at lower binding energy, 531.6eV) and >C-O- (at higher binding energy, 533.1eV) groups on the fibre surface. These binding energies vary by 0.6eV depending upon the

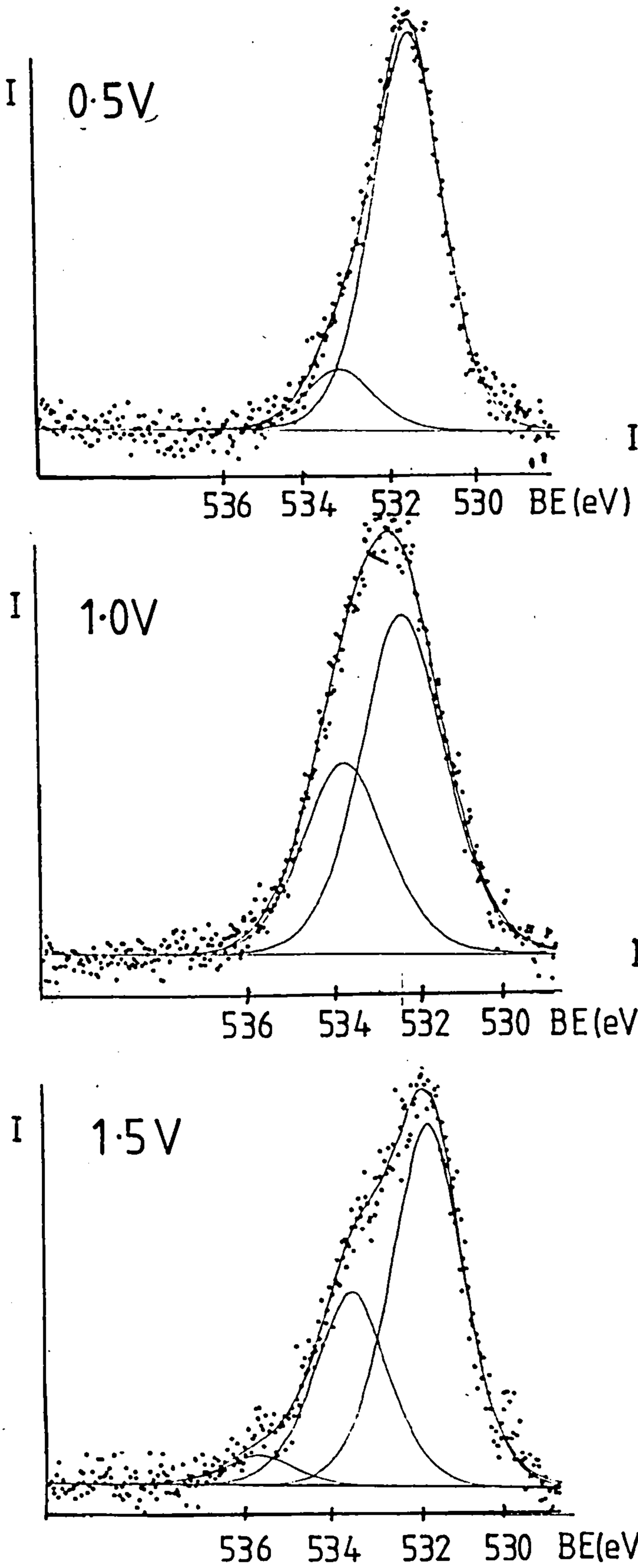

Fig.6.2 O1s Spectra of Fibres Polarised in 0·5MNaOH

TABLE 6.1

Relative C1s Peak Areas wrt the Graphitic Peak for Anodic Oxidation of Fibres in 0·5M NaOH Solution

Potential	Area Ratios Chemical Shift from Graphic Peak(eV)			
	6·9	6·0	4·0	1·6
0·5V	0·043	0·048	0·068	0·087
1·0V	0·012	0·040	0·044	0·046
1·5V	0·028	0·049	0·102	0·067
2·0V	0·006	0·072	0·099	0·061
2·5V	0·030	0·066	0·160	0·100

(Errors ±0·003)

TABLE 6.2

Curve Fitting Results of the C1s Spectra of Fibres Polarised at 2·0V in Solutions of Different pH

Solution	Chemical Shift	Relative Area	Ox 2 / Ox 1 (area ratio)	Graphitic peak FWHM
HNO_3	2·12 4·02 5·70	0·651 0·191 0·037	0·292	2·10
$NaNO_3$ pH=0·9	2·05 4·17 6·43	0·673 0·220 0·074	0·326	1·44
$NaNO_3$ pH=7·0	2·05 4·19 6·41	0·660 0·253 0·079	0·384	1·31
$NaNO_3$ pH=11·9	1·74 4·20 6·65	0·543 0·292 0·040	0·538	1·28
NaOH	1·60 4·00 6·00 6·90	0·095 0·112 0·032 0·068	1·181	1·01
Errors	(±0·01)	(±0·001)	(±0·004)	(±0·005)

potential. This variation may well arise from the steady change in suface enviroment caused by the varying amounts of the two groups as the potential is altered. At higher potentials the higher binding energy component increases until its area ratio is greater than that of the low binding energy component. This is due to the way in which the amount of -OH species increases, since the -OH contribution arises from carboxyl and alcohol groups, whereas =O species arise only from carboxyl groups.

6.2.3 Working Electrode Solution and Gases Evolved

The main gas evolved at the anode at potential above 0.5V was oxygen. At potentials above 1.5V the solution in the working electrode chamber darkened. At 3.0V the solution turned dark brown and fragments of fibre were dispersed in the solution. The UV spectra for these solutions, collected after polarisation to 2.0, 2.5 and 3.0V, showed an absorbance maximum between 204nm and 208nm (see Fig.6.3). This peak is representative of π to π transitions in conjugated carbon-carbon bonds, suggesting that small carbon fibre fragments were present in the solution.

6.2.4 SEM Studies of Fibres Treated in 2M Sodium Hydroxide

Plate 6.1 shows an SEM photograph of fibres polarised in 2M sodium hydroxide. Clearly, the physical mechanism of oxidation is different to that of fibres oxidised in acidic solutions. Circular holes are formed in the fibre surface. These appear to be the areas of localised attack and may provide suitable keying points to which the resin can adhere. There is no evidence of an 'oxide' layer as in the case of acidically treated fibres.

Plate 6·1 A Fibre after Polarisation in NaOH (2M)

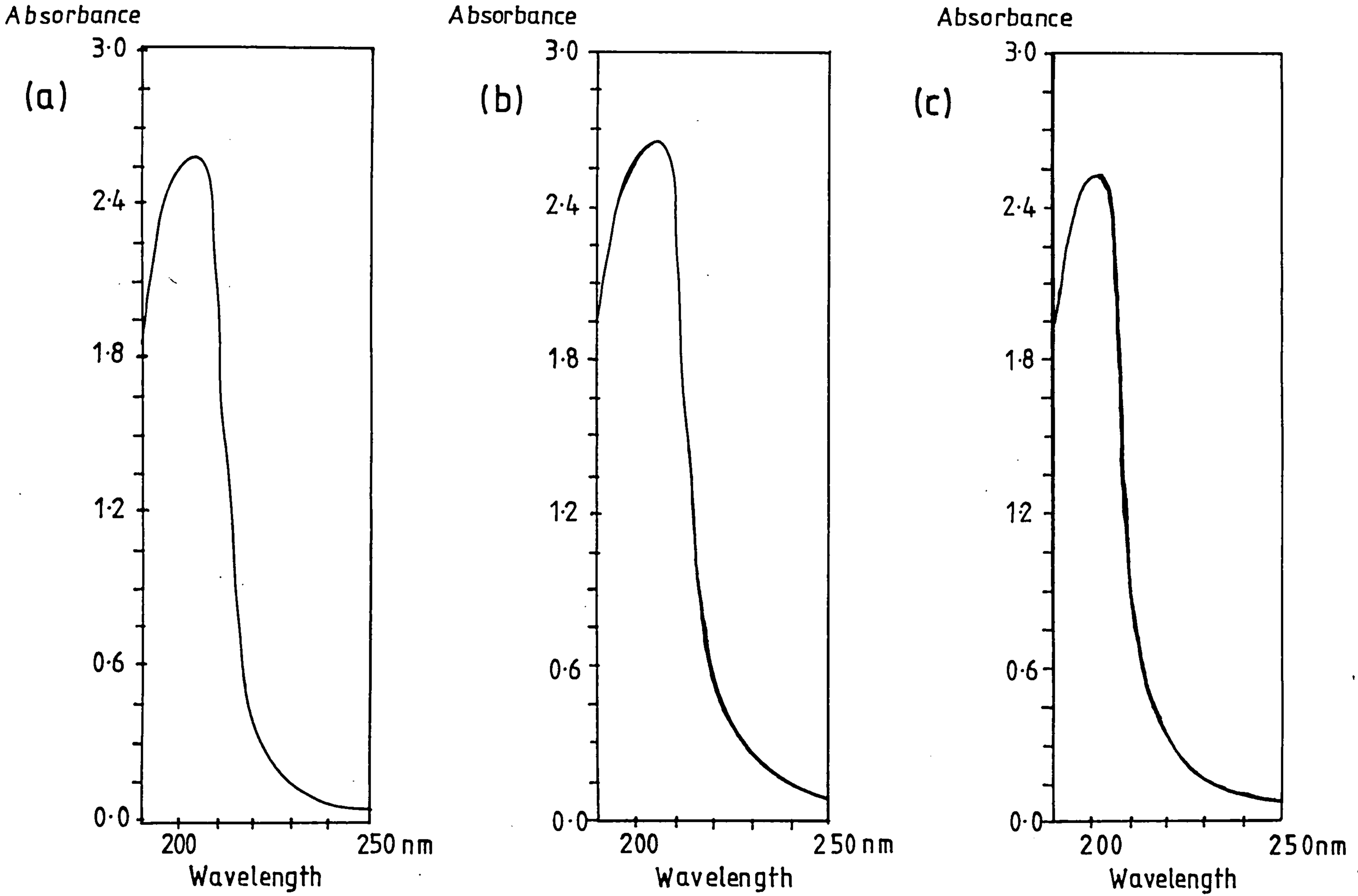

Fig.6.3 Ultraviolet Spectra of the solution in the working electrode chamber after the fibres had been polarised to (a) 2·0V, (b) 2·5V and (c) 3·0V.

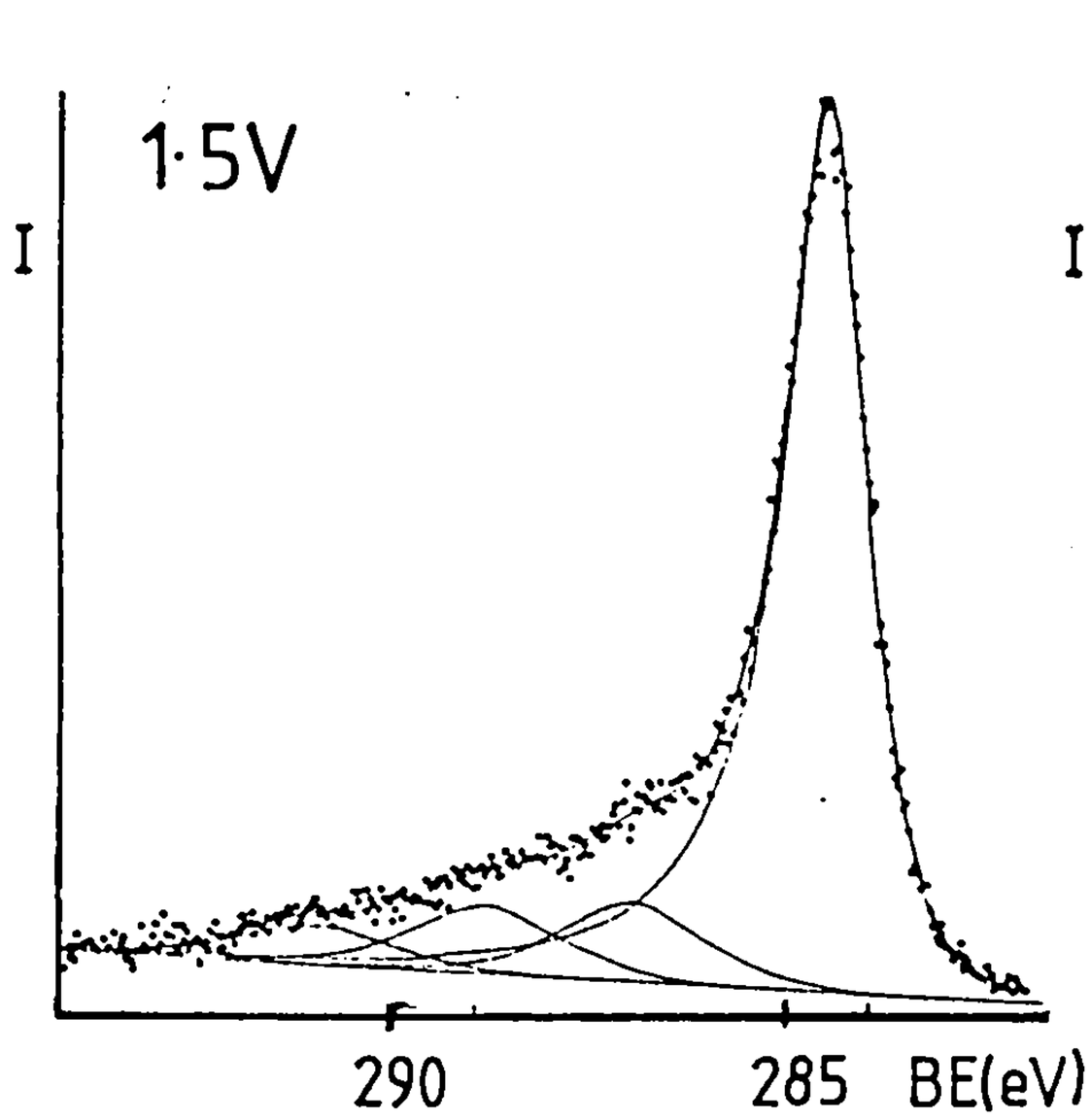

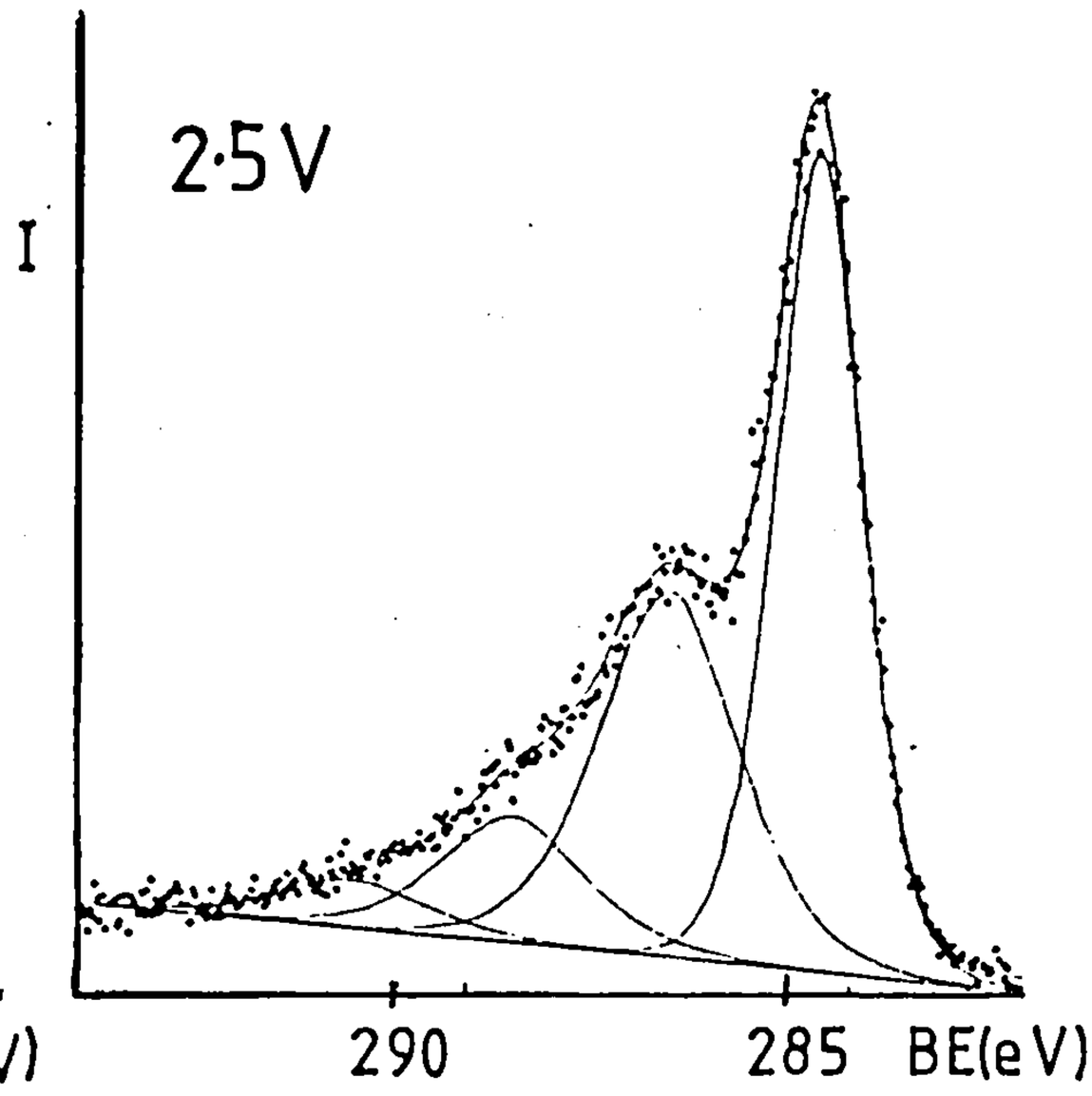

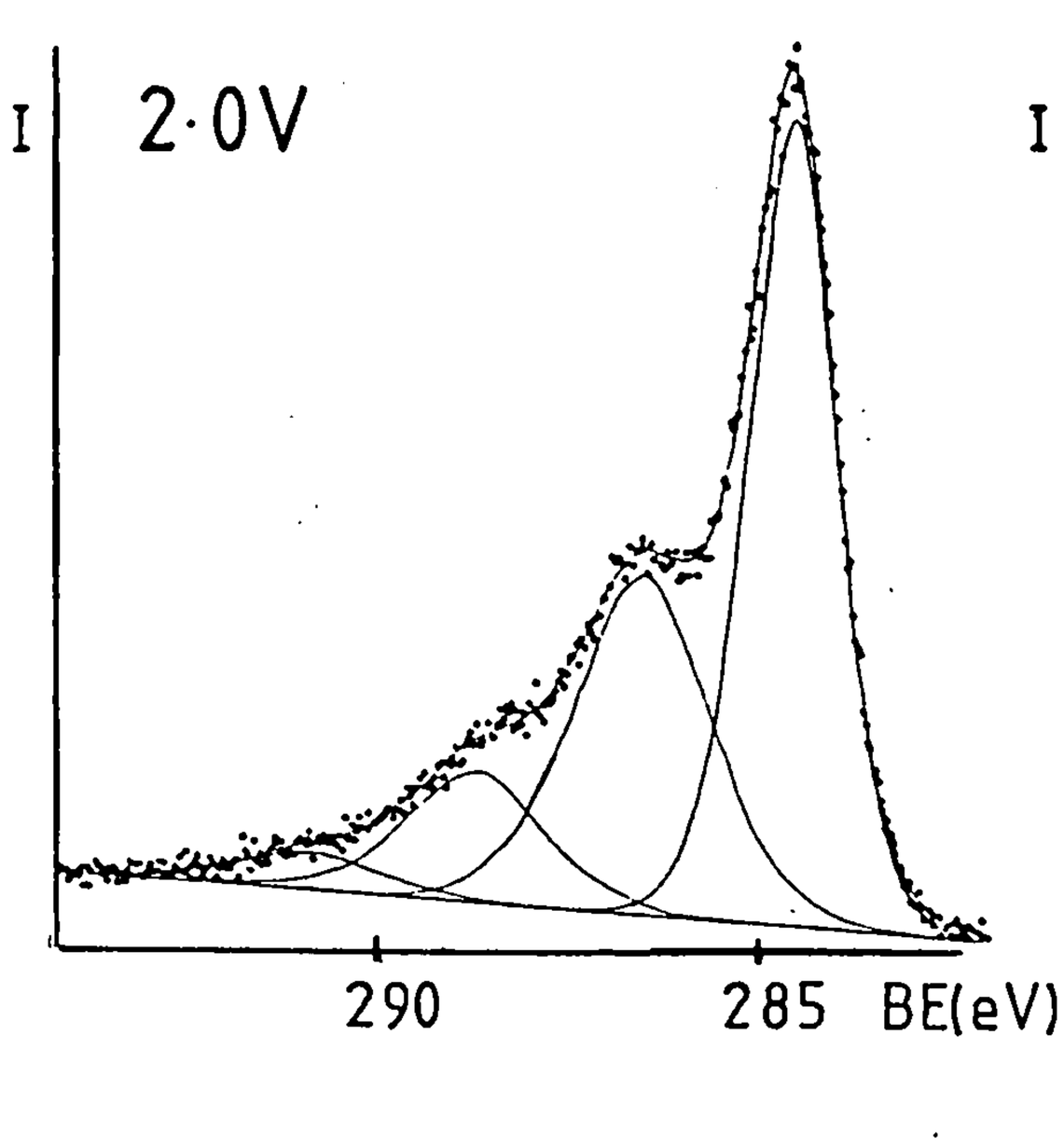

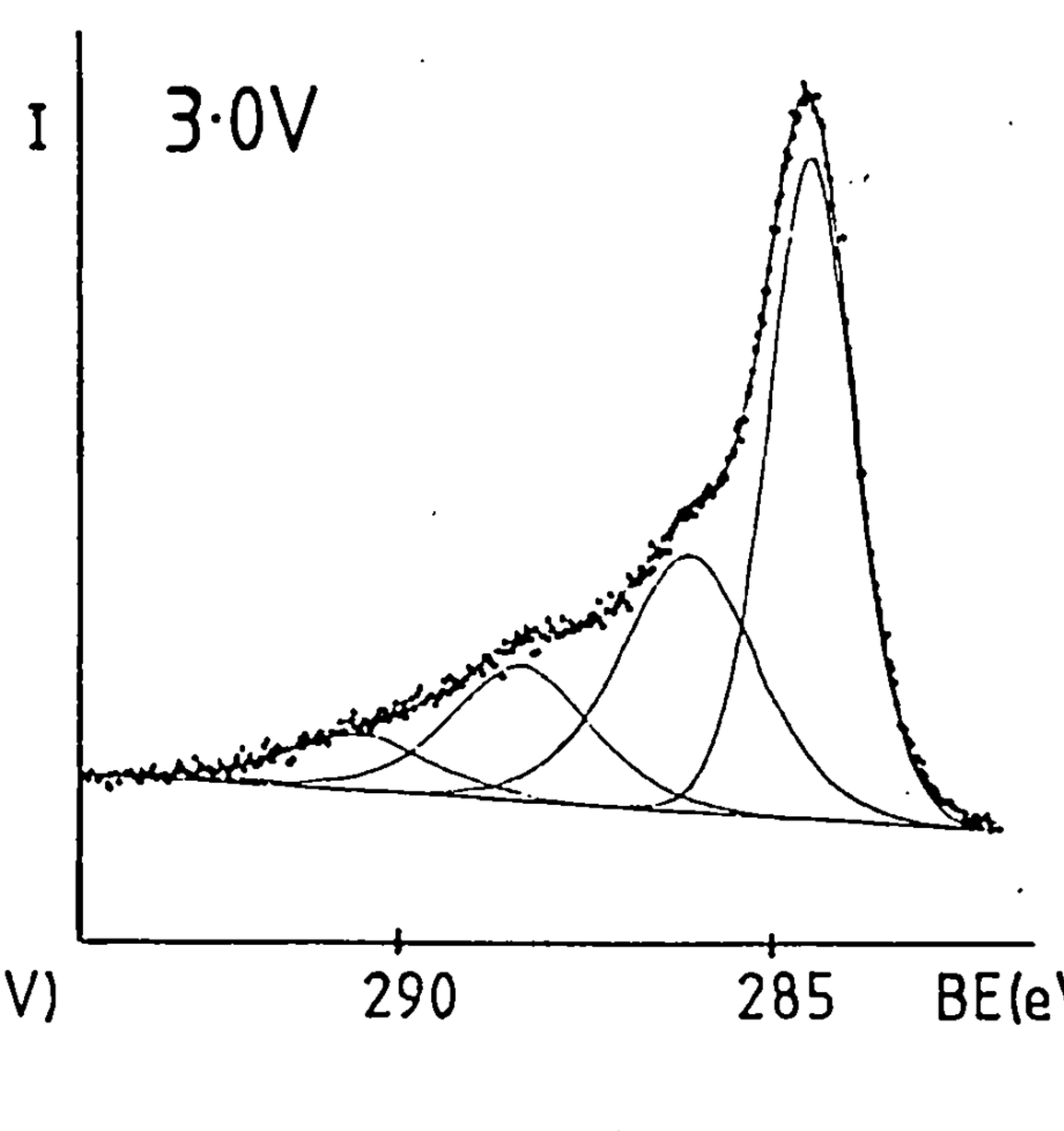

Fig. 6.4 C 1s Spectra of Fibres Polarised in $NaNO_3$

6.3 Anodic Oxidation in 2M Sodium Nitrate Solution

6.3.1 Features of the Carbon 1s Spectra

Fig.6.4 shows the fitted carbon 1s spectra of fibres polarised to several potentails. It can be seen that the overall oxidation increases with potential. These results are very similar to those found with nitric acid. The 'graphitic' carbon 1s peak loses its asymmetric tail at higher potentials due to exfoliation of the carbon fibre surface, as is seen for nitric acid treatments.

The 'oxide' region of the carbon 1s spectrum consists of three main components with chemical shifts from the 'graphitic' peak of 2.1eV (±.2eV), 4.1eV (±.1eV) and greater than 6.0eV. The first two components arise from carbonyl and related groups (2.1eV) and carboxylic acid/ester groups (4.1eV). The peak above 6.0eV arises from satellite and plasmon processes.

6.3.2 Features of the Oxygen 1s Spectra

The fitted oxygen 1s spectra of the fibre samples showed two oxygen species at all potentials with binding energies 533.0eV (±.3eV) and 531.4eV (±.3eV) due to >C-O- and >C=O groups respectively. In all spectra the peak at highest binding energy had the greater intensity, although this intensity did vary slightly (the ratio of the peak areas varied from 0.54 to 0.66).

6.4 Anodic Oxidation in Solutions of Different pH

In this section the results for solutions of different pH are discussed. Fibres were polarised to 2.0V for 20 minutes in 2M solutions of nitric acid, sodium nitrate at pH values 0.9, 7.0 and 11.9, and sodium hydroxide.

6.4.1 Features of the Carbon 1s Spectra

The 'graphitic' carbon 1s peak has a FWHM that varies from 1.01eV to 1.62eV with an exponential tail seen only in the sodium hydroxide case for the reasons discussed earlier.

The unfitted spectra (Fig.6.5) clearly show the effect of pH on the amount of surface oxidation. Acidic solutions give rise to substantial surface oxidation, in contrast to alkaline solutions.

The results of the fitted spectra are shown in Table 6.2. The relative carbon 1s area associated with carboxylic/ester groups increases with pH. The position of group 3 varies from 2.12eV to 1.6eV. It has already been stated that the values from 2.05eV to 2.12eV are due to >C=O and related groups and that the values from 1.74eV to 1.60eV are due to >C-OH type groups. In reality, the situation is probably more complex than this with the possibility of structures of the sort:

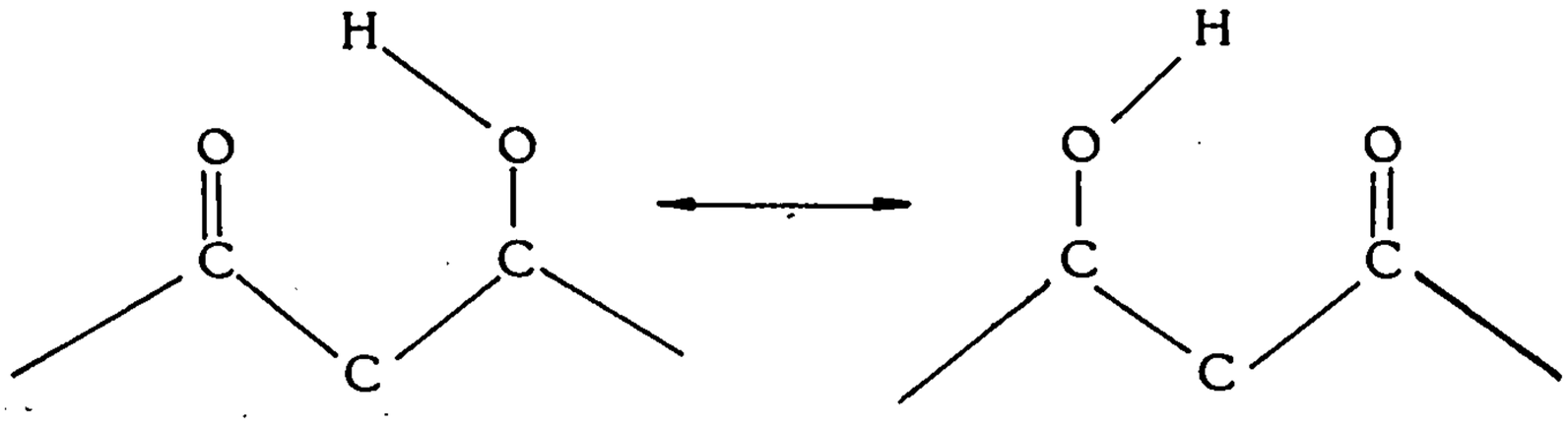

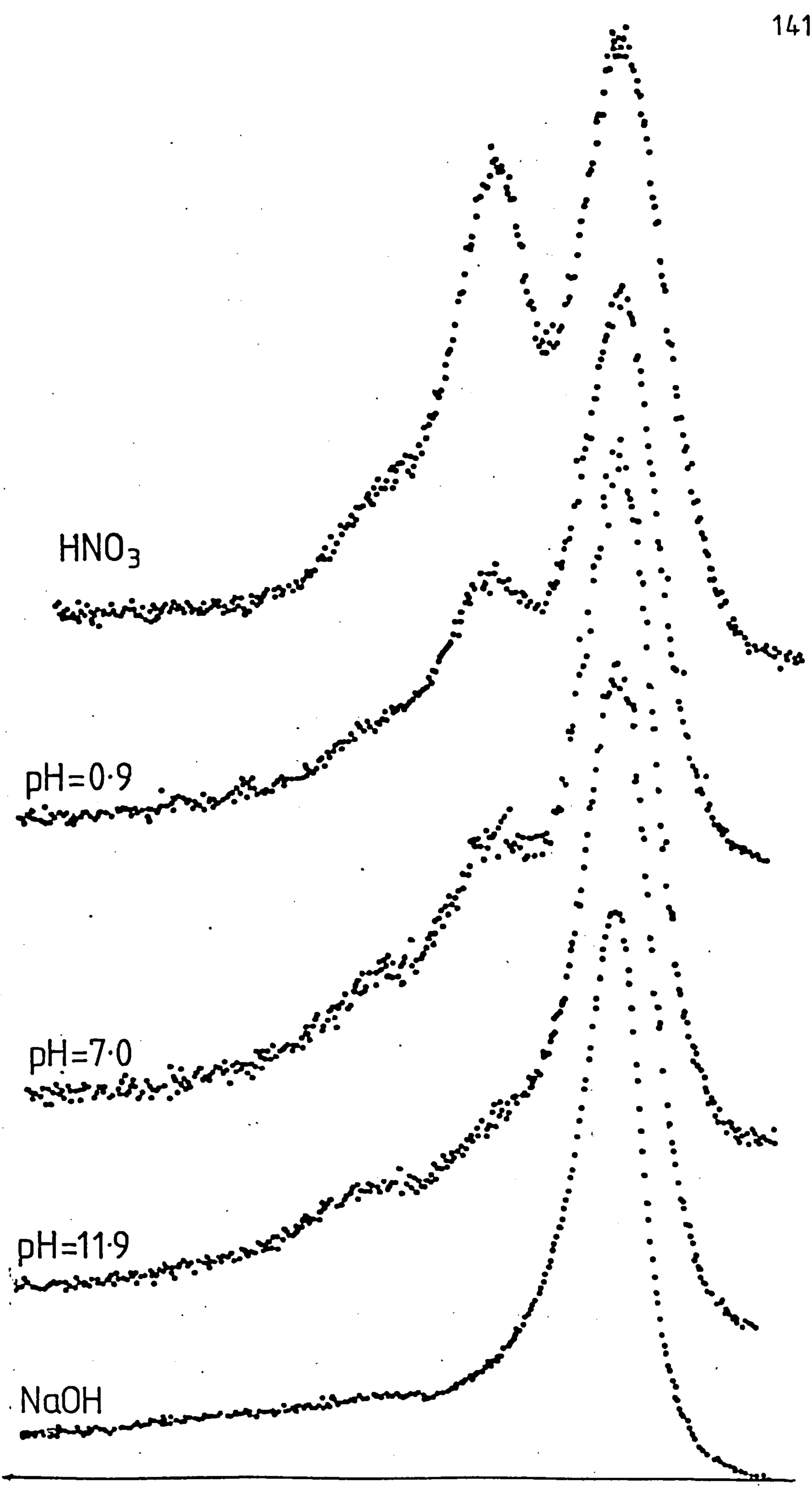

Fig.6.5 C1s Spectra of Fibres Polarised in Solutions of Different pH

where the net effect is to give two equivalent oxygen atoms leading to a carbon 1s binding energy intermediate between that of >C=O and >C-OH. A straightforward >C=O group would be expected to have a shift of around 3.0eV (87,95,96), and a straightforward >C-OH group around 1.6eV (see Appendix). Thus in this case intermediate behaviour is exhibited for all but the highest pH values. This resembles the situation discussed by Boehm (159) for graphitic oxide, which can be electrochemically produced from graphite in aqueous nitric acid (149).

6.4.2 Features of the Oxygen 1s Spectra

Fig.6.6 shows the fitted oxygen 1s spectra of the fibres samples, and Table 6.3 summarises the results. The oxygen 1s spectra reflect the changes observed in the carbon 1s region. Thus if one considers the two equivalent oxygen atoms discussed above and supposes that they have a binding energy intermediate (532.3eV) between that of >C=O (531.5eV) and >C-OH (533.5eV), then the changes seen in Table 6.3 can be understood. At low pH one peak is seen at 532.3eV, but as the pH is increased more individual >C-OH and >C=O character is present, so that for sodium hydroxide separate peaks are seen for these two groups. In addition, carboxylic acid/ester groups are present and were seen (carbon 1s region) to increase with pH. These groups would be expected to give two peak at 531.6eV and 533.1eV (the case of 0.5M sodium hydroxide is given above) and would overlap with the peaks above. The absence of any peak at around 533eV in the 2M nitric acid case (when the relative amount of carboxylic acid/ester groups is at its lowest) may be due to differences in

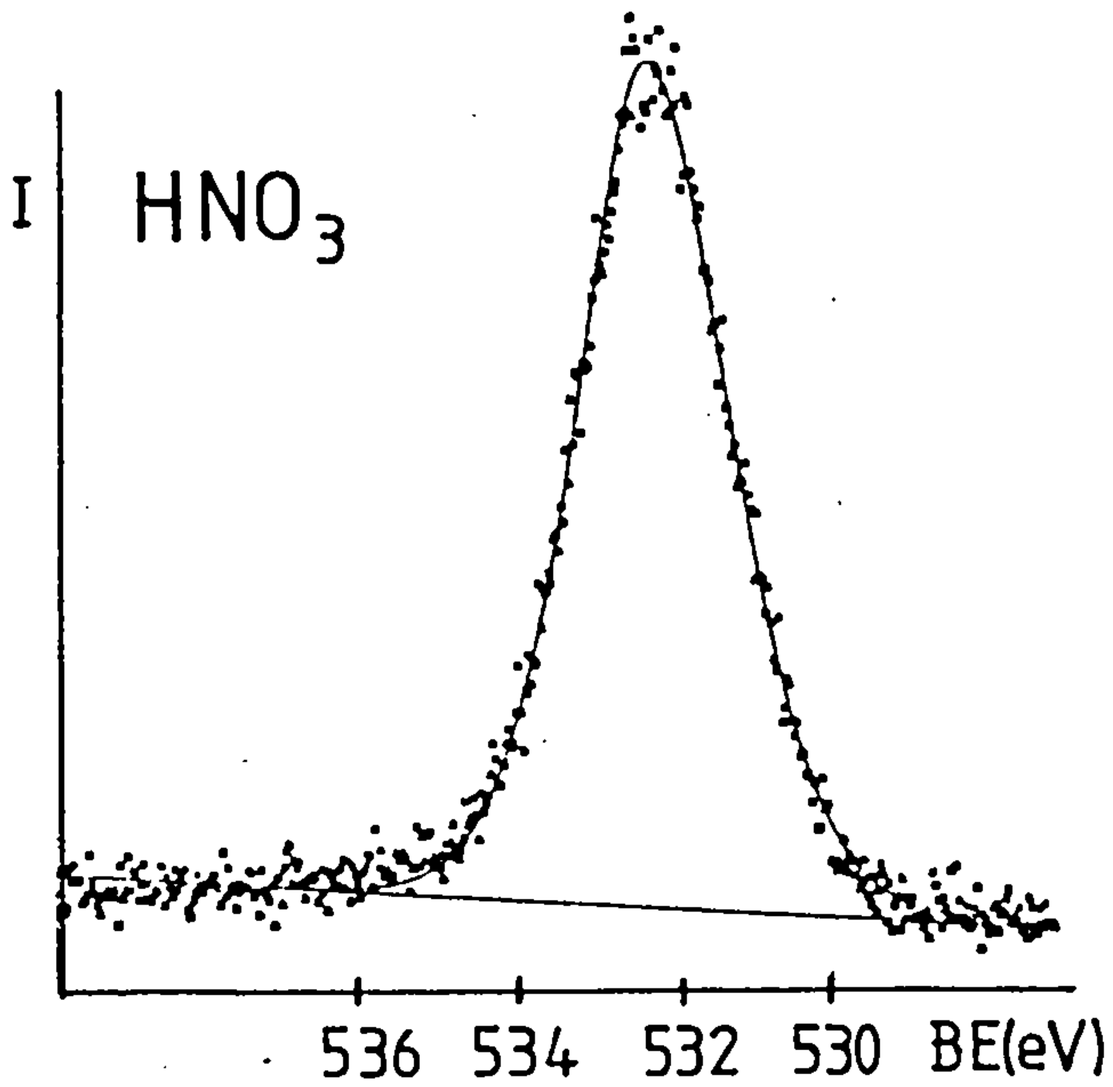

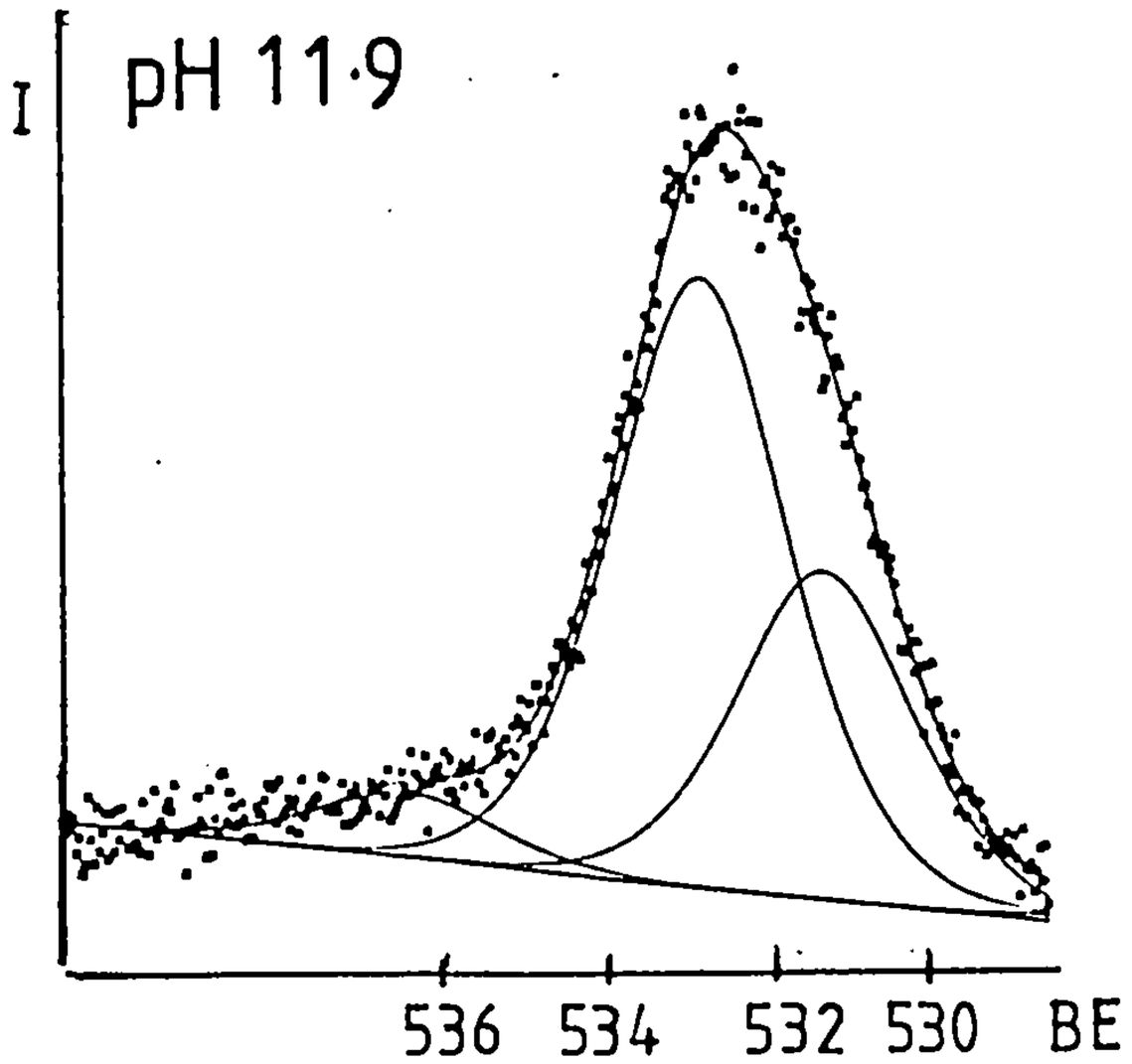

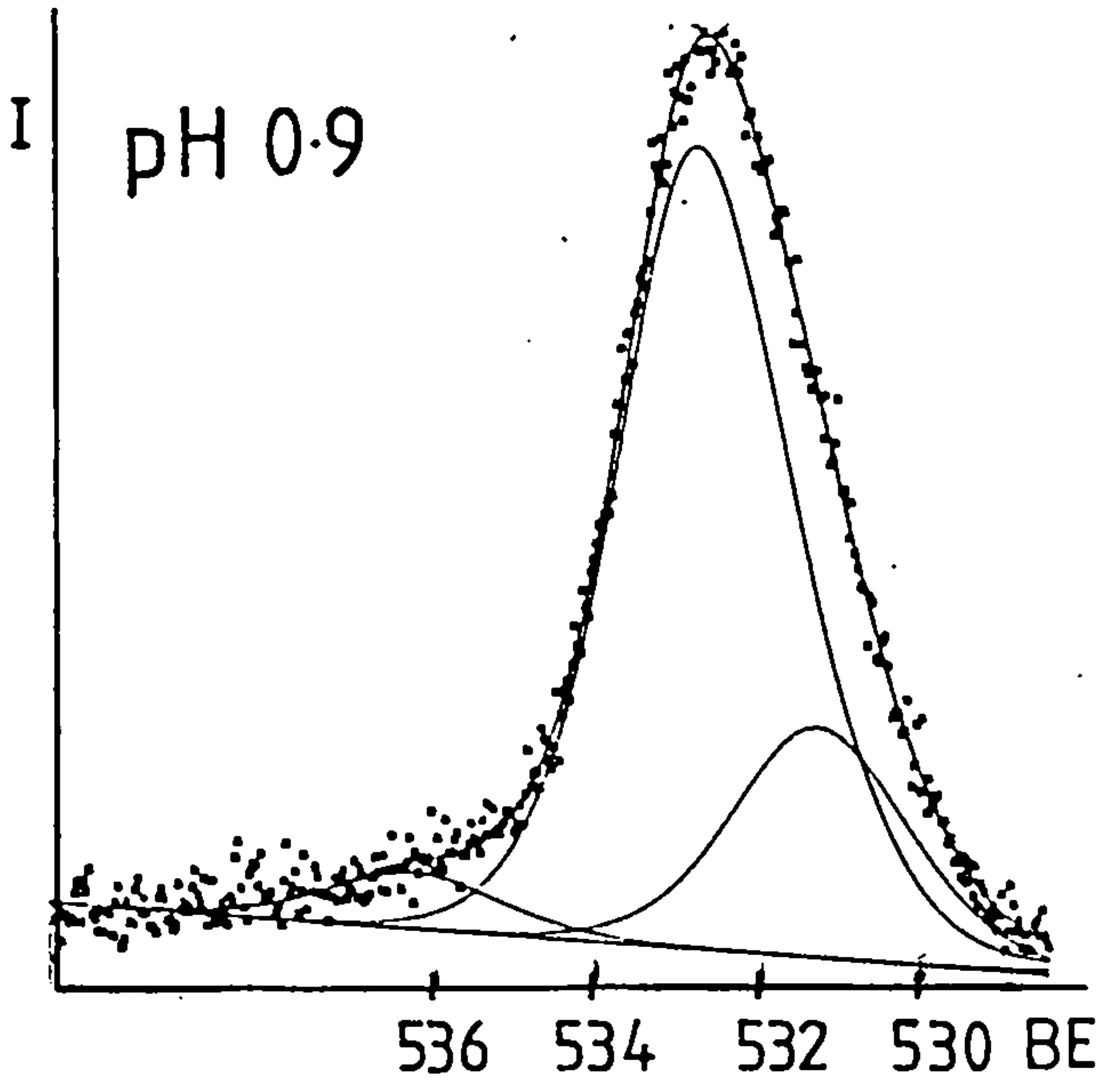

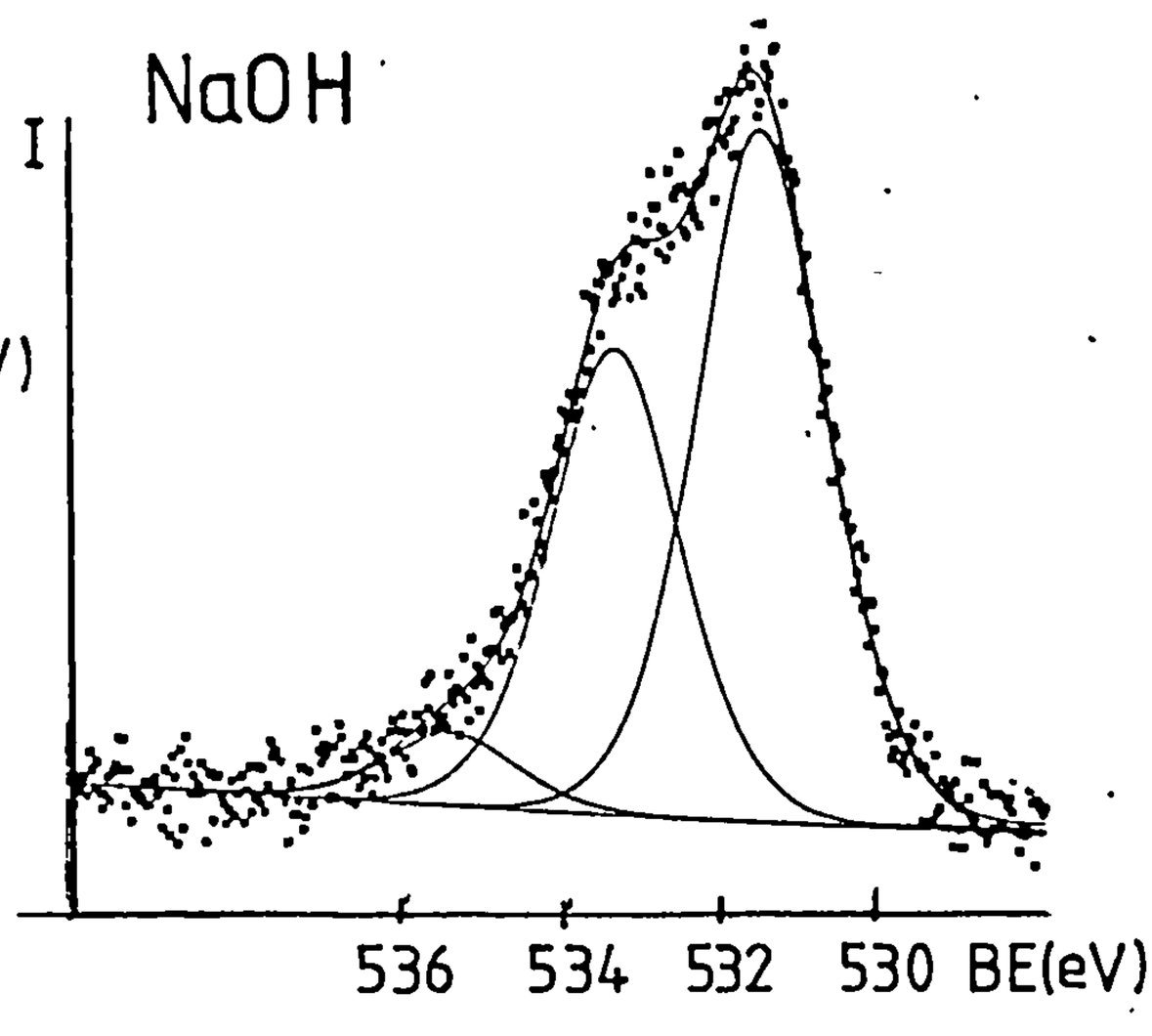

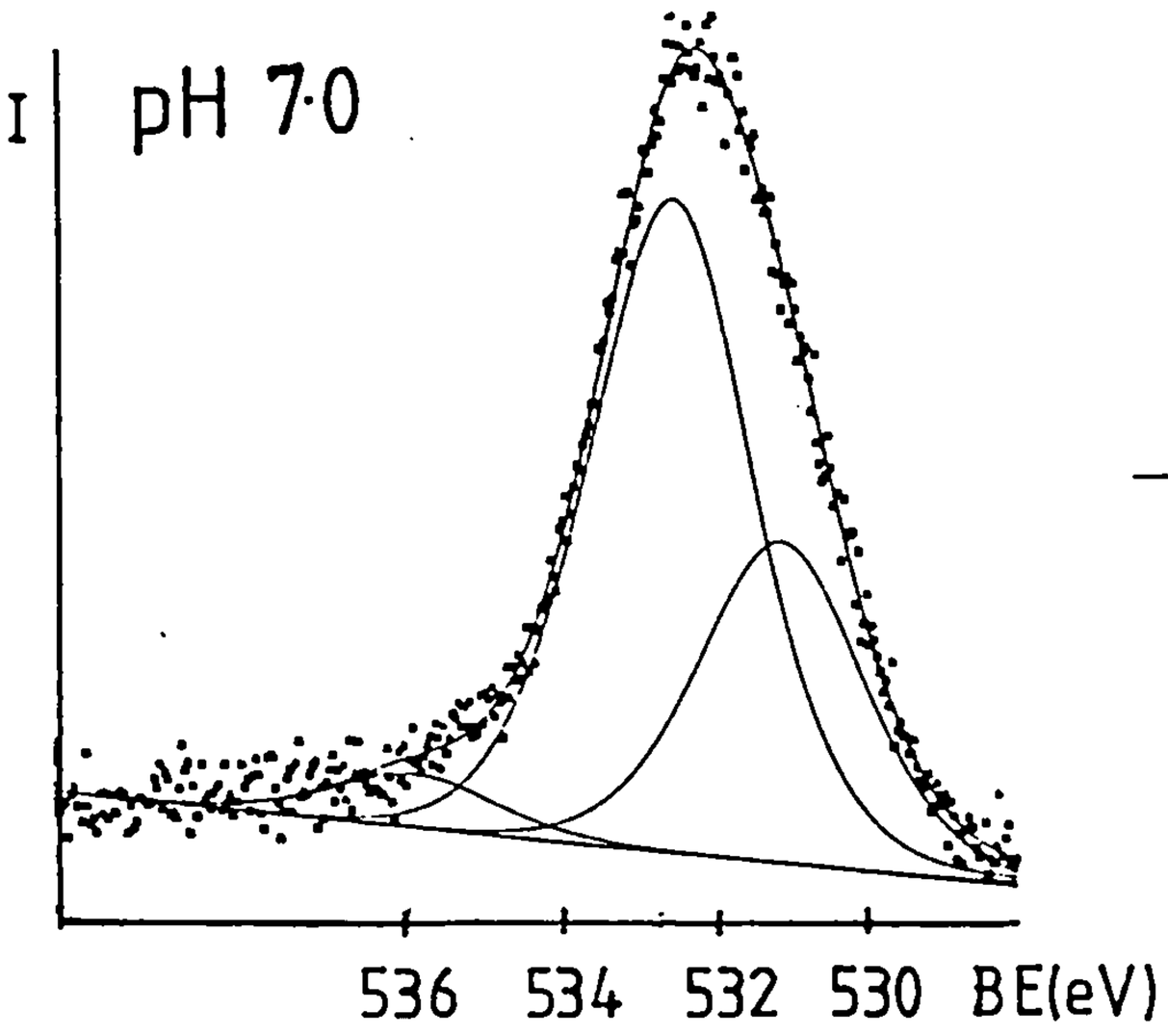

Fig.6.6 O1s Spectra of Fibres Polarised in Solutions of Different pH

TABLE 6.3

Curve Fitting Results from O1s Spectra of Fibres Polarised in Solutions with Different pH Values.

Solution	Peak 1		Peak 2		Peak 3	
	BE(eV)	Rel Area	BE(eV)	Rel Area	BE(eV)	Rel Area
HNO_3			532·3	1·0		
$NaNO_3$ pH=0·9	536·4	0·051	5328	0·734	531·4	0·209
$NaNO_3$ pH=7·0	536·2	0·053	532·7	0·662	531·7	0·338
$NaNO_3$ pH=11·9	536·7	0·064	533·1	0·607	531·5	0·328
NaOH	535·7	0·060	533·5	0·378	531·5	0·562

(Errors in BE ±0·2 eV Rel Area±0·004)

escape depth for the carbon 1s and oxygen 1s electrons (the oxygen 1s region is more sensitive to surface groups).

6.4.3 Working Electrode Solution and Gases Evolved

Different gases were evolved depending upon the pH. Thus, as discussed previously, in sodium hydroxide solution oxygen is evolved. In nitric acid solution carbon dioxide is evolved. These observations are probably explained by the different initial steps in the oxidation processes. A similar situation to that with graphite (83) probably occurs. Thus, in acid, carbon dioxide is evolved according to the following electrode process:

$$C_{(s)} + H_2O \text{ ------- } "C_{(s)}(O)_{(ads)}" + 2H^+ + 2e \qquad 6.1$$

followed by processes such as:

$$2"C_{(s)}(O)_{(ads)}" \text{ -------- } CO_2 + C \qquad 6.2$$

$$"C_{(s)}(O)_{(ads)}" \text{ -------- } CO_2 + 2H^+ + 2e \qquad 6.3$$

In base oxygen is evolved according to the electrode process:

$$C_{(s)} + OH^- \text{ ------ } "C_{(s)}(OH)_{(ads)}" + e \qquad 6.4$$

followed by processes such as:

$$"C_{(s)}(OH)_{(ads)}" \text{ ---- } C_{(s)} + OH^- \qquad 6.5$$

$$4OH^- \text{ ----- } O_2 + 2H_2O + 2H_2O + 4e \qquad 6.6$$

Many possible intermediate reactions for graphite have been discussed by Kokharov (84).

The working electrode solutions for fibre polarised in sodium hydroxide (2M) and sodium nitrate (pH 11.9) turned dark brown and fragments of fibres were dispersed in the solution as described above.

6.4.4 Other Features

Sodium was present on the fibres treated in sodium nitrate and sodium hydroxide. A large amount of these ions were removed after washing in triply distilled water, but some sodium ions always remained. Sodium is well known to intercallate with graphite and the same is probably true of carbon fibres.

6.5 Conclusions

These results show the important effects that pH and the nature of the electrolyte have on the resulting surface composition of electrochemically treated carbon fibres. The presence of hydroxide ions (high pH) leads to less surface oxidation and a breakup of the surface which gives rise to small carbon fibres fragments in the electrolyte. In high pH environments oxygen is evolved, but in neutral and in acidic environments carbon dioxide is produced. At the edge sites of untreated carbon fibres, carbon/ oxygen complexes are already present. These complexes can be of several types including >C-OH, >C=O and -COOH/ester. The alcohol and aldehyde type groups will be more readily oxidised than the graphitic lattice itself.

Alkaline electrolytes, as already stated, provide oxygen from OH ions at the anode. This form of oxygen is not very reactive and hence may only be able to oxidise edge site functionalities already present on the surface. They appear to be unable to oxidise the main graphitic structure. This would explain the holes produced on the fibre surface after treatment in sodium hydroxide solution, the edge sites being those of localised attack.

CHAPTER 7

THE USE OF AMMONIUM SALT ELECTROLYTES

7.1 Introduction

Most commercially treated fibre samples, eg. HMS,HTS and AS (treated types I, II, and III fibres respectively) have small amounts of nitrogen functionality on their surfaces(91). It was proposed that this is a result of nitric acid treatment, but it has been shown in preceding chapters that no nitrogen is produced when nitric acid is used as the electrolyte for a variety of polarising conditions. Proctor and Sherwood (87), using ammonium bicarbonate solution, found that nitrogen functionality was introduced onto the fibre surface in the form of amines or amides. They suggested that the surface nitrogen was introduced whilst the fibres were prepolarised to -1.3V. This chapter aims to expand this study using several ammonium salts and to observe any changes in the physical and chemical properties of the fibre surfaces.

The fibres were not prepolarised to a cathodic potential and then pulsed to a desired potential as in the work carried out by Proctor and Sherwood (87), but were polarised to the desired potential immediately on immersion into the electrolyte solution. This method was used because it more closely resembled the treatment used in the pilot plant (see next chapter). The ammonium salts used were ammonium nitrate, ammonium bicarbonate,

and ammonium sulphate.

7.2 Ammonium Nitrate Electrolyte

7.2.1 The Effect of Potential on Fibre Surfaces

Fig.7.1 shows the carbon 1s spectra from fibres polarised to several potentials in 10% ammonium nitrate solution for one minute. These spectra are very similar to those obtained for fibres polarised in acidic electrolytes. The main carbon peak loses its graphitic character at potentials above 1.5V, again due to exfoliation and break up of the extended π electron system. The 'oxide' region of the spectra consists of three chemically shifted species. The two main signals have chemical shifts of 2.2eV (±0.1eV) and 4.2eV(±0.1eV). The variation in area of these chemically shifted species is shown in Fig.7.2. It can be seen that only a small amount of oxidation is produced below 1.5V, but on polarising to potentials of 2.0V and above, a substantial amount of surface oxide is produced. The intensity of both chemically shifted species increases, although this increase is much larger for 'oxide' 1 (0.089 to 0.739) than for 'oxide' 2 (0.056 to 0.200). The ratio of 'oxide' 2 to 'oxide' 1 at low potentials, ie 0.5V, is 0.9, but as the potential increases this ratio decreases until there is only 30% as much 'oxide' 2 (carboxyl-type groups) as there is 'oxide' 1.

The area of the satellite/plasmon feature observed above 6.0eV remains constant (with respect to the graphitic peak) within the range 0.045-0.055.

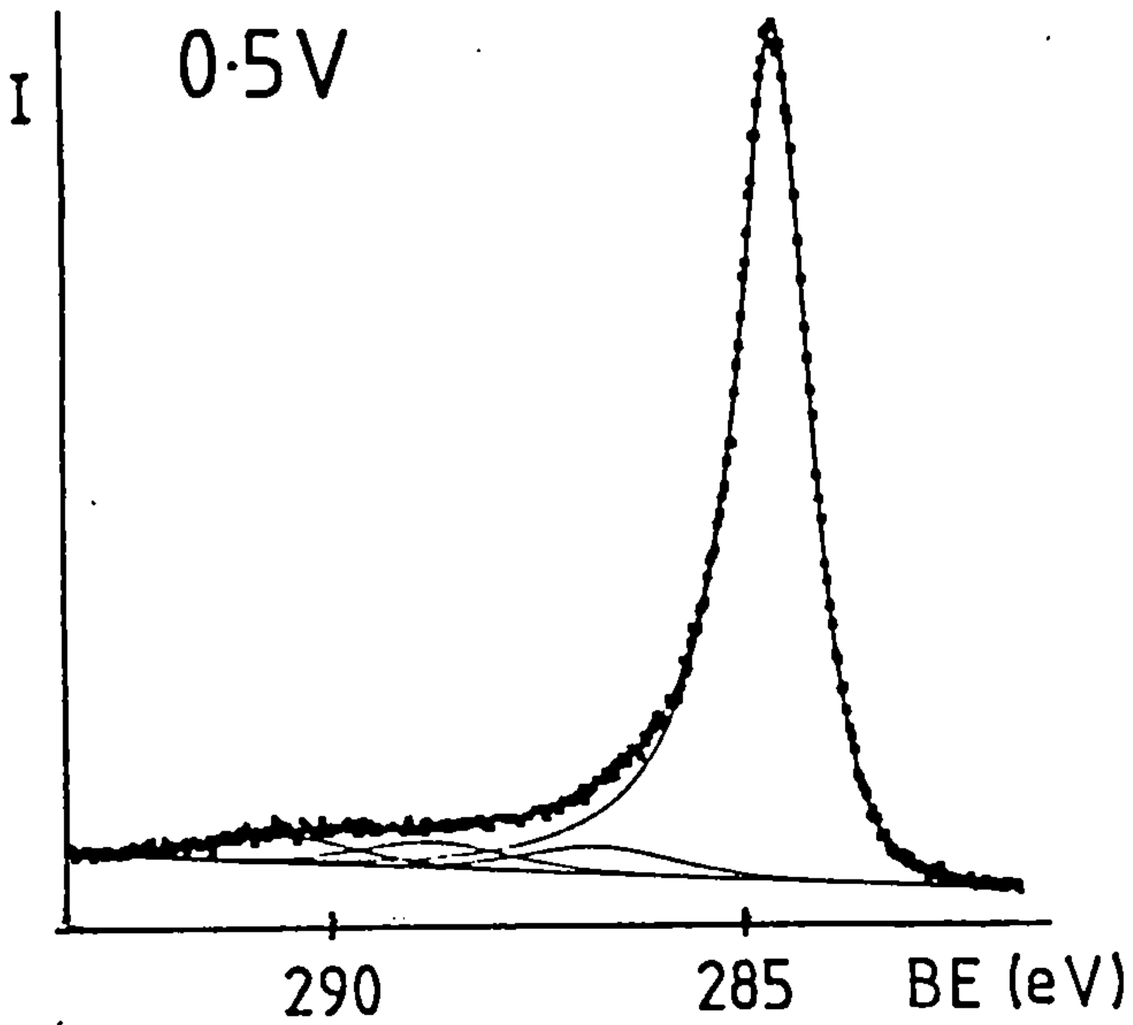

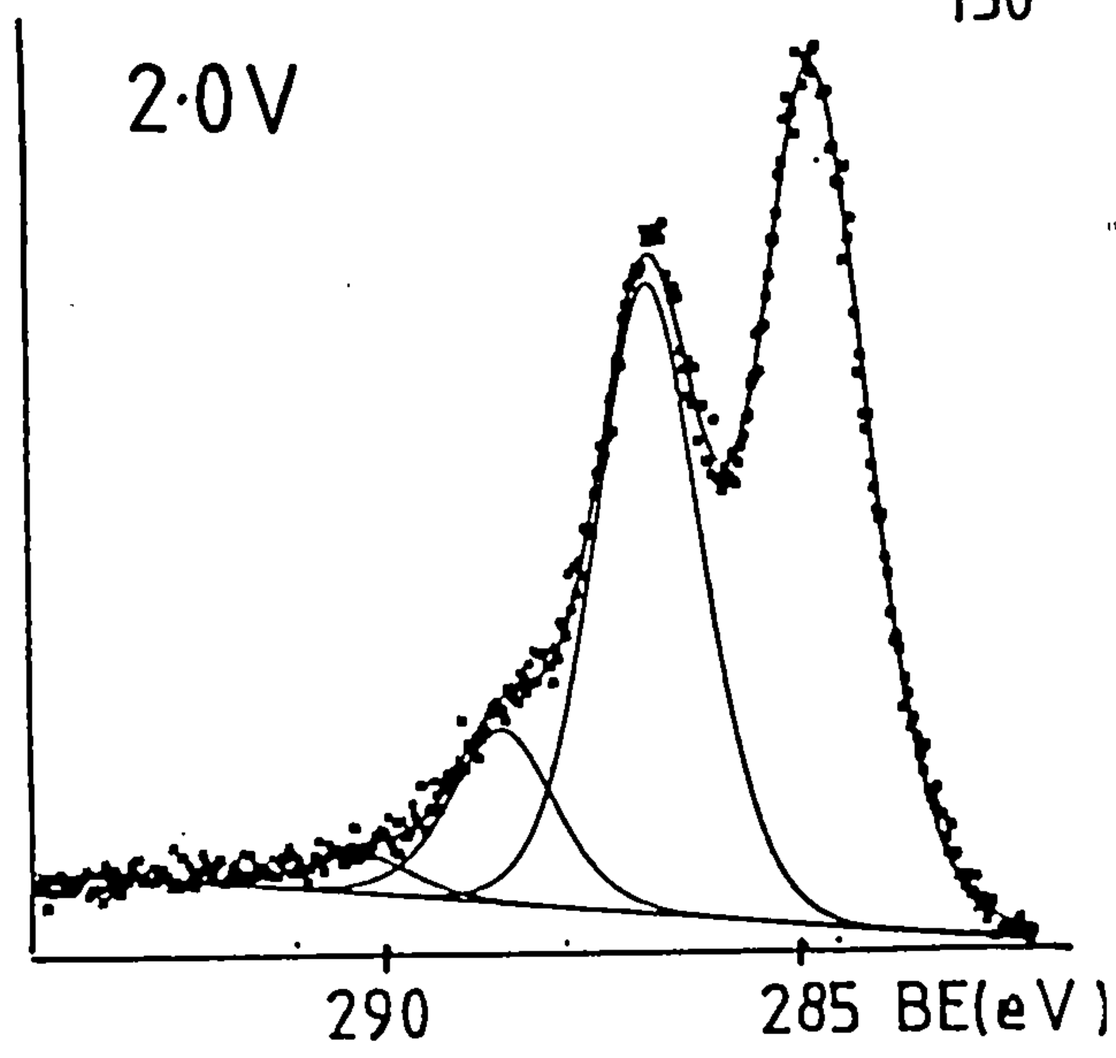

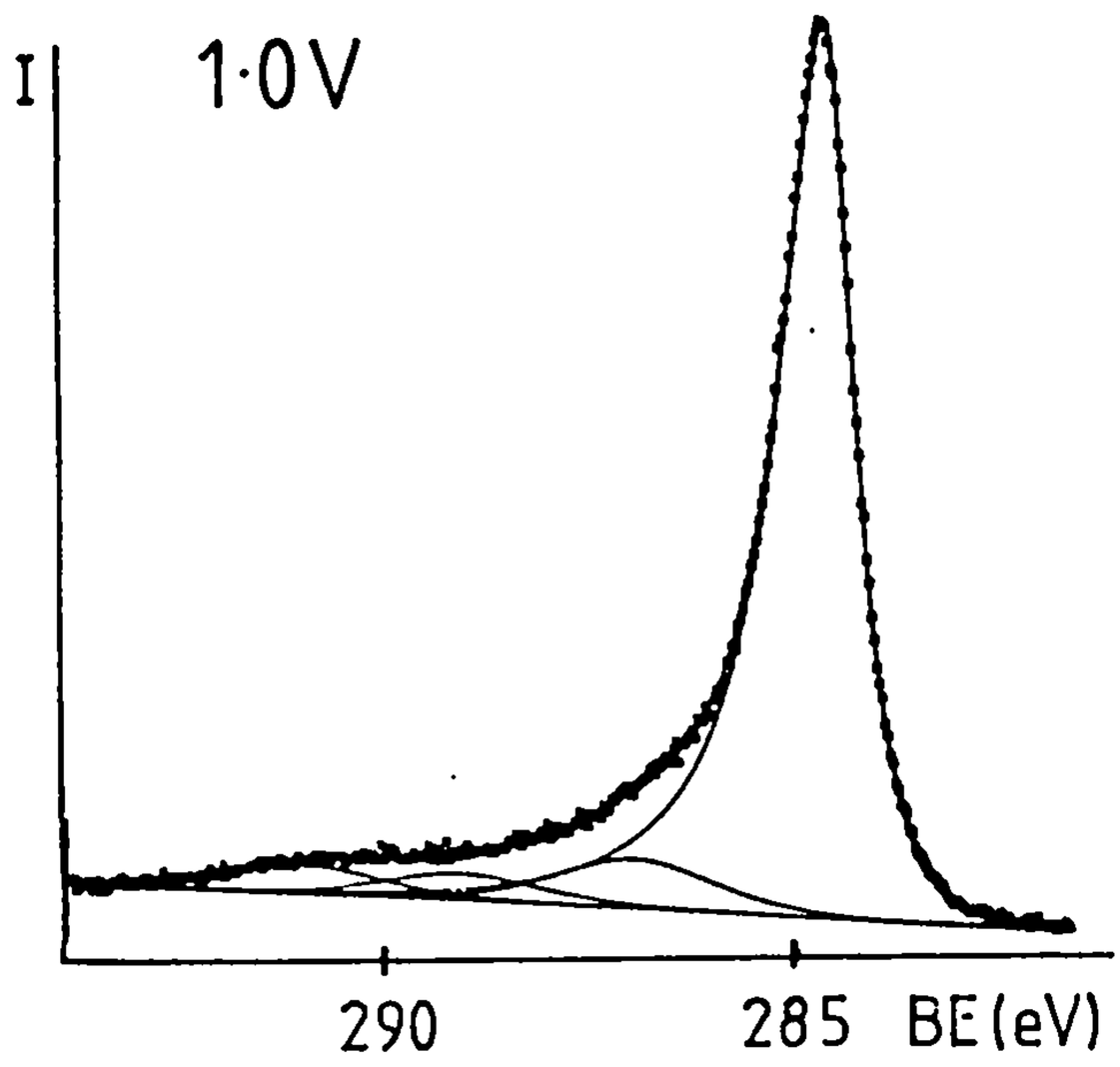

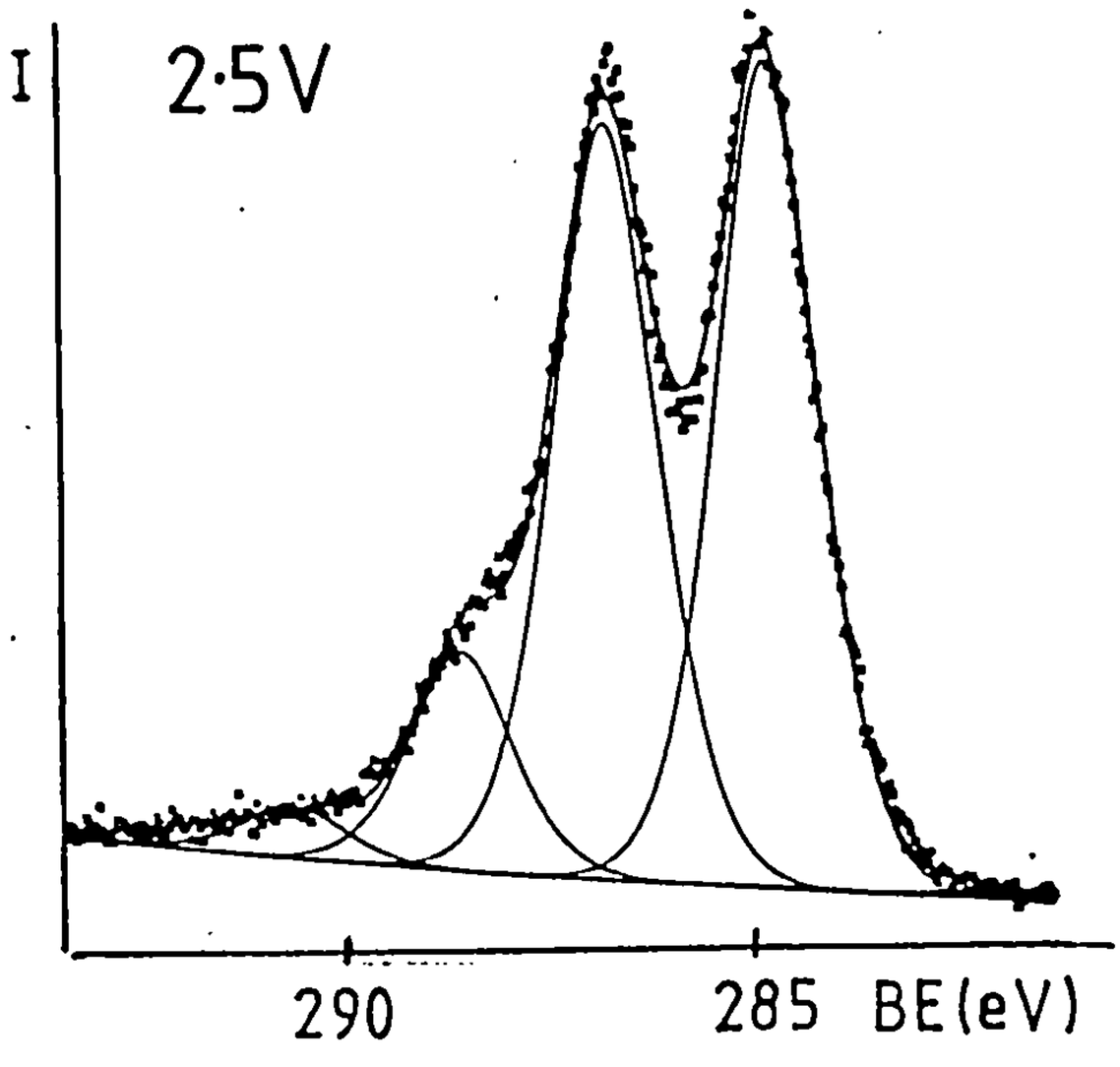

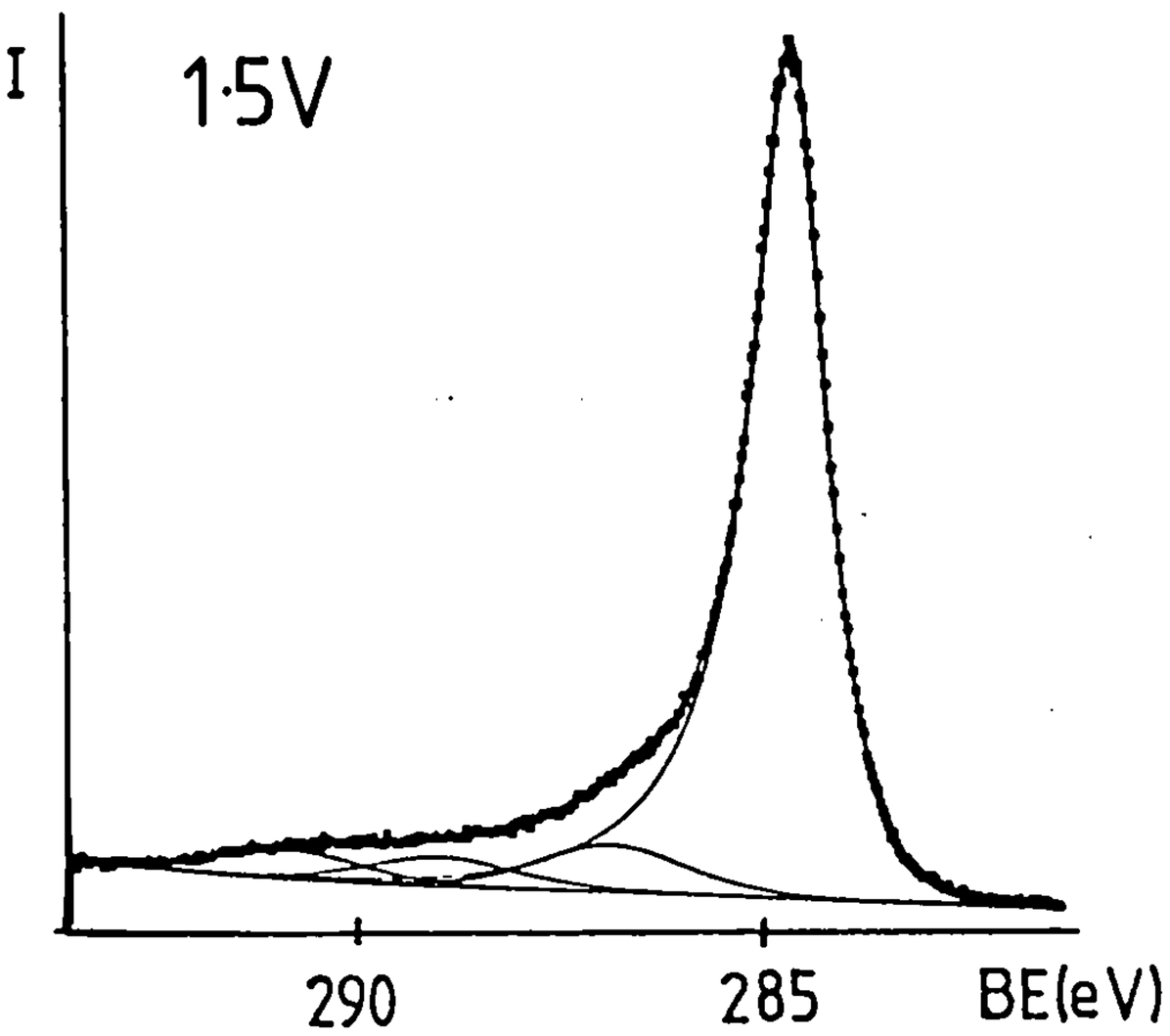

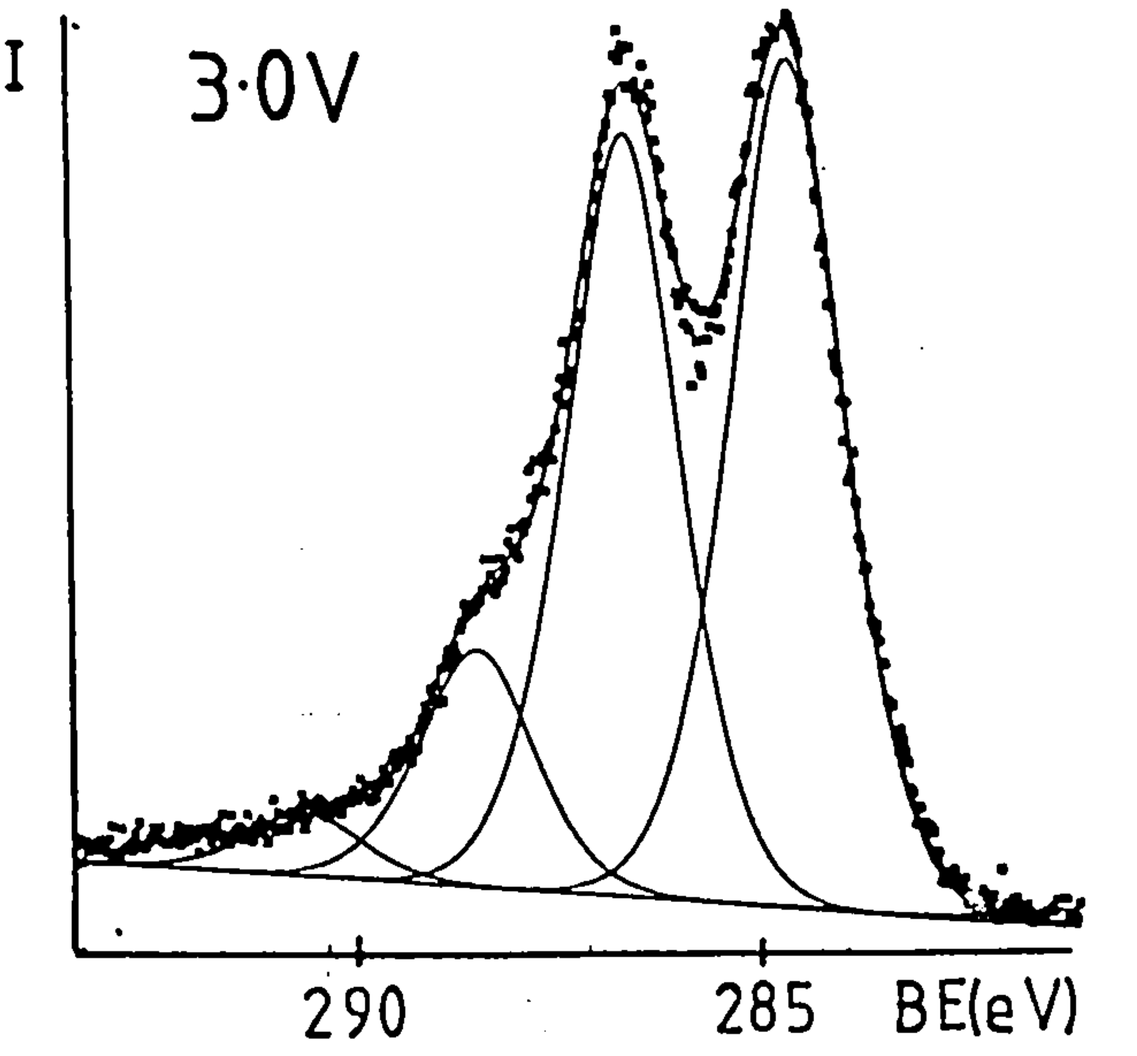

Fig.7.1 C1s Spectra of Fibres Polarised in 10% NH_4NO_3

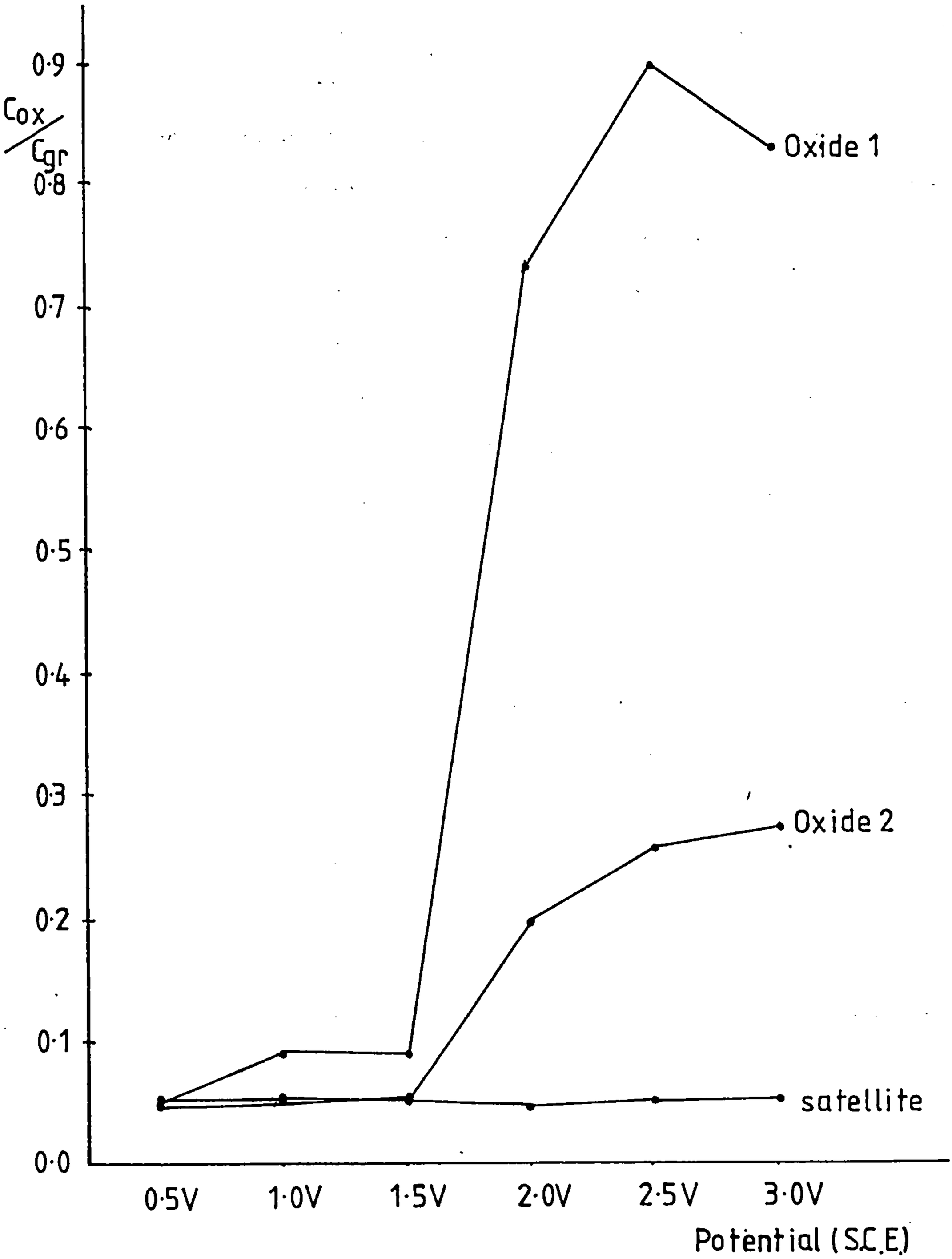

Fig.7.2 Variation of Chemically Shifted Species with Potential (for NH_4NO_3)

Table 7.1 shows the results obtained from fitting oxygen 1s spectra of these fibre samples. At low potentials (0.5-1.5V) the spectra consist of two resolvable oxygen species with binding energies 533.3eV (±0.2eV) and 531.8eV (±0.2eV). These correspond to =O and -O- type groups respectively. The ratio of these two species varies from potential to potential. At 0.5V the -O- type group is present in a larger amount but at 1.0V and 1.5V =O predominates. At potentials above 1.5V only one species is detected with a binding energy of 532.2eV. This may be due to functional groups of the type shown in chapter 6 for the fibres treated in nitric acid. These results are expected because the solution is slightly acidic (pH 4.7).

The O1s:C1s ratios are given in Table 7.2. The ratio increases with increasing potential from 0.0214 to 0.6411.

Small amounts of nitrogen were present on fibre surfaces treated above 1.0V. The statistics of the spectra were poor, even though they were collected over several hours, because of these very small nitrogen concentrations. There were two nitrogen species present with binding energies of aprox.401eV and 399eV These binding energies correspond to amine and amide functionality. As stated in chapter 5, nitrogen functionality is not produced as a result of nitric acid treatment and therefore the nitrogen functionality in this case occurs because of the reaction with ammonium ions. Amides can be produced by heating the ammonium salts of carboxylic acids. If amides are being produced, a photoelectron signal with a chemical shift of 2.1eV would be expected in the carbon 1s spectrum. Unfortunately, this would coincide with the keto-enol signal.

TABLE 7.1

Curve Fitting Results from the Oxygen 1s Spectra of Fibres Polarised in Ammonium Nitrate Solution (10%)

Potential	Binding Energy (eV)	Area Ratio
3·0V	532·2	1
2·5V	532·2	1
2·0V	532·2	1
1·5V	533·1 531·6	0·640 0·360
1·0V	533·5 532·4	0·718 0·282
0·5V	533·3 531·9	0·382 0·618
Errors	(±0·2)	(±0·005)

TABLE 7.2

O1s: C1s Ratios for Fibres Polarised in Ammonium Nitrate Solution (10%)

Potential	O1s : C1s
3·0V	0·641
2·5V	0·560
2·0V	0·494
1·5 V	0·100
1·0 V	0·077
0·5V	0·021
	(±0·006)

7.2.2 The Effect of Concentration of Ammonium Nitrate

Fig.7.3 shows the carbon 1s spectra of fibres which have been polarised to 2.0V for 20 mins in solutions of ammonium nitrate of different concentrations. Even at the lowest concentration, ie.10^{-4} M, there is a larger amount of chemically shifted species produced than in alkaline conditions. The spectra have been fitted to the same chemically shifted signals as mentioned above. The intensity of the chemically shifted species increases with the concentration of the solution. The increase in carboxyl-type groups ('oxide' 2) is not as great as that of 'oxide' 1. The increase in the amount of each group is given in Table 7.3. The area of the satellite peak remains fairly constant.

The O1s:C1s ratio increases steadily with concentration from 0.31 to 0.53. This ratio even at the lowest concentration, 10^{-4}M, is greater than that for fibres polarised to 1.5V in 10% ammonium nitrate, although the reaction time is shorter in the latter case. Very little gas was evolved at either electrode during polarisation in the solution with concentrations in the range 0.01-1M. The fibre sample turned blue in colour during polarisation. This colouring may be due to an interference pattern, because red and yellow colours were also observed.

Nitrogen was present on all fibre samples. The total intensity increased with concentration of the electrolyte. The binding energy of 400eV again suggests the presence of amides. This confirms that this functionality is a result of ammonium

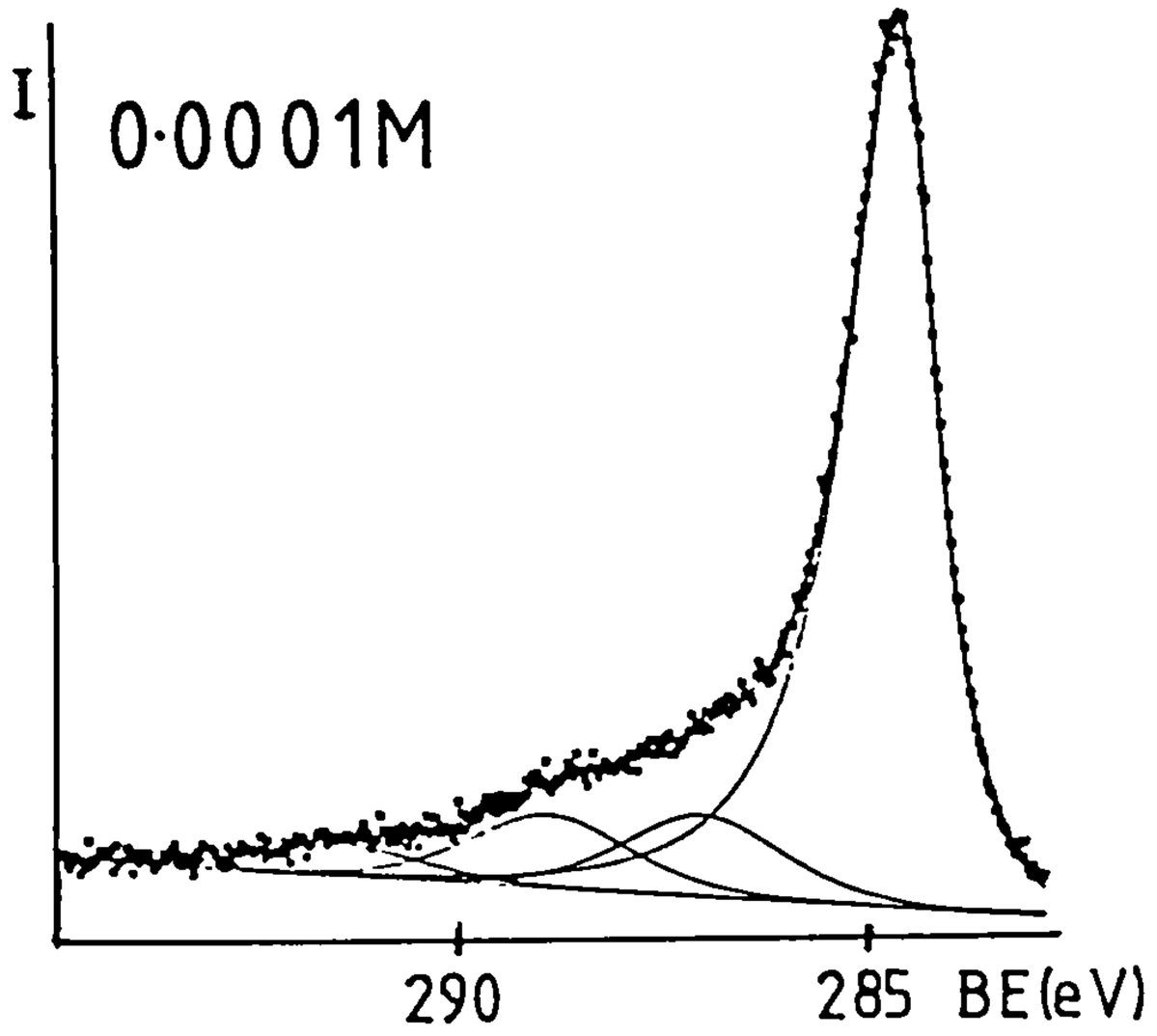

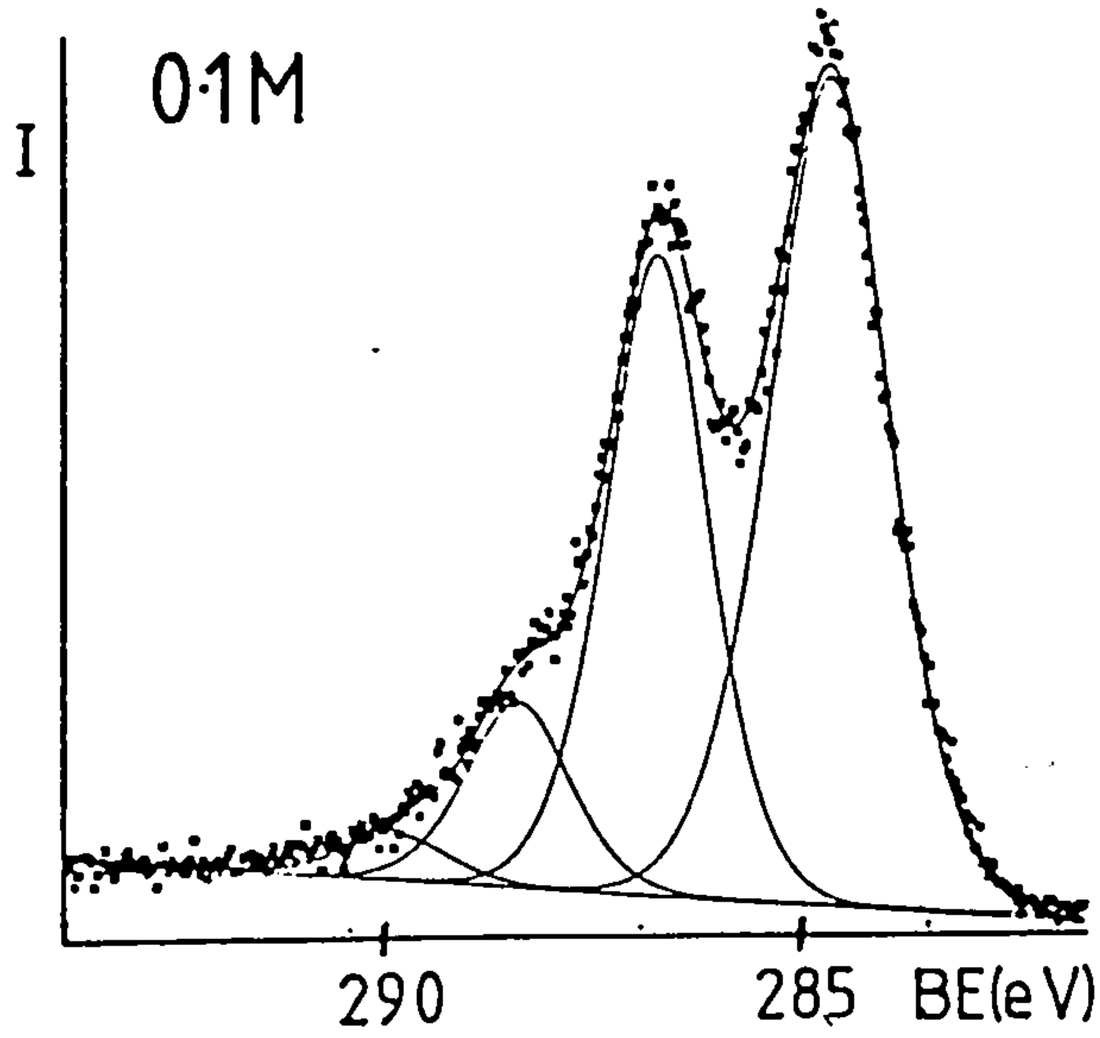

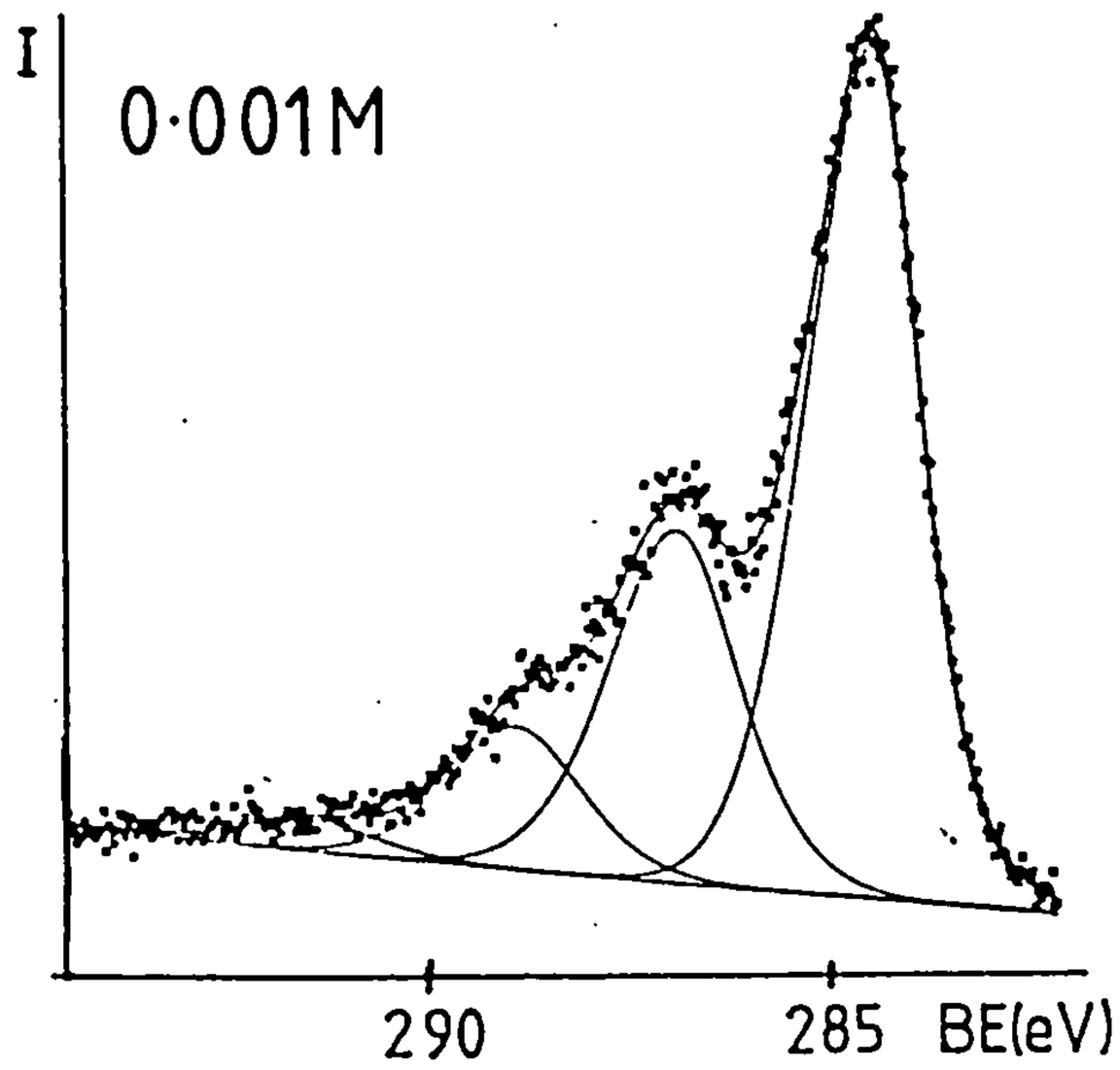

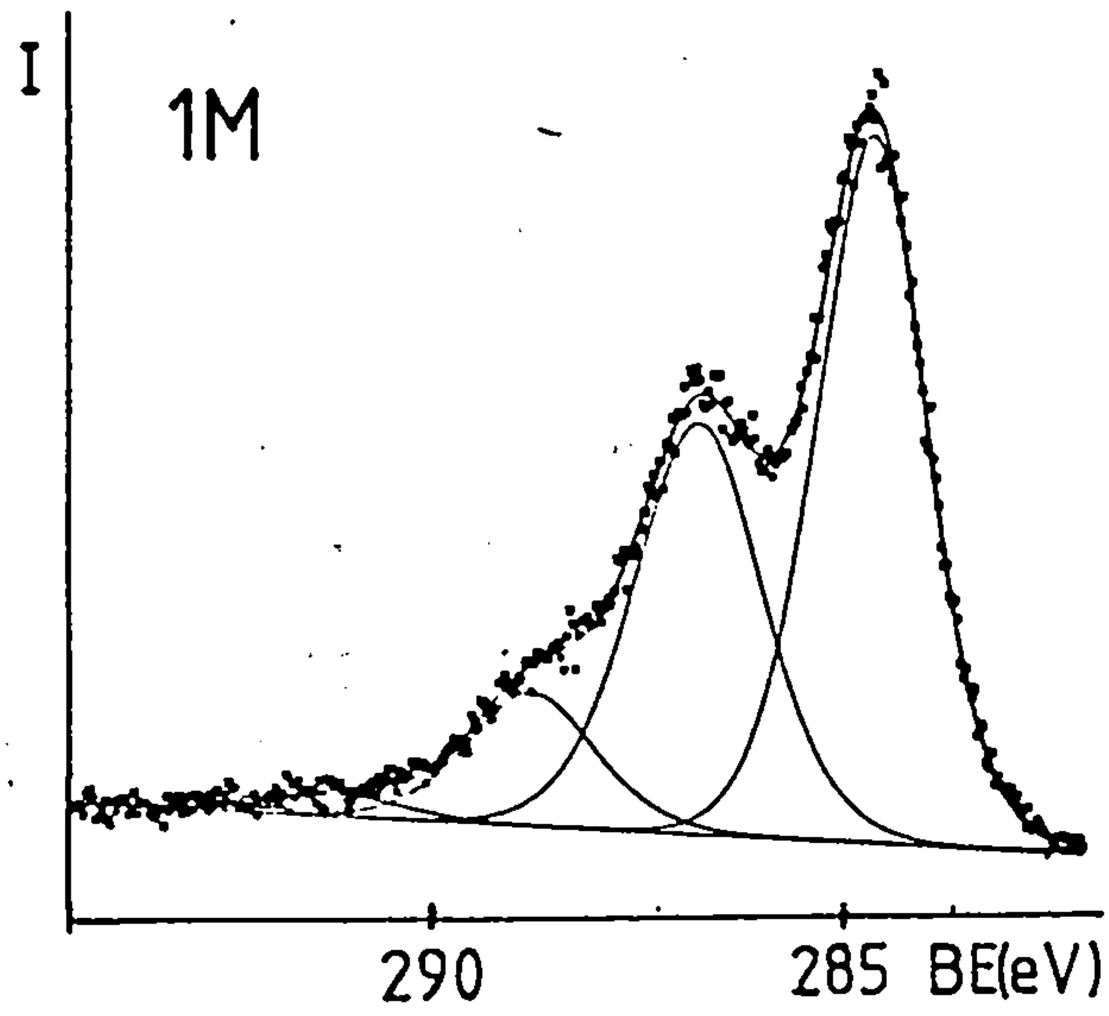

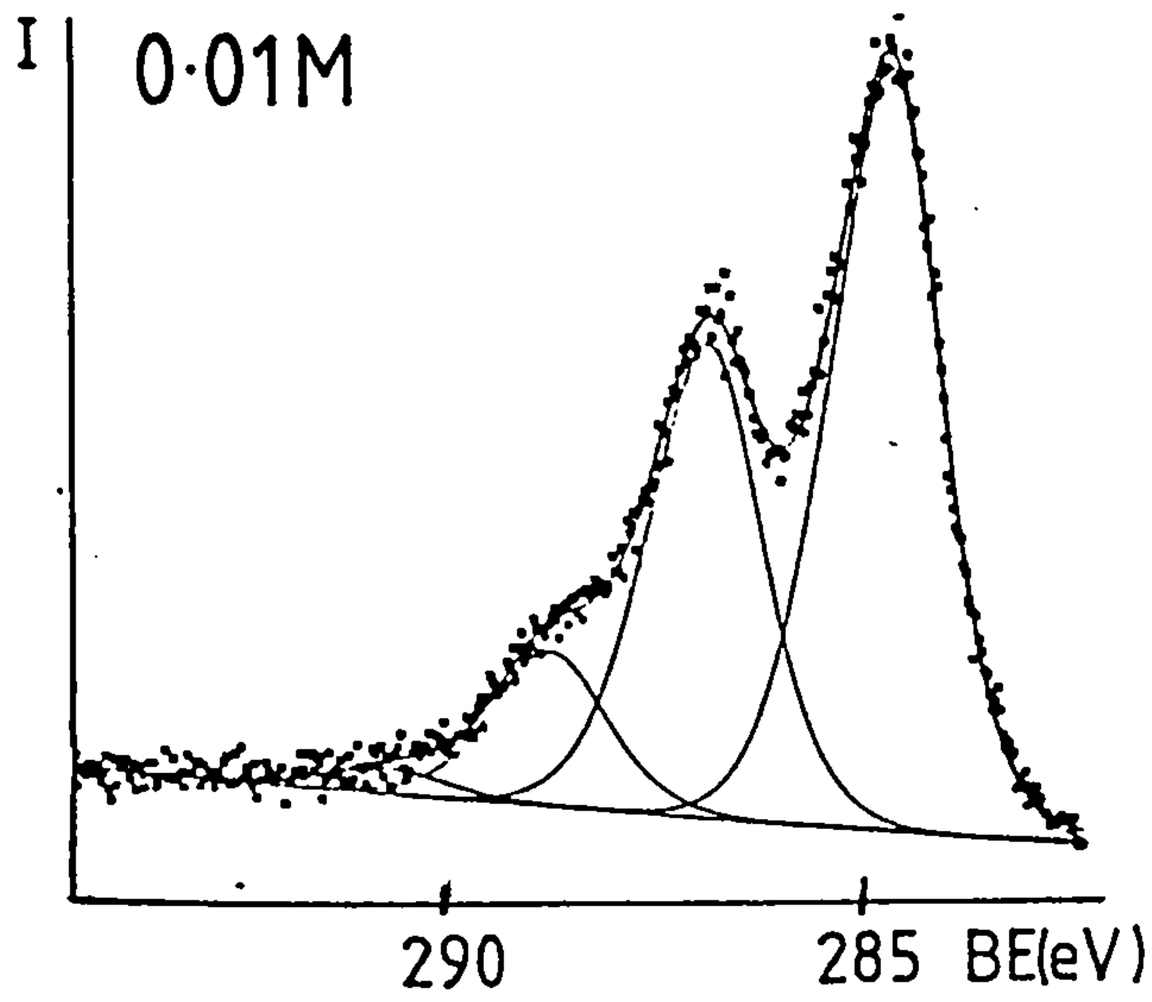

Fig.7.3 C1s Spectra of Fibres Polarised in NH_4NO_3 Solns. of Different Concentration

Fig.7.4

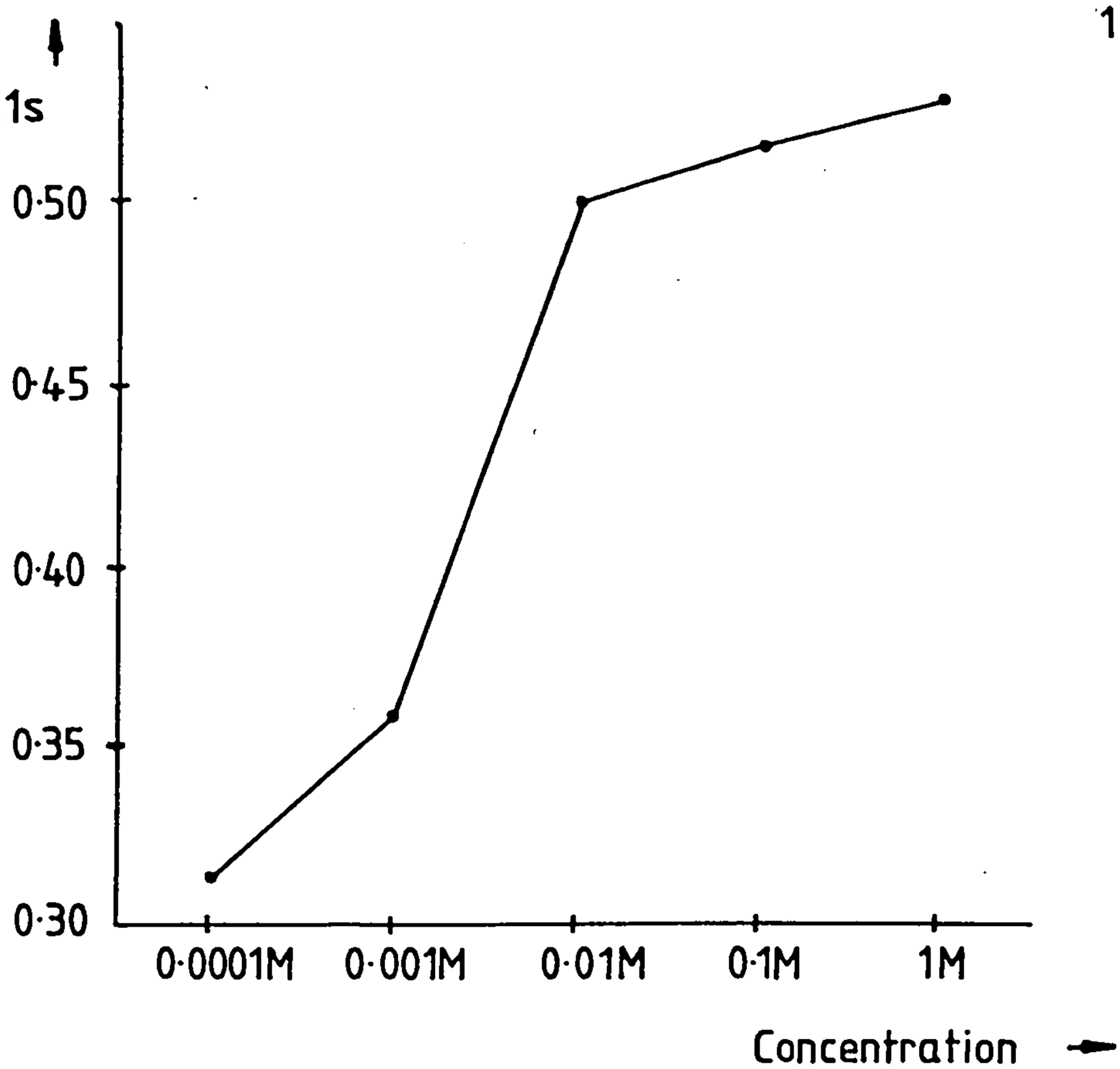

Table 7.3

Concentration	Chemical Shift	
	2·2eV	4·1eV
0·0001M	0·1223	0·1359
0·001M	0·1984	0·4835
0·01M	0·2103	0·6429
0·1M	0·1907	0·6632
1M	0·2242	0·6812

Fig.7.5

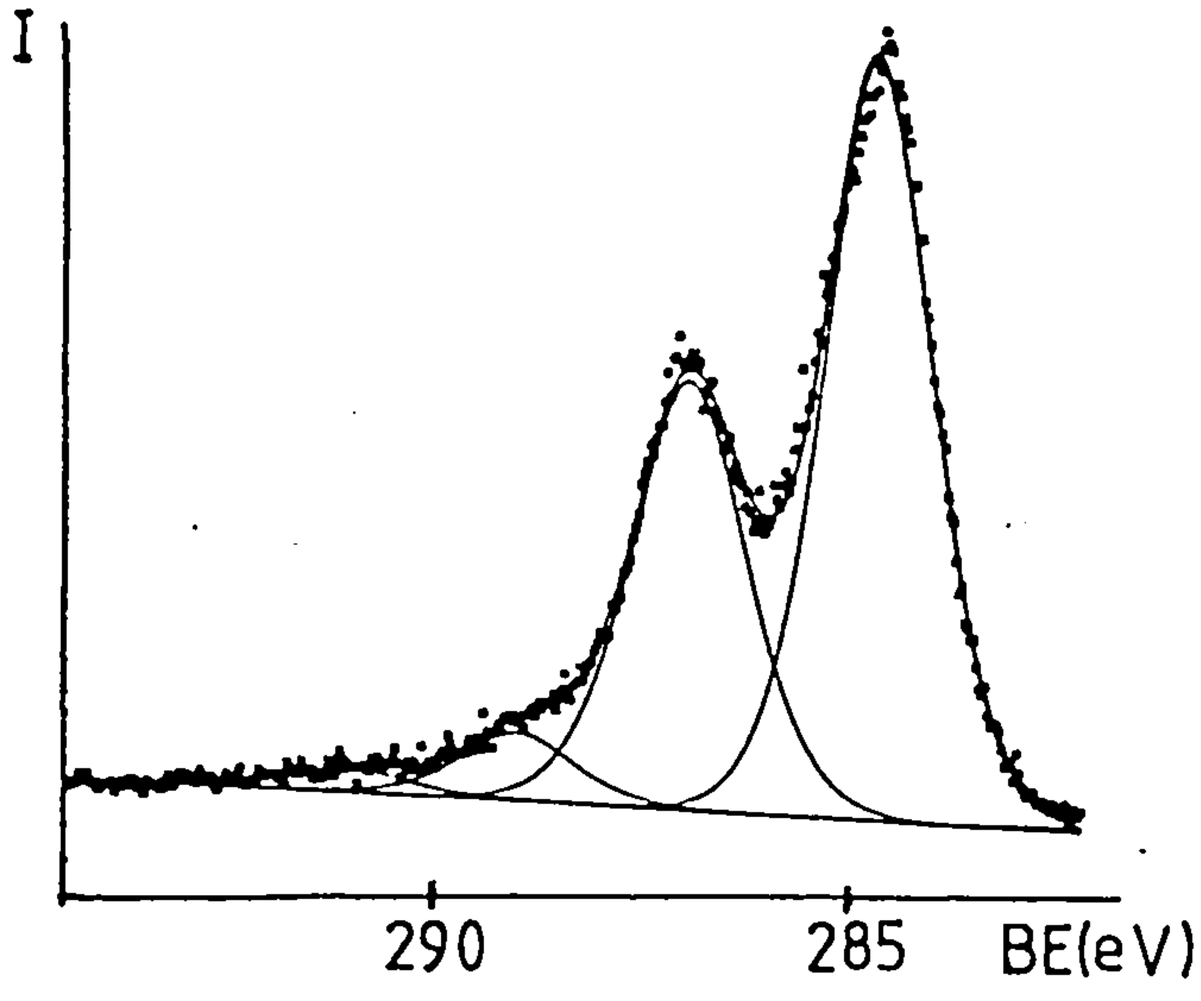

ions reacting with the surface. This probably takes place after the oxidation step occurs because ammonium ions are unlikely to be attracted to the anode.

7.2.3 Type I Fibres

Fig.7.5 shows the spectra obtained for type I fibres treated in 10% ammonium nitrate. Just as for the acid cases, the relative amount of carboxyl type functionality is far less than for the keto-enol type functionality. This again indicates that carboxyl type groups are produced at edge sites. This would be expected because surface oxygen complexes that already exist at these edge sites can be further oxidised (see section 5.13).

7.3 Ammonium Bicarbonate

The carbon 1s spectra for fibres treated in 10% ammonium bicarbonate solution at various potentials are shown in Fig.7.6. The pH of this solution is 7.66 (±0.1). It can clearly be seen that the amounts of chemically shifted species are much less than for fibres treated in ammonium nitrate. The main carbon peak retains its graphitic character at every potential (as for sodium hydroxide treatment). This implies that the bulk fibre structure and the extended π-system is not excessively disrupted during polarisation.

The 'oxide' region of the spectrum does not change significantly, although a slight variation is observed. These spectra were fitted to two main oxide signals. The positions of these two peaks were allowed to float using the curve fitting

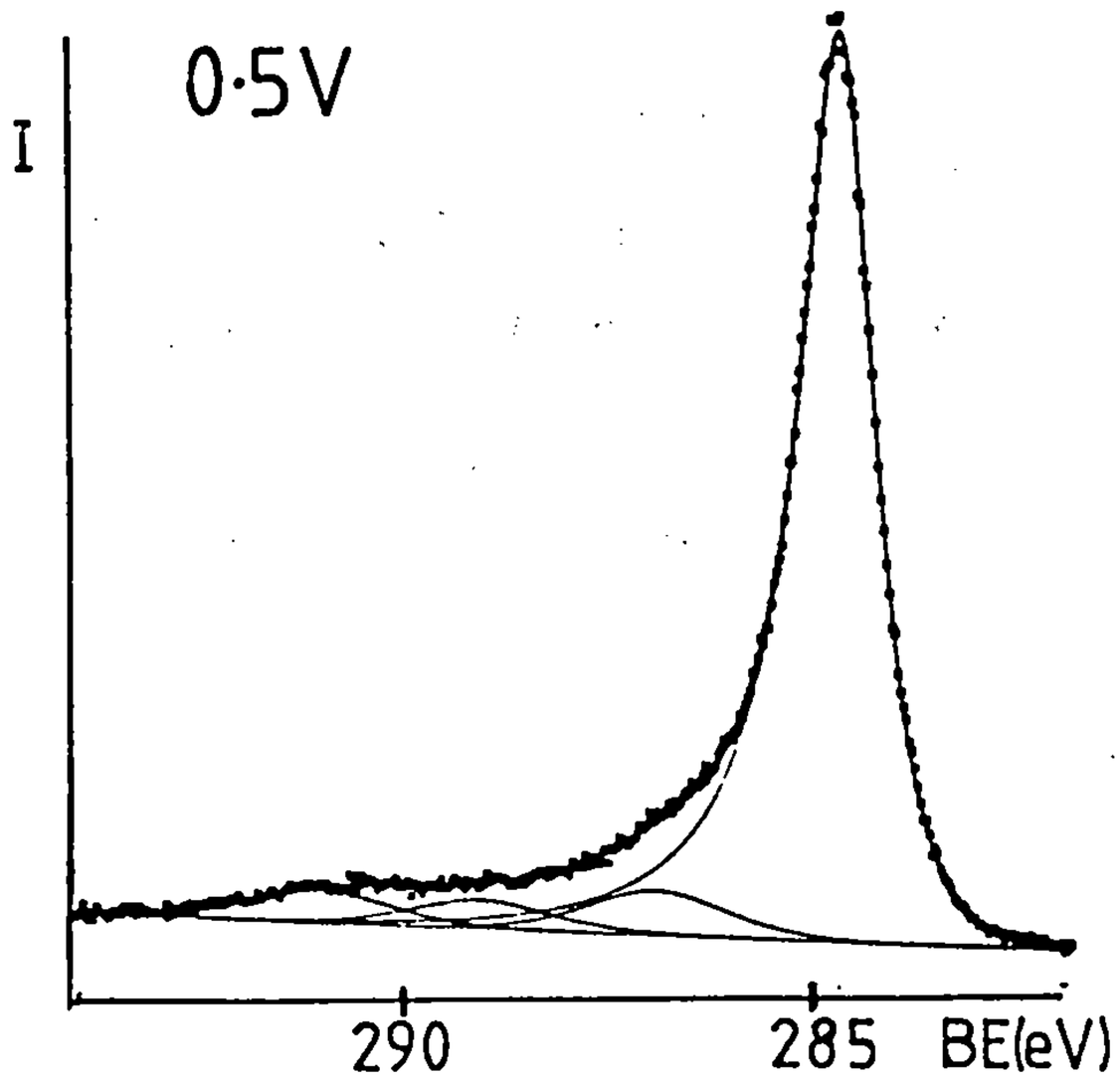

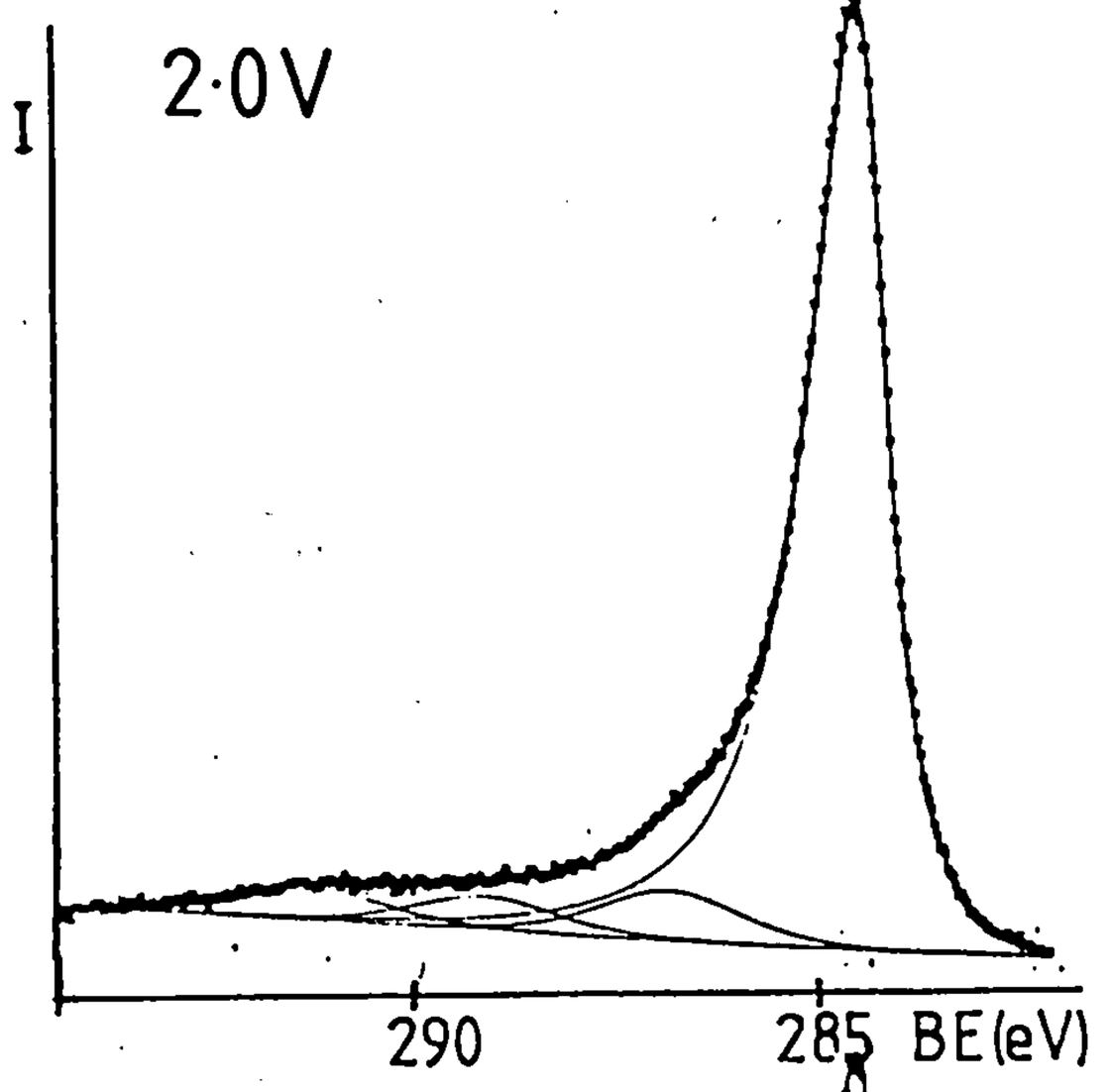

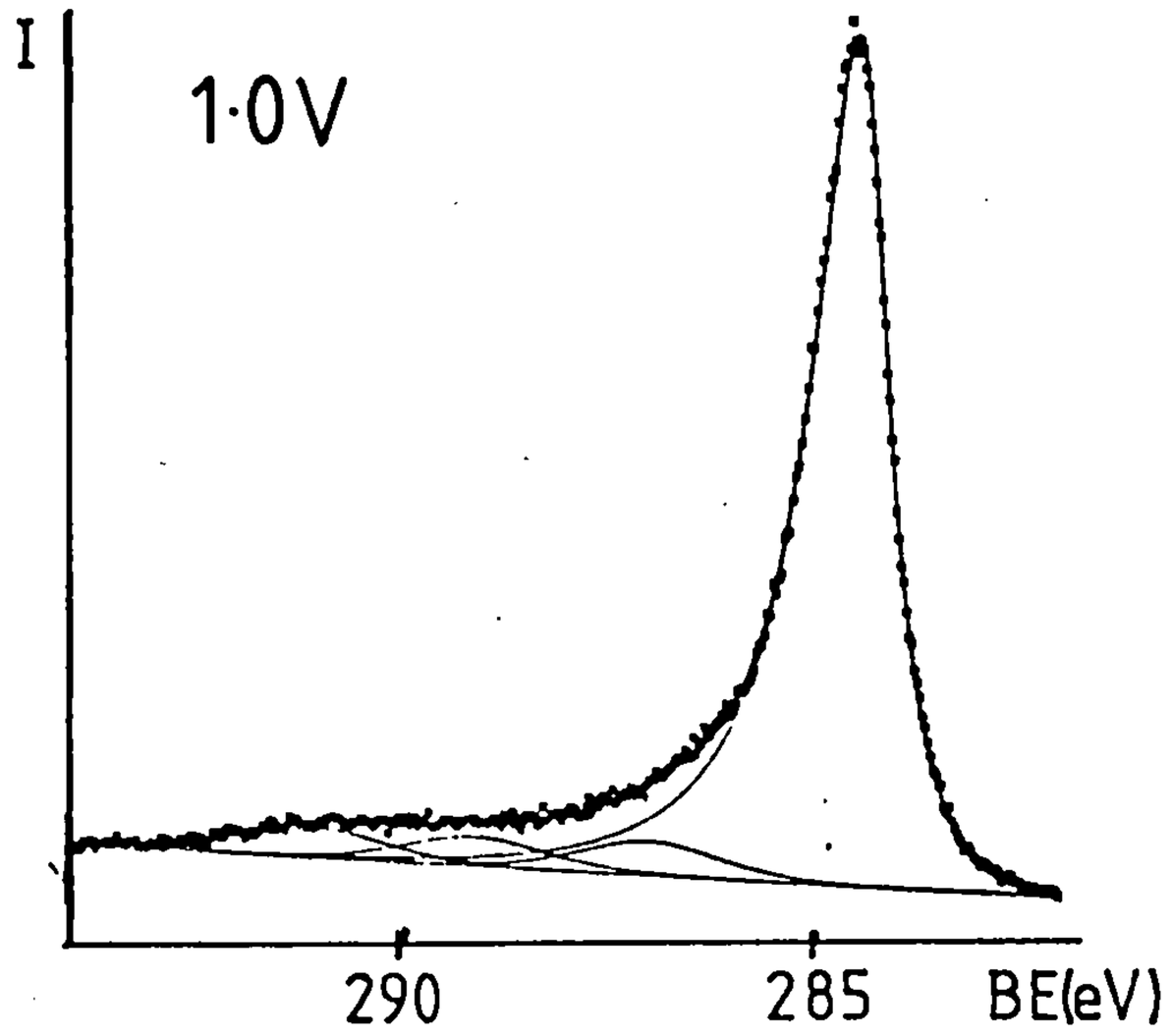

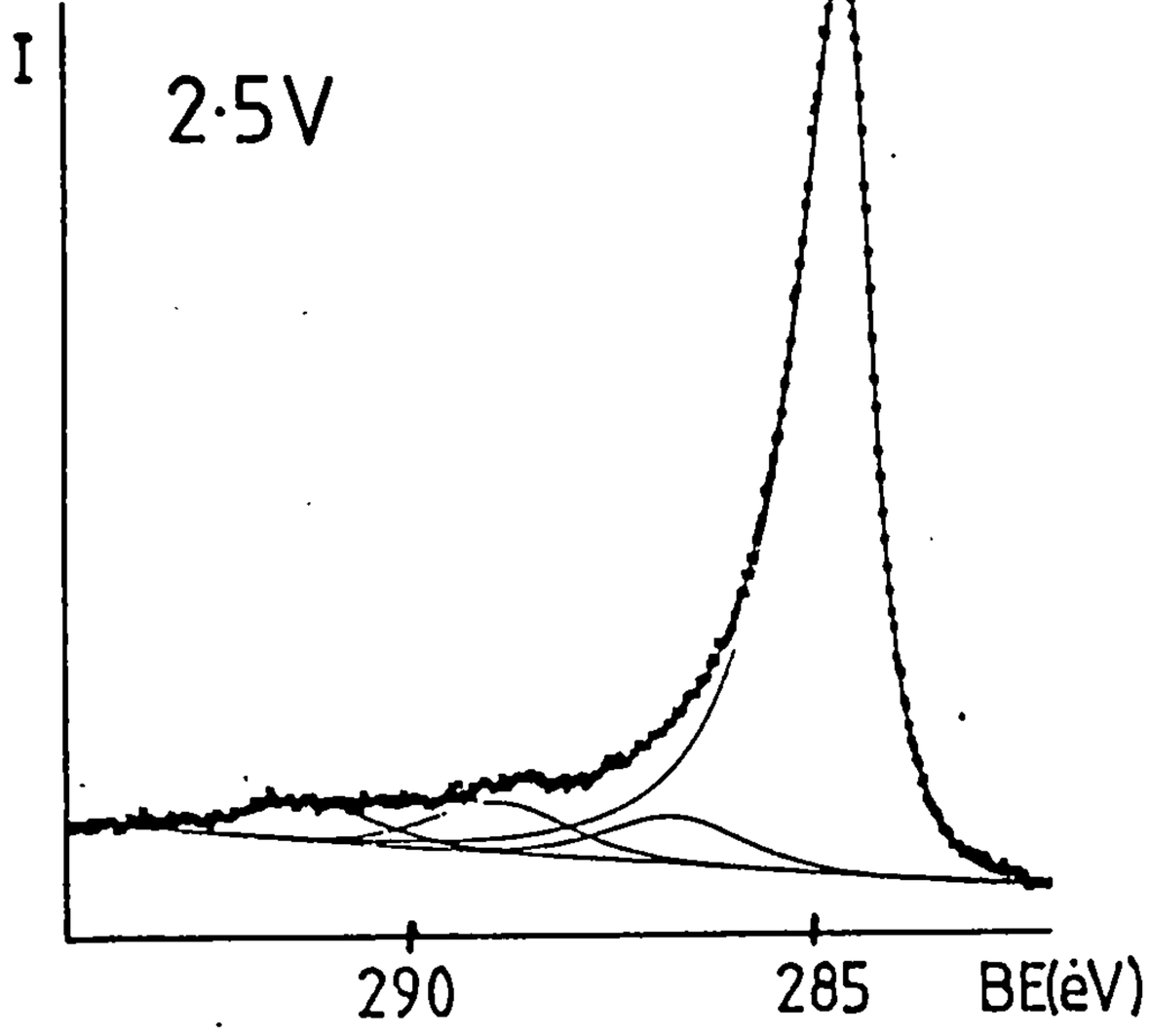

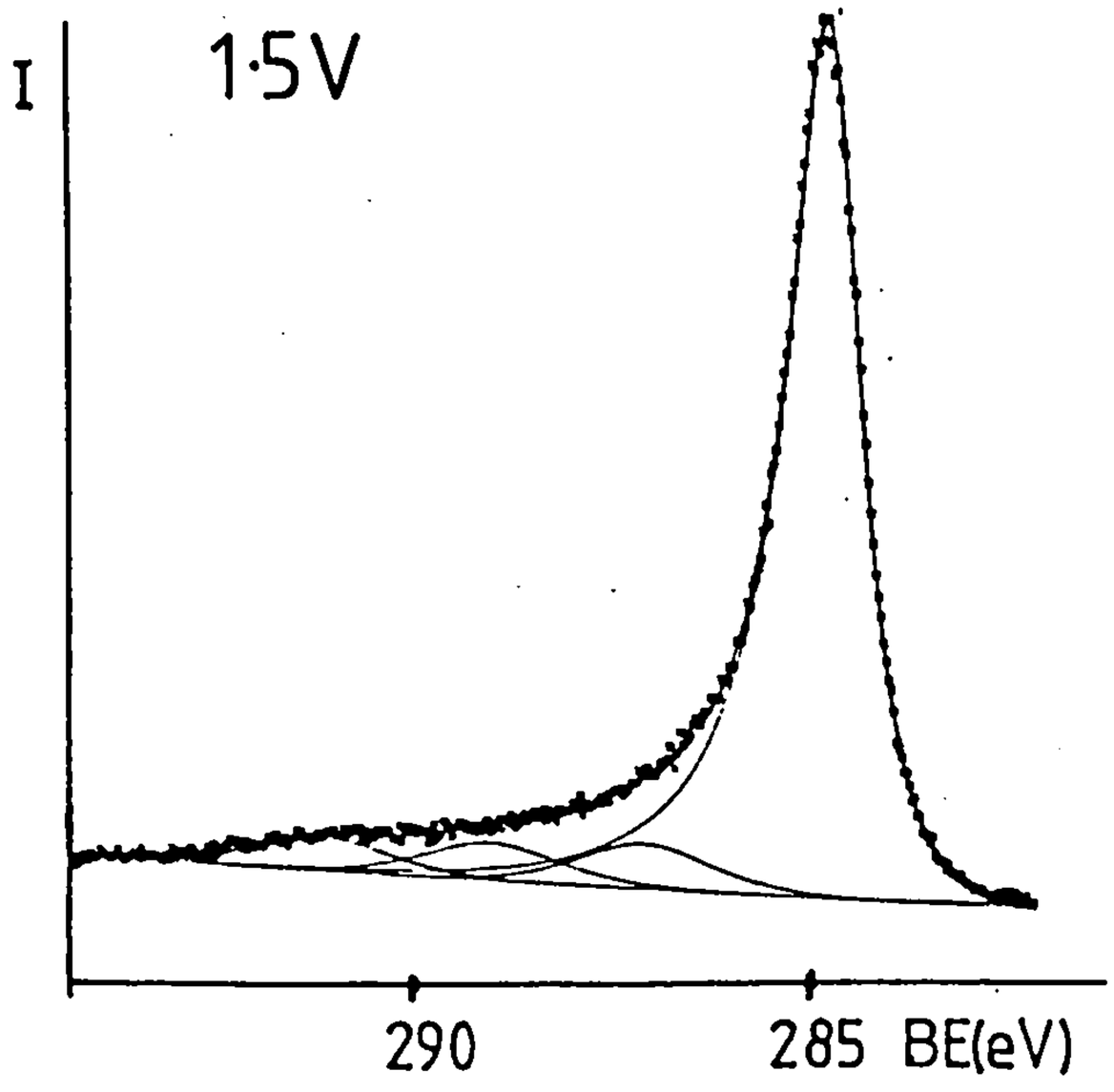

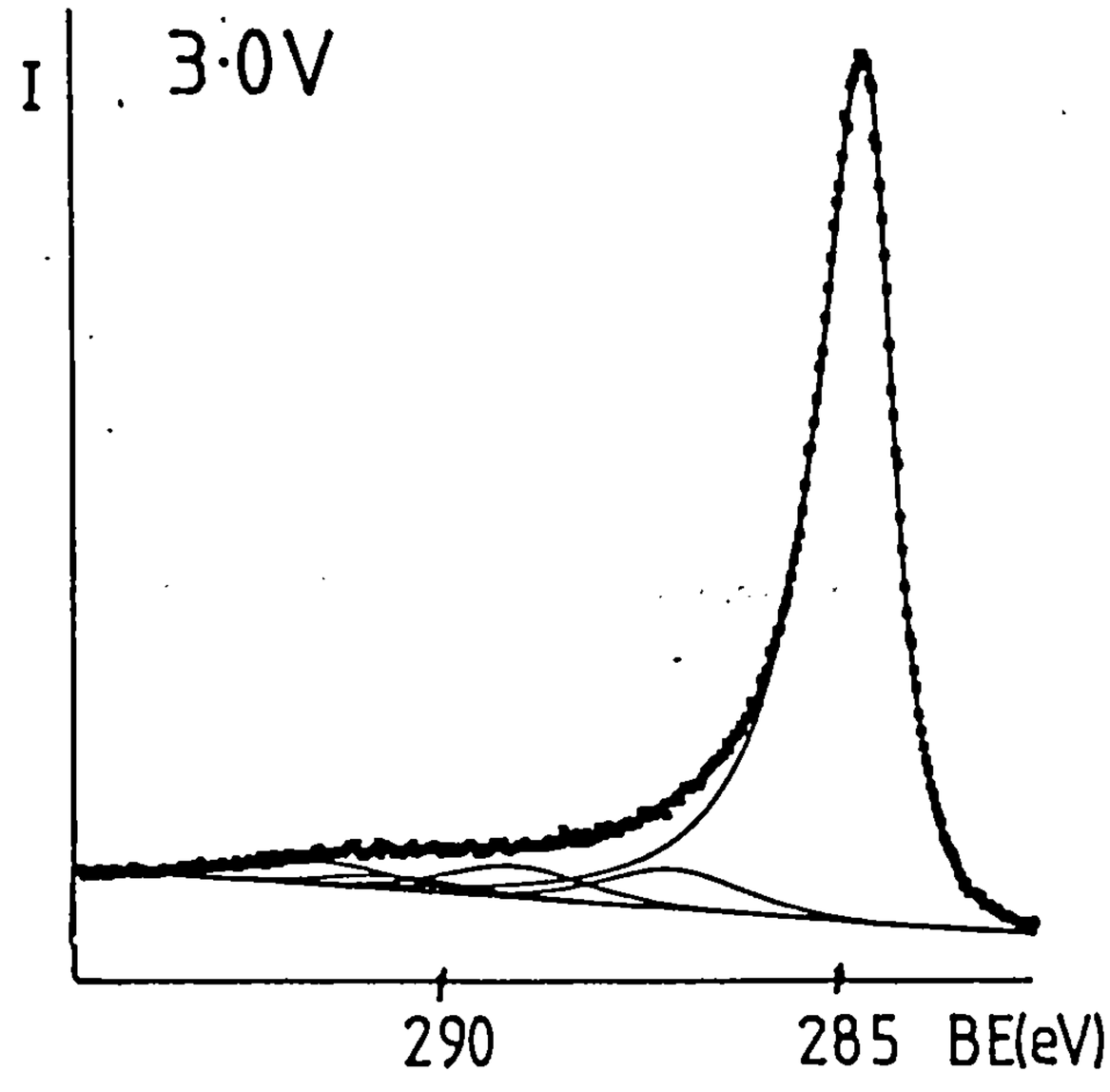

Fig.7.6 C1s Spectra of Fibres Polarised in NH_4HCO_3 Soln.

TABLE 7.4

The Curve Fitting Results from Carbon 1s Spectra of Fibres Polarised in Ammonium Bicarbonate Solution (10%)

Potential	Chemical Shift (eV)	C_{ox}/C_{graph} (Area Ratio)
3·0V	2·52 4·73 6·82	0·070 0·060 0·052
2·5V	2·21 4·45 6·62	0·072 0·077 0·056
2·0V	2·28 4·62 6·76	0·077 0·052 0·050
1·5V	2·38 4·38 6·53	0·073 0·062 0·053
1·0V	2·58 4·79 6·80	0·059 0·051 0·053
0·5V	2·37 4·58 6·52	0·074 0·048 0·053

(Figures quoted are within ± 0·01) (± 0·001)

TABLE 7·5

O1s:C1s Ratios for Fibres Polarised in Ammonium Bicarbonate Solution

Potential	O1s:C1s
3·0V	0·071
2·5V	0·124
2·0V	0·221
1·5V	0·085
1·0V	0·047
0·5V	0·058

(± 0·004)

program, and the resulting chemical shifts were slightly higher than those for ammonium nitrate, ie. 2.4eV(±0.2eV) and 4.5eV (±0.3eV). The area ratios with respect to the main graphitic peak are given in Table 7.4. The ratio of the two species varies to a small extent with potential. At most potentials the amount of 'oxide' 1 (ketone-type) is greater than that of 'oxide' 2 (carboxyl-type). The relative area of the signal above 6.0eV varies within a small range (0·050-0·056)

This lack of oxidation cannot be solely attributed to the pH of the electrolyte solution. The pH of 10% ammonium bicarbonate (7.66) is not as high as that of the sodium hydroxide solutions in chapter 6. The O1s:C1s ratios for fibres treated in sodium hydroxide solutions are four times as large as those obtained using ammonium bicarbonate. This suggests that the bicarbonate ion in some way inhibits the oxidation of fibres, not only by the removal of hydroxonium ions (countered by the removal of hydroxyl ions by ammonium ions), but also by the inability of the bicarbonate ions to react with the surface. Although no thorough investigation of surface reaction mechanisms was carried out, it is proposed that the reactions of bicarbonate ions at the fibre anode may be of the following type:

$$HCO_3^- = CO_2 + OH + e^- \qquad 7.1$$

$$2OH = H_2O + O \qquad 7.2$$

$$2O = O_2 \qquad 7.3$$

$$O + C_{(s)} = C_{(s)}(O)_{(ads)} \qquad 7.4$$

The overall effect can be written as

$$8HCO_3^- = 8CO_2 + 4H_2O + O_2 + C_{(s)}(O)_{(ads)} \qquad 7.5$$

The carbon dioxide will be unlikely to oxidise the fibre surface. The O1s:C1s ratios are given in Table 7.5, the largest ratio being found for fibres polarised at 2.0V.

All the oxygen 1s spectra consist of two oxygen species with binding energies 533.4eV (±0.2eV) and 531.7eV (±0.5eV). These correspond to =O and -O- type groups. Again, there is no trend in the relative area ratios for these two signals, but large variation is seen with potential. The oxygen spectra are shown in Fig.7.7.

Nitrogen was present on all fibres polarised above 1.0V, although its concentration was extremely small. The N1s:C1s values obtained here are much smaller than those obtained by Proctor and Sherwood (87), confirming that the surface functionality produced in that case was probably due to the prepolarisation at -1.3V before pulsing to a positive potential.

7.3.1 The Effect of Saturating the Ammonium Bicarbonate solution with Ammonia

It has already been suggested that surface nitrogen functionality is a result of the reaction of ammonium ions with the fibre surface. To maximise the amount of ammonium ions in solution, but to keep the concentration of the anion constant, the solution was saturated with ammonia.

Fig.7.8 shows the fitted carbon 1s spectra for fibres

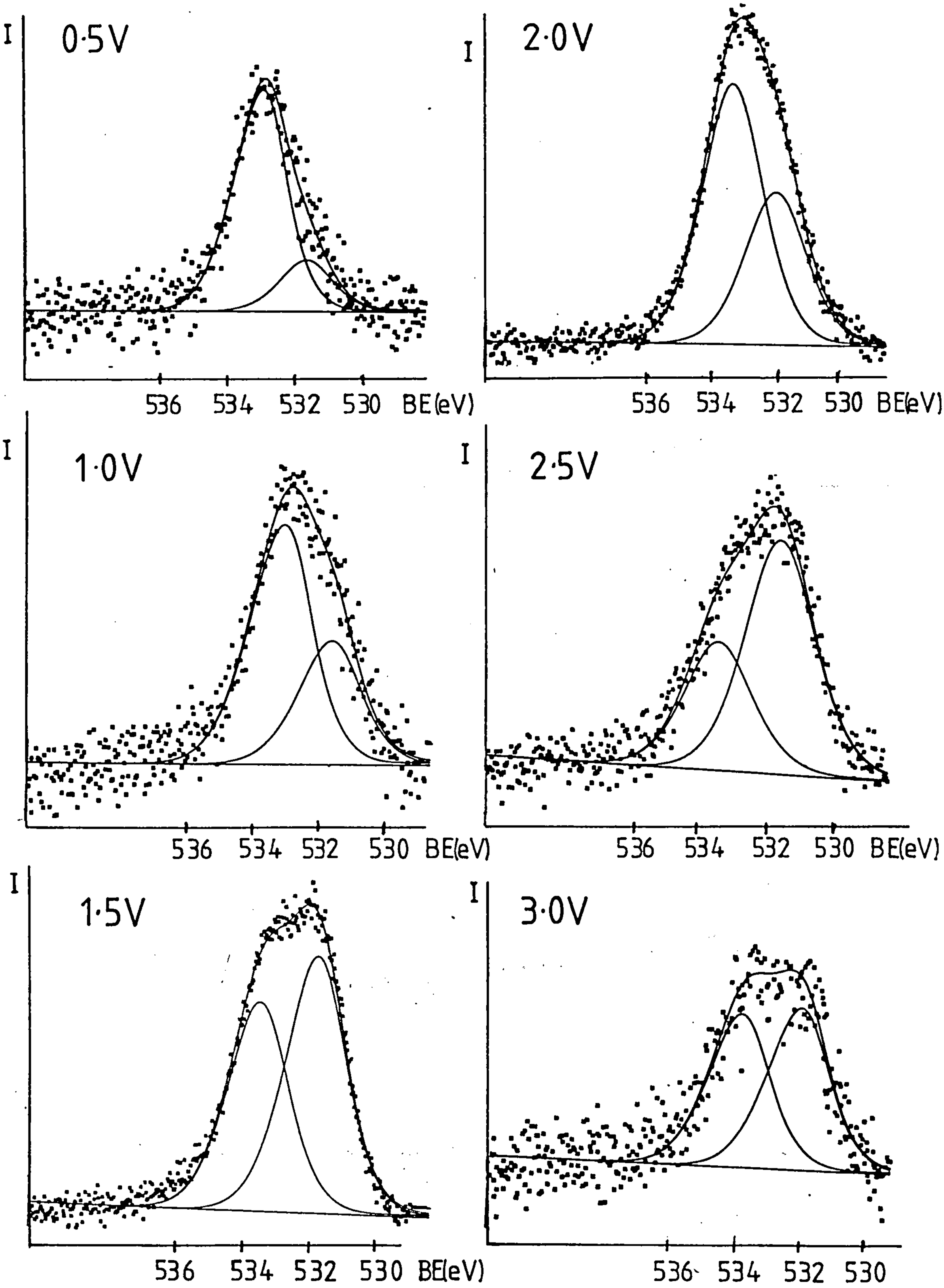

Fig.7.7 O1s Spectra of Fibres Treated in NH_4HCO_3

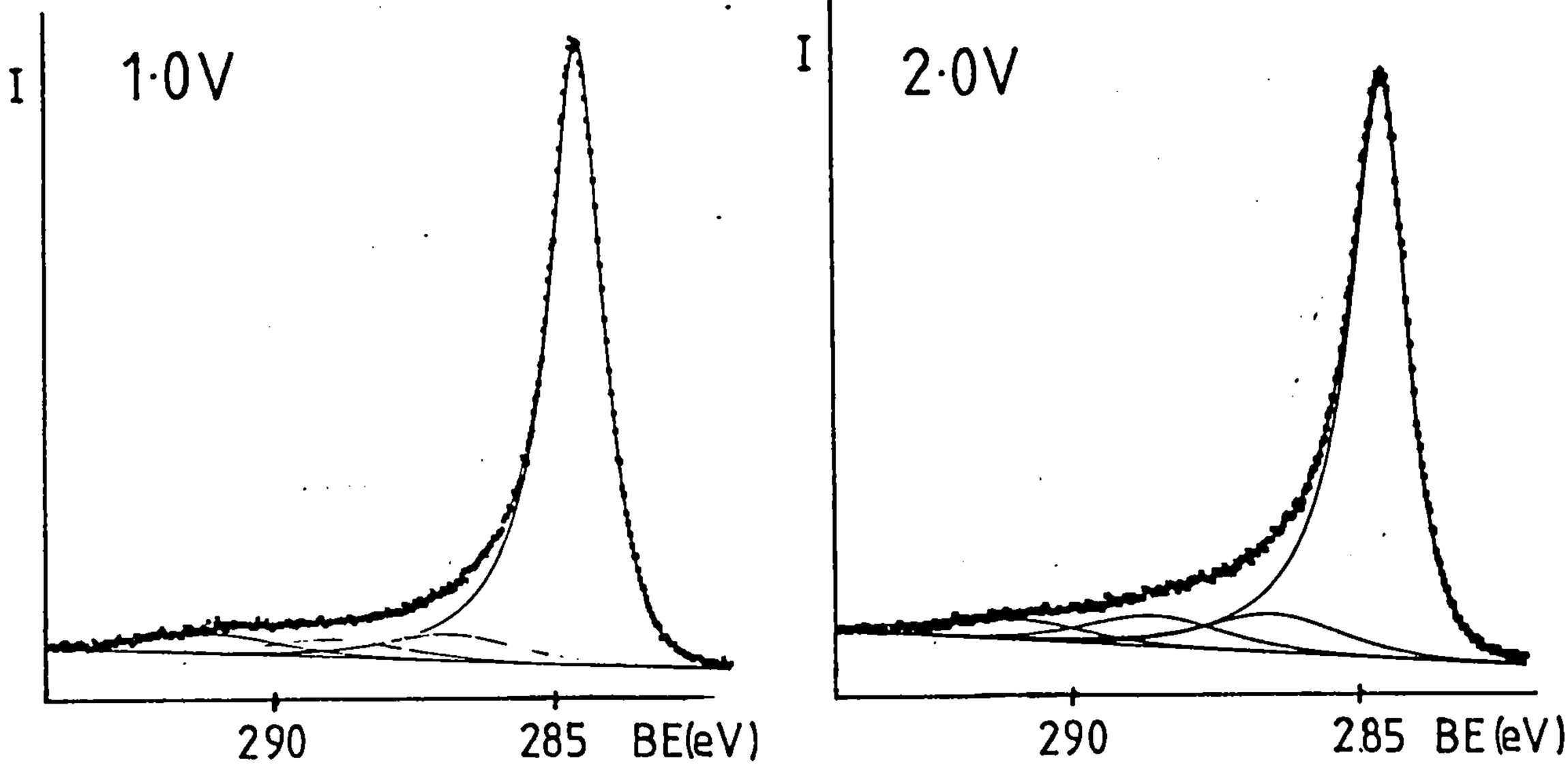

Fig.7.8 C1s Spectra of Fibres Polarised in NH_4HCO_3 Soln. Saturated with NH_3

polarised in these saturated solutions. The amount of chemically shifted species is far greater in these cases than for the unsaturated solutions. The area ratios and fitting results are shown in Table 7.6. The spectrum for fibres polarised at 1.0V consists of two chemically shifted species with binding energies similar to those seen in the case of the unsaturated solutions ie. 2.3eV (±0.05eV) and 4.5eV (±0.05eV). The binding energies for the chemically shifted species present in the other spectra (corresponding to 1.5, 2.0 and 3.0V) are 2.0eV (±0.1eV) and 4.1eV (±0.2eV), these being lower than for the unsaturated solutions.

The oxygen 1s spectra consist of two species for 1.0, 1.5 and 2.0V, and three in the case of 3.0V. This third peak is due to adsorbed water on the surface (B.E. 535.6eV). The two main species have binding energies 533.5eV (±0.4eV) and 531.7eV (±0.4eV). This large variation is probably due to the varying acidity of surface functional groups. The higher binding energy component decreases with increasing potential and, at 3.0V, =O predominates.

The nitrogen 1s spectra of these fibre samples consist of two chemically shifted species at 400.5eV (±0.3eV) and 399.0eV (±0.1eV). The latter's intensity always being greater than the former.

The O1s:C1s ratios vary from potential to potential although no trend was observed. The N1s:C1s ratios increase with increasing potential from 0.0314 to 0.1221. This may be due to the increase of carboxyl-type functionality with which the

TABLE 7.6

Curve Fitting Results for the C1s Spectra Polarised in Ammonium Bicarbonate Solution Saturated with Ammonia

Potential	Chemical Shift	C_{ox}/C_{graph}
3·0V	2·08 4·18 6·44	0·126 0·095 0·051
2·0V	1·98 4·10 6·60	0·128 0·102 0·068
1·5V	1·97 3·93 6·18	0·187 0·078 0·054
1·0V	2·40 4·47 6·73	0·088 0·057 0·065
Errors	(±0·02)	(±0·002)

ammonium ions may react and, upon heating, form amides.

The N1s:C1s ratio increases eightfold in the ammonia saturated solution as compared to the unsaturated solutions, and a slight increase in surface oxygen was produced. This is most probably due to the large increase in the number of ammonium ions available for reaction. The large increase in nitrogen suggests that the chemically shifted signals seen in the carbon 1s spectra are largely due to C/N functionality. If relaxation effects are taken into account, the peak with a chemical shift of 2.0eV is most probably due to $-NH_2$ groups associated with carbonyl functionality (see Appendix). Nitrogen substituents on carbon are not expected to give rise to chemical shifts of 4.1eV.

Fitzer (18) has proposed some reactions that may occur between the fibre functional groups and the nitrogen groups in the hardener of the resin. The hardener molecules are then said to react with the resin (see Fig.7.9a). If nitrogen groups were present on the surface, then they could react directly with the resin, as shown in Fig 7.9b.

7.4. Ammonium Sulphate

The solution used was 10% ammonium sulphate which has a pH of 4.5. Fig.7.10 shows the spectra obtained for fibres polarised in this solution at 2.0V for one minute. Large amounts of surface oxygen complexes were produced. The carbon 1s spectrum once more shows typical characteristics of fibres polarised to high potentials in acidic solutions. Two 'oxide' signals are seen at 2.07eV (±0.01eV) and 4.00 eV (±0.01eV) and a

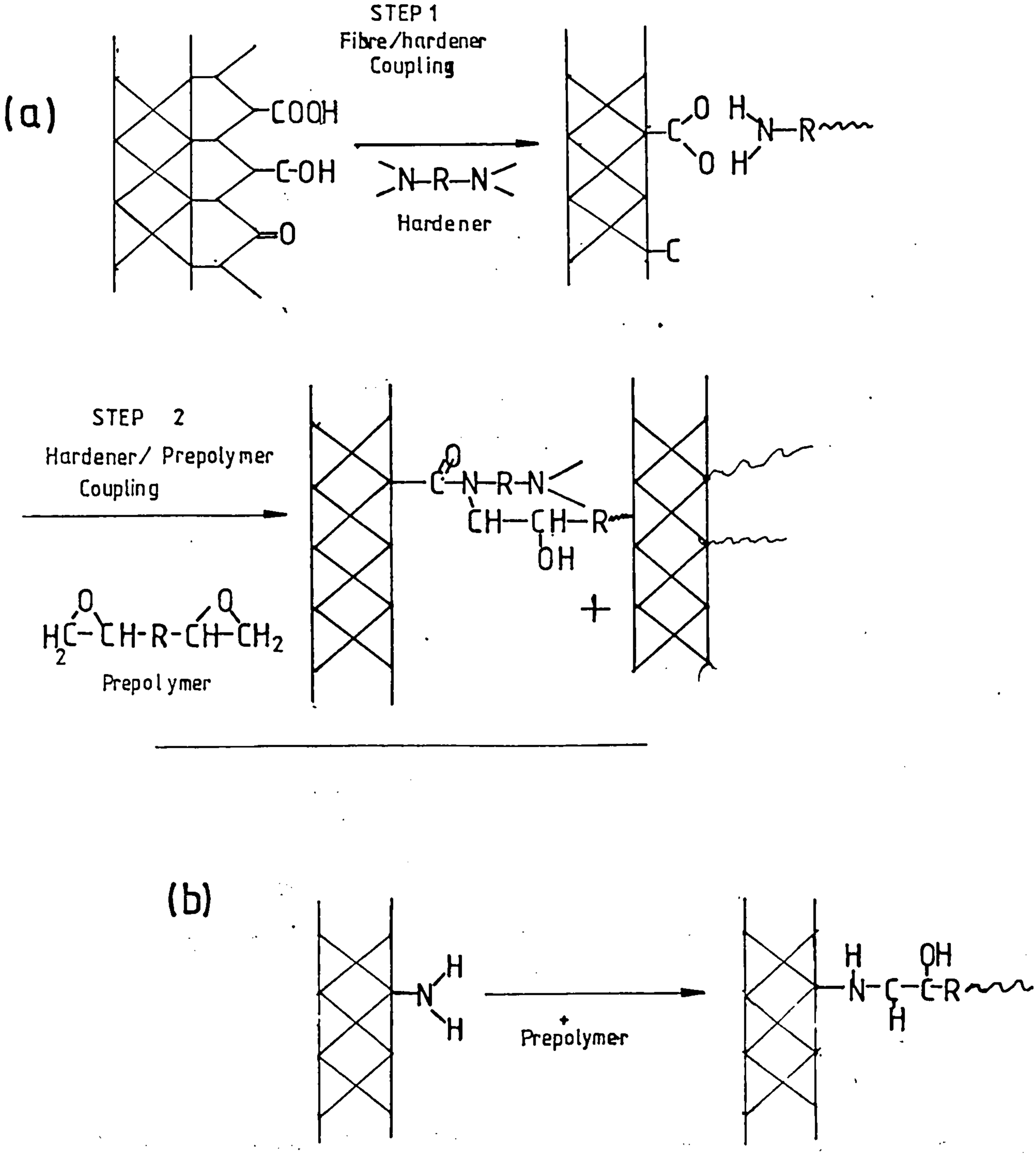

Fig.7.9 Possible Reactions between Fibre and Resin

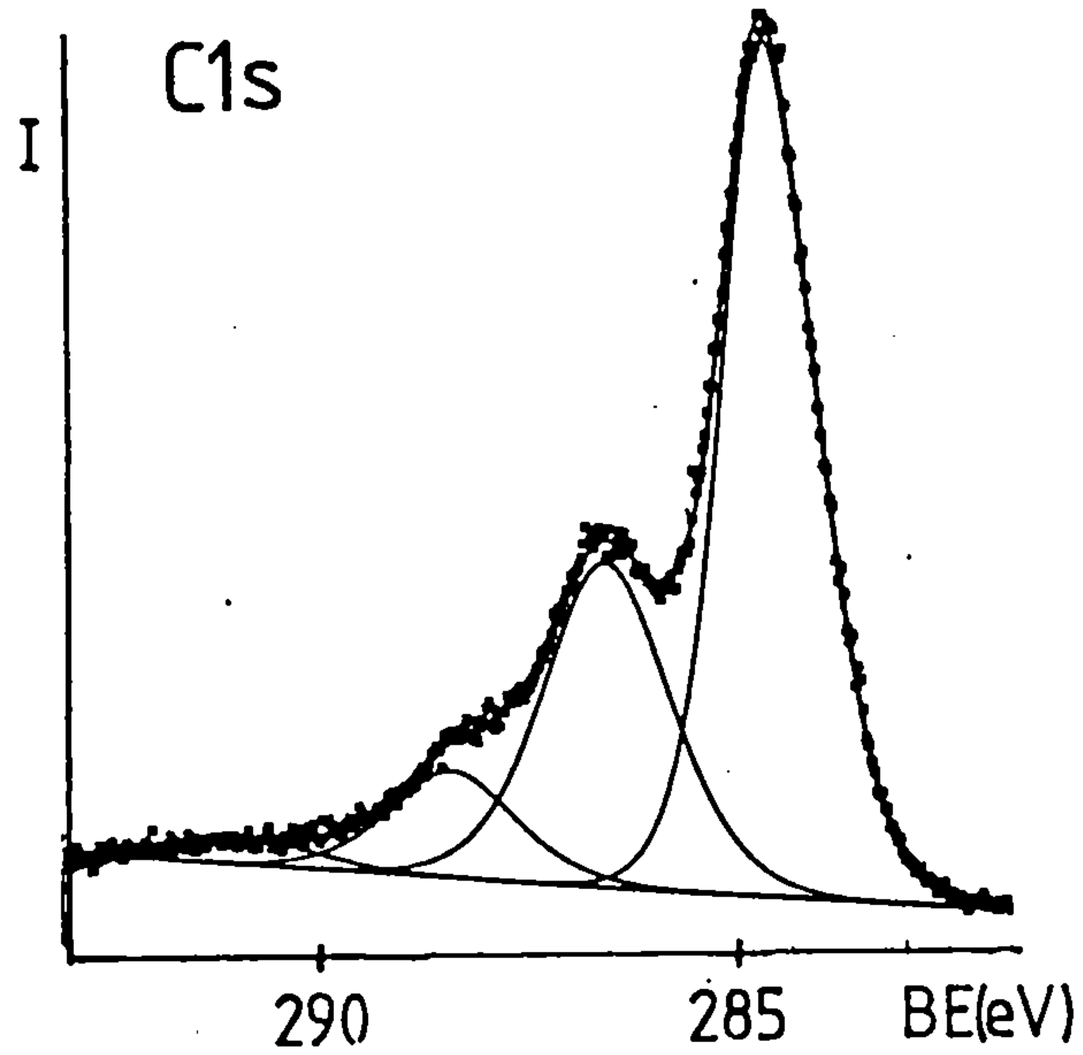

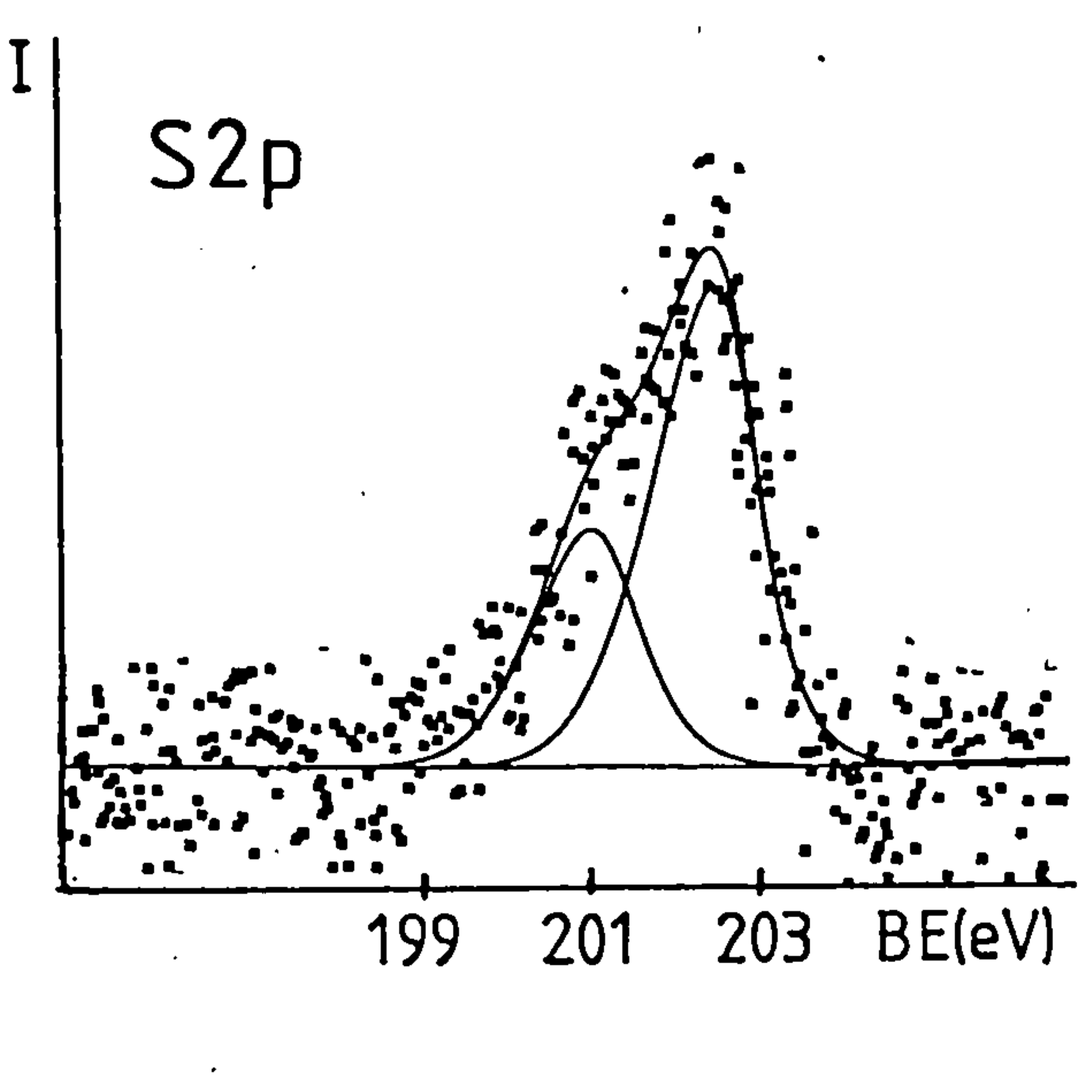

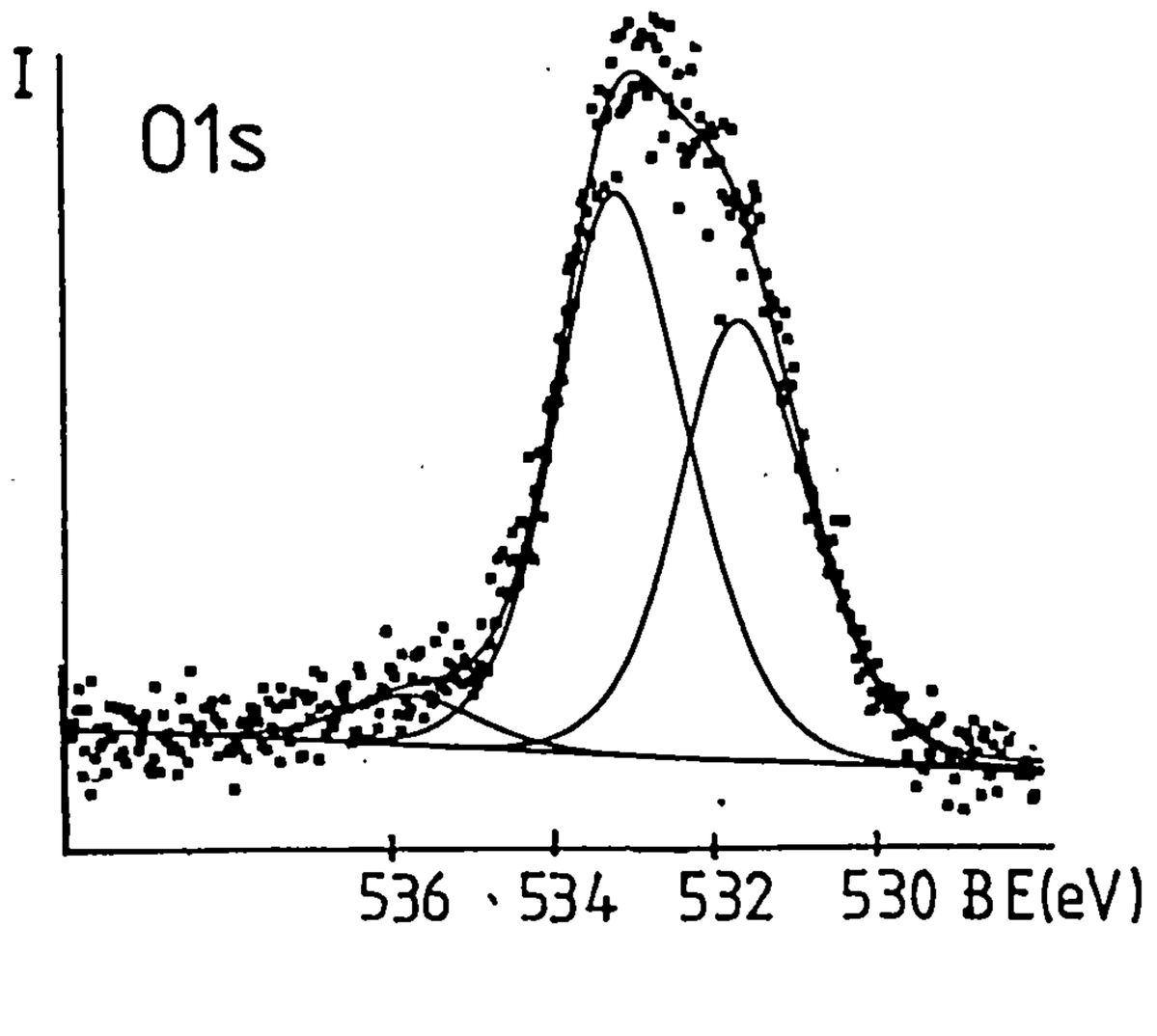

Fig.7.10 Spectra Obtained from Fibres Polarised in $(NH_4)_2SO_4$

satellite at 6.4eV.

The oxygen 1s spectrum consists of three shifted species with binding energies 535.46eV, 532.68eV and 531.40eV (all values given are ±0.02eV). The highest value corresponds to adsorbed water, the other two signals arising from =O and -O- respectively. The binding energy of these latter two species are similar to those found for phosphoric acid treatments. The =O in the sulphate ions contributes to the intensity of the lower binding energy component. The binding energy of the sulphur species corresponds to sulphate ions.

These fibres have a S:C ratio of 0.0066 and an O:C ratio of 0.2988. The S:O ratio was 0.0221. The sulphate may be in the form of graphite bisulphate which is known to exist on graphite electrodes used in sulphate solutions.

7.5 Conclusions

The oxidation of fibre surfaces is quite marked using solutions containing ammonium salts of hard acids. The surface functionality is very similar to that produced from the hard acid alone. Small amounts of surface nitrogen can be detected in some cases, and is probably due to surface oxygen complexes reacting with the ammonium ions in solution.

The use of ammonium bicarbonate as the electrolyte greatly reduces the amount of surface oxidation produced. The volume of gas evolved at the electrodes is far greater in this case than for other ammonium electrolyte solutions. The bicarbonate ions

tend to inhibit surface oxidation. This, plus the slightly alkaline conditions lead to low oxidation of the fibre surface.

Increasing the concentration of ammonium ions by saturating the solution with ammonia introduces relatively large ammounts of surface nitrogen. These nitrogen containing functional groups may react with the resin matrix if incorporated into composites and may lead to improved mechanical properties.

The amount of surface oxidation increases with increasing concentration in the range 10^{-4}M to 1M ammonium nitrate.

CHAPTER 8

CARBON FIBRE/EPOXY RESIN COMPOSITES

8.1 Introduction

It is well known that oxidative surface treatments of fibres prior to their incorporation into epoxy resins increases the ILSS of the resulting composites. Many workers have examined fibres that have been commercially treated, eg. HMS, HTS and AS (treated types I,II and III carbon fibres), but details of process conditions were unknown. It has already been shown, in previous chapters, that anodic oxidation of fibres in different electrolytes can produce a variety of changes in the chemical and physical nature of the fibre surfaces. All these treatments were carried out in the laboratory where the cell was extremely clean and electrolyte solutions were almost pure. On an industrial scale these stringent conditions are neither practical nor economical. This chapter reports a study of fibres treated in a commercial-type cell. The use of the commercial cell enables a continuous tow of fibres to be treated in sufficient quantities for composites to be made. This allows the effect of a known commercial-type pretreatment on the ILSS of the composite to be studied.

The two methods of controlling the electrochemical conditions are galvanostatic and potentiostatic. The experimental arrangements have been described in chapter 4. The aim was to discover which method of control was more satisfactory.

8.2 The Effect of Galvanostatic Oxidation on the Fibre Surface

Fibres were treated in several different electrolytes using a series of currents. These treated fibres were incorporated into the resin. It was not possible, because of the time needed for such an investigation, to examine fibre samples from all treatments. Instead, a series of fibre samples treated in sodium hydroxide and another treated in potassium dichromate were chosen for examination using X-ray photoelectron spectroscopy. The results of this study are discussed below.

8.2.1 The Carbon 1s Spectra of Treated Fibres

A unique solution from curve fitting a photoelectron spectrum is very difficult to obtain, even with experimental data consisting of non-overlapping peaks. The carbon 1s spectra from fibre samples treated in the same electrolyte but with a variety of cell currents show very small changes. Many attempts were made to minimise the chi square (see section 4.9.1.2.3) of these fitted spectra using a variety of fixed and floated parameters, but unique curve fitting solutions could not be obtained.

From laboratory treated fibres it is known that certain types of functional groups give rise to signals in the photoelectron spectrum with a particular range of binding energies. It has already been shown that functional groups giving rise to chemically shifted signals at 1.6, 2.1 and 4.0eV from the main carbon signal, can be produced from a variety of chemical treatments. There are also plasmon and satellite signals present in the spectra with kinetic energies 6.9eV

and 6.0eV less than this main peak. The spectra were fitted to several combinations of signals and the best fits taken for this discussion.

It was also found that fixing the position of a signal 6.0eV from the main peak did not give satisfactory curve fits to the experimental data. The peak position was allowed to float and in all cases iterations produced a signal at between 5.1-5.9eV (may be due to carbonate groups) from the main graphitic signal. This contrasts with results from laboratory treated fibres. For the model compounds reported in chapter 5 (see also the appendix) satellite peaks were detected with kinetic energies 5.8-7.8eV lower than the main carbon signal (BE=284.6eV). The kinetic energies of the satellite peaks are slightly lower than that of the signal detected in the carbon 1s spectra of galvanostatically treated fibres. The solutions used for this commercial-type treatment have not been deaerated. This may lead to dissolved oxygen reacting with carboxyl groups already present on the fibre surfaces. Carbonate is said to have been produced in potassium hydroxide solutions using other types of carbon. In both cases the carbon 1s spectra consisted of a graphitic peak whose exponential tail and Gaussian/Lorentzian mix were fixed at 0.0275 and 0.840. A plasmon signal was also included 6.9eV from the main peak and its position fixed.

8.2.1.1 The Effect of Sodium Hydroxide

Fig.8.1 shows the carbon 1s spectra of fibres treated in sodium hydroxide (0.5M) using several cell currents. It can be seen that very little surface oxidation has taken place compared

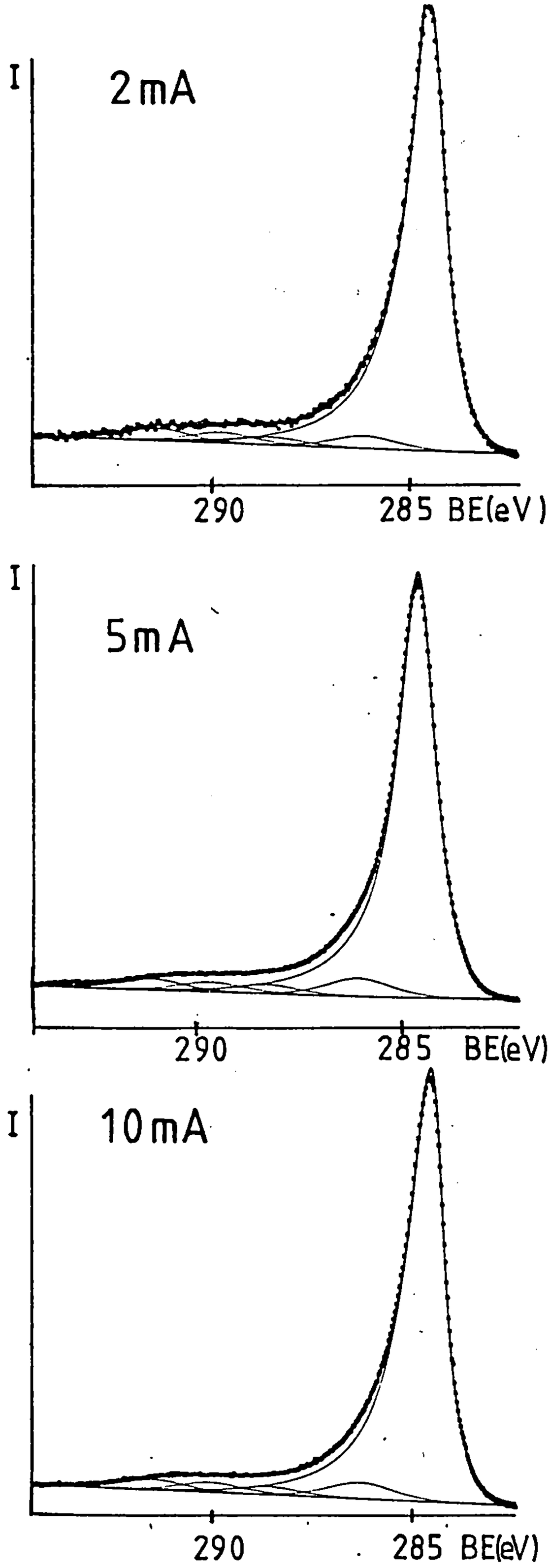

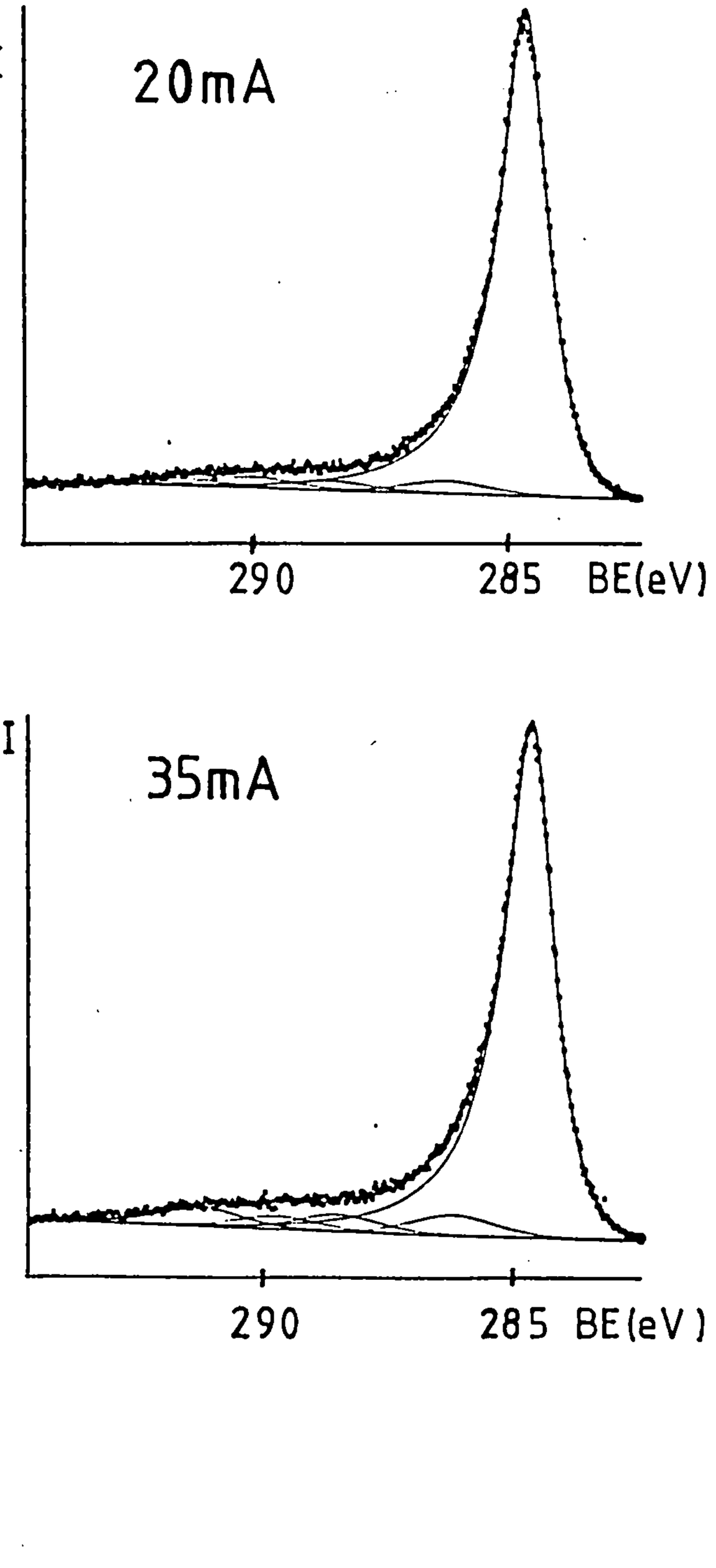

Fig.8.1 C1s Spectra of Fibres Treated in NaOH Soln.

to fibres treated under laboratory conditions. This is most probably due to the short reaction times (9 seconds). The variation in relative areas of the component peaks with respect to the main graphitic signal are given in Table 8.1.

It can be seen that for higher currents the amount of carboxyl/ester groups (4.0eV) is almost double the relative amount (with respect to the graphitic peak) produced using lower currents. The relative intensity of alcohol groups varies between 0.036 to 0.058, although there seems to be no relationship between their amount and cell current.

The relative intensity of the signal at 5.4eV remains almost constant (0.035-0.032).

The plasmon intensity decreases with current applied (with the exception of that corresponding to 35mA). This is to be expected because this plasmon is a feature of the main fibre lattice and, as the surface oxygen concentration increases, less of the bulk fibre structure is present in the sampling depth of the photoelectrons. (The reason for the exception is not known.)

8.2.1.2 The Effect of Potassium Dichromate

The fitted carbon 1s spectra from fibres treated in potassium dichromate are shown in Fig.8.2. These spectra were fitted to the same parameters as above, allowing the peak position at 6.0eV to float. The area ratios with respect to the main graphitic signal are shown in Table 8.2. As the current increases, the area ratio of the carboxyl groups also increases

TABLE 8.1

The Relative Area Ratios (wrt the Graphitic Peak) of Chemically Shifted Species in the C1s Spectra of Fibres Treated in NaOH

Current	Area Ratios			
	1·6eV	4·0eV	5·4eV	6·9eV
2mA	0·038	0·024	0·032	0·039
5mA	0·058	0·030	0·032	0·038
10mA	0·053	0·028	0·033	0·035
20mA	0·036	0·029	0·032	0·022
35mA	0·052	0·046	0·035	0·054

TABLE 8.2

The Relative Area Ratios (wrt the Graphitic Peak) of Chemically Shifted Species in the C1s Spectra of Fibres Treated in $K_2Cr_2O_7$

Current	Area Ratios			
	1·6eV	4·0eV	5·1eV	6.9 eV
0mA	0·067	0·017	0·047	0·028
2mA	0·061	0·031	0·034	0·022
5mA	0·139	0·009	0·057	0·035
			5·8eV	
10mA	0·033	0·044	0·028	0·037
20mA	0·032	0·056	0·023	0·042
35mA	0·041	0·066	0·032	0·035
50mA	0·049	0·069	0·031	0·035

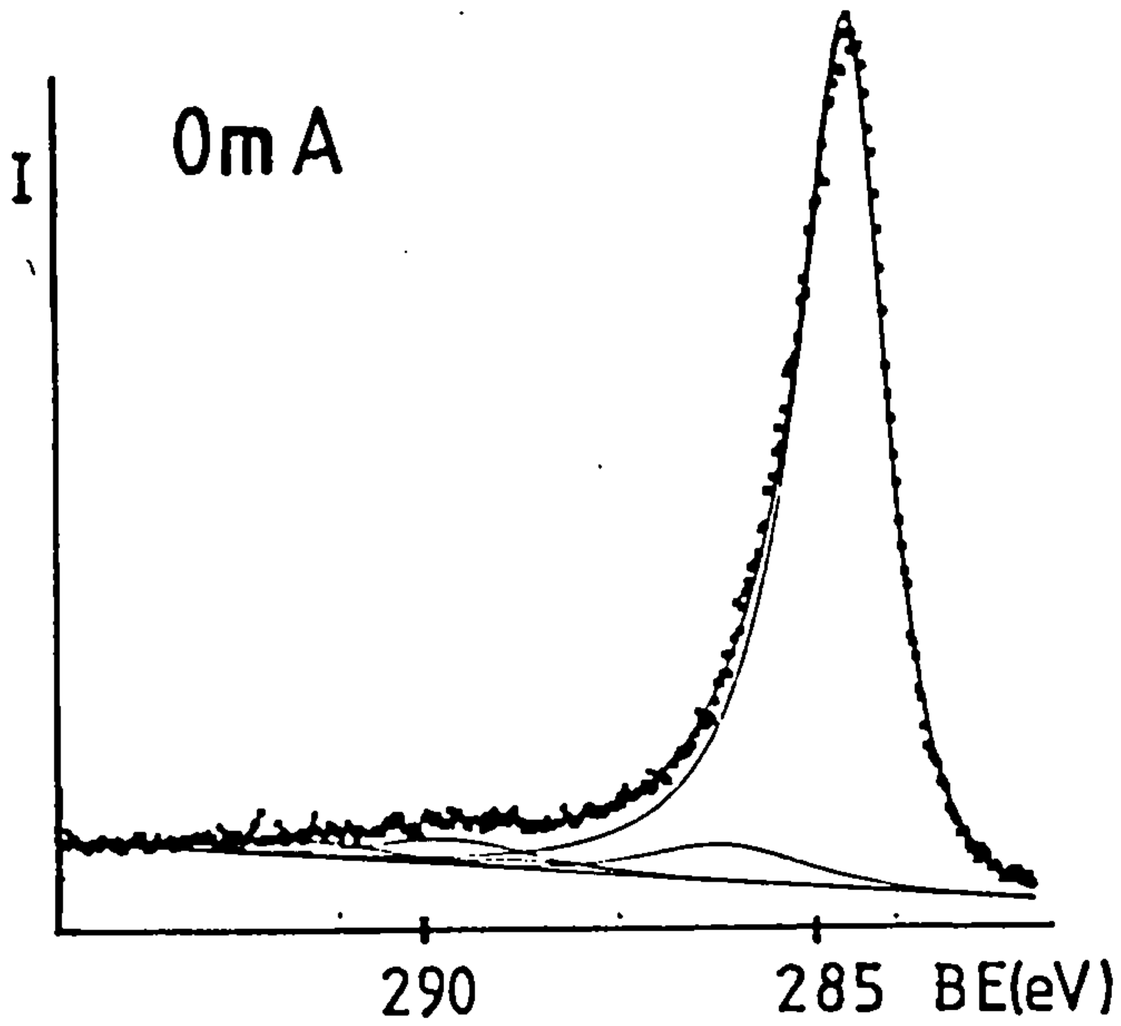

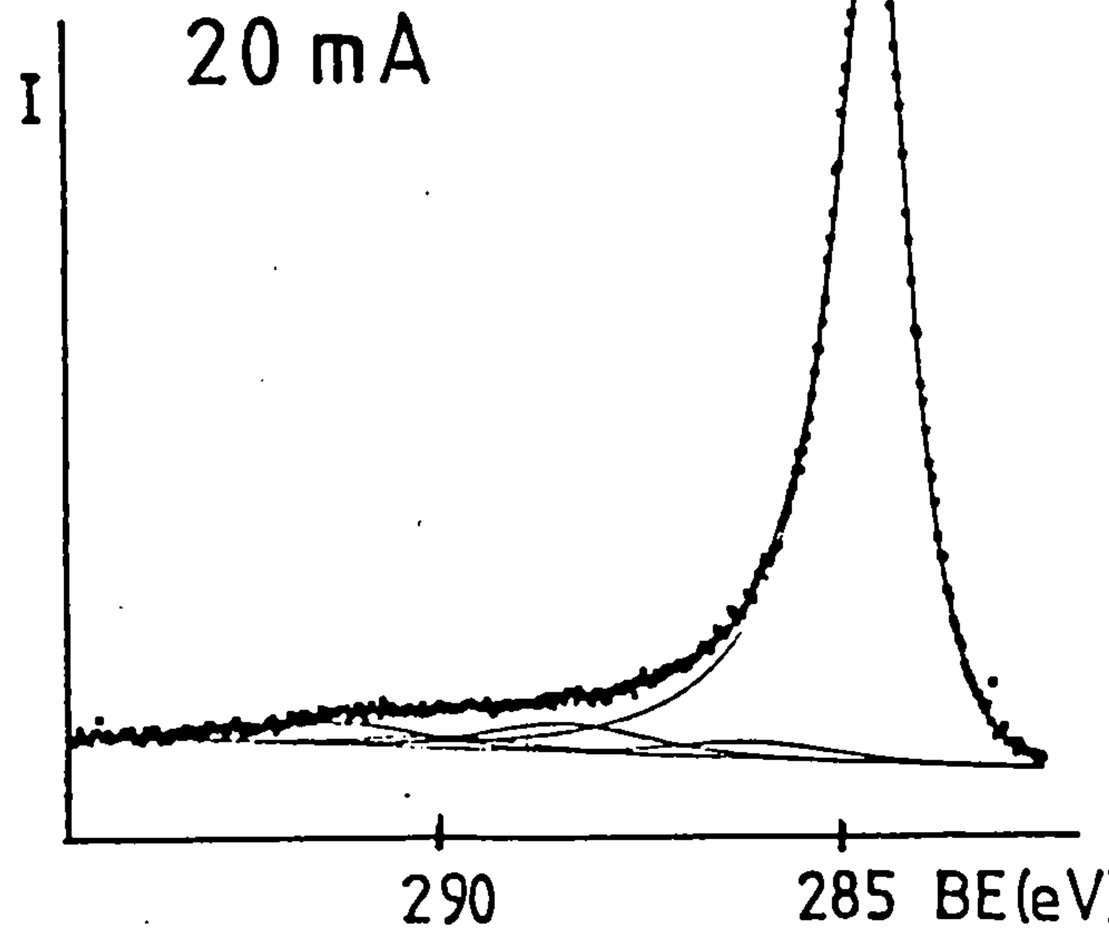

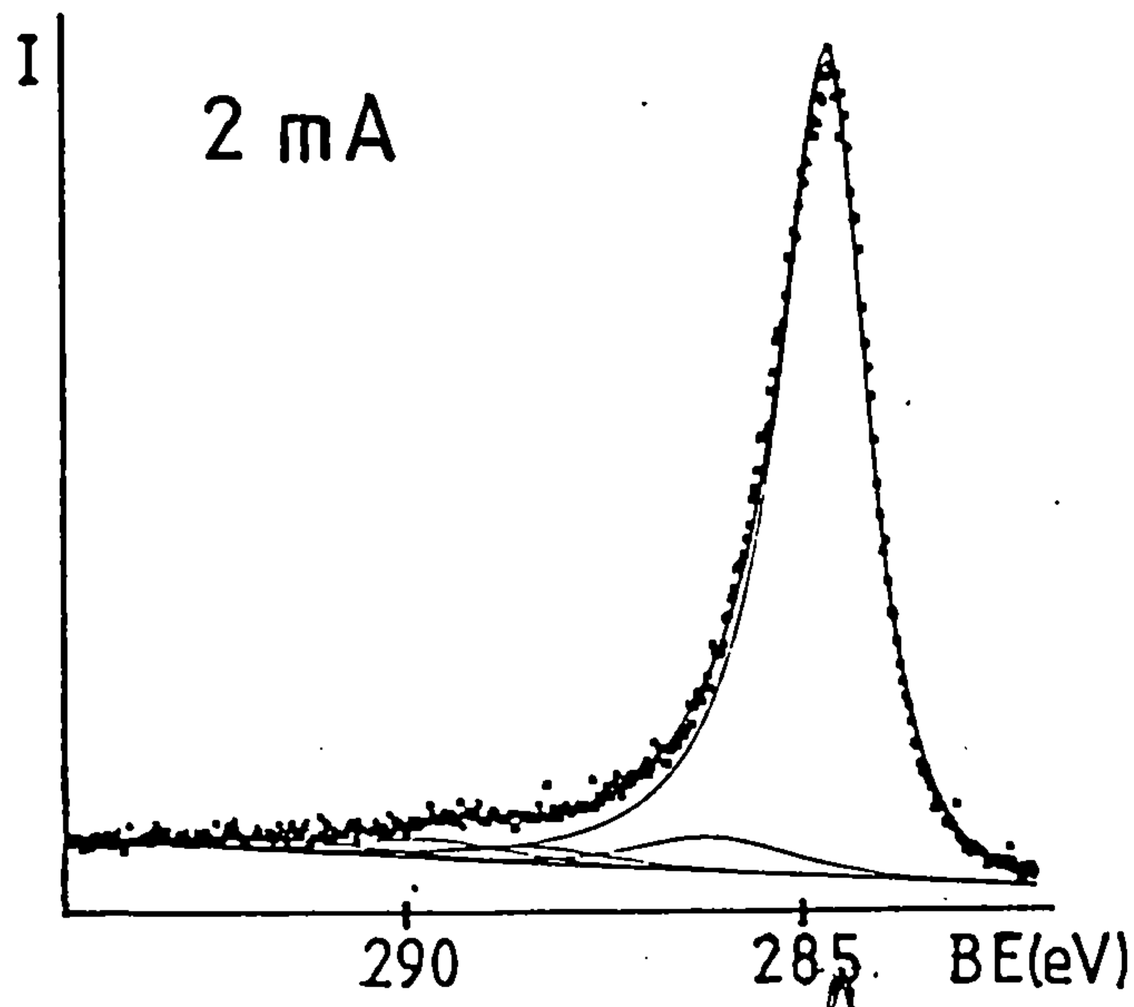

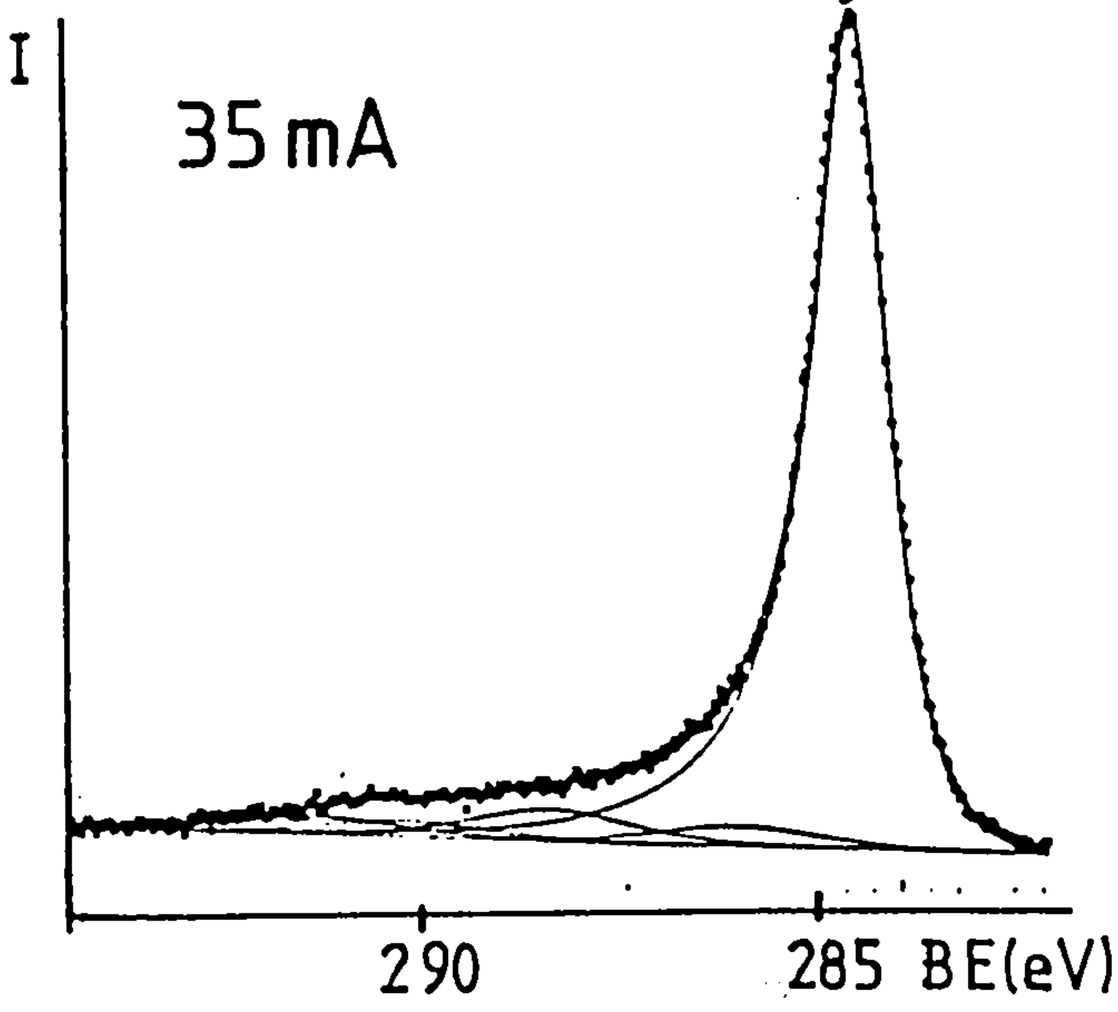

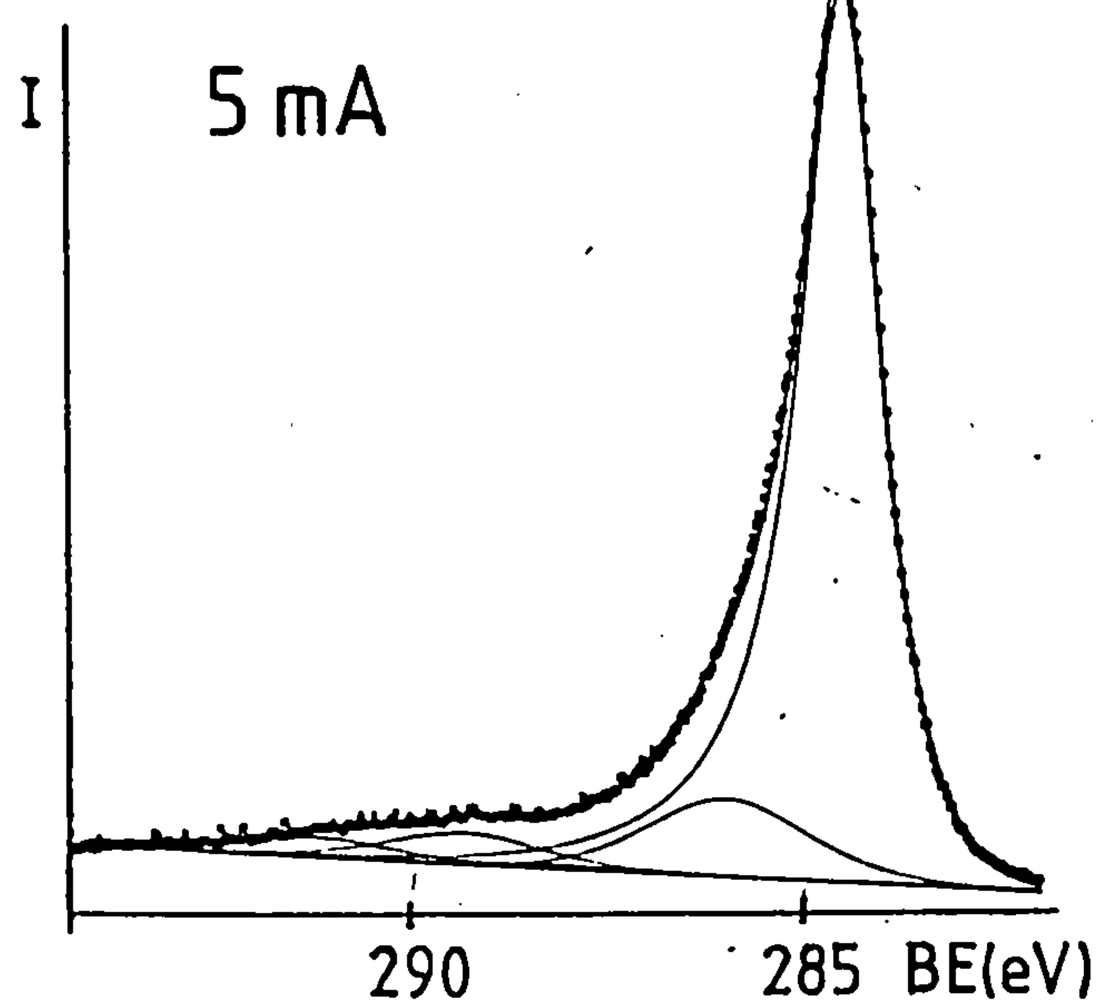

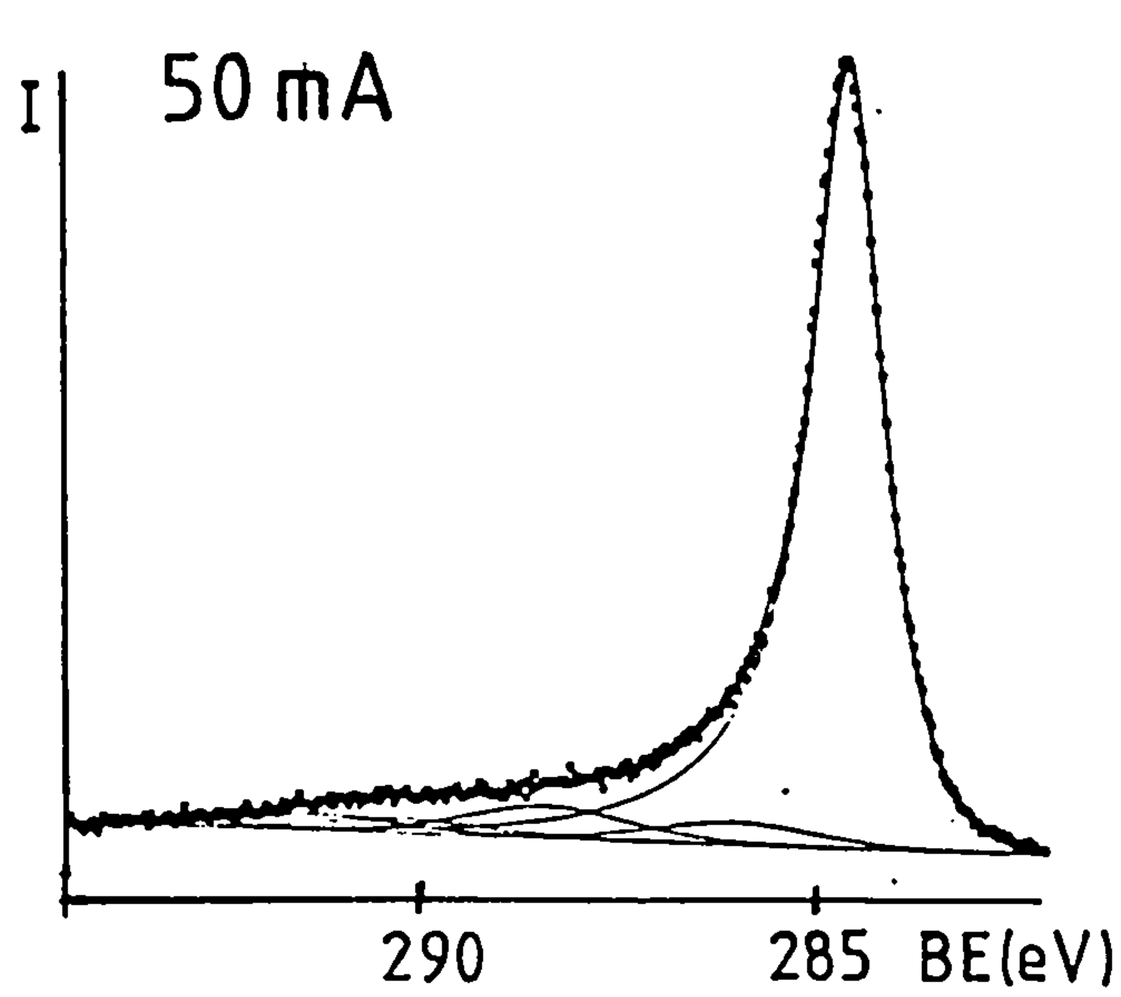

Fig. 8.2 C1s Spectra of Fibres Treated in $K_2Cr_2O_7$ Soln.

from 0.017 at 0mA to 0.069 for 50mA. The alcohol intensity varies with current, and in general there appear to be more alcohol type groups produced at low currents than at high currents. At 10mA and above, the carboxyl intensity is greater than the alcohol intensity. This is unlike the sodium hydroxide case where the number of carboxyl groups is always greater than the alcohol groups. This may be due to potassium dichromate being a good oxidizing agent, well known to be able to oxidise alcohols to carboxylic acids. The potassium dichromate was known to be reduced during treatment because the solution in the washing baths turned green due to the presence of Cr^{3+} aq. No chromium remained on the fibre after washing, as it was not detected in the spectrometer.

For high current (10mA-50mA) treatments a signal at 5.8 eV from the main peak was present. This peak position does suggest that it arises from satellite processes (see section 8.2.1). For lower current (0-5mA) a peak at 5.1. eV was present. This peak position (KE) is much higher than those found for satellite features. The chemical shift for carbonate type groups is approx. 5.4eV and this type of functionality may be responsible for observed chemical shift on these treated fibres.

8.2.2 The Oxygen 1s Spectra

8.2.2.1 The Effect of Sodium Hydroxide

Fig.8.3 shows the oxygen 1s spectra of these fibre samples. These spectra consist of two resolvable oxygen species with binding energies 533.9eV (.2eV) and 532.5eV (.2eV), an

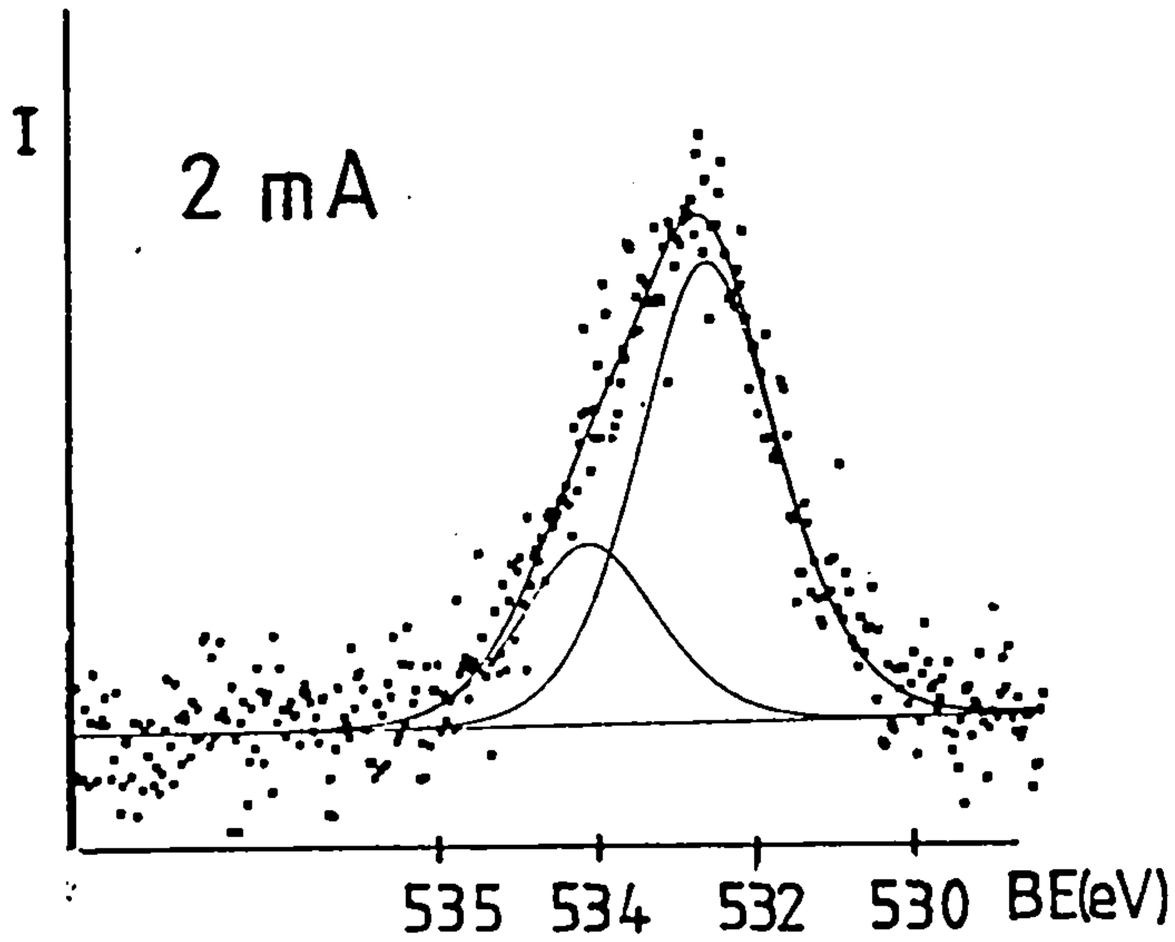

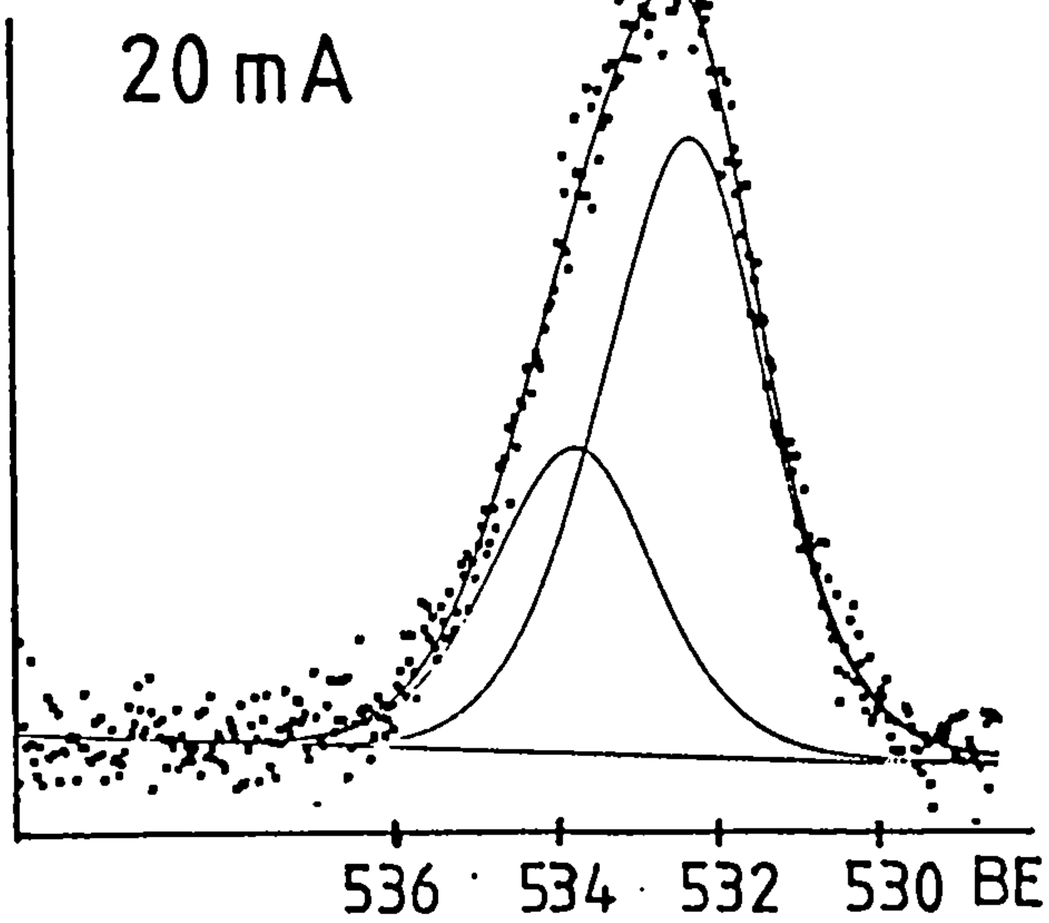

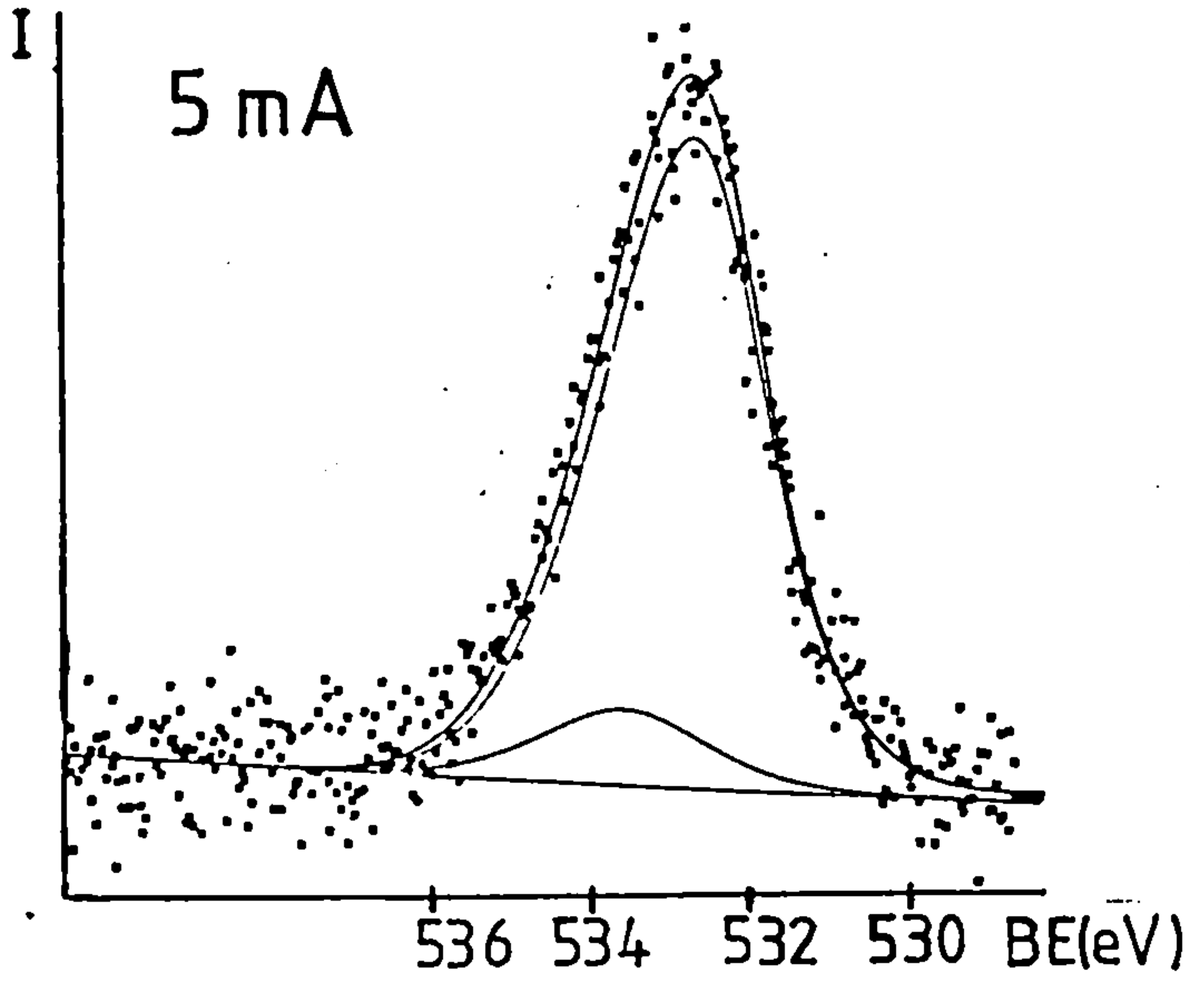

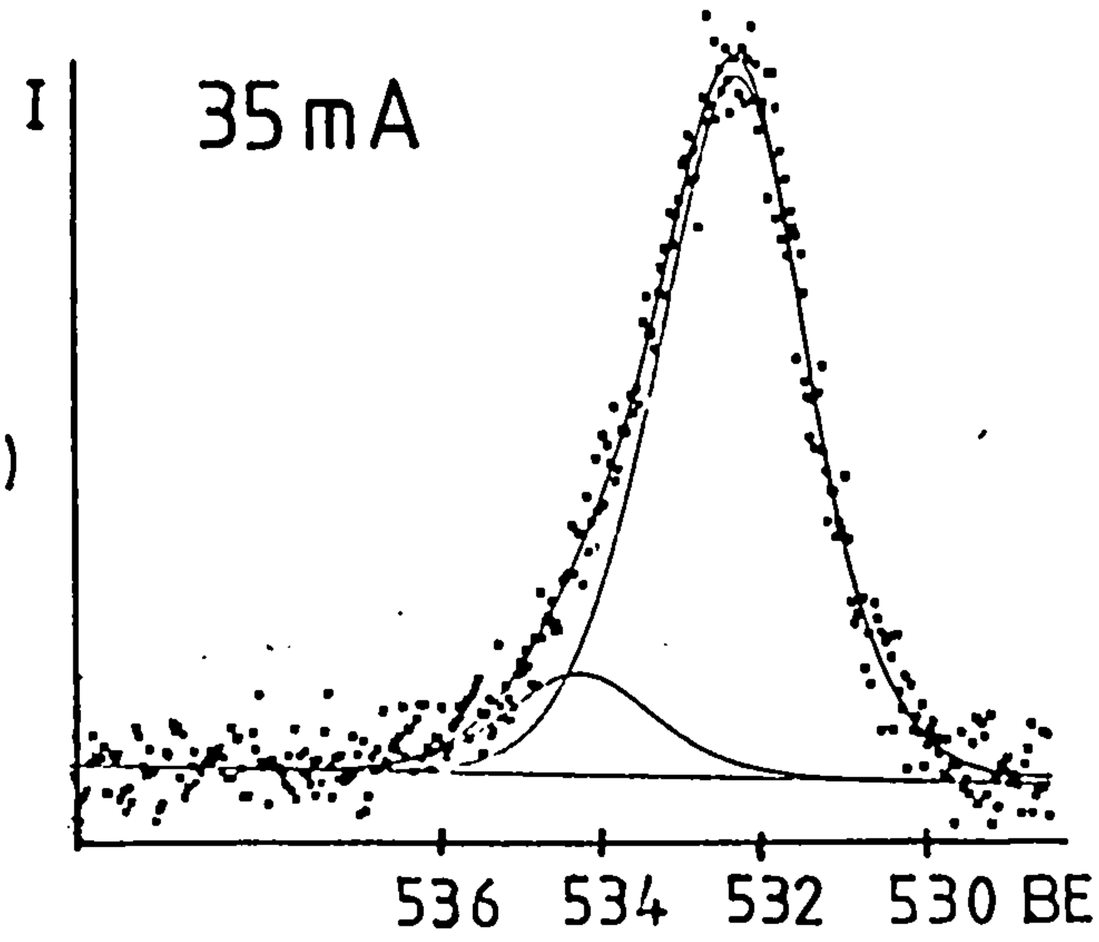

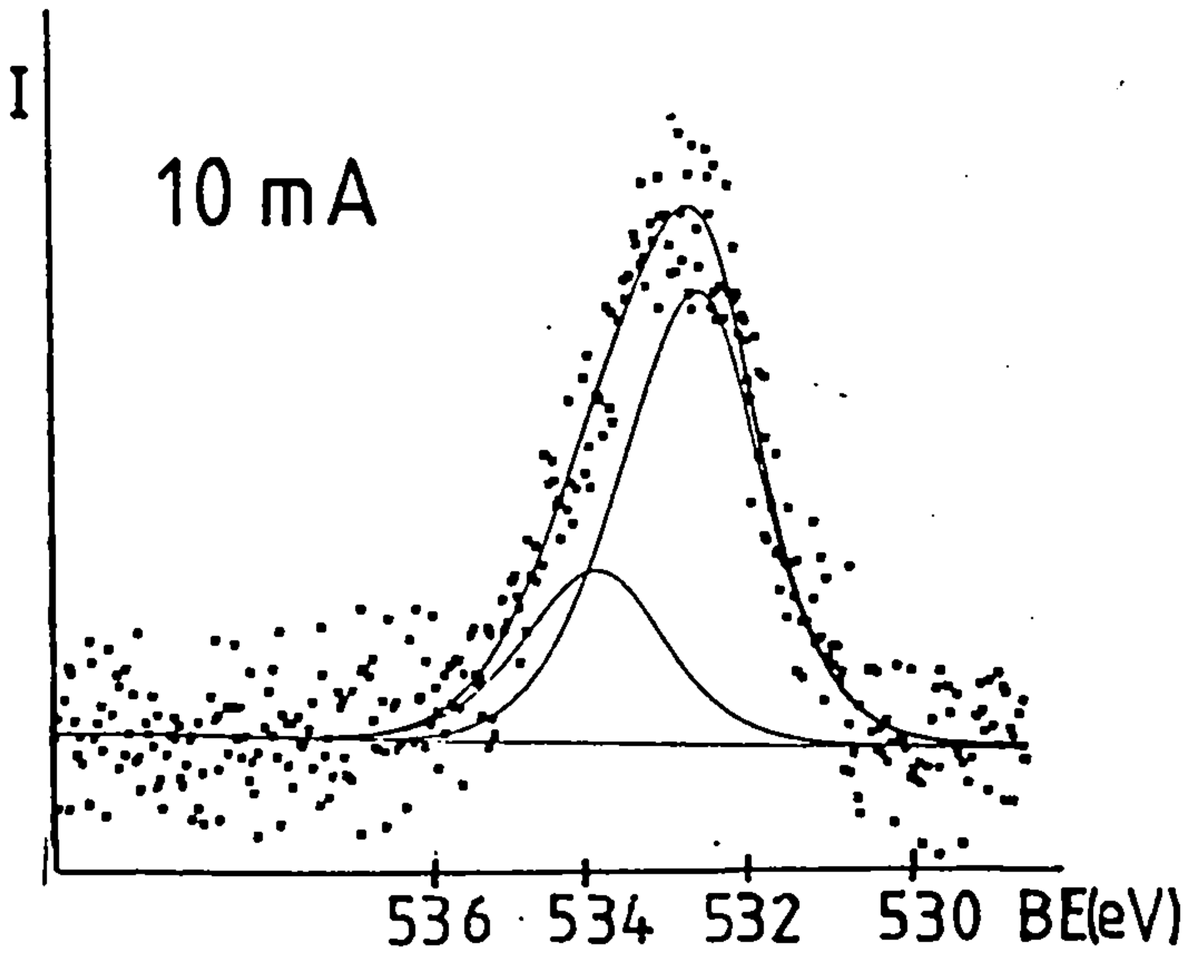

Fig. 8.3 O1s Spectra of Fibres Treated in NaOH Soln.

TABLE 8.3

Curve Fitting Results of O1s Spectra of Fibres Treated in NaOH

Current	Binding Energy	Area Ratio
2mA	532·4 533·9	0·719 0·281
5mA	532·7 533·8	0·855 0·145
10mA	532·6 533·7	0·723 0·277
20mA	532·4 533·7	0·669 0·331
35mA	532·4 534·2	0·874 0·126

TABLE 8.4

Curve Fitting Results of O1s Spectra of Fibres Treated in $K_2Cr_2O_7$

Current	Binding Energy	Area Ratio
0mA	532·6 533·9	0·819 0·181
2mA	532·3 533·8	0·756 0·244
5mA	532·5 533·7	0·788 0·212
20mA	532·1 533·4 536·0	0·562 0·370 0·068
35mA	531·8 533·3 536·0	0·514 0·389 0·097

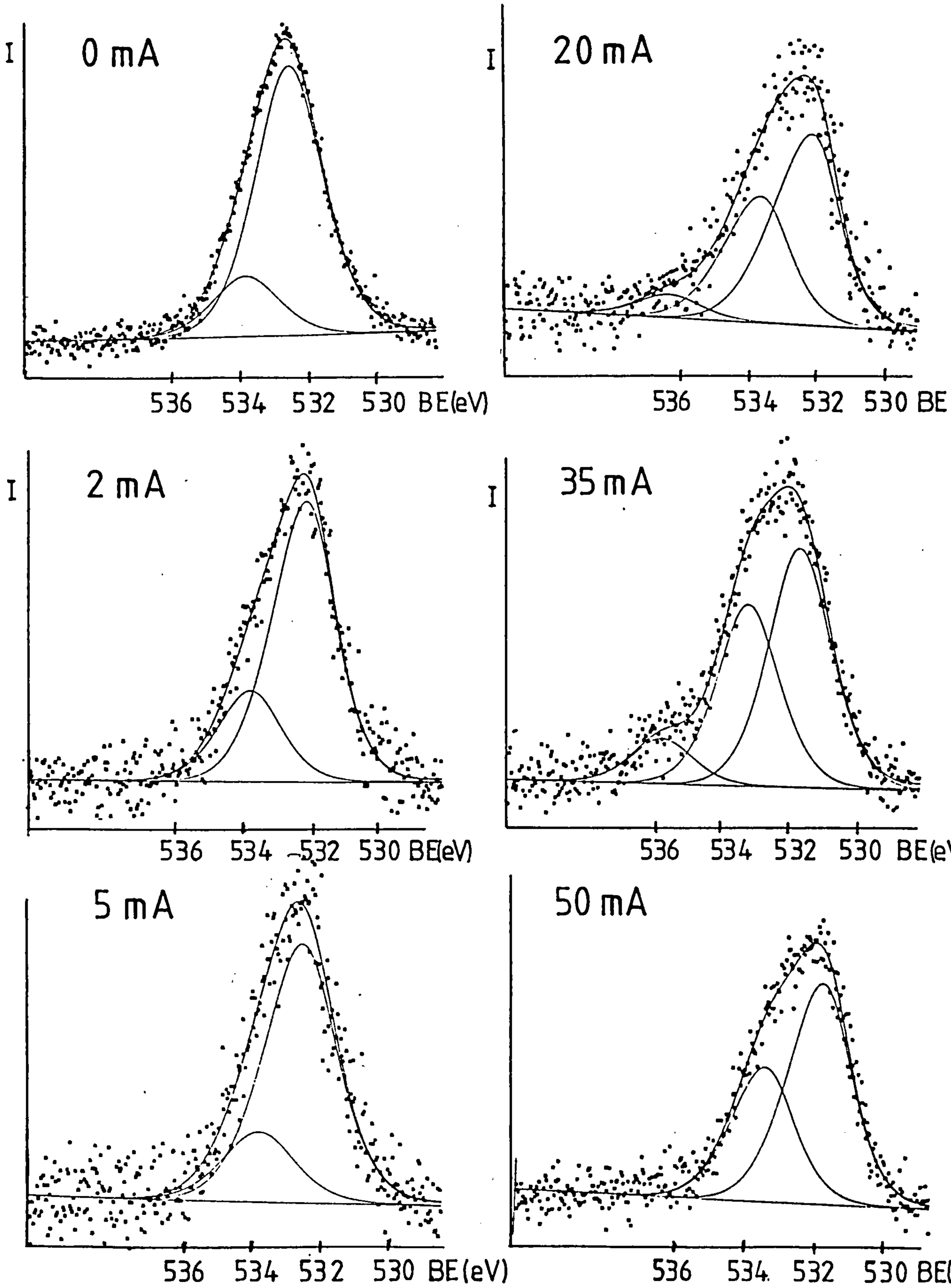

Fig.8.4 O1s Spectra of Fibres Treated in $K_2Cr_2O_7$ Soln.

exception being at 35mA where the higher component has a binding energy 534.2eV which is slightly higher than the others (see Table 8.3). In all cases the lower binding energy component is of higher intensity. The assignment of both peaks to a specific type of oxygen species is a little uncertain. Comparing these binding energies to those found on laboratory treated fibres in the same electrolyte shows that the higher binding energy component is common for all samples (within error limits), and it probably arises from -O- type groups. From the carbon 1s spectra it was found that there were more alcohol groups present than carbonyls. It would therefore be expected that a signal due to -O- type oxygen would have the larger intensity in the oxygen 1s spectra. The lower binding energy value, 532.4eV, is, in this case, higher than for laboratory treated samples (531.4eV). As found in the case of the oxygen 1s spectra for fibres polarised in nitric acid (B.E.=532.2eV), these oxygen species may have both =O and -O- character. No signal due to adsorbed water was present. This may be because the number of highly polar carboxyl groups is far less in this case, as compared to the laboratory treated fibres.

8.2.2.2 The Effect of Potassium Dichromate

The fitted oxygen 1s spectra for samples treated in potassium dichromate are shown in Fig.8.4. The binding eneries and area ratios are given in Table 8.4. At currents below 20mA only two oxygen species are produced, but above this cell current adsorbed water is present on the fibre surface. This is to be expected because carboxyl groups are the main functional group present on the fibre surface. The binding energies for both =O

TABLE 8.5

O1s : C1s Ratios

Current (mA)	O1s:C1s Ratio	
	NaOH	$K_2Cr_2O_7$
0	—	0·067
2	0·054	0·096
5	0·049	0·079
10	0·061	—
20	0·071	0·085
35	0·088	0·184
50	—	0·200

and -O- decrease with increasing current. (The reason for this is unknown.) There is a general trend for the intensity of the higher binding energy component to increase with increasing current, and that of the lower binding energy component to decrease with increasing current, although the intensity of the lower binding energy component is always greatest.

8.2.3 Oxygen/Carbon Intensity Ratios

For fibres treated in sodium hydroxide the O1s:C1s ratio varies for different cell currents, there being no observable trend in the results (see Table 8.5). The maximum ratio, 0.071, occurs for fibres at 20mA. These ratios were much smaller (approximately 1/4) than those found on laboratory treated samples due, in part, to the limited reaction times.

For fibres treated in potassium dichromate this ratio generally increases with increasing current from 0.067 to 0.200 (see Table 8.5). These ratios are higher than those for sodium hydroxide. This is not surprising because potassium dichromate is a good oxidising agent in itself and the pH of the solution is lower than for sodium hydroxide (see chapter 5).

8.3 The Effect of Galvanostatic Surface Treatment upon the ILSS of Composites

Figs.8.5a and b show the ILSSs of composites made from fibres treated with sodium hydroxide and potassium dichromate respectively. Both plots show that the ILSS initially increases with increasing all currents up to 20mA, thereafter remaining

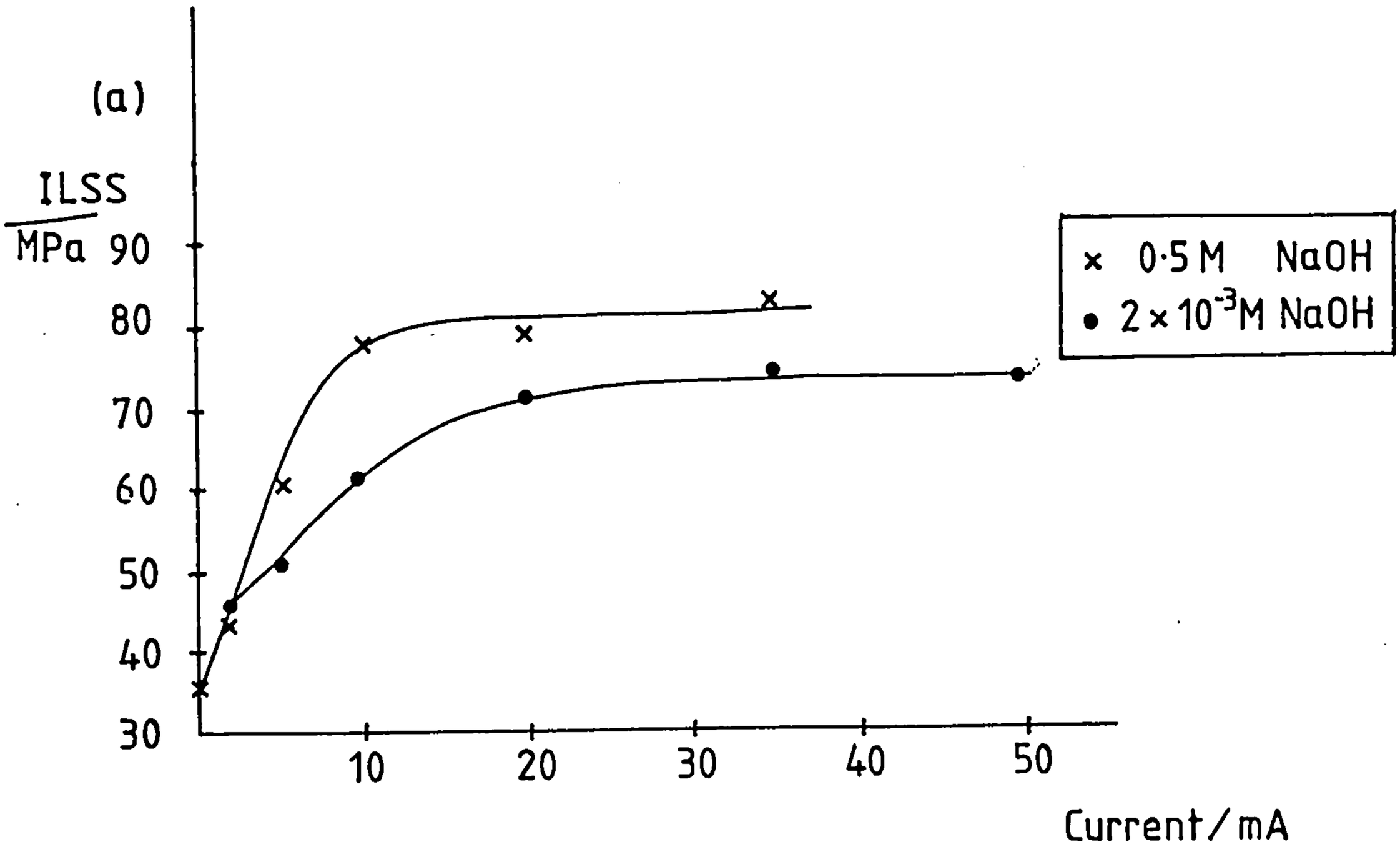

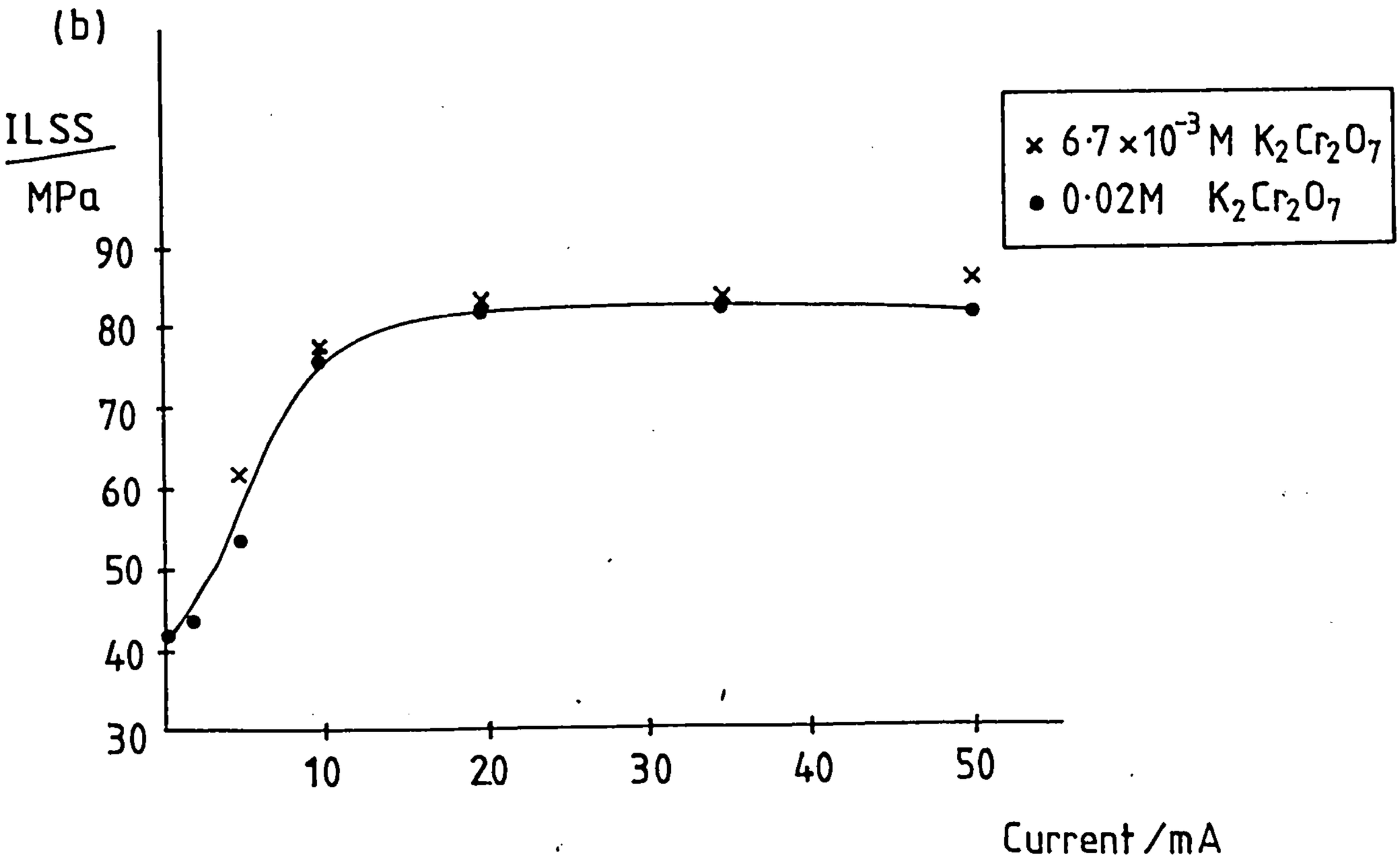

Fig. 8.5 ILSS vs. Cell Current

constant at 86MPa.This plateau in the ILSS could be due to several factors:-

(a) all the reactive sites on the fibre surface have been utilised and the maximum possible ILSS may have been achieved using that particular electrolyte;

(b) the limiting strength of the resin; or

(c) the limit of the ILSS test itself.

The rise in ILSS occurs at the same cell current suggesting that the same reaction is involved in both cases. There also seems to be a slight dependence upon concentration in the sodium hydroxide case.

Fig 8.6a shows a plot of ILSS against current for sodium chloride and oxalic acid treatments. The results for sodium chloride are very similar to those reported above. No chlorine was found on the surface. Oxalic acid, however, inhibited any increase in ILSS. This may be due either to a polymer being formed on the surface, preventing fibre resin bonding, or the oxalate ions inibiting the reaction responsible for good adhesion. The latter seems to be the case because there is no evidence in the carbon 1s spectrum of a large amount of any chemically shifted species (eg.C=O) due to a polymer being formed on the surface. The O1s:C1s ratio is very low, 0.0257, suggesting that the oxidation of the fibre surface has been inhibited by the electrolyte.

A set of reaction time dependent studies was also performed. The current used was 50mA in potassium dichromate solution. The

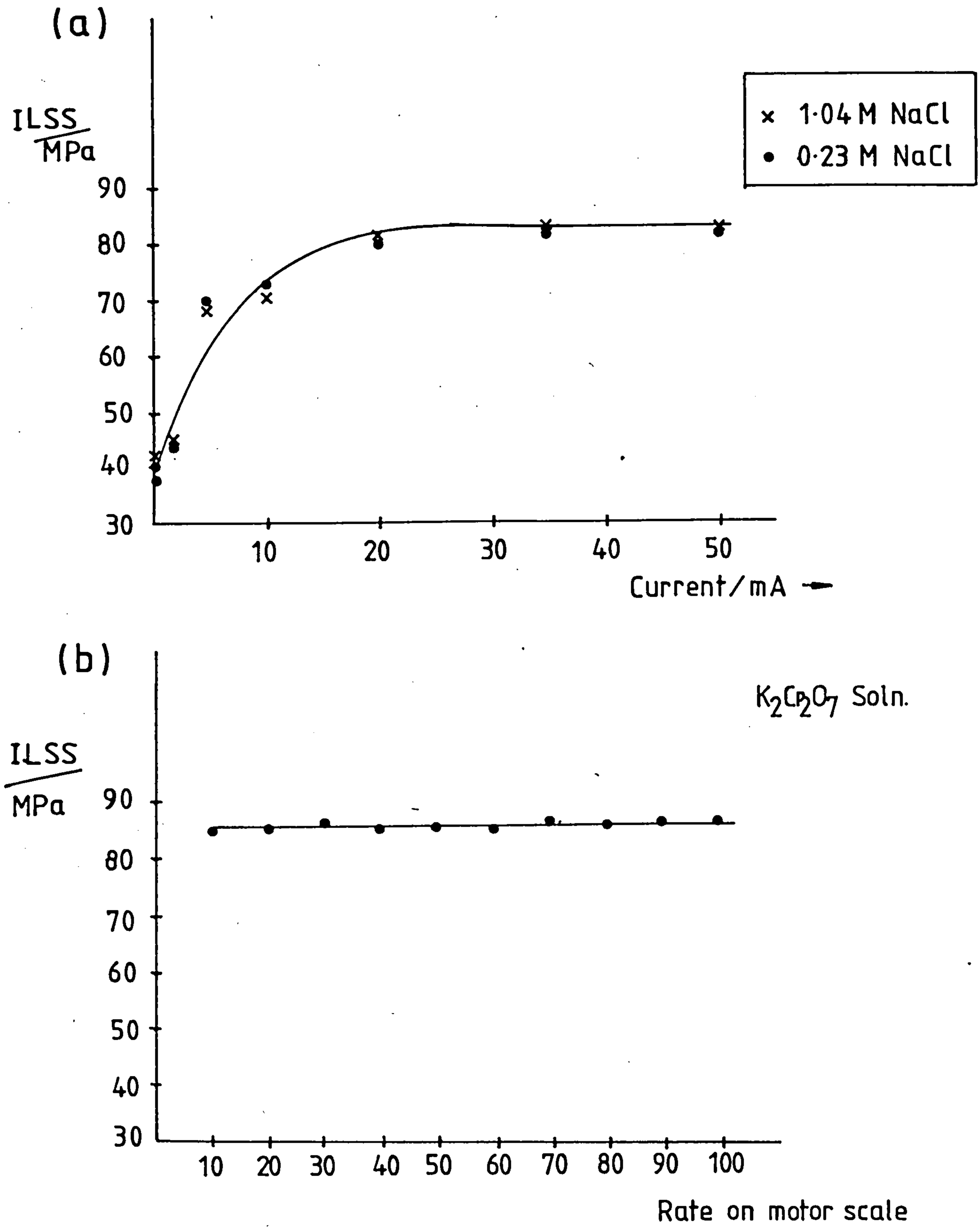
(a)
ILSS / MPa
90
80
70
60
50
40
30
10
20
30
40
50
Current/mA
× 1·04 M NaCl
• 0·23 M NaCl
(b)
ILSS / MPa
90
80
70
60
50
40
30
10
20
30
40
50
60
70
80
90
100
$K_2Cr_2O_7$ Soln.
Rate on motor scale

Fig. 8.6

ILSS of the composites remained constant, even though the time that the fibres spent in solution was increased (see Fig.8.6b). 86MPa seems to be the maximum ILSS value that can be obtained for this type of treatment and composite production. For a cell current of 15mA in $2x10^{-3}$M NaOH, the time spent in solution was doubled. The ILSS of the resulting composite increased 10 MPa compared to the lesser reaction time. The value achieved was the maximum value of ILSS obtained for that solution. This suggests that the same reaction can occur at lower currents if the reaction time is increased.

8.4 The Effect of Potentiostatic Treatment on Carbon Fibres

The only difference between these type of cell conditions and those mentioned previously is that in this case the potential is kept constant using a potentiostat and a calomel reference electrode. The time the fibres spent in solution was the same as before, 9 seconds.

It should be realised that the potentials measured on a digital volt meter (DVM) connected to the reference electrode and the working electrode for this type of cell arrangement are larger than the true potential between the fibres and the electrolyte solution. There are two reasons for the discrepancy in potential:-

(a) the ohmic drop due to the length of the Luggin tube,

(b) the ohmic drop along the length of the fibres.

Although this drop in the actual potential does occur the effect

will pobably be proportional to the potential, and can therefore be accounted for. (The potentials reported in this chapter have not been corrected.)

After ten seconds polarisation in nitric acid at 2.0V the C_{ox}/C_{graph} ratio was 0.48. The ratio for 'commercially' treated fibres polarised to 2.0V is 0.18. Clearly, the potential for the commercially controlled environment is not as high as the laboratory controlled potential. Assuming that oxide production is linear between 2.0V and 3.0V for commercially treated fibres, the ohmic drop in the cell causes an error of approximately 0.6V in measuring the voltage between 2V and 3V. For lower potentials this over-estimation will not be as large (at 1.0V the error will be 0.2V). The cell was set up for steady state conditions and the potential measured on the DVM remained constant (±0.0001V S.C.E.).

8.4.1 The Effect of Nitric Acid

Fig.8.7 shows the carbon 1s fibres polarised to several potentials. It can be seen that at high potentials the amount of chemically shifted species increases significantly. At potentials +3.0V and +4.0V, the graphitic nature of the main peak is lost, most probably due to exfoliation of the fibre surface.

The spectra have been fitted to four peaks (just as for the laboratory results for nitric acid), a main carbon peak, and three chemically shifted species at 2.1, 4.2 and >6.0eV. The peak above 6.0eV may have plasmon and satellite contributions, but using two separate peaks to describe this region did not

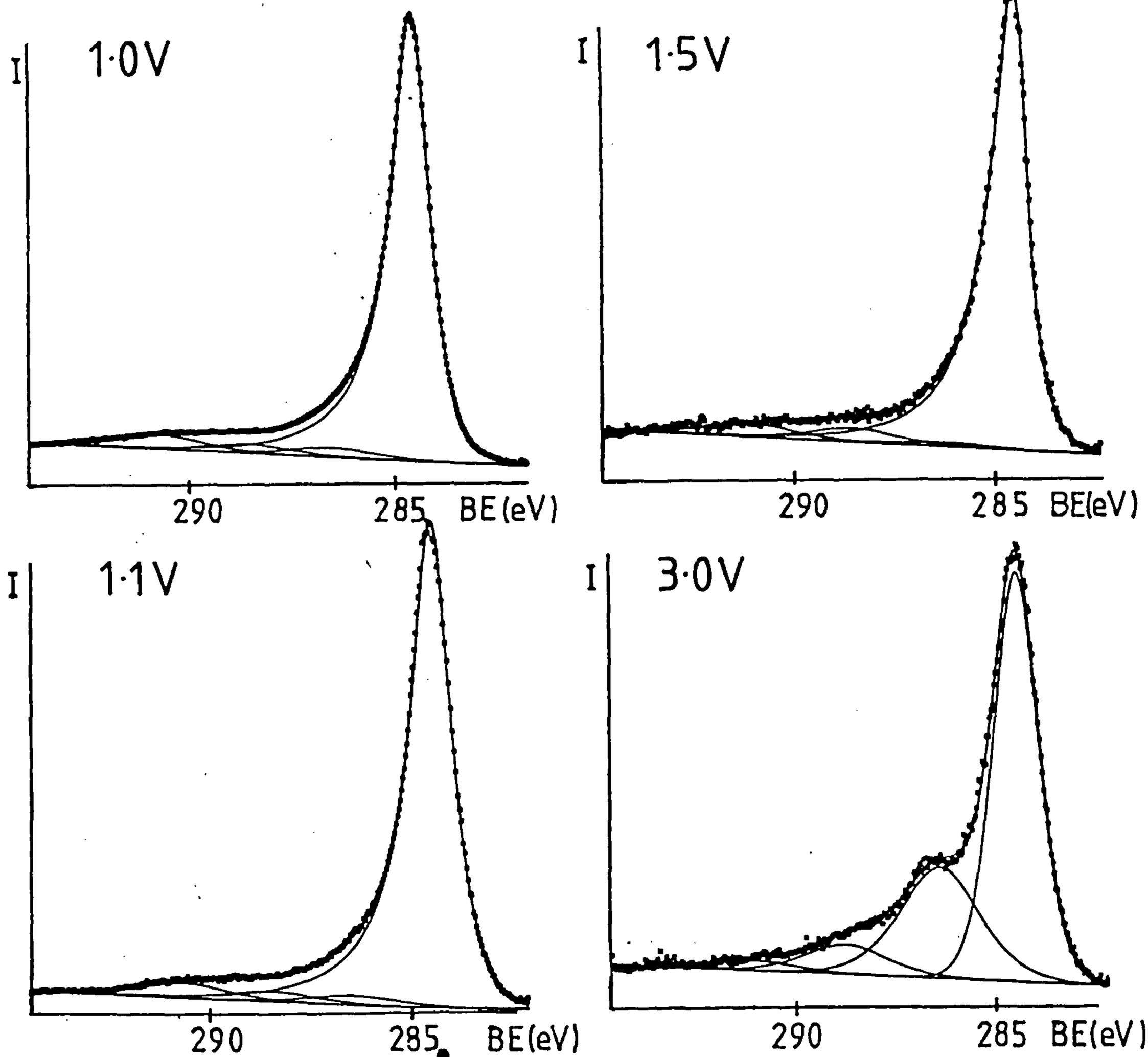

Fig.8.7 C1s Spectra of Fibres Polarised in Nitric Acid

allow the curve fitting program to converge. The variation in area ratio for the chemically shifted species (with respect to the main carbon peak) against potential is shown in Fig.8.8. The total intensity of chemically shifted species is also shown. It can be seen that a rise in oxidation starts to occur at 2.0V. The intensity of both 'oxide' 1 and 'oxide' 2 increases with potential, but as in the laboratory case the peak at 2.0V increases to a much greater extent. The signal intensity above 6.0eV remains constant (0·05-0·06)

Unlike the laboratory treated fibres (in HNO_3), the oxygen 1s spectra consist of two resolvable components at low potentials and three at higher potentials (3.0V and 4.0V). The binding energies for the two main components are 533.5eV (±0.2eV) and 532.1eV (±0.3eV). For higher potentials, eg.3.0V and 4.0V, these peak positions alter to 532.9 eV (±0.1 eV) and 531.9 eV (±0.1 eV) for fibres polarised at 3.0V and, 532.8 eV and 531.1 eV for fibres polarised at 4.0V. At 4.0V the fibres seem to have individual C=O and -O- character. The area ratios are given in Table 8.6.

There is a general trend for the O1s:C1s ratio to increase with increasing potential.

8.4.2 The Effect of Ammonium Bicarbonate

The fitted carbon 1s spectra are shown in Fig.8.9. There is very little change in the main profile of the spectra (just as in the laboratory case). The spectra were fitted to four peaks, with all the peak positions being allowed to float. The total

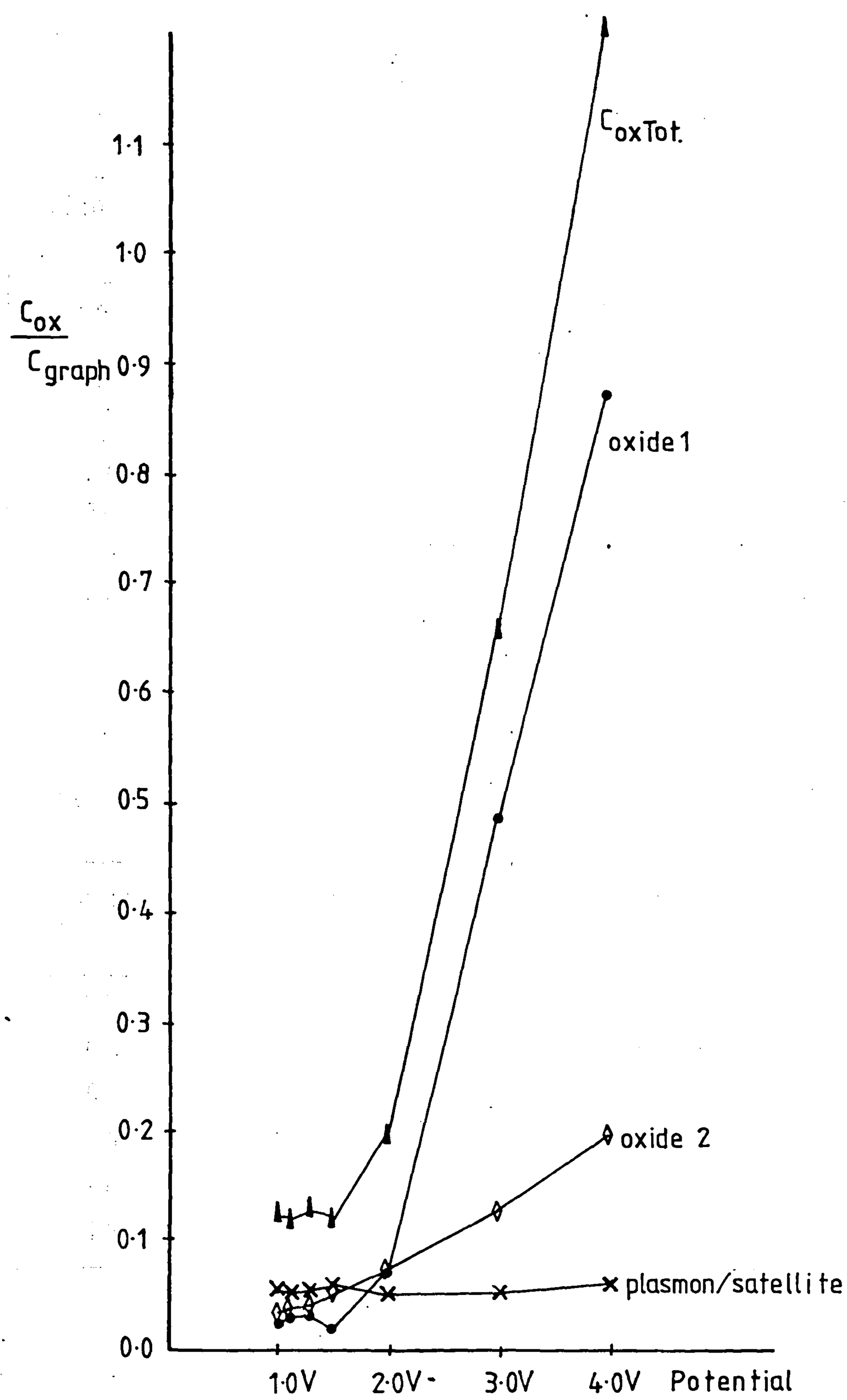

Fig.8.8 Variation of Chemically Shifted Species with Potential

TABLE 8.6

Curve Fitting Results of O1s Spectra of Fibres Polarised in HNO_3

Potential (V)	Binding Energies (eV)			Area Ratios		
	1	2	3	1	2	3
1·0	532·2	533·6	—	0·715	0·285	—
1·1	532·0	533·4	—	0·479	0·521	—
1·3	532·2	533·5	—	0·519	0·481	—
1·5	532·1	533·5	—	0·577	0·423	—
2·0	532·3	533·7	—	0·542	0·458	—
3·0	531·9	532·9	535·9	0·448	0·505	0·047
4·0	531·1	532·8	535·9	0·191	0·764	0·045

TABLE 8.7

Curve Fitting Results of C1s Spectra of Fibres Polarised in NH_4HCO_3

Potential (V)	Chemical Shifts (eV)			Area Ratios		
	1	2	3	1	2	3
0·1	2·74	5·01	6·73	0·039	0·050	0·052
0·4	2·65	5·03	6·61	0·049	0·050	0·051
0·6	2·37	4·80	6·60	0·057	0·049	0·053
0·7	2·64	5·07	6·93	0·050	0·052	0·057
1·0	2·64	5·05	6·82	0·036	0·055	0·052
1·5	2·73	4·99	6·81	0·041	0·050	0·052

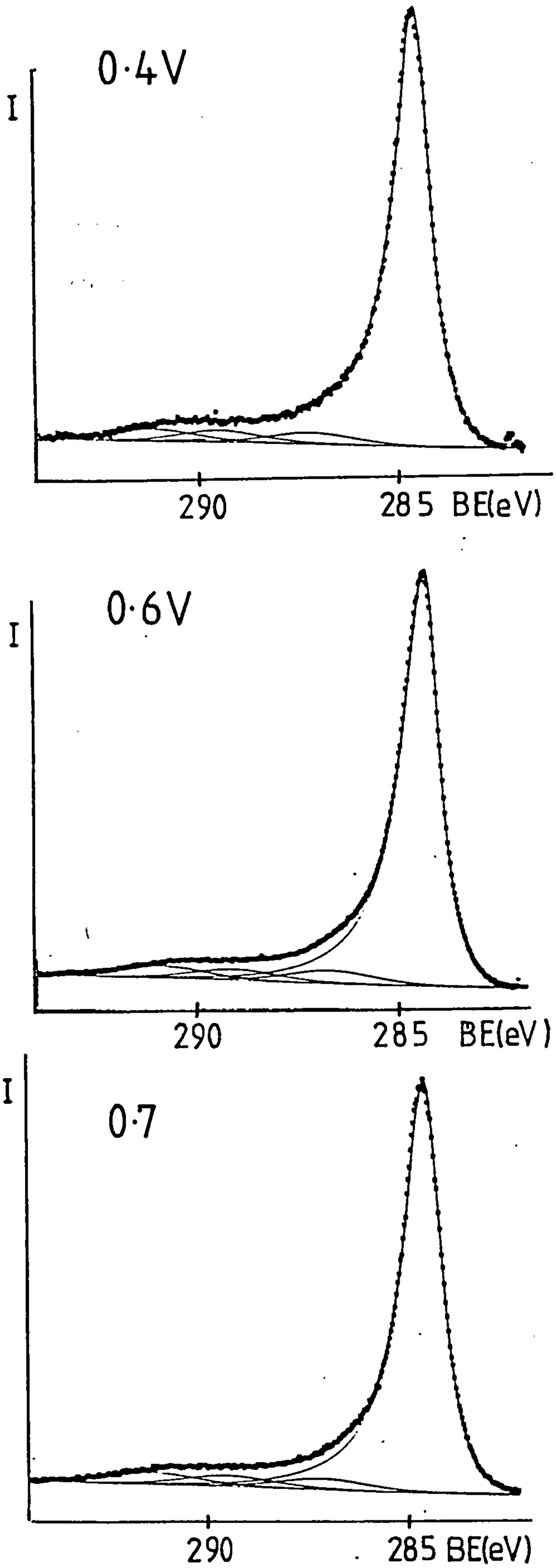

Fig. 8.9 C1s Spectra of Fibres Polarised in NH_4HCO_3 Soln.

area ratio of the chemically shifted species with respect to the graphitic peak is constant falling within the range 0.14-0.16 (see Table 8.7). This total ratio is only very slightly lower than that obtained for laboratory treated fibres in the same electrolyte over the same range of potentials. The chemical shifts are also much higher than those obtained with nitric acid, the 'oxide' chemical shifts being 2.64eV (±0.3eV) and 4.98eV (±0.2eV). These are also slightly higher than the laboratory fibres treated in ammonium bicarbonate. It has already been shown (see chapter 5) that the binding energy of a particular functional group can vary quite considerably depending on neighbouring functionalities. This is probably the reason for the observed changes in chemical shifts.

The oxygen 1s spectra for the above samples are shown in Fig.8.10. They consist of two resolvable species with binding energies 533.4eV (±0.2eV) and 532.1eV (±0.1eV). The area ratios vary with potential but show no trend, the lower binding energy component, corresponding to =O type groups, usually being of greater intensity. This is confirmed by the carbon 1s spectra in which the chemically shifted species at 2.64eV arises from ketone-type groups.

There is also a general trend for the O1s:C1s ratio to increase with potential. No nitrogen was present on the fibres. This is most likely to be due to the short reaction times. It has been suggested that the bicarbonate ion inhibits the oxidation of the surface (see section 7.3). The O1s:C1s ratios for commercially and laboratory treated fibres using ammonium bicarbonate have similar values, even though the reaction times

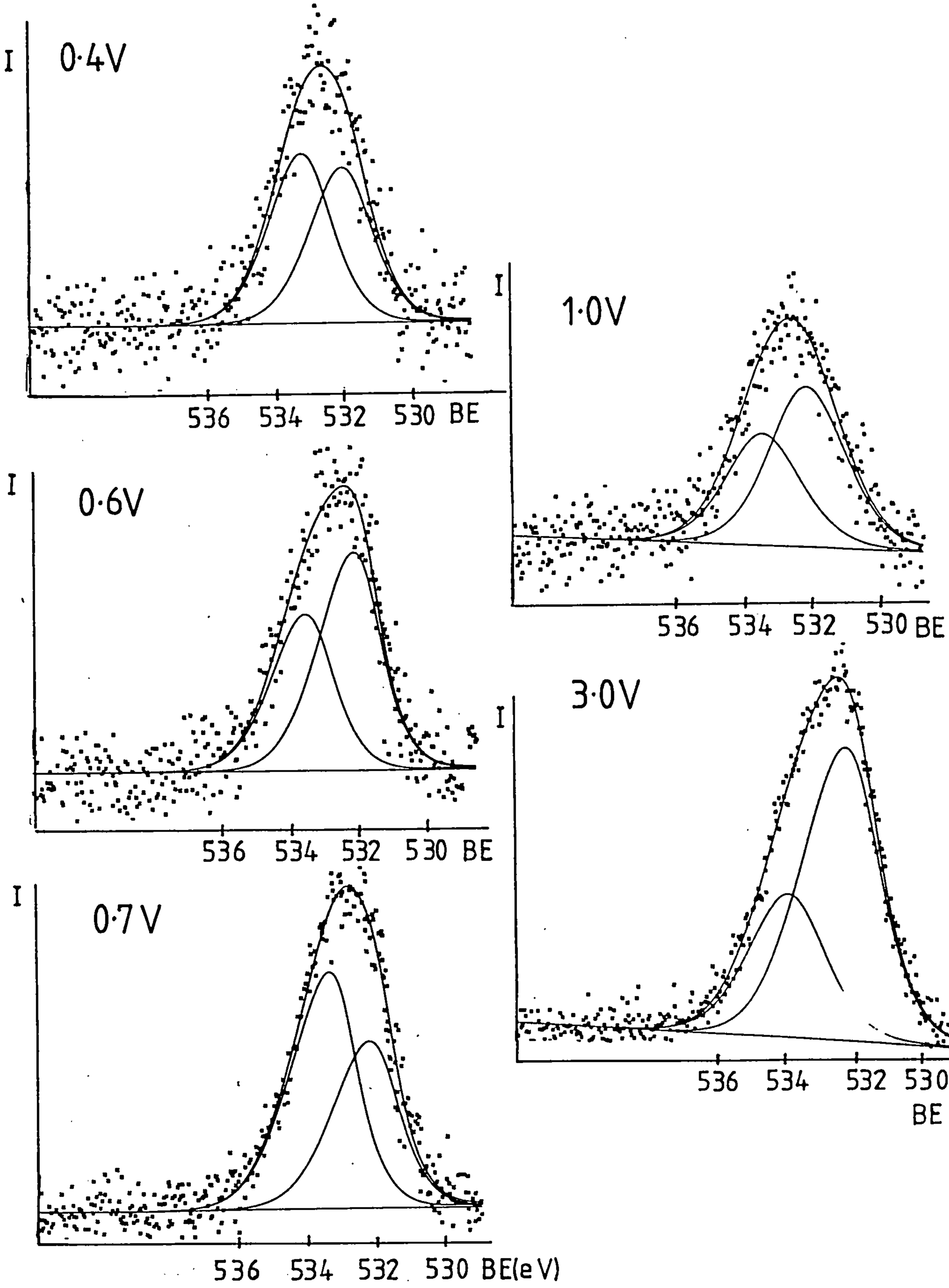

Fig. 8.10 O1s Spectra of Fibres Polarised in NH_4HCO_3 Soln.

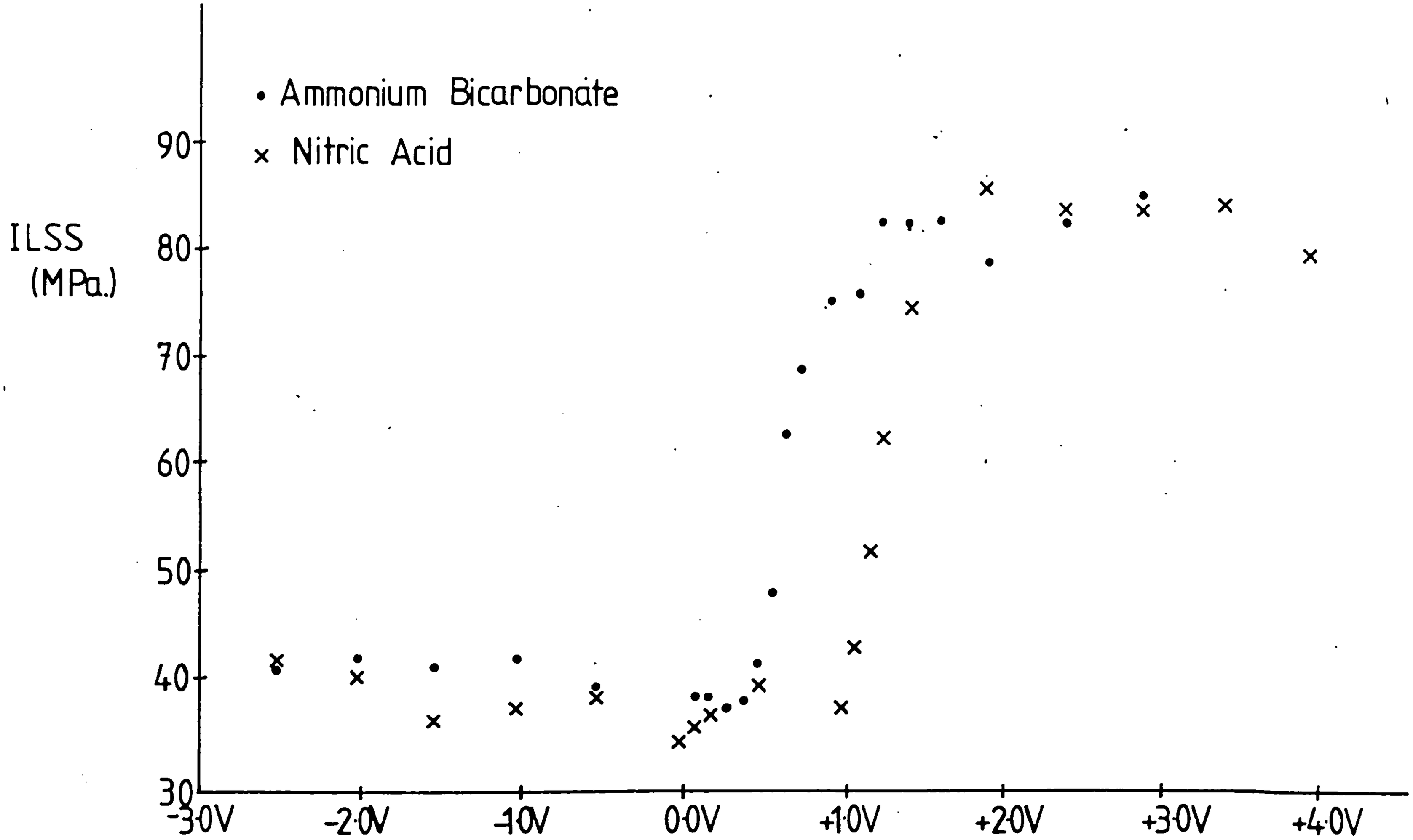
• Ammonium Bicarbonate
× Nitric Acid
ILSS (MPa.)
90
80
70
60
50
40
30
-3·0V
-2·0V
-1·0V
0·0V
+1·0V
+2·0V
+3·0V
+4·0V
Potential of Fibres (S.C.E.)

Fig.8.11

are vastly different.

8.5 The Effect of Potentiostatic Surface Treatment on the ILSS of the Composites

Fig.8.11 is a plot of ILSS against polarising potential for both electrolytes. The lowest ILSS values were obtained by polarising the fibre to 0.0V (SCE) in both electrolytes. Polarising to negative potentials causes only a very slight increase in ILSS, if at all, but polarising the fibres to positive potentials causes significant changes in the ILSS. This rise in the ILSS occurs at different potentials in the two electrolytes. For ammonium bicarbonate a rise from 40MPa to 84MPa occurs between 0.5V and 1.0V (SCE), whereas with nitric acid a similar rise in ILSS occurs between 1.0V and 1.3V. These voltages, if the ohmic drop is taken into account, are slightly lower than the oxygen potentials in both electrolytes.

Although the greatest ILSS is almost the same using both electrolytes, the O1s:C1s ratio is far greater for nitric acid, in some cases, than for those treated in ammonium bicarbonate.

8.5.1 SEM Studies of Composite Samples

For composites with low ILSS (eg. those produced from fibres that have been polarised to 1.0V in nitric acid, ILSS 36.21MPa) the composite consists of regions of high fibre concentration and others of only resin. This is shown in Plate 8.1a (a fracture surface of a composite bar). The specimen also has resin loosely bonded to the fibre surface, only attaching

(a)

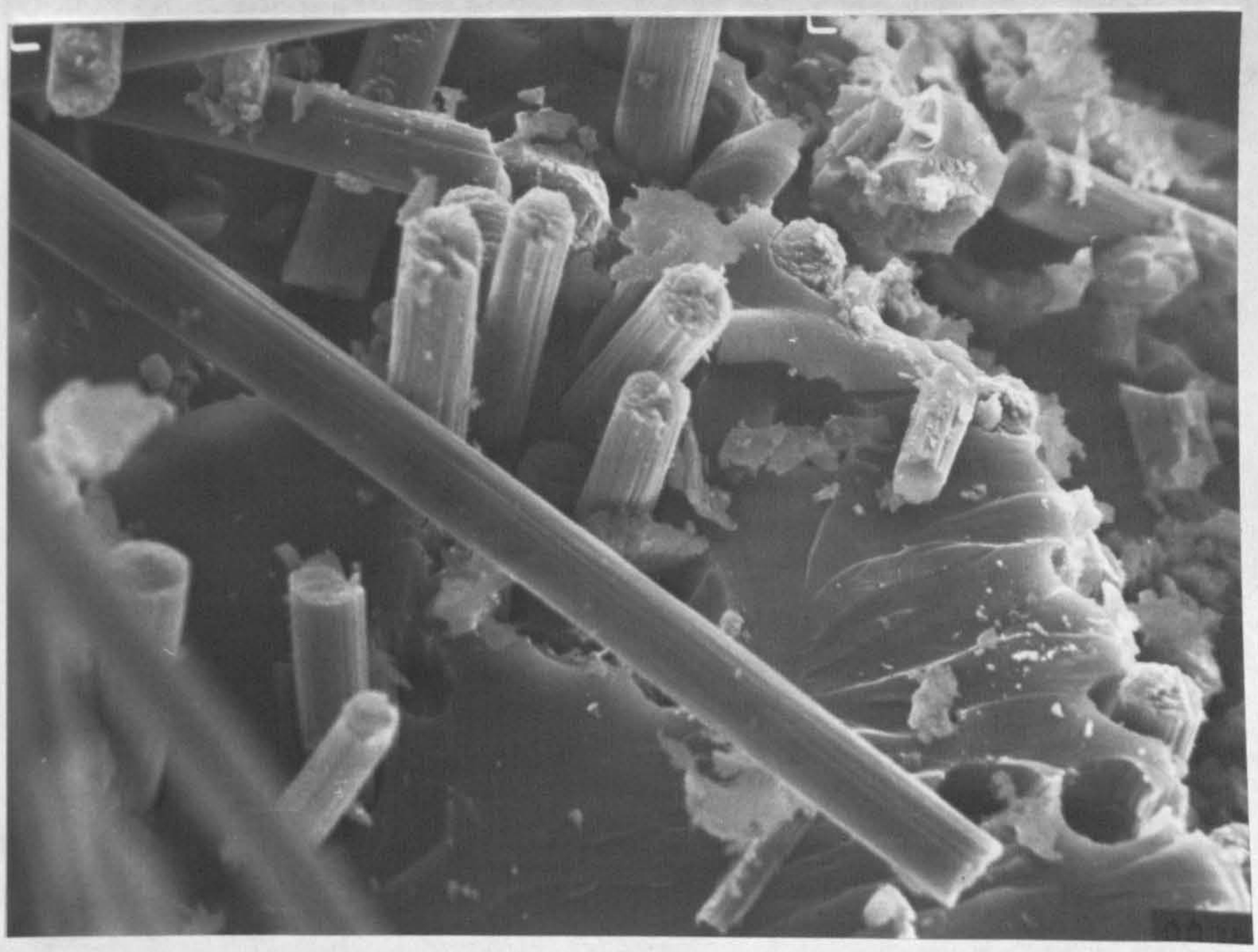

(b)

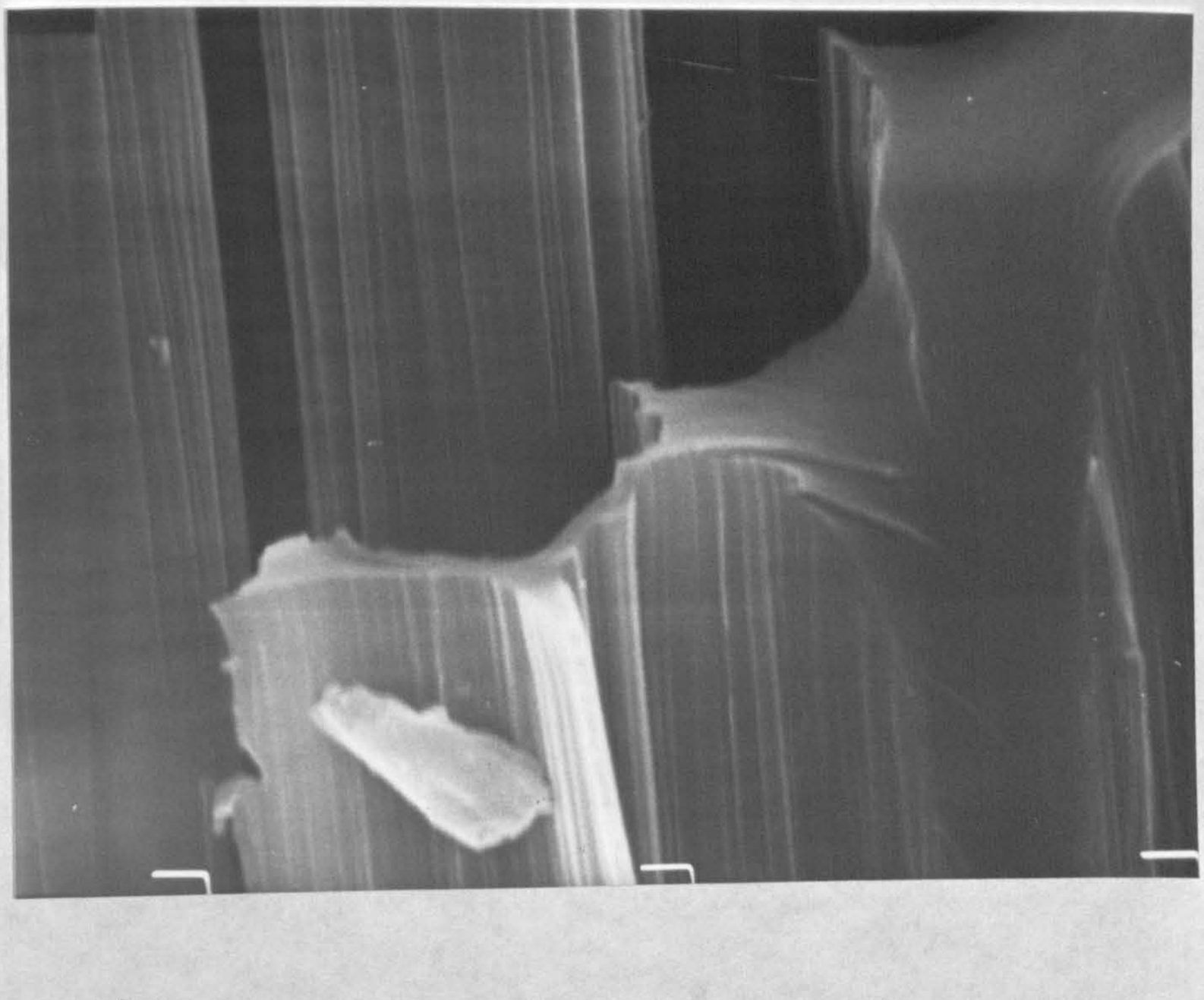

Plate 8.1 Composite with Low ILSS

(a)

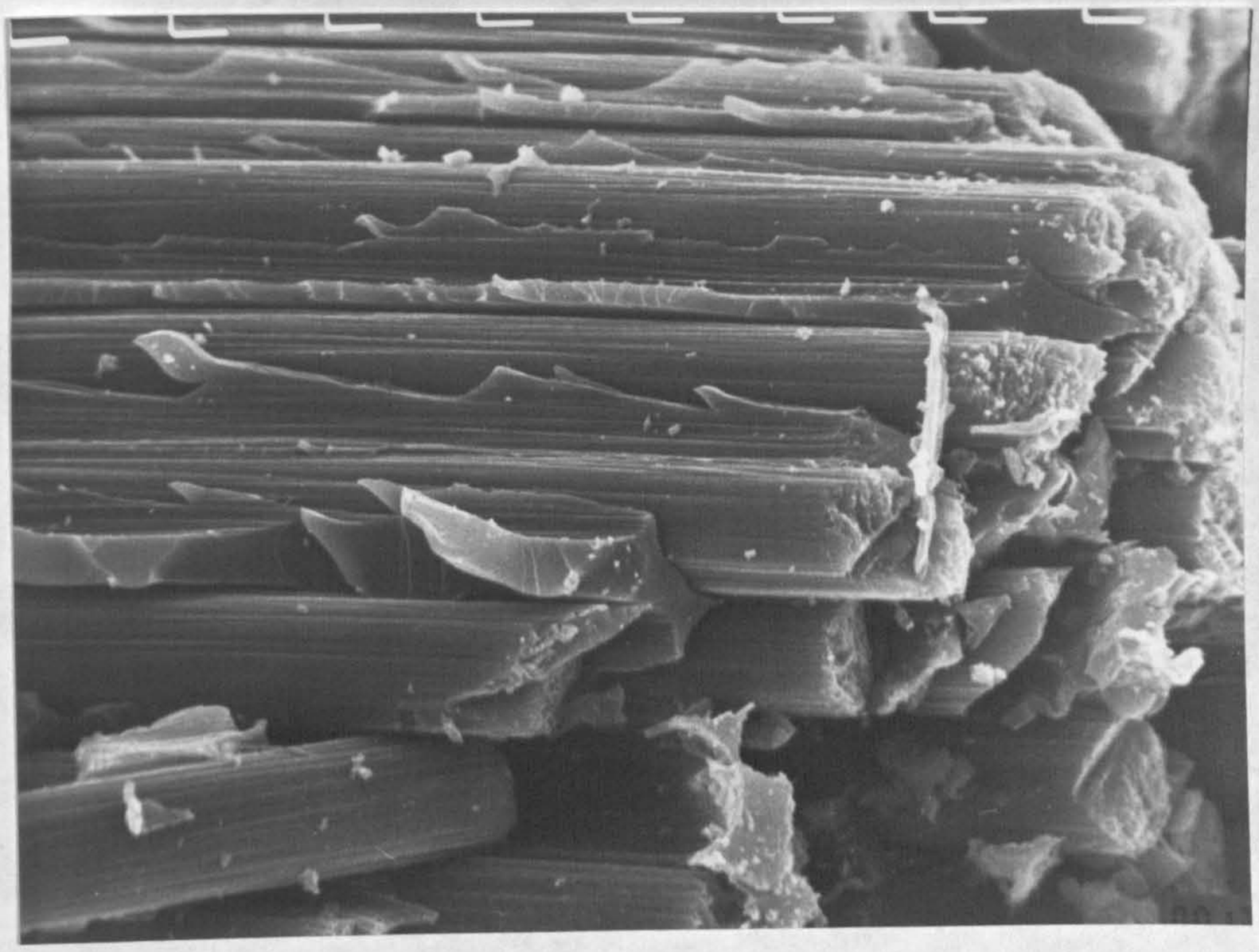

(b)

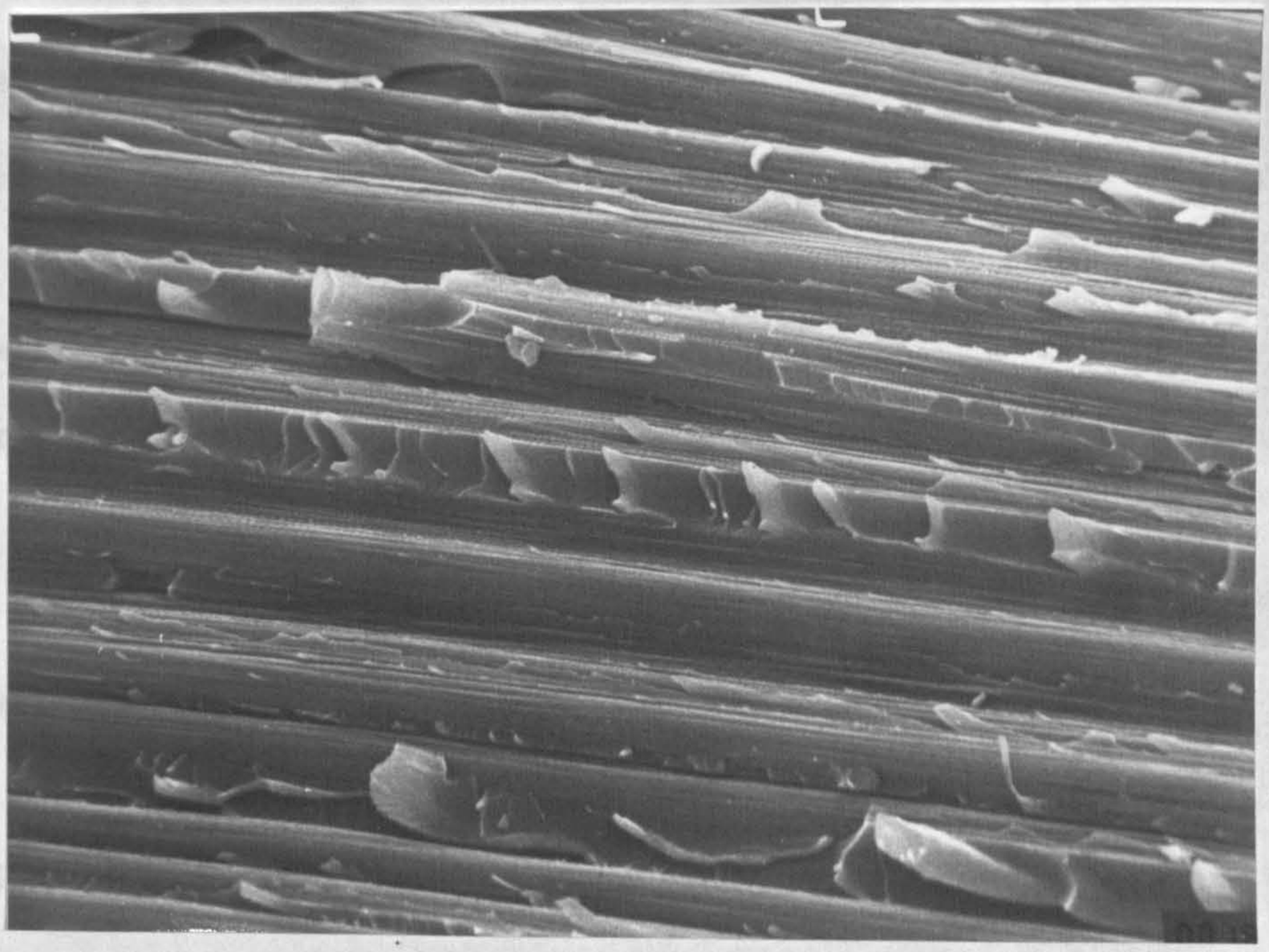

Plate 8.2 Composite with High ILSS

itself via a longitudinal groove in the fibre surface (see Plate 8.1b).

For composites made from fibres treated in ammonium bicarbonate, the ILSS is high (83.82MPa). The composite consists of a more even dispersion of fibre in the resin than those described above. The fibres also appear to be fully coated by the resin. Plates 8.2a and b show a longitudinal fracture surface. There are some regions where the resin appears to be loosely bonded to the fibre. This may, in this case, be due to the fracturing of the composite. This feature is not as common as in composites of low ILSS.

8.6 The Variation of ILSS with Surface Functionality

Fig.8.12 shows a plot of the ILSS of the composites against the O1s:C1s of their component fibres. Fig.8.13 shows a plot of ILSS against the relative amount of 'oxide'[2] on the fibre surface. It can be concluded that the ILSS of a composite does not directly depend upon the amount of surface oxygen, or upon the amount of acid/ester type groups.

If the effect of only nitric acid is studied, misleading results may be obtained because with this electrolyte the number of carboxyl-type groups increases with potential, as does the ILSS. A plot of ILSS against the O1s:C1s ratio for nitric acid treatment is shown in Fig.8.14. There is a clear trend in this case. The ILSS increases with surface concentration until an optimum value is reached (O1s:C1s = 0.25, ILSS = 83MPa). Further increase in the surface oxygen concentration leads to a decrease

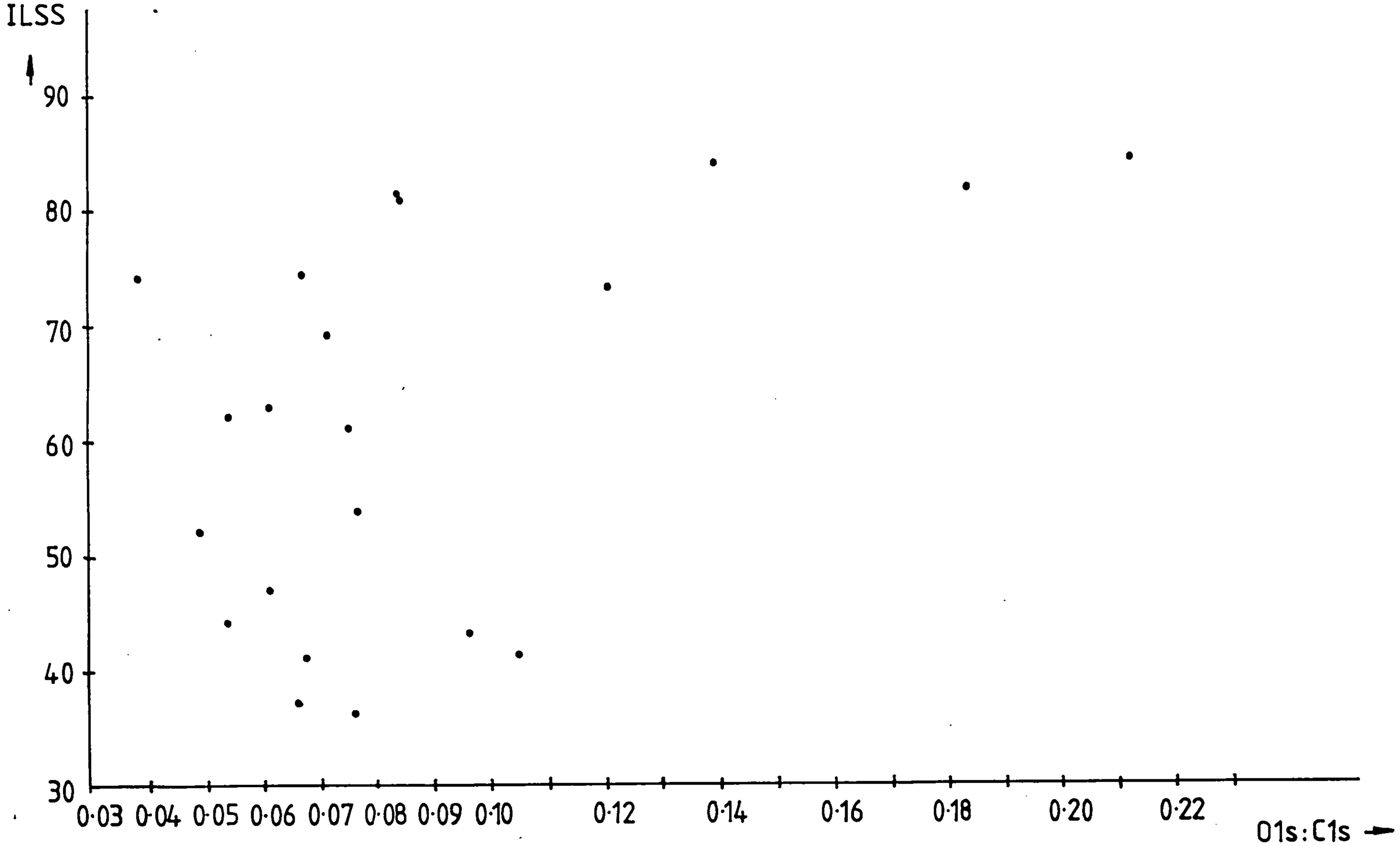

Fig.8.12 Variation of ILSS with O1s:C1s Ratio

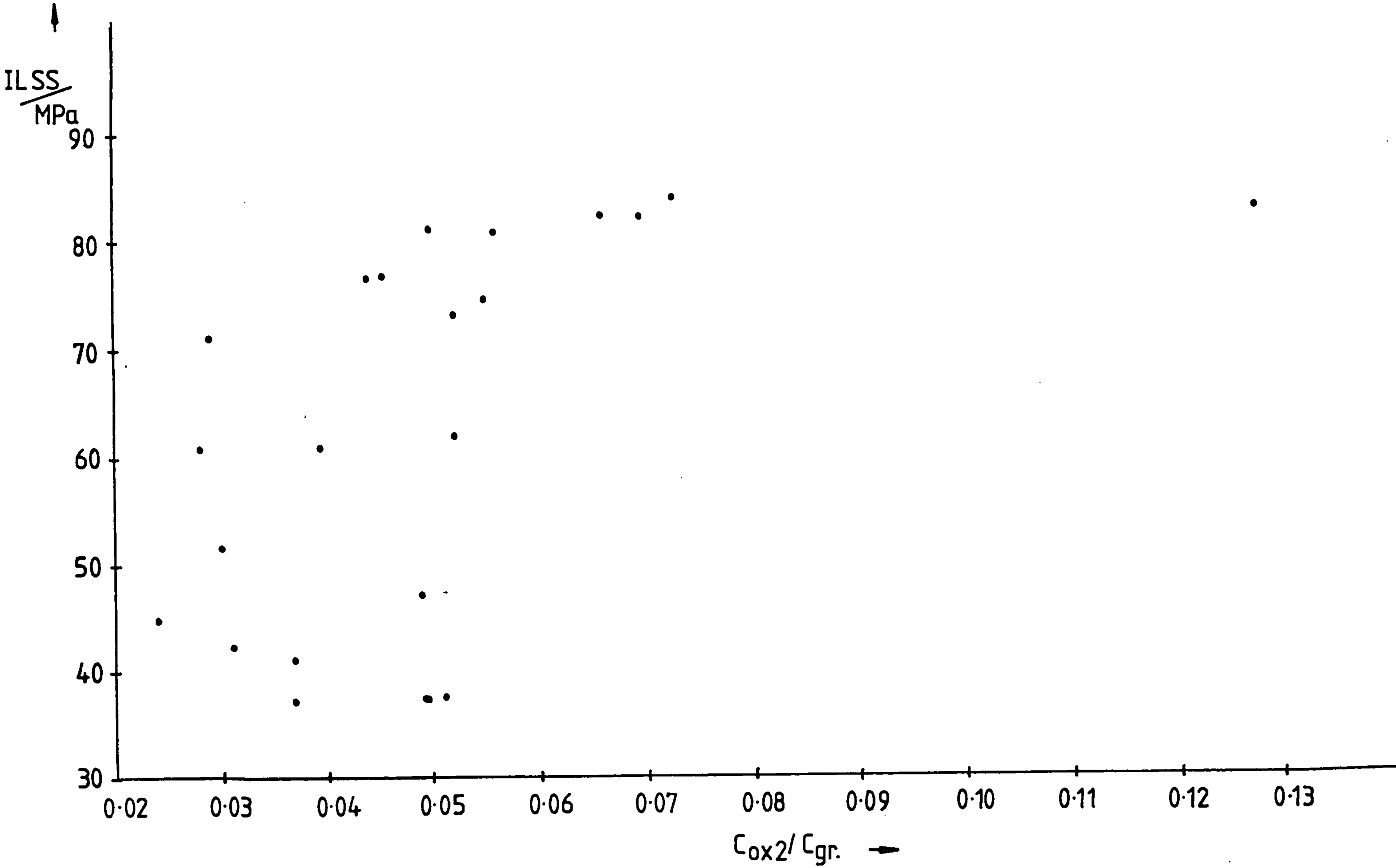

Fig.8.13 Variation of ILSS with Carboxyl Group Intensity

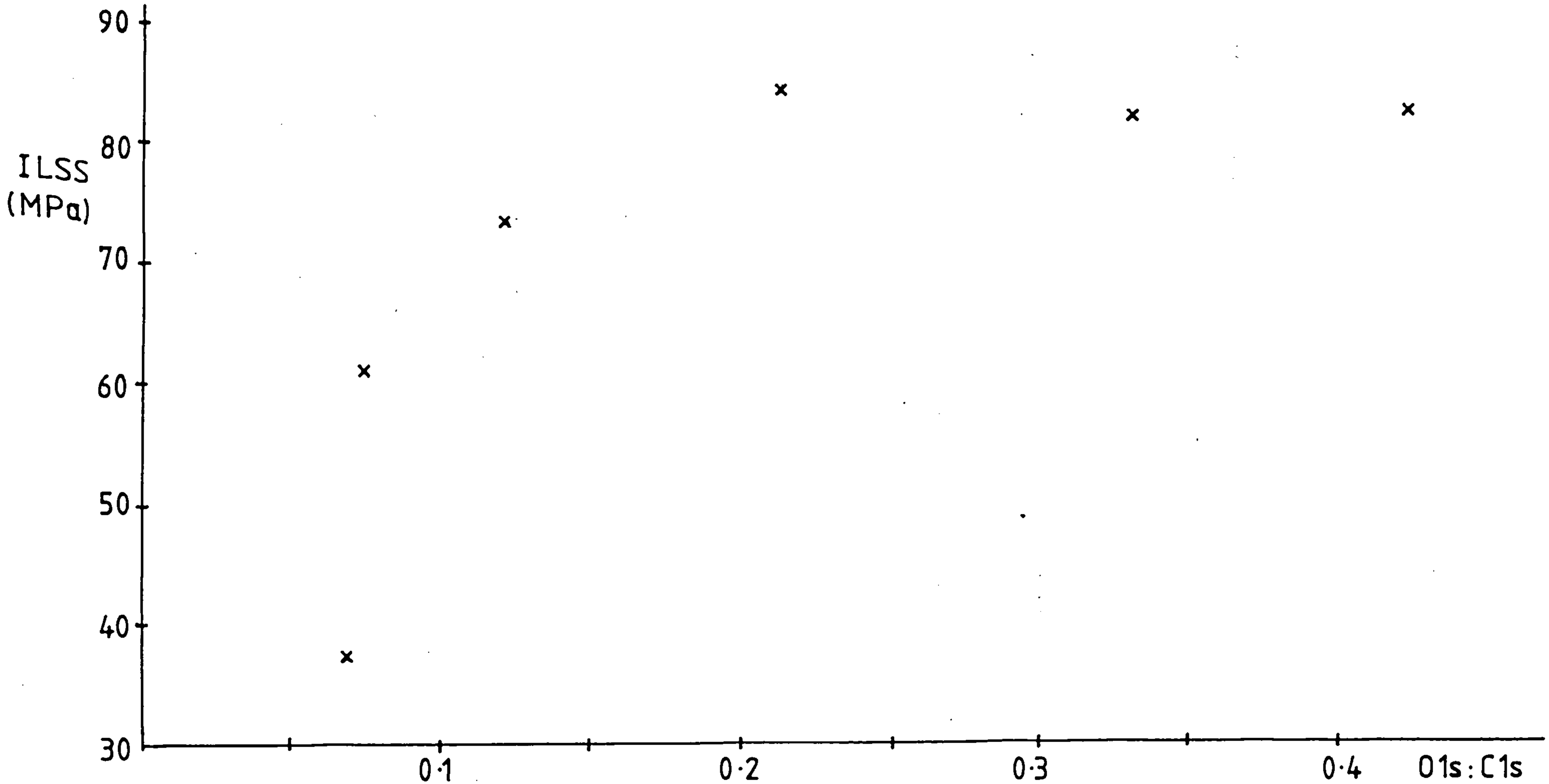

Fig.8.14 Variation of ILSS with O 1s:C 1s Ratio (for nitric acid only)

in ILSS. An extensive study of fibres treated with nitric acid has been carried out by Fitzer et al (3,18). Their conclusions can only be arrived at using nitric acid and cannot be applied to most other types of surface treatment.

8.7 The Effect of Reaction Time and Heat Treatment

Fibres were polarised to 3.0V in nitric acid using the commercial cell. The time the fibres spent in solution was varied using a D.C motor to pull the fibres through the system at different rates. The reaction times used were 36, 45, 60 and 120 seconds. Enough fibre was treated for two composite bars to be made for each reaction time. One set of composite bars (one for each reaction time) was made in the usual way, the other set of fibre samples was heated in a vacuum to 1000^{o}C prior to incorporation into the resin.

8.7.1 Reaction Time

As the reaction time was increased, the amount of chemically shifted species increased. The O1s:C1s ratio also increased with reaction time. The carbon 1s spectra of fibres treated for 45 and 120 seconds are shown in Fig.8.15.a. These spectra consist of chemically shifted signals at 2.1, 4.0 and >6.0eV from the main peak. This main peak has also lost its graphitic nature, suggesting that the bulk fibre lattice is not close to the surface, that is to say present in the escape depth of the photoelectrons.

A plot of ILSS against reaction time is shown in Fig.8.16.

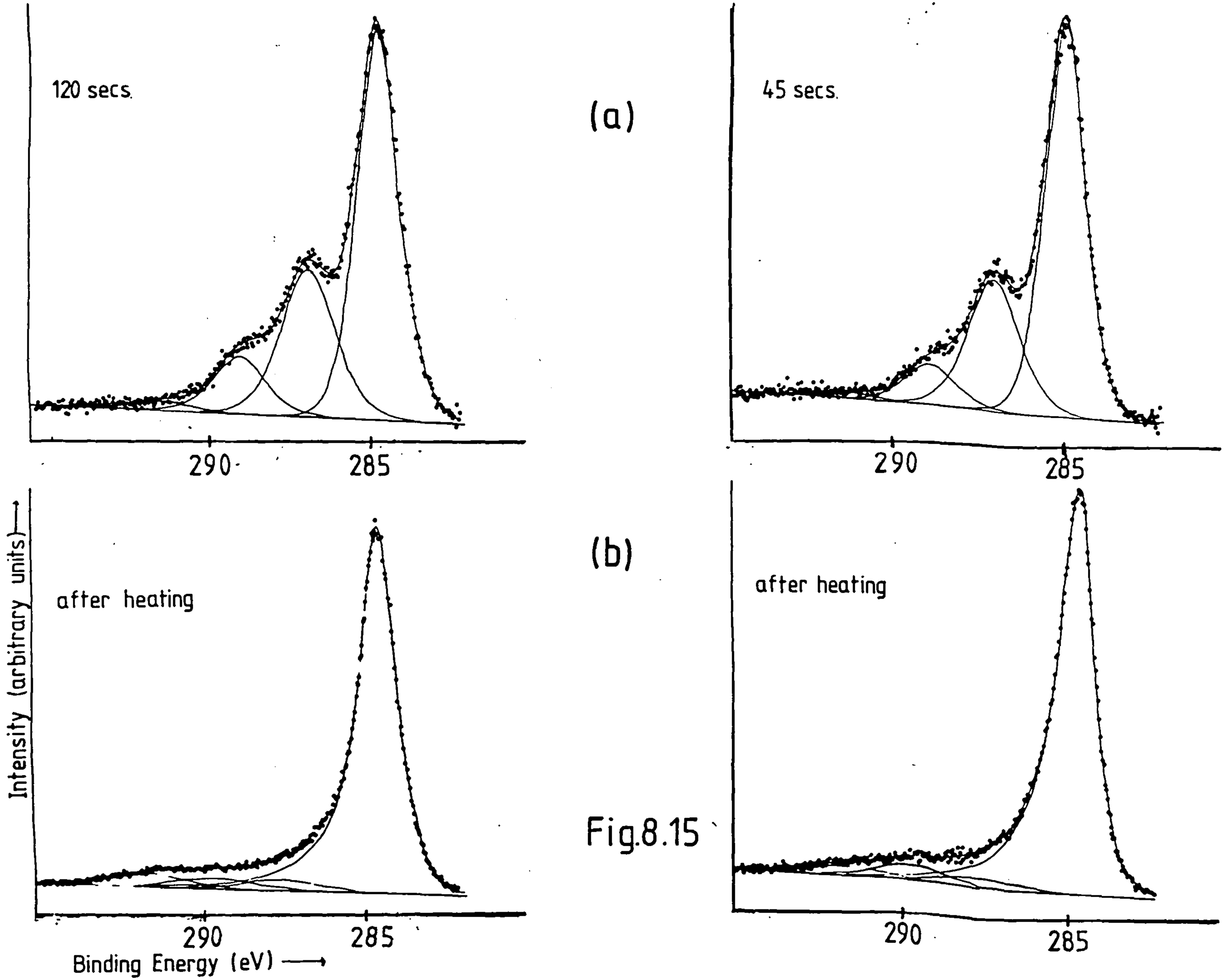
120 secs.
(a)
45 secs.
290
285
290
285
after heating
(b)
after heating
Intensity (arbitrary units)
290
285
290
285
Binding Energy (eV)

Fig.8.15

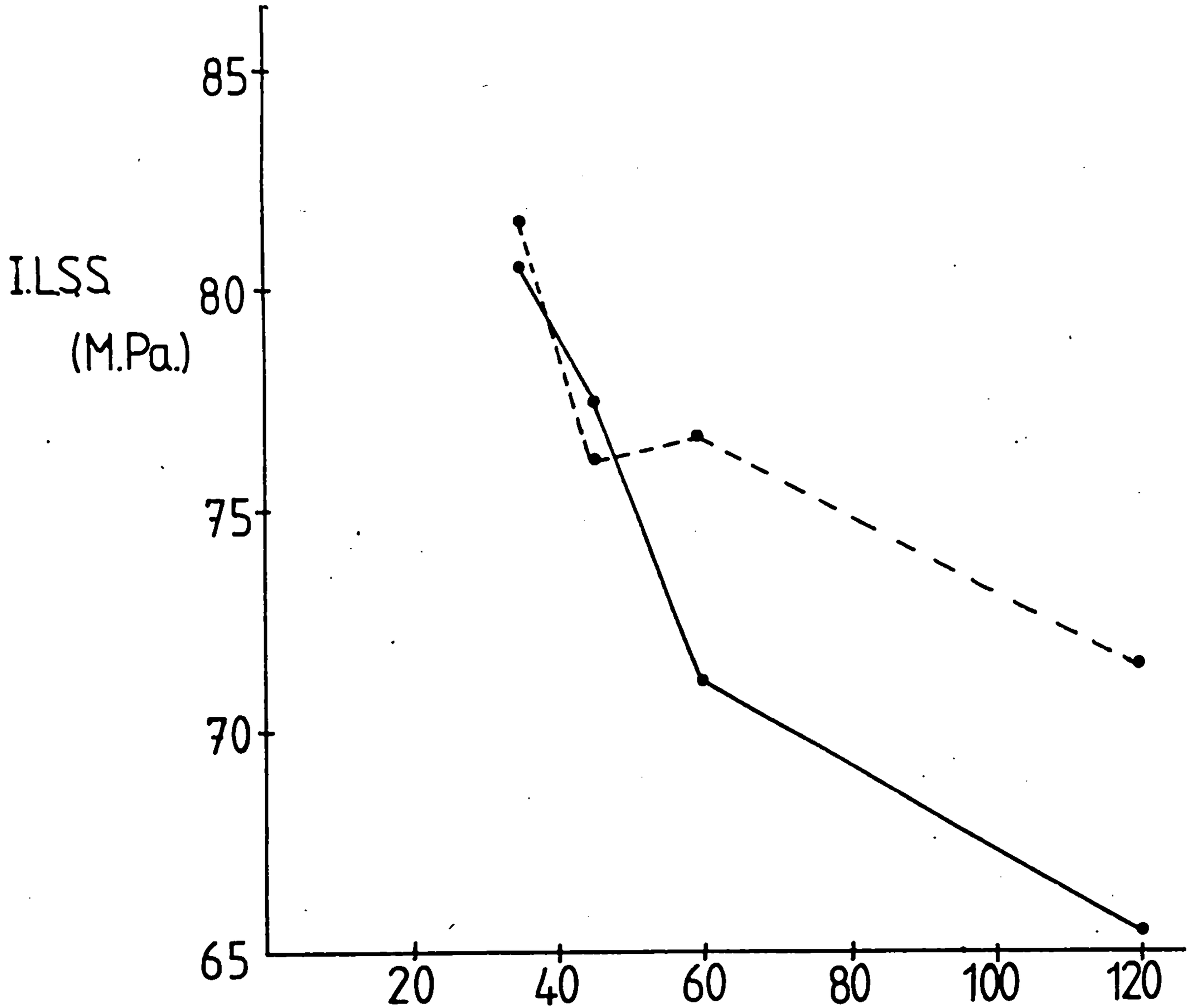

Fig.8.16

The solid line represents fibres which have not been heated prior to composite production. It shows that as the reaction time increases the ILSS of composites decreases significantly. This means that as the O1s:C1s ratio increases, the ILSS decreases. It is thought that this is due to the oxide layer causing the failure of the fibre-resin bond. The maximum O1s:C1s ratio before the ILSS of the composite decreases is 0.337. The same ILSS value can be achieved at an O1s:C1s ratio of 0.076 for the same electrolytic treatment (the latter level of oxidation being far more desirable because of the lower level of surface polarity).

8.7.2 Heating

It has been shown in a previous chapter that nitric acid produces an oxide layer resembling graphitic oxide. On heating, graphitic oxide decomposes at temperatures above 120°C. The carbon 1s spectra of fibres after heating are shown in Fig.8.15b. It can be seen that heating causes a decrease in the amount of carbon-oxygen complexes produced on the fibre surfaces. Some basic oxides may also have been produced after heating fibres in a vacuum; cooling, and exposing them to air. Fig.8.16 shows the ILSS of the fibre samples plotted against reaction time (represented by the broken line). For fibres treated for short reaction times (36 and 45 seconds) the ILSS remains roughly at the same level, but for longer reaction times heating causes an increase in the ILSS. This is probably due to the decomposition of the 'oxide' layer into gaseous products on heating. The evolution of gas was detected by monitoring pressure fluctuations during the heating process.

8.8 Summary

Both galvanostatic and potentiostatic control of cell conditions proved satisfactory in the treatment of fibres to produce composites with a high ILSS (80-90MPa). Slightly higher values of ILSS may be achieved by altering the volume fraction of fibres in the resin (usually 60% fibre). Epoxy resins contain highly polar functional groups and consequently readily absorb water. As these structures absorb water the resin becomes plasticised, with a resultant loss of strength. This strength is largely regained on drying. However, if the composite is subjected to moist conditions at high temperatures irreversible damage occurs. It is therefore necessary to produce composites with low hydrophilicity. This can be achieved by altering the resin to make it more moisture resistant and by decreasing the number of polar functional groups on the fibre surface. For the treatments carried out in this study, polarisation in ammonium bicarbonate solution results in the lowest O1s:C1s ratio for a satisfactory ILSS (ILSS= 86MPa, O1s:C1s =0.06).

Changing the electrolyte of the solution in which the fibres were treated results in a change in the amount of functional groups produced. The relative proportions of these functional groups is also altered. Proctor and Sherwood (87,96) reported that industrial treatment gave less control over fibre surface oxidation than in the laboratory treated fibres. To produce a composite with a high ILSS, the reaction time used was 9 seconds. In this study and in those of Proctor and Sherwood, the laboratory treated fibres were kept at an anodic potential for 20

minutes. This increased reaction time in both cases leads to functional groups being produced, the relative amounts being dependent on the electrolyte used.

The cell current needed to increase the ILSS of the composite is the same for a wide range of electrolytes. The potential applied between a reference electrode and the fibres is specific to the electrolyte used. This potential is close to the oxygen potential for a particular electrolyte.

The rise in ILSS is not dependent on the O1s:C1s ratios or the amount of carboxyl functionality present on the surface. Whilst it cannot be concluded, therefore, that the nature of the fibre resin bond is purely physical, mechanical keying of the resin to the fibre surface is likely to play a more important role in the fibre/resin bond then is appreciated by many research workers.

CHAPTER 9

CONCLUSIONS

XPS has proved to be a most useful method for examining carbon fibre surfaces. Complimentary information has also been obtained from FTIR spectroscopy. The treatments used in this study do not only change the surface functionality; significant changes in surface topography have also been observed using SEM. These physical and chemical changes in the fibre surface have been shown to depend on several factors:-

(1) the nature of the electrolyte,

(2) the anodic potential,

(3) the reaction time,

(4) the structure of the fibre surface,

(5) the pH of the electrolyte solution, and

(6) the concentration of the solution.

(1) The Nature of the Electrolyte

Electrochemical oxidation of the fibres has been carried out using acidic, salt and alkaline solutions. Each results in different types of functionality being produced on the fibre surface, depending upon the anions and cations present in solution. Phosphate, sulphate and nitrate ions, at potentials >1.5V, lead to extensive oxidation of the fibre surface, resulting in the production of an 'oxide' layer. This 'oxide'

layer is loosely attached to the bulk fibre and in some cases extensive flaking occurs. The surface topography of these treated fibres is greatly different for each of the above electrolyte solutions (see Plates 5.2, 5.3a, 5.3b and 5.4). Both phosphate and sulphate ions remain in the 'oxide' layer whereas nitrate ions do not.

Surface nitrogen functionality is a result of electrochemical oxidation in ammonium salt solutions, the amount depending upon the concentration of ammonium ions in solution. This surface nitrogen is probably in the form of amides and amines.

Sodium ions present in the solution always lead to sodium ions remaining on the fibre surface. These ions are well known to intercallate with graphite and they are probably situated between the graphitic surface layers of the fibre.

The presence of bicarbonate ions inhibits the oxidation of the fibre surface. This is most probably due to the formation of carbon dioxide (see section 7.3), which is unlikely to react with the fibre surface.

Electrochemical oxidation of the fibre surface in salt solutions in most cases produces similar changes in surface functionality and topography to those found with the corresponding acids alone.

(2) Anodic Potential

In general, increasing the positive potential of the fibre leads to an increase in the amount of surface oxygen (or nitrogen) complexes present on the fibre surface. At high potentials (~3V) in acidic solutions however, oxidation may lead to gaseous products, eg. CO and CO_2. This results in a decrease in the amount of 'oxide' remaining on the surface itself.

(3) Reaction Time

Increasing the reaction time increases the fibre surface functionality. Long reaction times result in a slight decrease in surface oxygen complexes, again probably due to the production of CO and CO_2.

(4) Structure of the Fibre Surface

Type I fibres are known to contain a lesser number of edge sites than type II fibres. The reactions occurring during electrochemical oxidation at the edge sites are different to those occurring at the basal planes of the fibre surface. It has been shown that oxidation of the edge sites produces acid/ester functionality, whereas oxidation of the basal planes results in keto-type functionality. These functional groups, ie keto- and carboxyl/ester, give rise to chemical shifts of 2.1eV and 4.0eV respectively. Their presence on the fibre surface was confirmed using FTIR spectroscopy. Stretching frequencies of 1690-1700cm^{-1} and 1730-1740cm^{-1} were obtained

respectively.

(5) The pH of the Electrolyte Solution

The pH of the electrolyte solution has been shown to markedly affect the type and extent of fibre surface oxidation. For acidic and neutral electrolytes extensive oxidation occurs, but this is not the case in alkaline solutions. For acidic treatments the carbon 1s spectra show the presence of 'oxide' 1 (keto-) and 'oxide' 2 (carboxyl/ester) groups. As the pH is increased, the ratio of 'oxide' 1 to 'oxide' 2 decreases. At pH greater than 7 the nature of 'oxide' 1 changes to alcoholic/hydroxyl and a signal with a chemical shift of 1.6eV is detected. In alkaline solutions the number of carboxyl/ester groups is far greater than the number of alcohol type functionalities. The oxygen provided in the form of OH^- ions in alkaline solution is not very reactive towards the fibre surface and may only be able to oxidise existing functionalities at the edge sites. The edge sites appear to be centres of localised attack. The SEM photographs (Plate 6.1) of fibres polarised in sodium hydroxide solution show small holes in the fibres. No oxide layer was present. The physical mechanism of oxidation is therefore different to that in acidic solutions.

(6) The Concentration of the Solution

For ammonium nitrate solutions, increasing the concentration of the electrolyte, within the range 0.0001M-1M, increases the amount of surface functionality.

The nature of the surface produced after treatment depends upon many factors, as explained above. However, it has also been shown that the large observed increase in the ILSS of composites made from fibres treated in a wide range of electrolyte solutions occurs for the same current passing through the cell. This increase in ILSS does, however, occur at different potentials in different electrolyte solutions. These potentials are just below the oxygen potential for each electrolyte solution.

It has been shown that there is no relationship between the amount of surface oxygen and ILSS. Also, there is no relationship between the number of carboxyl/ester functionalities and ILSS. The apparent relationship between ILSS and surface oxygen noted by Fitzer (3,18) and other workers (eg.91), using nitric acid treatments, is not borne out when other electrolyte solutions are used for the electrochemical oxidation of fibre surfaces.

The presence of moisture (attracted by polar groups) denatures the the matrix material with a resultant loss of strength. If, as the above results indicate, there is nothing to be gained by having large numbers of oxygen complexes present on the fibre surface, then to increase the moisture resistance of the composites it may be desirable to use a surface treatment which produces the minimum O1s:C1s ratio for the desired ILSS. Results obtained in chapter 8 indicate that this may be achieved by polarisations in ammonium bicarbonate solutions.

Further Work

This study has shown that useful complimentary information

can be obtained from XPS, FTIR and SEM analyses. Further information concerning carbon fibre surfaces may be obtained from the use of other techniques, such as SIMS (secondary ion mass spectroscopy), and the measurement of micropore volume.

An investigation using all of the above techniques may well succeed in establishing the relative importance of physical and chemical characteristics of fibre/resin bonding. The apparently anomalous dependence of ILSS on the O1s:C1s ratio for nitric acid treatment may also be explained.

APPENDIX

This appendix contains C1s, O1s and N1s binding energies for a number of organic compounds. These binding energies are mainly taken from the literature, though some results from aromatic compounds studied by the author (and described in Chapter 5) have been included.

Polymer Feature	Material	Binding Energy	
		C1s	O1s
$-C\overset{O}{\underset{OH}{}}$	Polyacrylic acid	289·1	533·0 534·3
$-C\overset{O}{\underset{O-C}{}}$	Polyalkyl acrylates	288·9 286·6	532·8 534·3
$-C\overset{O}{\underset{O-C}{}}$	Polyalkylmethacrylates	288·8 286·7	533·0 534·4
$-C-O-C-O-$	Polymethylene oxide	287·8	533·6
$\rangle C=O$	Poly acetyl-p-xylene	287·6	533·6
$-O\diagdown\ \diagup C=O$ $-O\diagup$	Polycarbonates	290·4	534·9 533·0

After Clark(59-65)

(all binding energies w.r.t. C C1s=285eV)

Compound	C1s shift	O1s B.E.
CH_3CH_2OH	1·6	533·6
$CH_3CH_2O\,CH_2CH_3$	1·5	533·6
$HC(=O)OCH_2CH_3$	1·6 4·3	534·5 533·3
$CH_3COOCH_2CH_3$	1·6 4·0	534·4 533·6
$CH_3COO\,CH(CH_3)_2$	1·7 4·2	534·5 533·5
$CH_3COOCH_2CH(CH_3)_2$	1·7 4·2	534·2 533·4
$CH_3CO\,CH_2COOCH_2CH_3$	2·2 1·3 3·9	533·6 534·4 533·1

(59-65)

Compound	C1s	Compound	C1s
methanol	1·6	acetone	3·1
1,3,5 trihydroxy-benzene	1·8	acetaldehyde	3·2
hexahydroxy-benzene	1·9	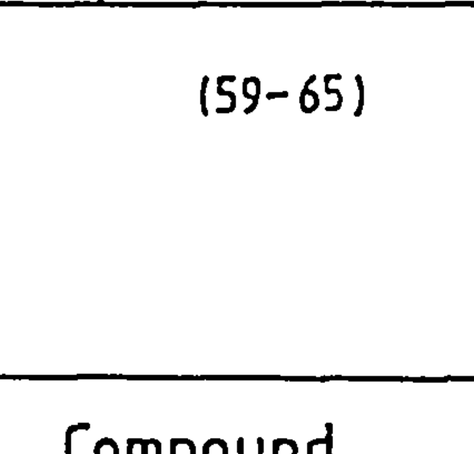	3·5
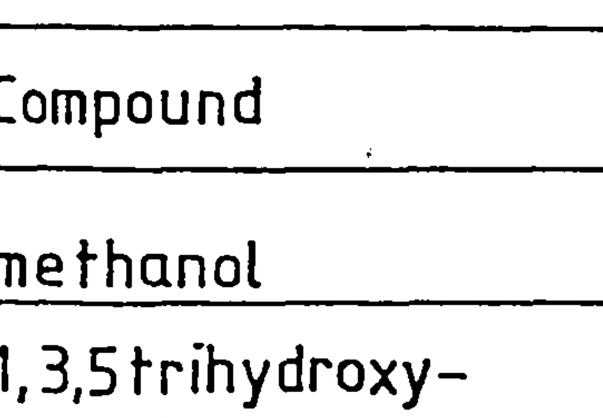	2·8	acetic acid	4·2

(59-65)

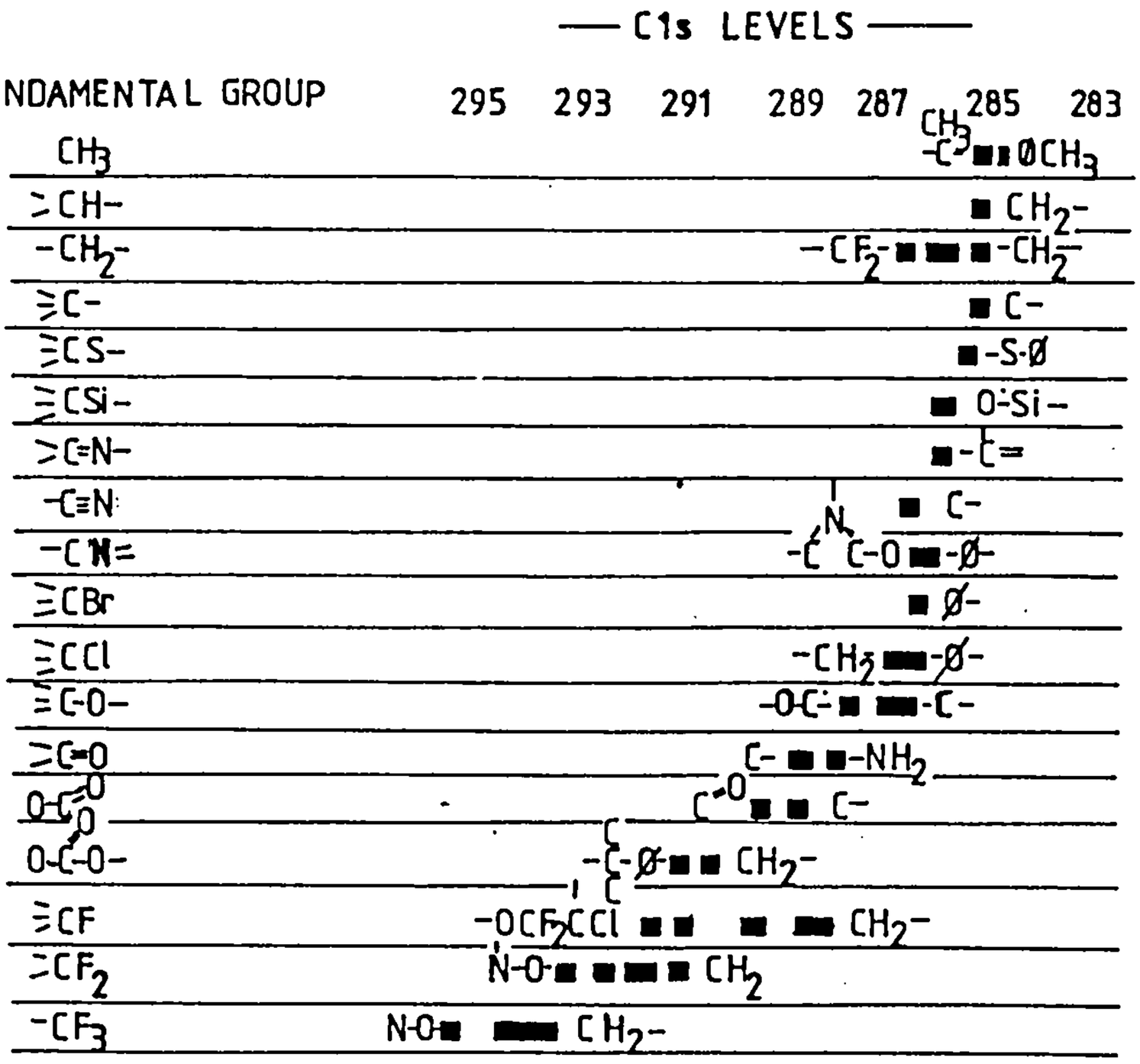

Correlation diagram for C1s levels in polmeric systems as function of electronic enviroment. (The horizontal scale for each block is taken to indicate the typical range of binding energies found for a given structural type.)

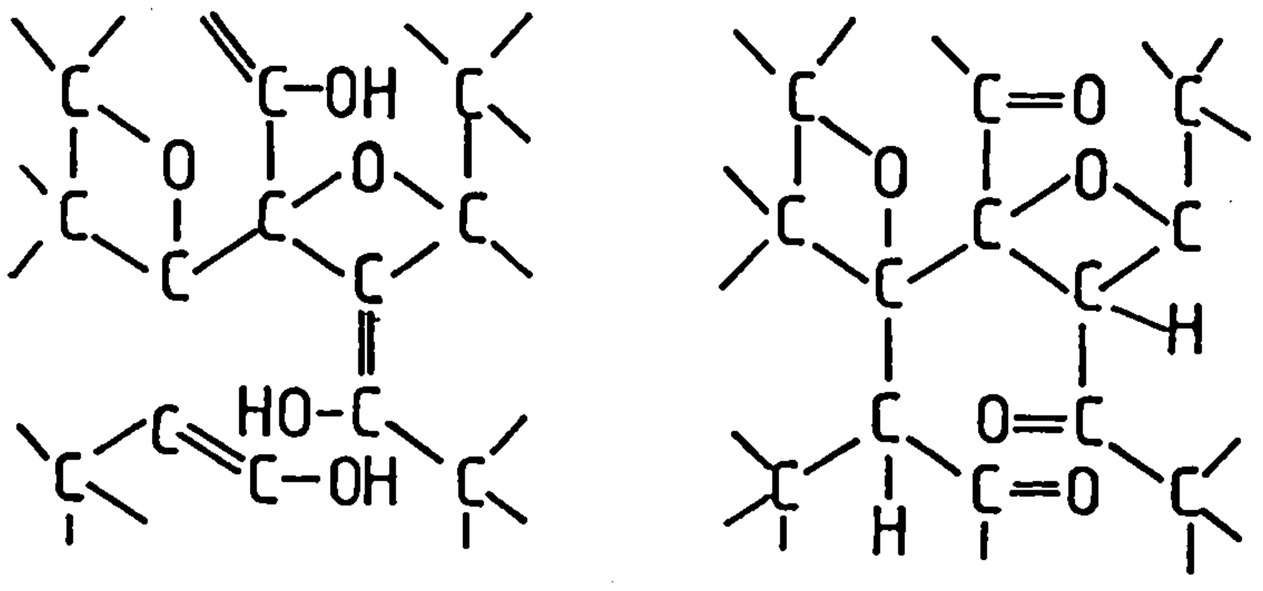

The keto and enol forms of graphite oxide.

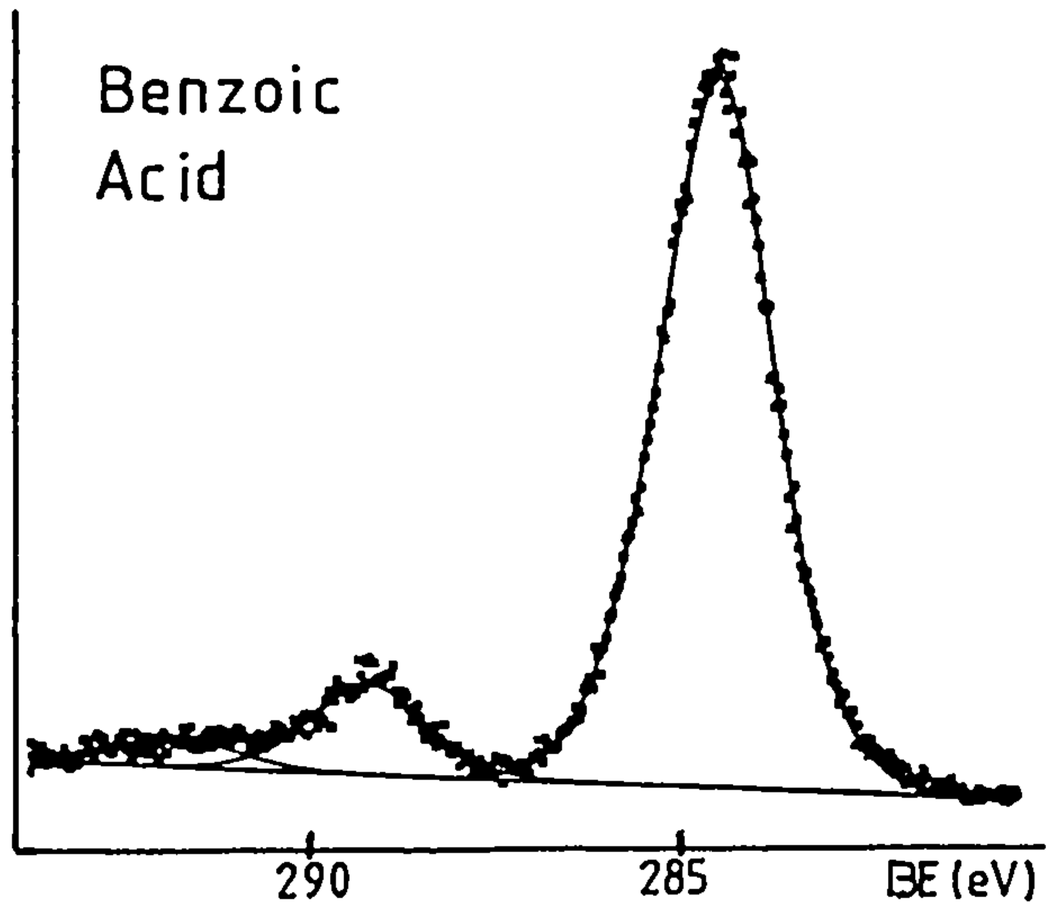

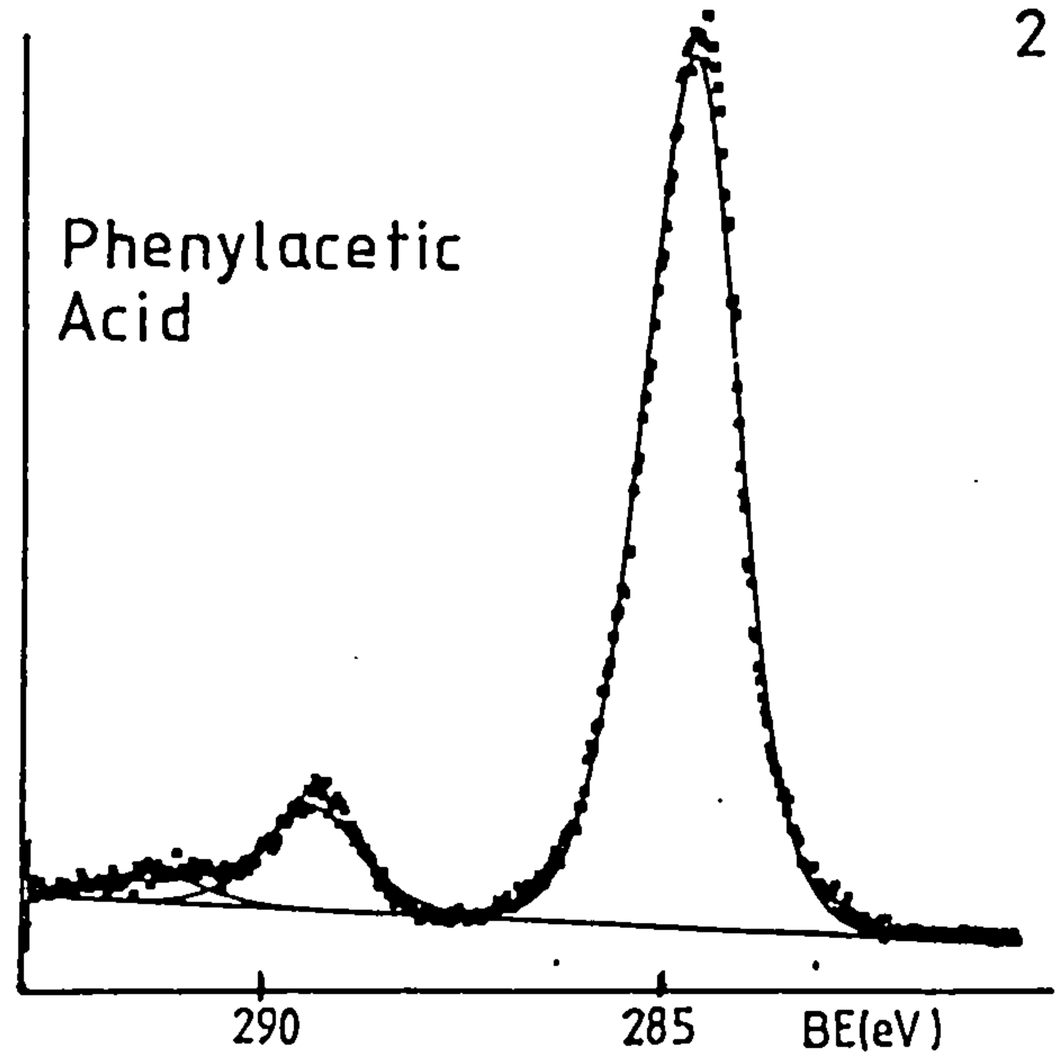

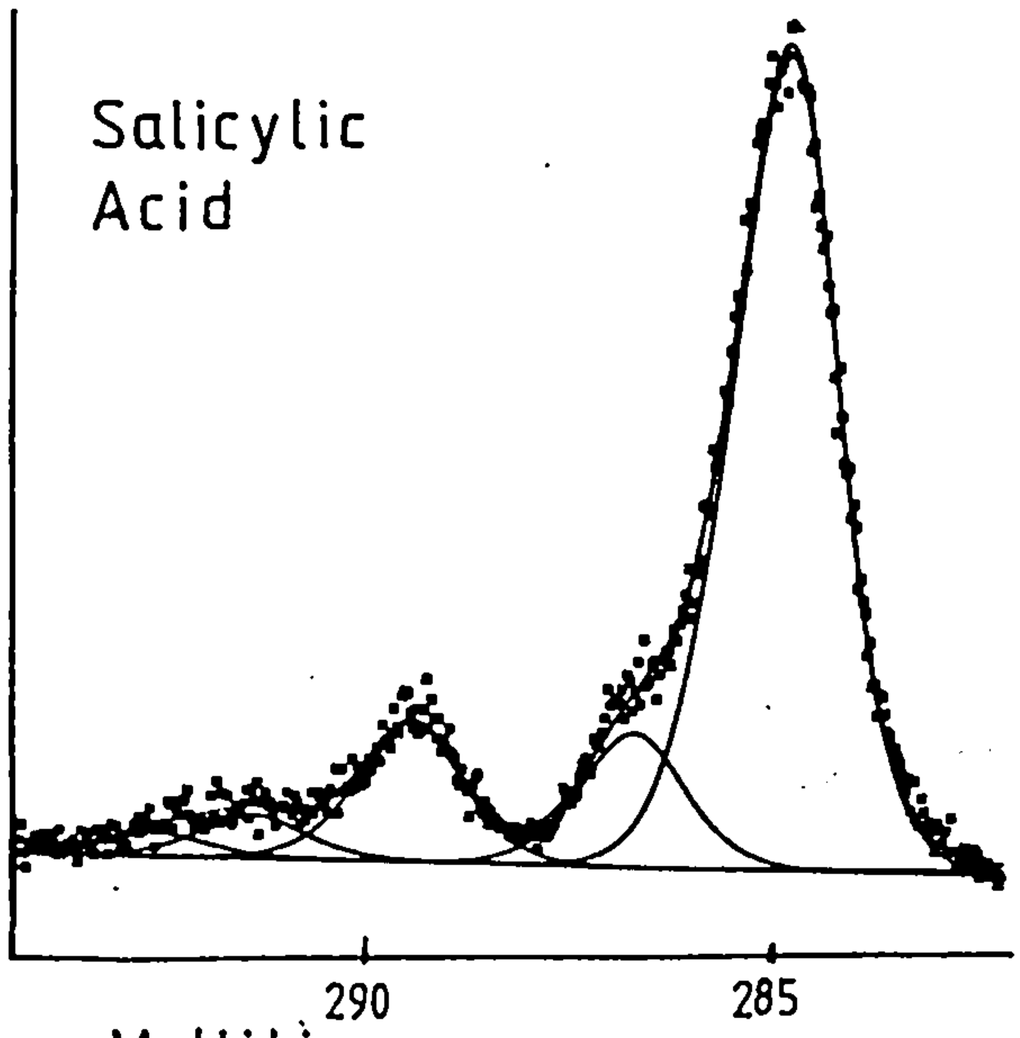

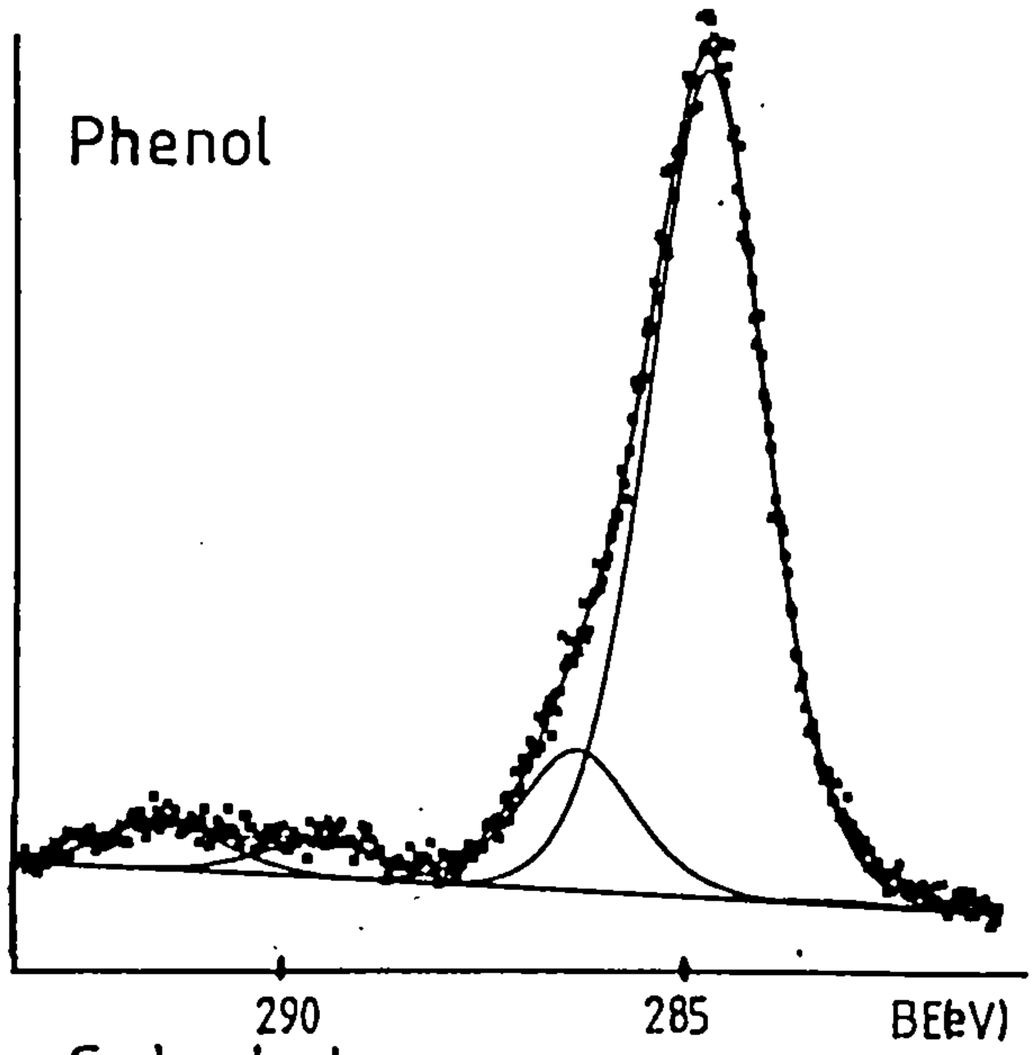

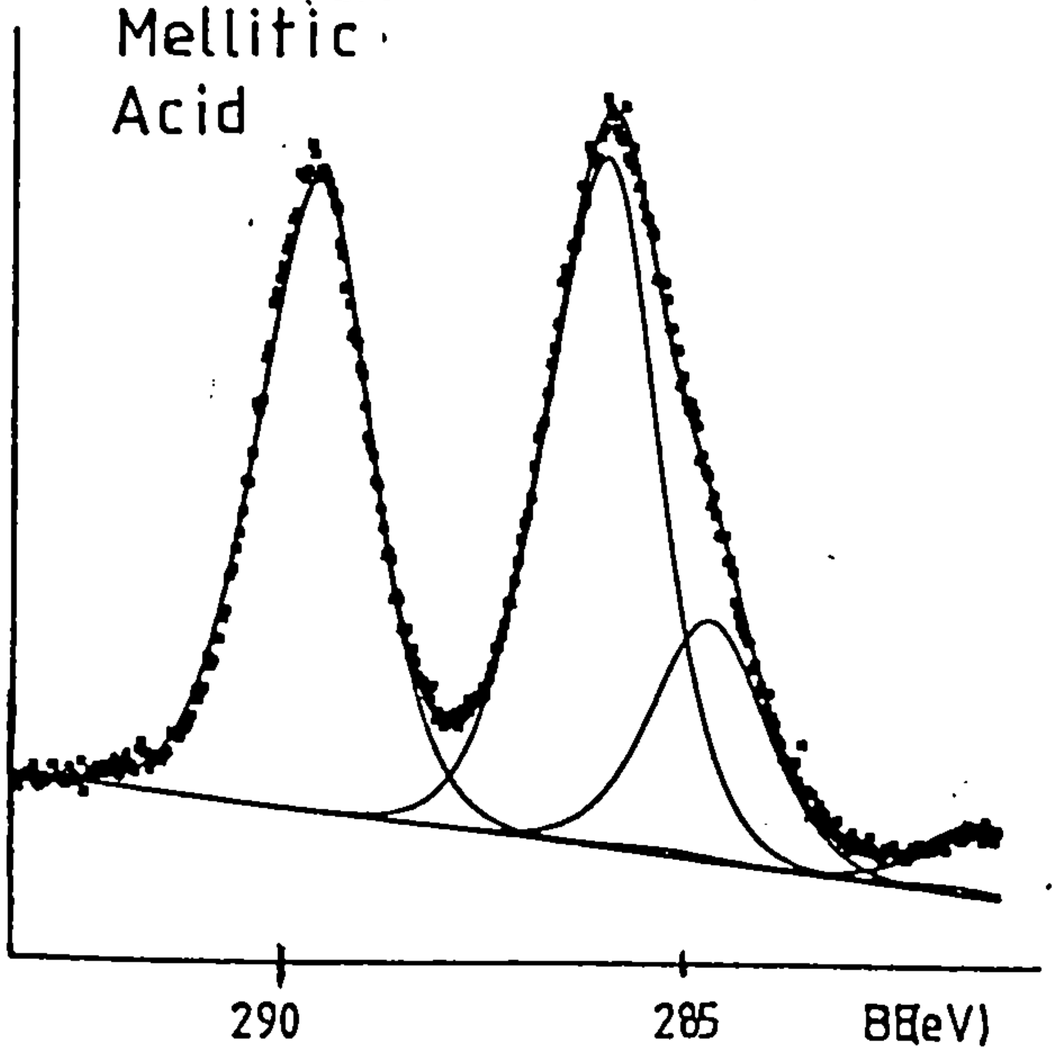

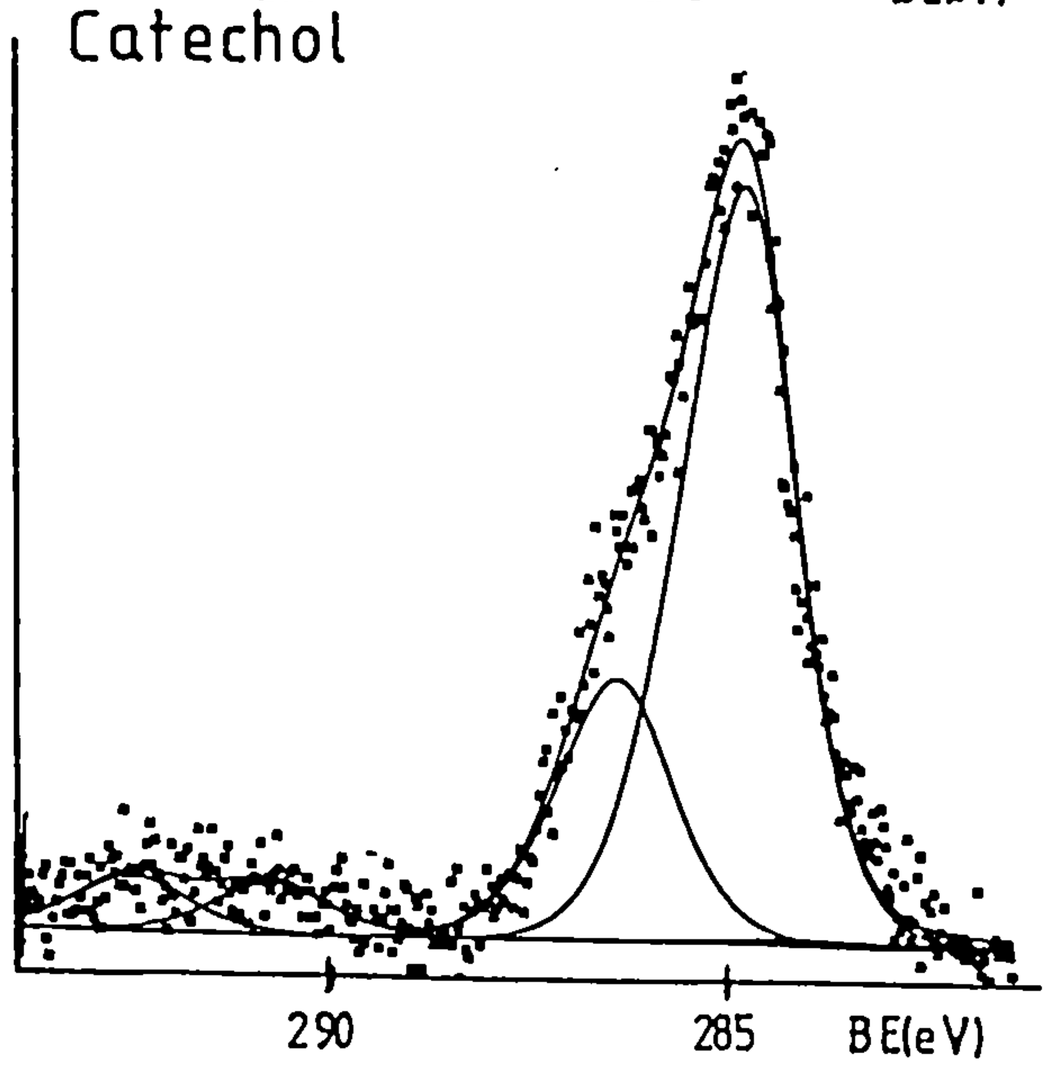

C1s Spectra of Acidic Compounds

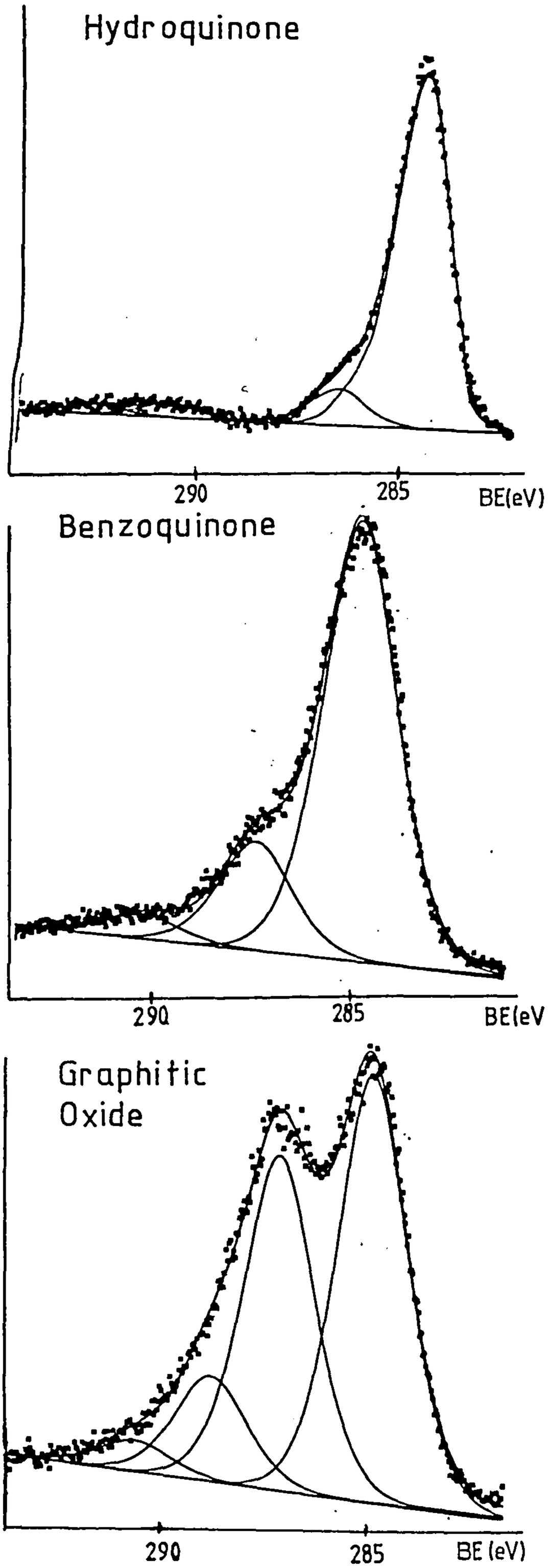

C1s Spectra of Aromatic Compounds

REFERENCES

1) D.W.McKee and V.J.Mimeault, "Chemistry and Physics of Carbon" Vol.8, p151, Dekker (N.Y.) 1973.

2) D.M.Brewis, J.Comyn, J.R.Fowler, D.Briggs and V.A.Gibson, **Fibre Sci. Technol.**, 12, p41 (1979).

3) E.Fitzer, **Proc. International Conf. "Interface-Interphase in Composite Materials", SYNERGIUM 83, Soc. Plastics Engineers,** 16-20 Oct. 1983.

4) J.W.Herrick, P.E.Gruber, F.T.Mausur, **23rd Hon. Tech. Conf. Reinforced Plastic Composites,** AFML-TR-66-178, p1 and p12 (1966).

5) V.J.Mimeault, D.W.McKee, **Proc. Xth Biennial Conf. on Carbon,** (1971).

6) N.L.Weinberg and T.B.Reddy, **J. Applied Electrochemistry,** 3, p73 (1973).

7) L.T.Drzal, **Carbon,** 15, pp129-138 (1977).

8) L.T.Drzal, J.A.Mescher and D.L.Hall, **Carbon,** 17, pp375-382 (1979).

9) C.Malstrom, R.Keen and L.Green, **J. Appl. Phys.,** 22, p593 (1951).

10) R.Franklin, **Proc. Roy. Soc.,** A209, p196 (1951).

11) R.Bacon, **J. Appl. Phys.,** 31, p284 (1960).

12) R.Bacon and M.M.Tang, **Carbon,** 2, p227 (1964).

13) R.Bacon and W.H.Smith, **Proc. 2nd. Ind. Carbon Graphite** Soc. Chem. Ind., London 1965.

14) W.Watt, **Carbon,** 10, pp121-143 (1972).

15) A.Shindo, **J. Ceram. Ass. Japan,** 69, p195 (1961).

16) A.Shindo, **Carbon,** 1, p391 (1964).

17) W.Johnson and W.Watt, **Nature,** 215, p384 (1967).

18) E.Fitzer, K.H.Geigl, W.Huttner and R.Weiss, **Carbon,** 18, pp389-393 (1976).

19) T.J.Lewis and P.E.Secker, "Science of Materials", p159, Harrap, London 1965.

20) H.L.Riley, **Chem. Ind.,** 58, p391 (1939).

21) J.B.Donnet and J.C.Bouland, **Rev. Gen du Caoutchouc,** 41, p407 (1964).

22) J.B.Donnet, J.Schultz and A.Eckhardt, **Carbon,** 6, p78 (1968).

23) F.A.Heckman and J.S.Clarke, **7th Biennial Conf. on Carbon,** Cleveland, June 1965.

24) R.D.Heindenreich, W.M.Hess and L.L.Ban, **J. Appl. Cryst.,** 1, p429 (1973).

25) W.Ruland, **Polymer,** 9, p17 (1967).

26) W.Ruland, "Chemistry and Physics of Carbon", Vol.4, Dekker, (N.Y) 1969.

27) D.J.Johnson and G.N.Tyson, **Brit. J. Appl. Phys.** (J. Phys. D.), 2, p787 (1969).

28) S.C.Bennet and D.J.Johnson, **Carbon,** 17, pp25-39 (1979).

29) B.L.Butler and R.J.Diendorf, **9th Conf. Carbon,** Boston, 1969.

30) D.Robson, F.Y.I.Assabghy, D.J.E.Ingram and P.G.Rose, **Nature,** 221, p51 (1969).

31) F.Tuinstra and J.L.Koenig, **J. Comp. Mater.,** 4, p492 (1970).

32) D.V.Badami, J.C.Joiner and G.A.Jones, **Nature,** 251, p386 (1967).

33) J.B.Donnet and A.Voet, "Carbon Black", Dekker, New York 1976.

34) J.B.Donnet, **Carbon,** 6, pp161-176 (1968).

35) H.P.Boehm, "Chemical Identification of Surface Oxides", in Advances in Catalysis, Vol.16, Academic Press, New York 1966.

36) D.Rivin, **Rubber Chem. Technol.,** 44, p307 (1971).

37) B.R.Puri, "Surface Complexes of Carbons" in "Chemistry and Physics of Carbon", Vol.6, p191, Edited by P.L.Walker, Dekker, New York 1970.

38) M.L.Diviney, **Adv. Colloid and Interface Sci.,** 2, p237 (1968).

39) M.S.Shah, **J. Chem. Soc.,** 261, p2676 (1929).

40) Yu A.Zarif'Yanz, V.F.Kisilev and N.N.Lezhnev, **Carbon,** 5, p127 (1967).

41) F.J.Vastola and P.L.Walker, **J. Chim. Phys.,** 58, p20 (1961).

42) J.Dubsky and S.Beran, **Surf. Sci.,** 79, pp53-63 (1979).

43) B.Steenberg, "Adsorption and Exchange of Ions on Activated Charcoal", Almquist and Wiksells, Uppsala, Sweden 1944.

44) D.S.Evehart and C.N.Reilley, **Anal. Chem.**, 53, p655 (1981).

45) D.Briggs and C.R.Kendall, **Int. J. Adhesion and Adhesives**, 2, p13 (1982).

46) D.Briggs and C.R.Kendall, **Polymer**, 20, p1053 (1979).

47) A.Bradley and M.Czuha, **J. Anal. Chem.**, 47, p1838 (1975).

48) M.Czuha and W.M.Riggs, **J. Anal. Chem.**, 47, p1836 (1975).

49) C.D.Batich and R.C.Wendt in "Photon Electron and Ion Probes of Polymer Structure and Properties", Eds. D.W.Dwight, T.J.Fabish and H.R.Thomas, AC Symposium Series, p221 (1981).

50) J.R.Rasmussen, E.R.Stedronsky and G.M.Whitesides, **J. Am. Chem. Soc.**, 99:14, p4736 (1977).

51) H.P.Boehm, E.Diehl, W.Heck and R.Sappock, **Angew. Chem. Internat.**, 3 (No.10), pp669-677 (1964).

52) H.P.Boehm, **Advan. Catal.**, 16, p179 (1960).

53) H.P.Boehm, E.Diehl and W.Heck, **Rev. Gen. du Caoutchouc**, 41, p444 (1964).

54) H.P.Boehm, **Angew. Chem. Int.**, 5, p533 (1966).

55) V.A.Garten, D.E.Weiss and J.B.Willis, **Aust. J. Chem.**, 10, p295 (1957).

56) J.B.Donnet, **Carbon**, 6, pp161-176 (1968).

57) V.A.Garten and D.E.Weiss, **Aust. J. Chem.**, 10, p309 (1957).

58) G.R.Hennig, **Proc 5th Carbon Conf.**, Vol.1, p143, Pergamon Press 1966.

59) D.T.Clark, **Macromol. Sci. Rev.**, Macromol. Chem. C., 12, p191 (1975).

60) D.T.Clark and H.R.Thomas, **J. Polym. Sci.**, Polym. Chem. Ed., 14, p1671 (1976).

61) D.T.Clark and A.Dilks, **Charact. Met. Polym. Surf.**, 2, pp5-52 (1977).

62) D.T.Clark, **Adv. Polym. Sci.**, 24 (Mol. Prop.), pp25-88 and pp101-132 (1977).

63) D.T.Clark, B.J.Cromarty and A.Dilks, **J. Polym. Sci.**, Polym. Chem. Ed., 16, p3173 (1978).

64) D.T.Clark, **J. Polym. Sci.**, Polym. Chem. Ed., 16, p791

(1978).

65) D.T.Clark and A.Dilks, **J. Polym. Sci.,** Polym. Chem. Ed., 17, p957 (1979).

66) Courtaulds LTD. Br. Pat. 144341 19th March, 1969.

67) J.D.Ray, S.Steinsiger and B.A.Cass, US Pat. 16251 (3rd March, 1970).

68) Morganite Research Development LTD., Br. Pat. 493571 (8th Oct., 1969).

69) J.T.Paul, Appl. No. 25208/74 Patent Specification 1433712.

70) J.W.Herrick, **Proc. 23rd Ann. Tech. Conf. Reinf. Plastics Division,** Sect.16A, Feb. 1968.

71) J.B.Donnet, **Carbon,** 20, p267 (1982).

72) C.Kozlowski and P.M.A.Sherwood, **J. Chem. Soc. Farad. Trans.1,** in press (1984).

73) J.C.Goan and S.P.Prosen, **71st. ASTM Meeting,** San Francisco 1978.

74) J.B.Donnet and P.Ehrburger, **Carbon,** 15, pp143-152 (1977).

75) J.C.Goan, L.A.Joo' and G.E.Sharpe, **Proc. 27th Ann. Tech. Conf.,** 27 Section 21E, p1 (1972).

76) I.D.Aitken, G.D.Rhodes and R.A.P.Spencer, **Harwell 7th Int. Conf. on Reinforced Plastics,** Paper 24 (1970).

77) J.P.Randin, "The Encyclopedia of Electrochemistry", Vol.8.

78) H.Marsh, A.D.Foord, J.S.Mattson, J.M.Thomas and E.L.Evans, **Jou. Colloid and Int. Sci.,** 49, No.35 (1974).

79) N.G.Bardina and L.T.Krishtalik, **Elecktrokhimiya,** 2, p216 (1966).

80) H.Binder, A.Kohling, K.Richter and G.Sandstede, **Electrochim. Acta,** 9, p255 (1964).

81) L.Redey and N.Lohonyai, **Abh. Saechs. Akad. Wiss Leipzig Math Naturwiss Kl,** 49, p97 (1968).

82) B.K.Brown and O.W.Storey, **Trans. Am. Electrochem. Soc.,** 53, p140 (1928).

83) Ngo Dai Viet, D.V.Kokoulina and L.I.Krishtalik, **Elecktrokhimiya,** 8, p225 (1972).

84) G.N.Kokhanov, **Elecktrokhimiya,** 7, p1606 (1971).

85) Bulygin, **Zh. Prikl. Khim.,** 32, p121 (1959).

86) G.N.Kokhanov and N.G.Milova, **Elecktrokhimiya,** 5,

p93 (1969).

87) A.Proctor and P.M.A.Sherwood, **J. Elec. Spec. and Rel. Phenomena,** 27, pp39-56 (1982).

88) A.Shindo, **Proc. Int. Conf. "Interface-Interphase in Composite Materials", SYNERGIUM 83, Soc. Plastics Engineers,** 16-20 Oct. 1983.

89) M.Barber, P.Swift, E.L.Evans and J.M.Thomas, **Nature,** 227, p1131 (1970).

90) M.Barber, E.L.Evans and J.M.Thomas, **Chem. Phys. Lett.,** 18, p423 (1973).

91) C.R.Thomas and E.J.Walker, **Proc. 5th Int. Carbon/Graphite Conf.,** London, pp520-531 (1978).

92) G.Gynn, R.N.King, S.F.Chappell and M.L.Deviney, AFWAL-TR-81-4096.

93) A.Ishitani, **Carbon,** 19, pp269-275 (1981).

94) T.Takahagi and A.Ishitani, **Carbon, 22, pp43-46** (1984).

95) A.Proctor and P.M.A.Sherwood, **J. Elec. Spec. and Rel. Phenomena,** 27, p39 (1982).

96) A.Proctor and P.M.A.Sherwood, **Surface and Interface Anal.,** 4, No.5 (1982).

97) A.Proctor and P.M.A.Sherwood, **Anal. Chem.,** 54, p13 (1982).

98) A.Proctor and P.M.A.Sherwood, **Anal. Chem.,** 52, p2315 (1980).

99) R.O.Ansell, T.Dickinson, A.F.Povey and P.M.A.Sherwood, **J. Electroanal. Chem.,** 98, p79 (1979).

100) B.Rand and R.Robinson, **Carbon,** 15, p2547 (1977).

101) R.V.Subramanian, J.J.Jakubowski and F.D.Williams, **J. Adhesion,** 9, (1978).

102) D.A.Scola and S.C.Brooks, 25th Soc. Plastics Ind. Meeting DC (1970).

103) R.V.Subramanian and J.J.Jabowski, **Polym. Eng. Sci.,** 18, p590 (1978).

104) S.Brelant, **Carbon,** 19, p329 (1981).

105) H.Hertz, **Ann. Physik.,** 31, p983 (1887).

106) A.Einstein, **Ann. Physik.,** 17, p132 (1905).

107) E.Sokolowski, C.Nordling and K.Siegbahn, **Arkiv. Physik.,** 12, p301 (1957).

108) C.Nordling, E.Sokolowski and K.Seigbahn, **Phys. Rev.**, 105, p1676 (1957).

109) S.Hagstrom, C.Nordling and K.Seigbahn, **Phys. Lett.**, 9, p235 (1964).

110) K.Seighbahn, C.Nordling, A.Fahlman, R.Nordberg, K.Hamrin, J.Hedman, G.Johansson, T.Bergmark, S.Karlsson, I.Lingreen, B.lindberg, "ESCA-Atomic, Molecular and Solid State Structure studied by means of Electon Spectroscopy" Almquist and Wiksell, Uppsala, Sweden (1976).

111) K.Seigbahn, **Pure Appl. Chem.**, 48, p77 (1976).

112) S.C.Avanzino, W.L.Jolly, **J. Amer. Chem. Soc.**, 100, p2228 (1978).

113) U.Gelius, **J. Electron Spec.**, 5, p985 (1974).

114) G.Ertl, **Angew Chem.**, 15, p391 (1976).

115) P.Auger, **J. Phys. Radium**, 6, p205 (1925).

116) P.Auger, **Surf. Sci.**, 48, p1 (1975).

117) A.F.Orchard, in "Handbook of X-ray and UV Photolelectron Spectroscopy", Edited by D.Briggs, p49, Heyden and Son, London 1977.

118) T.Dickinson, A.F.Povey and P.M.A.Sherwood, **J. Elec. Spec.**, 2, p441 (1973).

119) T.Koopmans, **Physical**, 1, p104 (1934).

120) P.S.Bagus, **Phys. Rev.**, 139, A619 (1965).

121) M.E.Schwartz, **Chem. Phys. Lett.**, 5, p50 (1970).

122) C.M.Moser, R.K.Nesbet and G.Verhagen, **Chem. Phys. Lett.**, 12, p230 (1971).

123) D.A.Shirley, **Advan. Chem. Phys.**, 23, p85 (1973).

124) P.M.A.Sherwood, **J. Chem. Soc. Farad. Trans. 2**, 72, p1791 (1976).

125) K.Seigbahn, C.Nordling, A.Fahlman, R.Nordberg, K.Hamrin, J.Hedman, G.Johansson, T.Bergmark, S.E.Karlsson, I.Lindgreen and B.Lindberg, **Nova Acta Regiae Societatis Scientarium Upsaliensis**, Ser IV, p20 (11967).

126) L.Hedin and G.Johansson, **J. Phys. B**, 2, p1336 (1969).

127) D.A.Shirley, **Chem. Phys. Lett.**, 16, p220 (1972).

128) L.Ley, R.A.Pollak, S.P.Kowalczyk, R.Mc.Feely, D.A.Shirley, **Phys. Rev. B**, 8, p641 (1973).

129) G.D.Mahan, **Phys. Rev.**, 163, p612 (1967).

130) P.Nozieres and C.T.de Dominics, **Phys. Rev.**, 178, p1097 (1969).

131) S.Doniach and M.Sunjic, **J. Phys. Chem.**, 3, p285 (1970).

132) S.Evans, in "Handbook of X-ray and UV Photoelectron Spectroscopy" Edited by D.Briggs. Heyden and Sons LTD., 1977.

133) P.A.M.Dirac, **Proc. Roy. Soc.**, A118, p351 (1928).

134) R.A.Pollak, L.Ley, F.R.Mc.Feely, S.P.Kowalczyk and D.A.Shirley, **J. Elec. Spec. and Rel. Phenom.**, 3R, p381 (1974).

135) P.Steiner, H.Hochst and S.Hufner, **Phys. Lett.**, 61A, p410 (1977).

136) A.Barrie, **Chem. Phys. Lett.**, 19, p109 (1973).

137) J.C.Fuggle, D.J.Fabian and L.M.Watson, **J. Electron Spec.**, 9, p99 (1976).

138) W.J.Pandee, **Phys. Rev. B.**, 5, p3512 (1972).

139) P.M.T.H.Van Attekum and G.K.Wertheim, **Phys. Review Lett.**, 43, p1896 (1979).

140) P.M.A.Sherwood, in "Practical Surface Analysis by Auger and X-ray Photoelectron Spectroscopy" Appendix 3, edited by D.Briggs and M.P.Seah, Wiley and Sons 1983.

141) A.M.Bradshaw, L.S.Cederbaum, W.Domcke and U.Krause, **Vac. Ultraviolet Radical Phys., Proc. Int. Conf. 4th,** pp625-628 (1974).

142) A.M.Bradshaw, L.S.Cederbaum, W.Domcke and U.Krause, **J. Phys. Chem: Solid State Phys.**, 7, pp4503-4512 (1974).

143) W.Brenig and C.Gaillard, **Physics Letters**, 54A, No.6.

144) R.Schogl and H.P.Boehm, **Carbon**, 21, pp345-358 (1983).

145) J.Houston, **Solid State Comm.**, 17, pp1165-1169 (1975).

146) H.Y.Hall and P.M.A.Sherwood, **J. Chem. Soc. Farad. Trans. 1**, 80, pp135-152 (1984).

147) B.J.Lindeberg, **J. Elect. Spec. and Rel. Phenomena,** 5, p149 (1974).

148) W.S.Hummers and R.E.Offeman, **J. Am. Chem. Soc.**, 80, p1339 (1958).

149) R.V.Subramanian, V.Sundaram and A.K.Patel, **Proc. 33rd Ann. Conf. Reinforced Plastics/Compos. Int. Soc. Ind.** Section 20-F, pp1-8 (1978).

150) D.W.Davis and D.A.Shirley, **J. Elec. Spec. and Rel. Phenom,** 3, pp137-163 (1974).

151) G.E.Bacon, N.A.Curry and S.A.Wilson, **Proc. Roy. Soc.** 279A, p98 (1964).

152) V.M.Kozhin and A.I.Kitagorodskii, **Zh. Fiz. Khim,** 29, p1897 (1955).

153) D.W.J.Cruikshank, **Acta Cryst.,** 10, p504 (1957).

154) J.M.Roberston, V.C.Sinclair, J.Trotter, **Acta Cryst.,** 14, p697 (1962).

155) A.Camerman and J.Trotter, **Acta Cryst.,** 18, p639 (1965).

156) A.Camerman and J.Trotter, **Proc. Roy. Soc.,** 279A, p129 (1965).

157) J.K.Fawcett and J.Trotter, **Proc. Roy. Soc.,** 289A, p366 (1966).

159) H.P.Boehm, U.Hofman and A.Clauss, **Proc. 3rd Conf. Carbon,** Buffalo, Pergamon Press, p241 (1959).

160) E.L.Evans, J.de D.Lopez-Gonzalez, A.Martin-Rodriguez and F.Rodriguez-Reinoso, **Carbon,** 13, pp461-464, Pergamon Press (1975).